# Identification of pyruvate decarboxylase/indole pyruvate decarboxylase gene family members from *Arabidopsis thaliana*

A DISSERTATION
SUBMITTED TO THE FACULTY OF THE GRADUATE SCHOOL
OF THE UNIVERSITY OF MINNESOTA
BY

Songqing Ye

IN PARTIAL FULFILLMENT OF THE REQUIREMENTS
FOR THE DEGREE OF
DOCTOR OF PHILOSOPHY

Jerry D. Cohen, Advisor

August, 2009

**Acknowledgements**

It is a pleasure to thank those who have helped and encouraged me during my doctoral studies and thus made this thesis possible.

First and foremost, I thank my advisor, Dr. Jerry Cohen, for his guidance, encouragement, and support during my research and study at the University of Minnesota. He was always accessible and willing to help his students with both patience and knowledge. His enthusiasm and perpetual energy has motivated and encouraged all of his advisees, including me. As an international student, I could not have wished for a better and friendlier supervisor. This thesis could not possibly have been written or completed without his input.

I also thank the members of my committee, Drs. Alan G. Smith, Min Ni, John Ward, and Gary Gardner. They consistently inspired me to explore new research areas and guided me to shape the scope of my research. Deserving of special mention were my interactions with Dr. Gary Gardner, who acted as a very involved and helpful "co-advisor". His insights and knowledge of photobiology and his supporting advice have helped to enlighten my understanding and direct my studies into the area of the SAR.

I thank the members of the lab group of Drs. Jerry Cohen, Gary Gardner, and Adrian Hegeman for their academic and technical support and research enlightenment. Dr. Adrian Hegeman was especially helpful in guiding me on development and interpretation of the enzymatic assays. Dr. Lana Barkawi provided guidance in many areas, especially in the complexity of IAA extraction and isotope dilution quantification. Doug Brinkman assisted me in setting up the simulated foliar shade conditions and took care of the required growth chambers. Dr. Wen-Ping Chen helped me on molecular cloning and collaborated with me on a project of identifying APK kinase. Students and members of our lab, including Dr. Jyh-Ching Chou, Dr. Seijin Park, Dr. Minsang Lee, Dr. Angela H. Culler, Dr. Xiaoyuan Yang, Dr. Charlie Rowher, Veronica Justen, Lynette Wong, Xing Liu and Mike Wilson, have offered helpful support and useful discussions.

I also thank Dr. Heather Nonhebel, University of New England, for working together with me on PDC enzymes, Dr. Chuanyou Li at Institute of Genetics and Developmental Biology, Chinese Academy of Sciences for a fruitful collaboration on the interactions between JA and auxin, Dr. Mark Estelle at the University of California, San Diego for providing some interesting mutants potentially related to auxin metabolism, Dr. Jennifer Normanly from the University of Massachusetts for helpful suggestions, Dr. Janet Slovin at the USDA-ARS in Beltsville for encouragement and Dr. Roger Becker for assisting me herbicide resistance assay. Dr. Changbin Chen also helped me with techniques for measurement of pollen germination.

I thank my fellow graduate students including officemates, researchers as well as the support staff of Department of Horticultural Science.

I am indebted to the U.S. National Science Foundation (NSF 2010 grant MCB0725149 and Plant Genome Research Program grant DBI0606666) and the U.S. Department of Energy (grant DE-FG02-00ER15079) for the financial support provided for my research, as well as the Plant Biological Sciences graduate program for summer and travel support. In addition, I thank the Microbial and Plant Genomics Institute, The

North American Arabidopsis Steering Committee, and Cold Springs Harbor Laboratories for travel and tuition support.

I also thank my wife Aimei, daughter Rebecca, my parents, and other family members, and friends who have supported me throughout my graduate school career.

Lastly, I offer my regards and blessings to all of those who supported me in any of the many ways required for the completion of this research project.

## Dedication

This dissertation is dedicated to my wife Aimei, and my parents, who have given and supported me a lot.

## Abstract

Several biologically important and diverse reactions are regulated by thiamine pyrophosphate (TPP) cofactor-dependent metabolic enzymes, including pyruvate decarboxylase (PDC), indole pyruvate decarboxylase (IPDC), and acetohydroxy acid synthase. PDC is a critical enzyme in plant metabolism that regulates energy production especially during periods of anaerobic stress. IPDC has long been proposed as a key enzyme in the biosynthesis of the plant hormone indole-3-acetic acid (IAA) from tryptophan. Six putative *Arabidopsis thaliana PDC* gene family members have been individually cloned and expressed in *E. coli*, and recombinant PDC proteins were purified and biochemically characterized. *At*PDC2 was identified as a unique functional PDC based on its measured biochemical activity. The pH and temperature optima for the recombinant protein were 6.2 and 55°C, respectively, and the Km was 3.5 mM. Also, addition of 0.5 mM TPP and 5 mM $Mg^{2+}$ resulted in the highest activity. However, *At*PDC2 lacked any measurable IPDC activity as determined by gas chromatography-mass spectrometry (GC-MS)-based methods. Thus, this mono-functional PDC was different from the more thoroughly studied microbial PDCs, which all have bi-functional activity toward both indole-3-pyruvate and pyruvate substrates. These findings suggest a potential regulatory role for the catalytically inactive PDC proteins in modulation of PDC activity, similar to a mechanism proposed for yeast. None of the *pdc* mutants showed a change in resistance to chlorsulfuron or imazamox herbicides, and this result was also consistent with the hypothesis that the inactive *AtPDC* genes may play a role in PDC activity regulation in *Arabidopsis*.

Studies presented here show that the genes most likely to encode proteins with PDC activity or IPDC activity, the PDC gene family, all lack IPDC activity and all except one lack PDC activity. Furthermore, all *Arabidopis PDC* T-DNA insertion mutants were found to share the same shade avoidance phenotype to as did wild-type plants. These findings bring into question the physiological significance of the IPA pathway for auxin biosynthesis as has been previously proposed.

Very low levels of IPDC activity are difficult to measure using procedures developed for the enzyme activity of proteins from bacteria, which produce substantial levels of indole acetaldehyde (IAAld) from indole-3-pyruvate (IPA). To determine the potential activity of plant enzymes, either expressed in *E. coli* or extracted from *Arabidopsis* plants, GC-MS assay methods were developed with high sensitivity and specificity. For expressed proteins, IAAld produced from IPA was measured directly using indole carboxaldehyde as an internal standard. This procedure failed, however, to detect IPA in the presence of plant protein extracts; thus, a coupled *in vitro* reaction with aldehyde dehydrogenase that produced IAA from IPA was developed, and the IAA was quantified using [$^{13}C_6$]IAA as an internal standard, methylation with diazomethane, and GC-MS detection. Together, these methods provide important sensitive and precise methods for the search for IPDC activity in the plant kingdom.

**Table of Contents**

## List of Tables

## List of Figures

Figure Page

## List of Abbreviations

2,4-D: 2,4-dichlorophenoxyacetic acid

2,4,5-T: 2,4,5-trichlorophenoxyacetic acid

AAO1: aldehyde oxidase

ABA: abscisic acid

ACC: 1-amino-1-cyclopropane carboxylic acid

ADH: alcohol dehydrogenase

AGI: Arabidopsis Genome Initiative

AHAS: acetohydroxy acid synthase

ALDH: aldehyde dehydrogenase

AMI1:amidohydrolase gene

ASA1: anthranilate synthase α1

ATP: adenosine triphosphate

ATTP: adenosine thiamine triphosphate

GA: gibberellin

GC-MS: gas chromatography-mass spectrometry

HET: 4-methyl-5-(2-hydroxyethyl)thiazole

HMP: 4-amino-5-hydroxymethyl-2-methylpyrimidine

IAA: indole-3-acetic acid

IAAld: indole acetaldehyde

IAM: indole-3-acetamide

IAN: indole-3-acetonitrile

IAOx: indole-3-acetaldoxime

IBA: indole-3-butyric acid

IEt: indole-3-ethanol (or indoleethanol)

IGP: indole-3-glycerol phosphate

ILA: indole-3-lactic acid

IPTG: isopropyl-β-D-thiogalactopyranoside

IMIs: imidazolinones

IPDC: indole-3-pyruvic acid decarboxylase

IPA: indole-3-pyruvic acid (or indole pyruvate)

JA: jasmonic acid (or jasmonate)

Jdl1: jasmonate-induced defective lateral root1

kDa: 1000 daltons

LR: lateral root

LRP: lateral root primordium

NAA: naphthalene acetic acid

NADH: reduced form of nicotinamide adenine dinucleotide

NIT: nitrilase (nitrile aminohydrolase)

orp: orange pericarp mutant

OxIAA: oxindole-3-acetic

PAA: phenylacetic acid

PAR: photosynthetically active radiation

PAT: polar auxin transport

PDC: pyruvate decarboxylase

POBs: pyrimidinyl oxybenzoates

qRT-PCR: quantitative RT-PCR

R:FR: the ratio of red light to far-red light

RT-PCR: Reverse transcription-PCR

SAR: shade avoidance response

SIM: selective ion monitoring

SUs: sulfonylureas

TAA1: tryptophan aminotransferase of *Arabidopsis*

TAM: tryptamine

TH3: transhydrogenase dIII

TMP: thiamine monophosphate

TPP: thiamine pyrophosphate

TPs: triazolopyrimidines

TTP: thiamine triphosphate

TDC: tryptophan decarboxylase

WT: wild type

# Chapter 1

# Literature Review

## 1.1 Introduction

Auxins are the general name for a group of plant hormones or phytohormones and the term “auxin” is derived from Greek “to increase or grow”. Auxins were the first major plant hormones to be discovered, with the first reports on such a mobile signal appearing more than 130 years ago (Ciesielski, 1872). Although auxins can be produced in most organs in plants, the most abundant levels of auxins are produced in the growth regions such as root and shoot meristems. Auxins play an essential role in plant viability and are involved in nearly every stage of a plant’s life cycle. Auxins regulate apical dominance and promote the growth of stems, coleoptiles, and leaves, and their action includes a rapid increase in the extensibility of the cell wall (Rayle and Cleland, 1992; Yang et al., 1993). Auxins promote floral bud development and fruit development, and they induce vascular differentiation (Okada et al., 1991; Aloni, 1995). Auxins also promote the formation of lateral and adventitious roots but inhibit primary root growth and delay the onset of leaf abscission (Thimann and Skoog, 1934). Commercially, auxins are used to promote initiation of root growth, to improve uniform flowering, to increase fruit set, and to prevent premature fruit drop. In addition, synthetic auxins have a variety of commercial uses and can be used as an herbicide to control dicot weeds (Taiz and Zeiger, 1998).

Active auxin compounds include naturally occurring substances and synthetic compounds and both have similar physiological effects in plants. Indole-3-acetic acid (IAA), the most studied auxin, is the principal form of auxin in higher plants. Therefore, we often refer to IAA with the generic term “auxin”. However, IAA is rather easily

oxidized in aqueous solutions and turns over rapidly once it enters the plant tissue; thus, IAA is not typically used commercially as a plant growth regulator. Besides IAA, there are a few other native free auxins such as indole-3-butyric acid (IBA), phenylacetic acid (PAA), and 4-Cl-IAA found in higher plants (Epstein, et al., 1989; Ludwig-Müller and Cohen, 2002; Reinecke, 1999) (Figure 1.1). IBA is found in several species such as *Arabidopsis*, pea, and maize (reviewed in Epstein and Ludwig-Müller, 1993) and has been confirmed as a resource for conversion to IAA in grapevine and olive (Epstein and Lavee, 1984). IBA is an important ingredient in commercial plant rooting horticultural products. 4-Cl-IAA, a chlorinated derivative of IAA, has been found in pea, bean, barley, pine, and other species (Pless et al., 1984; Reinecke, 1999; Engvild, 1996). An important biochemical effect of 4-Cl-IAA, which may in part be responsible for some of its effects, is its ability to regulate gibberellin (GA) synthesis in pea (Ozga and Reinecke, 2003), and this is similar to the mechanism of IAA changes in GA metabolism seen in *Arabidopsis* (Desgagné-Penix and Sponsel, 2008). PAA is present in citrus fruits, nasturtiums, and wheat (Khalifah et al., 1963; Ludwig-Müller and Cohen, 2002; Macháčkova et al., 1981). Though PAA is not commonly used in agriculture and horticulture due to its weak effects, it has been used in some perfumes and in medicine.

Synthetic auxins include naphthalene acetic acid (NAA), 2,4-dichlorophenoxyacetic acid (2,4-D), 2,4,5-trichlorophenoxyacetic acid (2,4,5-T), and a large number of other compounds with related structures (Figure 1.2). 2,4-D is the most widely used herbicide in the world in the control of broadleaf weeds and also is an important supplement in plant cell cultures. 2,4,5-T is another potent auxin herbicide also widely used to defoliate

broad-leafed plants. Dicamba (3,5-dichloro-o-anisic acid; its trade names include Banvel®, Oracle® and Vanquish®) and picloram (4-amino-3,5,6-trichloropicolinic acid; its trade names include Tordon® and Grazon®) are additional auxinic herbicides used for controlling annual and perennial broadleaf weeds. NAA is used for plant tissue culture and, like IBA, is also used for vegetative propagation of stem and leaf cuttings. In plant rooting practice it is used alone or as a mixture along with IBA.

### 1.2 Auxin metabolism

Plants have complex biochemical mechanisms to control IAA levels and this has been attributed to a critical role of this regulation for plant growth and development (Normanly et al., 2005). These mechanisms include biosynthesis, conjugation, transport, and degradation as well as control mechanisms related to biotic or non-biotic stress and even environmental factors such as light and temperature. Active auxins can be produced by *de novo* biosynthesis, by transport to a site for action, by conversion from another form (such as IBA, indole-3-lactic acid or indole-3-ethanol), or by conjugate hydrolysis (Normanly et al., 2005).

#### 1.2.1 Auxin conjugation

Most auxins are present in conjugated forms in plants (reviewed by Slovin et al., 1999; Cohen and Gray, 2006). Several auxin conjugates, including IAA linked to amino acids, sugars, and peptides, have been identified (Bandurski et al., 1995; reviewed in Woodward and Bartel, 2005). These conjugates have been classified into two groups

based on the nature of the bond: ester-linked and amide-linked (Slovin et al., 1999). Auxin conjugates are thought to serve as reservoirs of inactive IAA, as a form for long distance transport of active IAA, or as intermediates in IAA turnover, such as IAA-Asp in *Arabidopsis* (Tuominen et al., 1994; Normanly et al., 2005).

### 1.2.2 Auxin transport

Auxins are present in elevated amounts in young shoot meristems and leaf primordia and these have been postulated as major sources of synthesis. Auxins are involved in nearly every stage of a plant's life cycle, notably those processes resulting in the establishment of growth polarity. Therefore, auxin polar transport plays an essential role in plant growth and development. Polar transport can be studied by isotope labeling, and an effective control can be obtained by applying auxin transport inhibitors, especially N-1-naphthylphthalamic acid (NPA), which clearly defines polar movement as distinct from simple diffusion. Influx carrier proteins or proton co-transporters are involved in auxin uptake from outside into the cell, while efflux carrier proteins that are associated with pin-formed (PIN) proteins transport auxin out of cells (Taiz and Zeiger, 1998).

### 1.2.3 IAA degradation

In general, there appear to be three routes of IAA degradation based on the reaction products. A decarboxylation pathway carried out by most peroxidase enzymes, the so-called 'IAA oxidase', has a long history of study but now appears to have little, if any, role for normal auxin metabolism in intact plants (Normanly et al., 1995). More recently,

the direct ring oxidation route has been described in many species (Normanly et al., 2005). In such pathways, IAA is converted first into oxindole-3-acetic acid (OxIAA) by oxidation, as has been shown in maize endosperm (Reinecke and Bandurski, 1983), and then the subsequent metabolism appears varied across species (reviewed in Normanly et al., 2005), but in maize the OxIAA yields 7-OH-OxIAA-glucoside via the intermediate 7-OH-OxIAA. The third route that has been shown to occur in *Arabidopsis* involves IAA-aspartate oxidation. Free IAA is first conjugated to an amino acid and some of these IAA-amino acid conjugates can produce free IAA by hydrolysis (reviewed in Woodward and Bartel, 2005) and others can enter into a catabolic route via the formation of OxIAA-aspartate or Hexosyl-1-N-IAA-aspartate (Tuominen et al., 1994; Cohen and Gray, 2006). This pathway is especially significant since it provides a direct connection between IAA conjugation and degradation (Cohen and Gray, 2006).

### 1.2.4 Interaction among hormones

Plant hormones include the auxins, but also consist of gibberellins, cytokinins, abscisic acid, ethylene, brassinolides, salicylic acid, jasmonates, and a variety of other identified plant growth regulators. Many of these hormones have also been implicated in regulating auxin levels in plants (for example, JA; Sun et al. 2009) and, in some cases, auxin alters the levels of these hormones as well (for example, GA; Ngo et al., 2002; Desgagné-Penix et al., 2005; Desgagné-Penix and Sponsel, 2008).

Both GA and IAA control stem elongation in plants. Not only does IAA increase GA biosynthesis by increasing the expression of the gene encoding GA 20-oxidase (van

Huizen et al. 1997; Ross et al. 2001), but GA also promotes IAA biosynthesis (Davies, 2005) and, similarly, a known molecular response to 4-Cl-IAA in pea is to regulate GA biosynthesis through altered expression of GA 20-oxidase (Ozga and Reinecke, 2003).

Although auxin biosynthesis has been ascribed as mainly originating in young shoot organs, it also plays an essential role in root growth and development as well as in shoot and root vascular differentiation (Shininger, 1979; Cooke et al., 2002; Cheng et al., 2006). The main location of cytokinin synthesis has been ascribed to the root tip, specifically the root cap cells (Jacobs, 1952; Letham, 1994; Aloni et al., 2004). Auxins appear to function in some cases to regulate the biosynthesis of cytokinins (Nordström et al., 2004). It is less clear, however, if cytokinins can function to increase or decrease auxin levels because such studies have been done in plants by overexpressing a microbial isopentenyltransferase (*IPT*) gene (Bourquin and Pilet, 1990; Eklöf et al., 2000) and the biochemical phenotypes are complex. One thing that appears well established is that the ratio of auxins to cytokinins is crucial for the regulation of root tropism, apical dominance, and the differentiation of plant tissues (see Nordström et al., 2004).

Abscisic acid (ABA) is involved in senescence, stress responses, seed dormancy, and seed germination. It has been shown that in senescing flowers of *Cucumis melo*, ABA induces the conversion of free IAA to esterified IAA (Dunlap and Robacker, 1990), but how this might impact physiological processes regulated by ABA remains unclear. While brassinolides have been long known to work synergistically with auxins to promote cell expansion and cell elongation (Nemhauser et al., 2004), their effects on

auxin metabolism are not well established (Cohen and Meudt, 1983; Khripach et al., 1999).

Jasmonic acid (or jasmonate, JA) has been shown to have important roles in regulating different aspects of plant development and defense. We have shown, in an international collaborative study (Appendix 1) that JA treatment can increase free IAA levels in 12 day seedlings of *Arabidopsis* (Sun et al., 2009). In this case, we used the mutant *jdl1-1*, a loss-of-function T-DNA line with the insert in the *ANTHRANILATE SYNTHASE α1* (*ASA1*) gene. Anthranilate synthase is the rate-limiting enzyme for the production of all indolic compounds including tryptophan, the amino acid precursor for several pathways proposed for auxin biosynthesis. The mutant line showed reduced numbers of lateral roots, a phenotype that is potentially due to the much lower auxin level in the mutant as compared to the wild type (WT) (Appendix 1; Sun, et al., 2009). These findings are consistent with the hypothesis that JA activates the transcriptional expression of *ASA1* and perhaps other auxin biosynthetic genes as well, which would be expected to result in increased rates of auxin biosynthesis. At the same time, JA was shown to negatively effect local auxin distribution in roots. The combination of effects should be expected to result in the observed promotion of lateral root formation (Appendix 1; Sun, et al., 2009).

### 1.2.5 Environmental factors and others

Many environmental factors including light, temperature, biological and physical stress, and wounding appear to modify auxins and other aspects of indolic metabolism

(Tao et al., 2008; Gray et al. 1998; Rapparini et al., 2002; O'Donnell et al., 2003; Sztein et al., 2002). Wounding can induce altered auxin biosynthesis (Sztein et al., 2002), where tryptophan dependent IAA biosynthesis is enhanced. Consistent with this observation, CYP79B2, a cytochrome P450, is wounding inducible and can catalyze the conversion of tryptophan to indole-3-acetaldoxime, an intermediate of one of the proposed tryptophan-dependent auxin biosynthesis pathways (Mikkelsen et al., 2000).

Gray et al. (1998) observed that 7-day-old seedlings have longer hypocotyls following treatment for 2 days at 29°C compared with those grown at 22°C and we have confirmed this finding (S. Ye, unpublished). While we did not observe an increase in IAA levels in the aerial parts of *Arabidopsis* seedling, Gray et al. (1998) found increased IAA levels for hypocotyls under high temperature. The reason for this difference may be explained by the fact that the hypocotyl accounts for just a small percentage of the total of the aerial parts. Rapparini et al. (2002) found that *Lemna gibba*, when planted at 30°C, has a normal growth rate and normal IAA levels; however, when the temperature decreases to below 15°C, the plants have a reduced rate of growth and elevated IAA levels. When labeled with [$^{2}H_{5}$]tryptophan and [$^{15}$N]anthranilic acid, Rapparini et al. (2002) found that the tryptophan-independent pathway was the major route for IAA biosynthesis under moderate temperatures and, when plants were grown under low temperature, the tryptophan dependent pathway was then more active and was the predominate route for IAA biosynthesis.

**1.3 Auxin biosynthesis**

Due in part to the multiple developmental and growth regulating roles auxins serve in plants, the mechanisms for their biosynthesis and its regulation have remained of considerable interest for more than sixty years. IAA biosynthesis has often been described as being associated with rapidly dividing tissue, such as shoots, young leaves, and developing fruits, based primarily on the fact that these tissues have high steady-state levels of auxins (Taiz and Zeiger, 1998). Many different pathways and the possibility of plants using multiple pathways for IAA biosynthesis have been proposed (Normanly et al., 1995). IAA is generally regarded as a derivative of tryptophan due to the structural similarity of the two compounds and the fact that two sequential oxidations are sufficient to convert the amino acid to the auxin. *De novo* synthesis is regarded as the conversion of a non-aromatic precursor to indole and then to IAA. IAA has been shown to be produced either *in vivo* or *in vitro* in many studies using either various labeled intermediates as well as in unlabeled precursor studies. Since studies with tryptophan auxotrophic mutants plant lines in the early 1990's (Wright et al., 1991; Normanly et al., 1993), IAA biosynthesis pathways have been grouped into two classes: tryptophan-dependent pathways and one or more tryptophan-independent pathways (Figure 1.3). However, no specific auxin biosynthesis pathways in plants have, so far, been fully elucidated.

### 1.3.1 Tryptophan dependent pathways

In plants, the tryptophan-dependent pathways have at least four proposed routes: the indole-3-pyruvic acid (or indole pyruvate, IPA) pathway, the tryptamine (TAM) pathway,

the indole-3-acetamide (IAM) pathway, and the indole-3-acetonitrile (IAN) pathway. In many cases multiple routes using these defining intermediates have been proposed and in some cases there are overlapping reactions that are in common with more than one pathway.

#### 1.3.1.1 The IAN pathway

The IAN pathway has been proposed to proceed from tryptophan to IAA via indole-3-acetaldoxime (IAOx) and indole-3-acetonitrile (IAN). The conversion of tryptophan to IAOx can be catalyzed by two cytochrome P450s, CYP79B2 and CYP79B3 from *Arabidopsis* (Mikkelsen et al., 2000; Sugawara et al., 2009), and the conversion from IAOx to IAN has been detected by isotopic tracer analysis of plasma membrane preparations from Chinese cabbage (Ludwig-Müller and Hilgenberg, 1990). IAOx could be an important metabolic branch point since it is also a precursor of indole glucosinolates, a series of secondary metabolites which are plant defense compounds that accumulate in members of the *Brassicaceae* and may be important for human health. Overexpression of CY79B2 in *Arabidopsis* showed elevated levels of indolic glucosinates, IAN, and IAA conjugates (reviewed in Bartel et al., 2001), whereas the biosynthesis of IAOx was nullified in *CYP79B* mutants (Sugawara et al., 2009). These results seem to add additional support for the idea that plants regulate IAA levels in part through regulation of conjugation. IAN can be hydrolyzed by nitrilase (nitrile aminohydrolase, NIT, EC 3.5.5.1) directly to IAA or via a two-step pathway where IAN is converted to indole-3-acetamide by nitrile hydratase, and subsequently an amidase

converts indole-3-acetamide into IAA, as has been found in microbes (Kobayashi et al., 1992). There are four differentially expressed nitrilase genes (NIT1-4) in *Arabidopsis thaliana* and three of the four genes are tandemly located together on chromosome III (Bartel and Fink, 1994). It has been demonstrated that IAN has auxin-like effects through its hydrolysis to IAA, and this hydrolysis can be achieved *in vivo* by NITl or NIT2 (Normanly, et al., 1997). However, the role of NIT3 or NIT4 is unknown. L-tryptophan and the glucosinolate glucobrassicin can be precursors for IAN in the *Brassicaseae* (Mahadevan, 1963). Schmidt et al. (1996) observed that an auxin overproduction phenotype resulted from increased auxin levels after treatment of *Arabidopsis* and transgenic tobacco with IAN. Also, endogenous IAN has been detected in *Arabidopsis* (Normanly et al., 1995). This adds evidence to support a potential role for the IAN pathway contributing to IAA biosynthesis. Evidence for the IAN pathway has been found primarily in the *Cruciferae*, *Graminae*, and *Musaceae* (Thimann and Mahadevan, 1964); therefore, the IAN pathway, if functional, may not be wide spread (Normanly et al., 1995).

#### 1.3.1.2 The TAM pathway

TAM is present as a native compound in tomato (Cooney and Nonhebel, 1989), as well as many other plant species. TAM was tentatively identified as an auxin precursor due to its auxin effect on the elongation of coleoptiles and pattern of its labeling and that of IAA in $^{2}H_2O$ labeling experiments (reviewed in Bartel et al., 2001). Tryptophan can be converted to TAM by decarboxylation, and TAM can then be further metabolized to

indole acetaldehyde (IAAld) or IAA in the TAM pathway. TAM can also be converted into N-hydroxyl-tryptamine, as has been proposed for YUCCA, a gene encoding a flavin monooxygenase (FMO)-like enzyme (Zhao et al., 2001). Overexpressing YUCCA plants showed a high auxin phenotype although *yucca*, a single gene mutant, did not reveal a change in its endogenous IAA levels (Zhao et al., 2001). Surprisingly, even triple or quadruple *yucca* mutants did not show decreased auxin levels (Culler, 2007). This phenomenon may be explained in part by the complexity contributed to the analysis of the pathway because YUCCA is a multiple gene family in *Arabidopsis*. Although YUCCA-like genes have been identified in other species (Yamamoto et al., 2007; Gallavotti et al., 2008), an experiment using a transgene approach with the tryptophan decarboxylase (TDC) gene from *Catharanthus roseus* to elevate TAM levels in tobacco did not result in an accumulation of IAA (Songstad et al., 1990). These findings may suggest that YUCCA is one of the rate limiting enzyme steps in the TAM pathway or that the process in tobacco is different (Bartel et al., 2001). It would be helpful to see the effect of TDC in plants known to use the YUCCA pathway as well as in plants over or under expressing specific YUCCA genes. It also may be surmised from the evidence to date that some plants may not have this pathway (Normanly et al., 1995; reviewed in Bartel et al., 2001). Mainly because of the lack of detectable TAM in some species, the TAM pathway has for many years been considered as one that is not a universal pathway of auxin biosynthesis.

#### 1.3.1.3 The IAM pathway

The IAM pathway, also tryptophan-dependent, had long been thought to exist only in bacteria. The formation of IAA from tryptophan is attributed to the sequential action of two enzymes, tryptophan 2-monooxygenase (*IaaM* gene) and indoleacetamide hydrolase (*IaaH* genes; Patten and Glick, 1996). IAM has recently been identified as a natural compound in *Arabidopsis* (Pollmann et al., 2002). A putative amidohydrolase gene (*AMI1*) was described from *Arabidopsis*, and *in vitro* assays show that IAM can be converted into IAA by the AMI1 protein (Pollmann et al., 2003). These reports suggest IAM is a possible pathway in plants as well, although conformation that the pathway is fully operative in plants remains for future studies to determine.

#### 1.3.1.4 The IPA pathway

The IPA pathway has often been proposed as the main auxin biosynthesis pathway (Costacurta and Vanderleyden, 1995; Taiz and Zeiger, 1998) and has a long history in studies of auxin biosynthesis (Dannenburg and Liverman, 1957). It has been proposed that tryptophan is converted into IPA by a tryptophan transaminase (or transferase), followed by either spontaneous or, more likely, enzymatic decarboxylation to IAAld, which is further oxidized by an indole-3-acetaldehyde oxidase to IAA. IPA has been identified as a native compound in tomato and *Arabidopsis* (Cooney and Nonhebel, 1991; Tam and Normanly, 1998). TAA1 (Tryptophan aminotransferase of *Arabidopsis*, EC 2.6.1.27) can potentially be a control point for the formation of IPA from L-tryptophan (Tao et al., 2008; Stepanova et al., 2008). Under simulated foliar shade conditions (low red to far-red ratios), plants have longer hypocotyls, and the longer hypocotyl has been

ascribed to increased auxin levels (Tao et al., 2008). However, contrary to these previous reports, I have shown that under simulated foliar shade treatment (reduced red/far-red light conditions) that the increase in IAA levels is short-lived and does not appear to persist throughout the period of enhanced growth (unpublished data). The final step in this pathway has been proposed to be catalyzed by the acetaldehyde oxidase (AAO1) protein. It was observed, for example, that AAO1 had increased activity in *superroot1* (*sur1*), an auxin over-producing mutant (Seo et al., 1998). Indole-3-pyruvic acid decarboxylase (IPDC) is the key enzyme in the IPA pathway in several microbes (Costacurta et al., 1994) where this has been studied. The second step, a rate-limiting step in microbes, is the formation of IAAld from IPA by IPDC. However, a gene(s) encoding this enzyme has not been identified in plants. Through sequence analysis, including motif identification, it has been shown that there are a few decarboxylases that could be candidates for an IPDC in *Arabidopsis*. Identifying this gene or gene family is critical to confirming this pathway, or even to clarifying the relationships among the whole array of enzymes involved in proposed auxin biosynthetic pathways.

### 1.3.2 Tryptophan independent pathway

Using stable isotope labeling methods, Baldi et al. (1991) observed that [$^{15}$N]-D-tryptophan could not be converted into IAA while even [$^{15}$N]-L-tryptophan was converted at only very low rates in *Lemna gibba*. They showed that this rate was too low to account for the expected needs for the growing plants and suggested another route not using tryptophan must be present. Endogenous tryptophan was also shown in subsequent

studies to be converted into IAA at lower rates than exogenous tryptophan (Rapparini et al., 1999; Cohen and Gray, 2006). Therefore, the primary contribution of the tryptophan dependent pathways in auxin biosynthesis has been critically challenged. Tryptophan independent pathways have now been found in several plant species. Indole is converted into tryptophan by tryptophan synthase β (encoded by the gene *TRP-2*). Free IAA levels did not change in the tryptophan synthase β defective *Arabidopsis* mutant *trp2-1*; however, the levels of amide-linked and ester-linked IAA increased dramatically and, in *trp2-1* plants grown in the presence of $^{15}$N-antranilate, IAA was more enriched in $^{15}$N than was tryptophan (Normanly et al., 1993). The orange pericarp mutant (*orp*) in maize is a double mutant line that lacks functional tryptophan synthase β genes; tryptophan, therefore, cannot be synthesized from indole in this line and the plants survive for only about 20 days post-germination (Wright and Neuffer, 1989). However, the level of total IAA was found to be significantly increased in *orp*; mutant seedlings grown on media containing stable isotope labeled precursors resulted in IAA more enriched than was tryptophan and no incorporation of label into IAA from tryptophan could be detected (Wright et al., 1991). In addition, an *in vitro* system showed that seedlings of normal maize and *orp* maize could convert [$^{14}$C]indole to IAA; however, the system did not convert [$^{14}$C]tryptophan to [$^{14}$C]IAA (Östin et al., 1999). Therefore, [$^{14}$C]indole must be converted into [$^{14}$C]IAA via a pathway independent of the formation of a tryptophan intermediate. These results reveal that indole and/or indole-3-glycerol phosphate (IGP) may be used as precursors in the tryptophan-independent pathway(s) (Ouyang et al. 2001). A pathway from indole does not rule out the potential that IGP or indole may be

converted first to an indolic precursor, such as IAOx or to IPA, and then be subsequently metabolized via an IAN-like or IPA-like pathway. Such a scenario might define a simplified mechanism to account for the observations that different developmental stages, tissues, and environmental conditions have been shown to affect which pathways, tryptophan-independent and tryptophan-dependent, are used predominately (Michalczuk et al., 1992; Koshiba et al., 1995; Sztein et al., 2002; Epstein et al., 2002; Rapparini et al., 2002) and, in an evolutionary context, that the tryptophan-independent pathway and tryptophan dependent routes seem to have both been present in plants through out the entire green plant lineage (Sztein et al. 2000). Possibly because of this redundancy, or because of the need for some IAA production to have a viable plant, no mutant that has completely lost the ability to produce IAA has been identified in plants. The above observations further highlight the complexity that continues to obscure the individual roles of the multiple auxin biosynthesis pathways (Patten and Glick, 1996).

### 1.3.3 Protein-linked system

As discussed above, there are tryptophan-dependent and tryptophan-independent pathways that have been proposed to be involved in auxin biosynthesis. Both classes of pathways appear to produce auxin by one or a few intermediates. In maize endosperm, none of these intermediates were able to be identified as being involved in auxin biosynthesis. Interestingly, a novel pathway without low molecular weight intermediates has been proposed recently in maize endosperm (Culler, 2007). A small protein of 8-16 kDa covalently binds to tryptophan and then, while bound to the protein, tryptophan is

converted into IAA. Based on LC-MS-MS analysis of candidate proteins, this protein probably is a phytosulfokine precursor that contains two cysteines which are capable of being linked to tryptophan (Culler, 2007). This particular pathway is still under active study and it will be very interesting to identify this peptide via *in vivo* and *in vitro* assays and explore its importance in maize and possibly in other plant species as well.

### 1.3.4 Other auxins

Many compounds with structures that suggest they could be metabolites with a potential role in auxin biosynthesis, such as IBA, indole-3-lactic acid **(**ILA), and indole-3-ethanol (or indoleethanol, IEt, also called tryptophol, TOL), have been identified as endogenous metabolites with auxin activity, likely by conversion to IAA, when fed to higher plants.

#### 1.3.4.1 IBA

IBA is found as a native compound in many plants (Epstein et al., 1989; Epstein and Ludwig-Müller, 1993; reviewed in Bartel et al., 2001**).** IBA has been widely used for induction of adventitious roots in horticulture though its role as an endogenous plant growth regulator is largely unknown. The difference between IBA and IAA is that the IBA side chain has two more carbons than IAA and these may be added and removed in a biochemical pathway similar to the mechanism of fatty biosynthesis in the peroxisome. Free IBA has been proposed to be much more stable than IAA *in vivo* and, like IAA, can be inactivated by conjugation. Many studies indicate that the IBA peroxisomal β-

oxidation could be another source of providing free IAA, making the formation of IBA a reserve or storage form, although the activity of IBA as an auxin in its own right has not been ruled out (reviewed in Bartel et al., 2001).

#### 1.3.4.2 IEt

IEt is a naturally occurring indole derivative in cucumber (*Cucumis sativus* L.) seedlings (Rayle and Purves, 1967) and other plants (Magnus et al., 1973; Lacan et al., 1985; Sandberg et al., 2006). The enzyme indole-3-ethanol oxidase was purified and identified from cucumber seedlings by using a $^{14}$C-substrate labeling procedure. This enzyme was shown to be capable of catalyzing the oxidation of IEt to IAAld and a similar activity was also reported from bean (Vickery and Purves, 1972; Zhu and Scott, 1995). The reverse reaction, from IAAld to IEt can also occur, in the presence of NADH (reduced form of nicotinamide adenine dinucleotide), by a specific alcohol dehydrogenase. The quantitative measurement of IAAld, the product of the reaction controlled by this oxidase, was established in these early studies only by using the colorimetric Salkowski reagent (Vickery and Purves, 1972). The physiological effects of IEt have been attributed to its conversion to IAA (Rayle and Purves, 1967).

#### 1.3.4.3 ILA

ILA is thought to be a good candidate for an auxin analogue due to the structural similarity of the two compounds (Sprunck et al., 1995). ILA is a by-product of IPA reduction by lactate dehydrogenase in the presence of NADH (Trinchant and Rigaud,

1974). Several products including IAA, IAAld, IEt, and tryptophan were identified when ILA was used as a precursor (Rigaud, 1970). ILA is found as a natural compound in low amounts in plants. However, this intermediate has primarily been studied in several microbes. ILA is a weak IAA analogue, but its specific physiological role in *Pisum sativum* L., where it was identified, is unknown. Biochemical analysis showed ILA does not, like the synthetic auxin analogue NAA, exhibit a high affinity to $ABP_{44}$, an auxin-binding protein (Sprunck et al., 1995), but the physiological role for this binding protein remains obscure so that the significance of this difference in binding cannot be assessed.

**1.4 Thiamine biosynthesis**

Free thiamin or thiamine, also known as vitamin $B_1$, is a water soluble vitamin which is an essential molecule for all living organisms. Its chemical structure contains a pyrimidine ring and a thiazole ring (Figure 1.4). Thiamine naturally occurs as free thiamine and as four phosphorylated derivatives: thiamine monophosphate (TMP or ThMP), thiamine pyrophosphate (TPP) or thiamine diphosphate (ThDP), thiamine triphosphate (TTP or ThTP), and adenosine thiamine triphosphate (ATTP or AThTP; Figure 1.4). In addition, several thiamine disulfide derivatives, analogs including thiamine tetrahydrofurfuryl disulfide (TTFD) and thiamine propyldisulfide (TPD), have been identified as a group of 'fat-soluble thiamines' which are more stable and have increased efficacy for thiamine activity than does free thiamine (Pincus et al., 1973).

TPP, also known as *cocarboxylase*, is a major biologically active derivative of thiamine. TPP is synthesized from free thiamine and adenosine triphosphate (ATP) by

thiamine pyrophosphokinase, which requires magnesium or other divalent cations as a cofactor. TPP is a prosthetic group or cofactor in many important enzymes that catalyze the decarboxylation of alpha-keto acids.

TTP is found in many organisms including bacteria, fungi, animals, and plants (Makarchikov et al., 2003). In *E. coli*, TTP is induced transiently by hypoxia, and it may be involved in the response to amino acid starvation (Lakaye et al., 2004; Bettendorff et al., 2007). It also has been observed that TTP specifically phosphorylates histidyl residues on rapsyn, a protein essential for the clustering of nicotinic receptors, in the electric organ of *Torpedo marmorata* (Nghiêm et al., 2000). The histidyl phosphorylation in two-component kinase systems is a major regulatory scheme in prokaryotes; whereas, signal transduction pathways in eukaryotes are mainly through specific phosphorylation at Ser, Thr or Tyr residues (West and Stock, 2001). In this way, TTP could be involved in potential signaling pathways. Although complete details of all TTP functions remain elusive, plants appear to have retained the capacity for its synthesis. TTP has been found, for example, in very low amounts in bean (*Phaseolus vulgaris*) and sphagnum (*Sphagnum palustre*). In *Arabidopsis thaliana*, TTP was detected only after the plants were removed from the soil and at the onset of wilting, suggesting a response to environmental stress (Makarchikov et al., 2003).

ATTP or thiaminylated adenosine triphosphate (TATP) has recently been detected in bacteria, yeast, animals, and higher plants (Bettendorff et al., 2007). ATTP, the first discovered adenine nucleotide containing vitamin B1, may serve as a precursor to TPP

and as a more stable 'storage' form for TTP when carbon is available (Jordan, 2007). In *E. coli*, the accumulation of ATTP is induced in the absence of any carbon source whereas ATTP decreases and TTP increases when glucose is provided (Bettendorff et al., 2007). Based on these results, it has been postulated that ATTP may be involved as part of the response to carbon starvation and may serve as a signal instead of as an enzyme cofactor (Bettendorff et al., 2007).

### 1.4.1 Thiamine biosynthetic pathways

Thiamine *de novo* biosynthesis is only found in most microorganisms and higher plants (Nosaka, 2006). TPP, a product of thiamine metabolism, is a cofactor for a specific family of enzyme proteins that includes the known pyruvate decarboxylase (PDC, EC 4.1.1.1) and IPDC enzymes. Though animals can synthesize thiamine phosphorylated esters, their only source of free thiamine is dietary. TMP is formed by thiamine phosphate synthase (TPS) by condensation of two substituted compounds: 4-methyl-5-(2-hydroxyethyl)thiazole phosphate (HET-P) and 4-amino-5-hydroxymethyl-2-methylpyrimidine diphosphate (HMP-PP; Figure 1.5). The two compounds are synthesized in separate branches of the thiamine biosynthetic pathway.

So far, two pathways for HET-P biosynthesis have been indentified (reviewed in Roje, 2007). In bacteria, the thiazole moiety (HET-P) is formed from three different substrates: 1-deoxy-D-xylulose-5-phosphate, cysteine, and glycine or tyrosine (reviewed in Settembre et al, 2003). It has been postulated that plants may use $NAD^+$ (nicotinamide adenine dinucleotide) to form HET-P via a pathway similar to that in yeast (Chatterjee et

al., 2007). Thi4, a thiazole synthase, controls the biosynthesis of the thiamine thiazole in *S. cerevisiae* (Chatterjee et al., 2006). Thi4 has been shown to bind tightly to an ADP-containing intermediate derived from $NAD^+$ and may form HET-P from cysteine, glycine, and $NAD^+$ (reviewed in Roje, 2007). The homologs of the yeast thiazole (HET-P) synthase (THI4) have been identified in *Zea mays*, *Arabidopsis thaliana*, and *Oryza sativa* (Belanger et al., 1995; Machado et al., 1996; Wang et al., 2006). The gene that encodes HET-P synthase has been cloned in *Zea mays* and *Arabidopsis thaliana*, and the distribution of GUS expression suggests this gene may be localized to the plastids and/or mitochondria (Belanger et al., 1995; Chabregas et al., 2001).

There are two HMP-PP biosynthetic pathways that have been identified. In bacteria, HMP-PP is synthesized from 5-aminoimidazole ribonucleotide (AIR; reviewed in Settembre et al., 2003). The formation of HMP-PP from AIR is attributed to the sequential action of three enzymes: ThiC, ThiD and an unidentified enzyme. The conversion of AIR to 4-amino-5-hydroxymethyl-2-methylpyrimidine phosphate (HMP-P) is catalyzed by ThiC together with an unidentified protein in *E. coli* (Lawhorn et al., 2004b). The next step is the phosphorylation of HMP-P to HMP-PP by ThiD (or HMP-P kinase; Lawhorn et al., 2004a). The findings from numerous studies have supported the concept that plants apparently synthesize HMP-PP via the bacterial pathway. For example, the first *BTHI* gene cloned from plants (*Brassica napus*) involved in thiamine biosynthesis encodes a bifunctional 4-amino-5-hydroxymethyl-2-methylpyrimidine monophosphate kinase (HMP-P kinase)/thiamine-phosphate pyrophosphorylase **(**TMP-PPase; Kim et al., 1998). Additionally, the homologs of bacterial ThiC have been

identified in many plant species including *Arabidopsis* (reviewed in Roje, 2007). However, in yeast, pyridoxal 5′-phosphate (PLP) and L-histidine are thought to be the precursors for the pyrimidine unit of thiamine (Nosaka, 2006).

Thiamine is hydrolyzed from TMP by a phosphatase, an enzyme that releases a phosphate group from its monoester substrate and forms a free hydroxyl group (Figure 1.5). In *E. coli*, ATTP is synthesized from TPP and ADP or ATP by a thiamine diphosphate adenylyl transferase (Makarchikov et al., 2007). Though TTP and ATTP have been detected in higher plants, genes involving their biosynthesis have not been identified.

As mentioned above, the concentration of the TPP cofactor regulates PDC enzymes, which are involved in fermentation and many stress responses. In addition, thiamine phosphate esters, including TTP and ATTP, may act as metabolic signals. These observations suggest it is very important to maintain TPP levels by regulating the flux through its biosynthetic pathway. Consistent with this suggestion, exogenous thiamine severely represses the expression level of many genes involved in thiamine biosynthesis (Miranda-Rios et al., 2001; Croft et al., 2007). The expression of several genes involved in thiamine biosynthesis is regulated by riboswitches, short sequence mRNAs that bind a small target metabolite and undergo a conformational change. The metabolite-bound riboswitches then affect the expression of the operon or gene(s) encoding the target metabolite at the level of transcription and/or translation (Mandal et al., 2003).

Riboswitches are widespread in bacteria. TPP riboswitches also have been found in fungi, algae, and higher plants (Cheah et al., 2007; Croft et al., 2007; Thore et al., 2006). A TPP riboswitch, for example, has been identified in the 3'-UTR (untranslated region) in *Arabidopsis thaliana* (Sudarsan et al., 2003). A riboswitch consensus motif has been identified in both rice and bluegrass for a protein homologous to the bacterial ThiC protein, an enzyme that catalyzes the formation of HMP-P from AIR (Sudarsan et al., 2003).

### 1.4.2 TPP - dependent enzymes

As briefly discussed above, TPP and $Mg^{2+}$ are required for the activity of the enzymes of TPP-dependent family in microbes. Free $Mg^{2+}$ can potentiate the catalytic activity of TPP dependent enzymes (Koga et al., 1992). The amino acids of the catalytic center of PDC and $Mg^{2+}$ binding sites are highly conserved in all species (Hawkins et al., 1989; Dyda et al., 1993). TPP-dependent enzymes include pyruvate dehydrogenase (PDH), 2-ketoglutarate dehydrogenase (KGDH), transketolase, PDC, IPDC, and acetohydroxy acid synthase (AHAS, EC 2.2.1.6, also known as acetolactate synthase, ALS; reviewed in Hohmann and Meacock, 1998). Most PDC-like enzymes including PDC, IPDC, and AHAS are homotetramers. TPP-dependent enzymes share a conserved pyrophosphate domain and a pyrimidine domain, and TPP is tightly bound to the interface of both domains (Todd et al., 2001; Costelloe et al., 2008). Both ends of TPP, the pyrophosphate group and the aminopyrimide group, associate with the pyrophosphate domain and pyrimidine domain, respectively, of different subunits, thus forming tight dimers or tetramers (Dyda et al., 1993; Costelloe et al., 2008). These domains might have

evolved from a common ancestor (Todd et al., 2001). Based on domain architecture, all TPP-dependent enzymes have been grouped into three classes: sulfopyruvate decarboxylase (SPDC) and phosphopyruvate decarboxylase (PPDC), PDC-like enzymes, and TKC (transketolase C-terminal domain)-containing enzymes (Costelloe, et al., 2008). A third or central domain, the transhydrogenase dIII (TH3)-domain exists only in all PDC-like enzymes, which include PDC, IPDC, phenylpyruvate decarboxylase (PhPDC), pyruvate oxidase (PO), AHAS, glyoxylate carboligase (GXC), benzaldehyde lyase (BAL), oxalyl CoA decarboxylase (OCADC), and benzoylformate decarboxylase (BFDC; Costelloe et al., 2008). Pyrophosphate, TH3, and pyrimidine domains in PDC-like enzymes also are called α, β, and γ domains, respectively. Although the order of TPP-binding domains varies and they may be located on the same or different subunits, their structure is highly conserved (Muller et al., 1993). IPDCs and PhPDCs form mixed clades close to PDCs, suggesting they might catalyze some common reactions, which is consistent with the observation that PDC/IPDC enzymes are bi-functional in microbes (Koga, 1995).

#### 1.4.2.1 Bacterial IPDC homologs in *Arabidopsis*

Many rhizosphere microbes synthesize IAA. The microbial IAA biosynthetic pathways have been well-studied and therefore offer a range of genomic information about the enzymes involved in IAA biosynthesis (Patten and Glick, 1996; Normanly et al., 2005). The post-genome-sequence era allows a shift from single-gene research to whole-system global analysis of gene expression, metabolite and protein dynamics,

molecular interaction, and comparative genomics. New technologies such as proteomics and metabolomics will be helpful to find gene functions, and sequence analysis is useful for discovering structural, functional, and evolutionary information about genes. Sequences that are alike or similar may have similar biological functions, similar biochemical functions, and similar three-dimensional structures. The amino acid sequence of IPDC from bacteria (*Enterobacter cloacae*) has an extensive similarity (36%) to that of PDC from yeast (Koga et al., 1991b). Sequence analysis of *Arabidopsis*, including motif identification, has shown a few candidate orthologs of *E. cloacae* IPDC. These *Arabidopsis* genes consist of four *PDC/IPDC* genes, one *PDC*-like gene, and one *AHAS* gene. The following sections will discuss the particular characteristics of PDC, IPDC, and AHAS enzymes.

#### 1.4.2.2 PDC enzymes

Pyruvate is a key metabolite at the branch point between anaerobic and aerobic respiratory pathways. Pyruvate can be converted into lactate or ethanol under anaerobic conditions for anaerobic metabolism. PDC converts, by decarboxylation, pyruvate into acetaldehyde, and then alcohol dehydrogenase (ADH, EC 1.1.1.1) reduces acetaldehyde into ethanol. Many *PDC* genes in several microbial and plant species have been cloned and identified, and some PDC enzymes have been partially purified and characterized. *PDC* is encoded by a gene family of at least six members (Flikweert, 1999). Based on their function, *PDC* genes have been classified into two groups: structural genes and regulatory genes. It has been suggested that *Saccharomyces* has an elaborated mechanism

to regulate PDC activity (Schaaff, et al., 1989). Due to its essential role in oxygen related stresses including flooding, PDC has been investigated in reference species as well as crop plants, including maize, pea, barley, and rice. The molecular weight of this enzyme was found in plants to be about 240 kDa, consisting of 4 subunits. The optimal pH of PDC enzymes is in the range of 6.0 - 6.5 at 30°C in most plants studied to date.

**1.4.2.3 IPDC enzymes**

IPA has been identified as a native compound of tomato, mung bean, and *Arabidopsis* (Cooney and Nonhebel, 1991; Tam and Normanly, 1998). The IPA pathway, a proposed main auxin biosynthetic pathway, remains to be demonstrated in plants (Costacura and Vanderleyden, 1995; Patten and Glick, 1996; Taiz and Zeiger, 1998). The second step, a rate-limiting step in microbes, is the formation of IAAld from IPA by IPDC. While IPDC is a key enzyme in the IPA pathway in microbes (Costacura et al., 1994), a gene(s) encoding this enzyme has so far not been identified in plants. In the bacterium *Pseudomonas fluorescens*, tryptophan is also converted to IAAld directly by a side chain oxidase (Narumiya et al., 1979) obviating the need for an IPDC activity.

In *E. cloacae*, IPDC has two forms; an inactive monomer and an active homotetramer with a molecular weight of 240 KDa (Koga et al., 1991a). The active form of this enzyme requires cofactors of $Mg^{2+}$ and TPP. Hohmann and Meacock (1998) found that TPP could be produced *de novo* in plants and in several microorganisms. In *S. cerevisiae*, the single copy gene *thi80* encodes thiamine pyrophosphokinase (TPP kinase), which catalyzes the final step of TPP anabolism. Mutation of this gene (*thi80-1*) resulted

in a 25% decrease in the activity of TPP-kinase (Nishimura et al., 1991). In *Arabidopsis*, there are two genes, At1g02880 and At2g44750, which were annotated as TPP-like genes. Surprisingly, Hohmann and Meacock (1998) also found that *thi3,* one of the positive regulators of TPP biosynthesis in *S. cerevisiae,* had a striking similarity (52% identity) to PDC. This seems like an interesting system where the enzyme regulating the synthesis of a cofactor shares similarity to the enzyme that requires the cofactor. Clearly, TPP biosynthesis and its role in the IPA pathway in plants still have much that needs to be determined.

The microbial PDC/IPDC enzymes can use both pyruvate and IPA as substrates; however, they have different affinities and specificities for these substrates (Koga, 1995). Boiteux and Hess (1970) observed that PDC from *Saccharomyces cerevisiae* has low specificity and affinity for pyruvic acid ($K_m$ = 1.3 mM) and can only slowly catalyze the decarboxylation of IPA ($K_m$ = 15 mM). IPDC from *E. cloacae* has higher affinity and specificity for IPA ($K_m$ = 0.015 mM) than for pyruvic acid ($K_m$ = 2.5 mM; Koga et al., 1992). These results indicated that IPDC potentially has a specific role in regulating IAA biosynthesis in *E. cloacae*.

As the free acid, IPA is very unstable and degrades over time to IAA and other compounds. Thus, special precautions and proper controls are required for measurement of enzymes that act on this substrate. IPDC catalyzes the decarboxylation of IPA to form IAAld and ILA. IAAld and ILA are interconvertable by IAAld reductase and ILA oxidase (or IEt oxidase) respectively (Bartel, 1997). Traditionally, IPDC activity was

best assayed by measuring the amount of IAAld and IEt produced using HPLC to fractionate the reaction products on a $C_{18}$ reverse phase column (Koga et al., 1991a). Due to the potential instability of the substrate this assay was not without concerns, and it was important, for example, to do careful analysis of zero time controls using parallel sample preparations. Product identity can be confirmed either using LC-MS-MS or by derivatization and GC-MS, as described previously (Tam and Normanly, 1998).

#### 1.4.2.4 AHAS enzyme

This enzyme, also known as ALS in the literature, catalyzes the first step in *de novo* synthesis of the branched-chain amino acids including valine, leucine, and isoleucine. The products of this step are 2-acetolactate (AL) from a single substrate (pyruvate) or 2-aceto-2-hydroxybutyrate (AHB) from substrates pyruvate and 2-ketobutyrate. AHAS apparently is present in fungi, bacteria, and plants (Falco et al., 1985; Chipman et al., 1998; reviewed in Duggleby et al, 2008). The AHAS gene has been identified in many higher plants including *Arabidopsis*, corn, soybean, and wheat (Chang and Duggleby, 1997; reviewed in Green et al., 2008). In higher plants, AHAS is a nuclear encoded enzyme but is localized in the plastid by way of a transit peptide. Though *ILVBL* (also called ilvB, or bacterial acetolactate synthase-like), a homolog of *AHAS*, is present in humans, the pathway of *de novo* synthesis of the branched-chain amino acids does not exist in humans and other animals (Joutel et al., 1996).

Besides using TPP and divalent metal ions such as $Mg^{2+}$ as cofactors, AHAS can also bind flavin adenine dinucleotide (FAD) and serves as a cofactor in some biochemical

reactions. AHAS is present in most of the sequenced genomes and AHAS has three isoenzymes in *E. coli* (reviewed in Duggleby et al, 2008). The AHAS enzyme is a heterotetramer of two large and two small subunits. The large subunit (about 65 kDa) is catalytic, and the small subunit is regulatory and has a much more diverse range of molecular weights, between 9 and 54 kDa (Hill et al., 1997; Chipman et al., 2005). The regulatory domain of *E. coli* AHAS isoenzyme III is a homo-dimer and the monomer is 18.1 kDa (Dugglegy et al., 2008). The regulatory subunit modifies the AHAS activity of the catalytic subunit, for example by binding branched-chain amino acids which act as negative feedback regulators (Mendel et al., 2001). AHAS I, which is only regulated by cAMP and the ‘‘catabolite repression system,’’ has unique catalytic and regulatory properties (Vinogradov et al., 2006) where the catalytic subunit alone has 10–20% of the holoenzyme’s catalytic activity while the isolated catalytic subunit of AHAS III has only 3–5% of the holoenzyme’s activity. *E. coli* isoenzyme I and III are negatively regulated by valine in the reconstituted system while isoenzyme II is intrinsically insensitive to valine (Hill et al., 1997; Lee and Duggleby, 2001). AHAS III is a ‘‘typical’’ bacterial AHAS and has a somewhat larger regulatory subunit (Vinogradov et al., 2006).

The eukaryotic AHAS have been less well studied. In plants, both subunits are synthesized from larger precursors containing an N-terminal transit peptide, which is removed after the protein is localized into the plastids. In *Arabidopsis*, the catalytic subunit is a homo-tetramer and each monomer consists of three domains (α, β, and γ) and a C-terminal tail (McCourt et al., 2006). When either the fungal or plant AHAS catalytic subunit is expressed in *E. coli*, it is not regulated by branched-chain amino acids, whereas

AHAS extracted from eukaryotes is sensitive to one or more of branched-chain amino acids (Singh et al., 1992). Recently, the regulatory subunit of *Arabidopsis thaliana* AHAS was identified and its *in vitro* reconstitution showed that the AHAS enzyme was inhibited by all three branched-chain amino acids (Lee and Duggleby, 2001).

### 1.4.3 AHAS-inhibiting herbicides

Since all branched-chain amino acids are essential and play an important role in protein synthesis and as metabolic precursors, any unique enzymes required for synthesis of any of the three branched-chain amino acids could potentially be a target for development of specific herbicides. Inhibiting those enzymes may result in the decreased level of one or more branched-chain amino acids, thus interfering with protein synthesis. Indeed, AHAS, threonine deaminase (TD, EC 4.3.1.19), ketol-acid reductoisomerase (KARI, EC 1.1.1.86), and dihydroxyacid dehydratase (DHAD, EC 4.2.1.9) inhibition has lead to a group of herbicides inhibiting production of branched-chain amino acids (reviewed in McCourt and Duggleby, 2006). Herbicides inhibiting plant AHAS enzymes, the first common enzyme of the branched-chain amino acids biosynthetic pathway, are called AHAS-inhibiting herbicides. The inactivation of the AHAS enzyme leads to a shortage of branched-chain amino acids, which eventually results in inhibition of DNA synthesis as well. The first AHAS-inhibiting herbicides were discovered by George Levitt of DuPont in 1975 (Shaner and O'Connor, 1991; Stetter, 1994; Green, 2007). There are five different chemical classes of AHAS herbicides or inhibitors: sulfonylureas (SUs), imidazolinones (IMIs), triazolopyrimidines (TPs), pyrimidinyl

oxybenzoates (POBs), and sulfonylamino carbonyl triazolinones (SCTs; reviewed in Green et al., 2008). Among these, SUs and IMIs are the most popular commercial herbicides in the world. These herbicides are also some of the safest; not only does AHAS not exist in humans and other animals, but also they are highly active at controlling a wide spectrum of grasses and dicots. In addition, a mutated AHAS gene can be used as a selectable marker. For example, a mutated AHAS gene from rice has been used in wheat transformation (Ogawa et al., 2008). Therefore, AHAS and the herbicides have attracted considerable interest from many scientists, with most of the focus being upon the interaction between AHAS enzymes and herbicides and identification of mutant alleles that are resistant to herbicides (Chipman et al., 2005).

It has been demonstrated by 3D structural analysis of the target enzymes that sulfonylureas and imidazolinones share some overlapping binding sites on AHAS in *Arabidopsis* (McCourt et al., 2006). When herbicides bind to those target sites, AHAS activity is inhibited. AHAS displays quite diverse affinities to different target herbicides. For example, the $K_i$ of AHAS in *Arabidopsis* for imazaquin (IQ, a member of the IMI family) and chlorimuron ethyl (CE, a member of the SU family) is 3.0 μM and 10.8 nM, respectively (McCourt et al., 2006).

It is possible that over-expression of the rate-limiting enzyme, a target for a particular herbicide, can result in herbicide resistance. However, this mechanism has not been identified for AHAS-inhibiting herbicides (Chang and Duggleby, 1998). Indeed, there are three mechanisms of AHAS-inhibiting herbicide resistance in plants: resistance

due to change in enzyme structure, metabolic detoxification or degradation, and prevention of the herbicide from reaching the target site (Sherman, et al., 1996). Many crops are naturally resistant to some specific AHAS-inhibiting herbicides due to the ability to rapidly degrade the herbicides (Chang and Duggleby, 1997). Mutations that result in a still functional AHAS enzyme, but with somewhat decreased enzymatic activity in the presence of herbicides, yield an herbicide resistant phenotype. Based on studies to date, this would appear to be clearly a major route for acquiring herbicide resistance (Chang and Duggleby, 1998). There is also evidence that higher plants can be modified to have increased herbicide resistance by over-expression of mutant AHAS genes (Harms, et al., 1992; Tourneur, et al., 1993). A single plant species can have different types of AHAS-inhibiting resistances due to the numbers of possible different mutations and their mechanisms (Hattori et al., 1992). Not all mutations result in cross-resistance to all AHAS-inhibiting herbicides (Anderson and Georgeson, 1989). In *Arabidopsis*, herbicide resistance is induced by one or more substitutions at six conserved amino acid residues, Ala122, Pro197, Ala205, Trp574, Ser653 and Asp376 of the AHAS gene product (Tranel and Wright, 2002; Whaley, et al., 2007; Yu et al., 2008). These mutations can result in three kinds of grouped phenotypes: broad cross-resistance to SUs, IMIs, TPs and PTBs; resistance to IMIs and PTBs only; and resistance to SUs and TPs only (Green et al., 2008). Weeds frequently gain natural resistance predominantly by mutating the gene encoding AHAS, as contrasted to metabolic degradation mechanisms, and in this way form what has been referred to as “superweeds” (Sherman et al., 1996; Green et al., 2008). Recent studies have addressed the public concern about

"superweeds" resulting from the prevalence of AHAS-resistance. Since many instances of AHAS resistance do not cause any perceptible reduction in fitness (Green et al., 2008), there have been at least 97 weed species that have been reported to have such resistance to AHAS-inhibiting herbicides (Heap, 2009).

## 1.5 Conclusion

Auxin biosynthesis consists of several potential routes of *de novo* synthesis, and IAA can be also obtained by IBA β-oxidation and the hydrolysis of some conjugates. It is difficult to study phenotypes that might result from defects in a single gene or single pathway due to the apparent redundant methods of IAA production, though recent advances in technologies have broadened our understanding of auxin biosynthesis mechanisms. Findings support a working hypothesis that a tryptophan-independent pathway is the major pathway to produce IAA under normal conditions, while tryptophan-dependent pathways are active and may predominate for IAA biosynthesis under special developmental needs or under different stress conditions.

The IPA pathway has long been proposed as a main tryptophan-dependent auxin biosynthetic pathway. Identifying an IPDC gene is a critical test of the hypothesis concerning the possible function of this pathway in plants, or even to clarify the relationships among the whole array of enzymes involved in proposed auxin biosynthetic pathways. Herein I report cloning each of these candidate IPDC genes, I have obtained a set of T-DNA insertion lines, and I have produced overexpression lines for each of these genes. In this study I have also developed an analytically precise enzyme assay for IPDC activity and used it to check IPDC activity of all the proteins encoded by these candidate genes over-expressed in *E. coli*. I also analyzed the overexpression lines and plants expressing a bacterial bifuctional PDC/IPDC enzyme.

## 1.6 References


Aloni, R. (1995) The induction of vascular tissue by auxin and cytokinin. In Plant Hormones and Their Role in Plant Growth Development, 2nd ed., P.J. Davies, ed., Kluwer, Dordrecht, Netherlands, pp. 531–546

Aloni, R., Langhans, M., Aloni, E. and Ullrich C.I. (2004) Role of cytokinin in the regulation of root gravitropism. Planta 220(1): 177–182

Anderson, P.C. and Georgeson, M. (1989) Herbicide-tolerant mutants of corn. Genome 31(2): 994–999

Bandurski, R.S., Cohen, J.D. and Slovin, J.P. (1995) Auxin biosynthesis and metabolism. In: Plant Hormones: Physiology, Biochemistry and Molecular Biology. P.J. Davies, ed. Kluwer Academic Publ., Dordrecht, pp. 35–57

Baldi, B.G., Maher, B.R., Slovin, J.P. and Cohen, J.D. (1991) Stable isotope labeling, *in vivo*, of d- and l-tryptophan pools in *Lemna gibba* and the low incorporation of label into indole-3-acetic acid Plant Physiology 95(4): 1203–1208

Bartel, B. (1997) Auxin biosynthesis. Annual Review of Plant Physiology and Plant Molecular Biology 48: 51–66

Bartel, B. and Fink, G.R. (1994) Differential regulation of an auxin-producing nitrilase gene family in *Arabidopsis thaliana*. Proc. Natl. Acad. Sci. USA 91: 6649–6653

Bartel, B., LeClere, S., Magidin, M. and Zolman, B.K. (2001) Inputs to the active indole-3-acetic acid pool: *de novo* synthesis, conjugate hydrolysis, and indole-3-butyric acid β-oxidation. Journal of Plant Growth Regulation 20: 198–216.

Belanger, F.C., Leustek, T., Chu, B. and Kriz, A.L. (1995) Evidence for the thiamine biosynthetic pathway in higher-plant plastids and its developmental regulation. Plant Mol. Biol. 29: 809–821

Bettendorff, L., Wirtzfeld, B., Makarchikov, A.F., Mazzucchelli, G., Frédérich, M., Gigliobianco, T., Gangolf, M., De Pauw, E., Angenot, L. and Wins, P. (2007) Discovery of a natural thiamine adenine nucleotide. Nature Chemical Biology 3: 211–212

Boiteux, A. and Hess, B. (1970) Allosteric properties of yeast pyruvate decarboxylase. FEBS Letter 9: 293–296

Bourquin, M. and Pilet, P.E. (1990) Effect of zeatin on the growth and indolyl-3-acetic acid and abscisic acid levels in maize roots. Physiologia Plantarum 80: 342–349

Chabregas, S.M., Luche, D.D., Farias, L.P., Ribeiro, A.F., van Sluys, M.A., Menck, C.F.M. and Silva-Filho, M.C. (2001) Dual targeting properties of the N-terminal signal

sequence of *Arabidopsis thaliana* THI1 protein to mitochondria and chloroplasts. Plant Mol. Biol. 46: 639–650

Chang, A.K. and Duggleby, R.G. (1997) Expression, purification and characterization of *Arabidopsis thaliana* acetohydroxyacid synthase. Biochem. J. 327: 161–169

Chang, A.K. and Duggleby, R.G. (1998) Herbicide-resistant forms of *Arabidopsis thaliana* acetohydroxyacid synthase: characterization of the catalytic properties and sensitivity to inhibitors of four defined mutants. Biochem. J. 333: 765–777

Chatterjee, A., Jurgenson, C.T., Schroeder, F.C., Ealick, S.E. and Begley, T.P. (2006) Thiamin biosynthesis in eukaryotes: characterization of the enzyme-bound product of thiazole synthase from *Saccharomyces cerevisiae* and its implications in thiazole biosynthesis. Journal of the American Chemical Society 128: 7158–7159

Chatterjee, A., Jurgenson, C.T., Schroeder, F.C., Ealick, S.E. and Begley, T.P. (2007) Biosynthesis of thiamin thiazole in eukaryotes: conversion of NAD to an advanced intermediate. Journal of the American Chemical Society 129: 2914–2922

Cheah, M.T., Wachter, A., Sudarsan, N. and Breaker, R.R. (2007) Control of alternative RNA splicing and gene expression by eukaryotic riboswitches. Nature 447: 497–500

Cheng, Y., Dai, X. and Zhao, Y. (2006) Auxin biosynthesis by the YUCCA flavin monooxygenases controls the formation of floral organs and vascular tissues in *Arabidopsis*. Genes and Dev. 20: 1790–1799

Chipman, D.M., Barak, Z. and Schloss, J.V. (1998) Biosynthesis of 2-aceto-2-hydroxy acids: acetolactate synthases and acetohydroxyacid synthases. Biochim Biophys Acta 1385: 401–419

Chipman, D.M, Duggleby, R.G. and Tittmann, K. (2005) Mechanisms of acetohydroxyacid synthases. Current Opinion in Chemical Biology 9: 475–481

Ciesielski, T. (1872) Untersuchungen uber die Abwartskrummung der Wurzel. Beitraege zur Biologie der Pflanzen 1: 1–17

Cohen, J.D. and Gray, W.M. (2006) Auxin metabolism and signaling. In: Plant Hormone Signaling (Annual Plant Reviews, Vol. 24). Hedden, P., Thomas, S. (eds), Blackwell Publishing, Oxford, pp. 37–66

Cohen, J.D. and Meudt W.J. (1983) Investigations on the mechanism of the brassinosteroid response. I. Indole-3-acetic acid metabolism and transport. Plant Physiol. 72: 691-694

Cooke, T.J., Poli, D.B., Sztein, A.E. and Cohen, J.D. (2002) Evolutionary patterns in auxin action. Plant Mol. Biol. 49: 319-338

Cooney, T.P. and Nonhebel, H.M. (1989) The measurement and mass spectral identification of indole-3-pyruvate from tomato shoots. Biochem. Biophys. Res. Commun. 162: 761–766

Cooney, T.P. and Nonhebel, H.M. (1991) Biosynthesis of indole-3-acetic acid in tomato shoots: measurement, mass spectral identification and incorporation of $^{2}H$ from $^{2}H_2O$ into indole-3-acetic acid, D- and L-tryptophan, indole-3-pyruvate and tryptamine. Planta 184: 368–376

Costacurta, A., Keijers, V. and Vanderleyden, J. (1994) Molecular cloning and sequence analysis of an *Azospirillum brasilense* indole-3-pyruvate decarboxylase gene. Mol. Gen. Genet. 243: 463–472

Costacurta, A. and Vanderleylden, J. (1995) Synthesis of phytohormones by plant-associated bacteria. Crit. Rev. Microbiol. 21: 1–18

Costelloe, S.J., Ward, J.M. and Dalby, P.A. (2008) Evolutionary analysis of the TPP-dependent enzyme family. J. Mol. Evol. 66: 36–49

Croft, M.T., Moulin, M., Webb, M.E. and Smith, A.G. (2007) Thiamine biosynthesis in algae is regulated by riboswitches. Proc. Natl. Acad. Sci. USA 104: 20770–20775

Culler, A.H. (2007) Analysis of the tryptophan-dependent indole-3-acetic acid biosynthesis pathway in maize endosperm. PH.D. thesis, University of Minnesota, Twin Cities.

Dannenburg, W.N. and Liverman, J.L. (1957) Conversion of tryptophan-2-C14 to indoleacetic acid by watermelon tissue slices. Plant Physiology 32: 263–269

Davies, P. (2005) Regulatory factors in hormone action: level, location and signal transduction. In: Plant Hormones: Biosynthesis, Signal Transduction, Action! (3rd edition). Davies, P.J. ed. Kluwer Academic Publ., Dordrecht, pp. 16–35

Desgagné-Penix, I., Eakanunkul, S., Coles, J.P., Phillips, A.L., Hedden, P. and Sponsel, V.M. (2005) The auxin transport inhibitor response 3 (*tir3*) allele of BIG and auxin transport inhibitors affect the gibberellin status of *Arabidopsis*. Plant J. 41: 231–242

Desgagné-Penix, I. and Sponsel, V.M. (2008) Expression of *gibberellin 20-oxidase1* (*AtGA20ox1*) in *Arabidopsis* seedlings with altered auxin status is regulated at multiple levels. J. Experimental Botany 59: 2057-2070

Duggleby, R.G., McCourt, J.A. and Guddat, L.W. (2008) Structure and mechanism of inhibition of plant acetohydroxyacid synthase. Plant Physiology and Biochemistry 46: 309–324

Dunlap, J.R. and Robacker, K.M. (1990) Abscisic acid alters the metabolism of indole-3-acetic acid in senescing flowers of *Cucumis melo* L. Plant Physiology 94: 870–874

Dyda, F., Furey, W., Swaminathan, S., Sax, M., Farrenkopf, B. and Jordan, F. (1993) Catalytic centers in the thiamin diphosphate dependent enzyme pyruvate decarboxylase at 2.4-Å resolution. Biochemistry 32: 6165–6170

Eklöf, S., Astot, C., Sitbon, F., Moritz, T., Olsson, O. and Sandberg, G. (2000) Transgenic tobacco plants co-expressing *Agrobacterium* iaa and ipt genes have wild-type hormone levels but display both auxin- and cytokinin-overproducing phenotypes. Plant Journal 23: 279–284

Engvild, K.C. (1996) Herbicidal activity of 4-chloroindoleacetic acid and other auxins on pea, barley and mustard. Physiologia Plantarum 96: 333–337

Epstein, E., Chen, K-H. and Cohen, J.D. (1989) Identification of indole-3-butyric acid as an endogenous constituent of maize kernels and leaves. Plant Growth Regulation 8: 215–223

Epstein, E., Cohen, J.D. and Slovin, J.P. (2002) The biosynthetic pathway for indole-3-acetic acid changes during tomato fruit development. Plant Growth Regulation 38: 15–20

Epstein, E. and Lavee, S. (1984) Conversion of indole-3-butyric acid to indole-3-acetic acid by cuttings of grapevine (*Vitus vinifera*) and olive (*Olea europa*). Plant Cell Physiol. 25: 697–703

Epstein, E. and Ludwig-Müller, J. (1993) Indole-3-butyric acid in plants: occurrence, synthesis, metabolism and transport. Physiologia Plantarum 88: 382–389

Falco, S.C., Dumas, K.S. and Livak, K.J. (1985) Nucleotide sequence of the yeast *ILV2* gene which encodes acetolactate synthase. Nucleic Acids Res. 13: 4011–4027

Flikweert, M.T. (1999) Physiological roles of pyruvate decarboxylase in *Saccharomyces cerevisiae*. PhD thesis, Delft University of Technology, Delft.

Gallavotti, A., Barazesh, S., Malcomber, S., Hall, D., Jackson D., Schmidt, R.J. and McSteen, P. (2008) *Sparse inflorescence1* encodes a monocot-specific *YUCCA*-like gene required for vegetative and reproductive development in maize. Proc. Natl. Acad. Sci. USA 105(39): 15196–15201

Gray, W.M., Ostin, A., Sandberg, G., Romano, C.P. and Estelle, M. (1998) High temperature promotes auxin-mediated hypocotyl elongation in *Arabidopsis*. Proc. Natl. Acad. Sci. USA 95: 7197–7202

Green, J.M. (2007) Review of glyphosate and ALS-Inhibiting herbicide crop resistance and resistant weed management. Weed Technology 21: 547–558

Green, J.M., Hazel, C.B., Forney, D.R. and Pugh, L.M. (2008) New multiple-herbicide crop resistance and formulation technology to augment the utility of glyphosate. Pest Manag. Sci. 64: 332–339

Harms, C.T., Armour, S.L., DiMaio, J.J., Middlesteadt, L.A., Murray, D., Negrotto, D.V., Thompson-Taylor, H., Weymann, K., Montoya, A.L., Shillito, R.D. and Jen, G.C. (1992) Herbicide resistance due to amplification of a mutant acetohydroxyacid synthase gene. Mol. Gen. Genet. 233: 427–435

Hattori, J., Rutledge, R., Labbé, H., Brown, D., Sunohara, G. and Miki, B. (1992) Multiple resistance to sulfonylureas and imidazolinones conferred by an acetohydroxyacid synthase gene with separate mutations for selective resistance. Mol. Gen. Genet. 232: 167–173

Hawkins, C.F., Borges, A. and Perham, R.N. (1989) A common structural motif in thiamin pyrophosphate-binding enzymes. FEBS Letter 255: 77–82

Heap, I. The international survey of herbicide resistant weeds. February 06, 2009. [Online available at http://www.weedscience.org/summary/MOASummary.asp]

Hill, C.M., Pang, S.S. and Duggleby, R.G. (1997) Purification of *Escherichia coli* acetohydroxyacid synthase isoenzyme II and reconstitution of active enzyme from its individual pure subunits. Biochem J. 327: 891–898

Hohmann, S. and Meacock, P.A. (1998) Thiamin metabolism and thiamin diphosphate-dependent enzymes in the yeast *Saccharomyces cerevisiae*: genetic regulation. Biochim. Biophys. Acta 1385: 201–219

Jacobs, W.P. (1952) The role of auxin in differentiation of xylem around a wound. American Journal of Botany 39: 301–309

Jordan, F. (2007) Adenosine triphosphate and thiamine cross paths. Nature Chemical Biology 3: 202–203

Joutel, A., Ducros, A., Alamowitch, S., Cruaud, C., Domenga, V., Maréchal, E., Vahedi, K., Chabriat, H., Bousser, M.G., and Tournier-Lasserve, E. (1996) A human homolog of bacterial acetolactate synthase genes maps within the CADASIL critical region. Genomics 38: 192–198

Khalifah, R.A., Lewis, L.N. and Coggins, C.W. (1963) New natural growth promoting substance in young *Citrus* fruit. Science 142: 399–400

Khripach, V.A., Zhabinskii, V.N. and de Groot, A.E. (1999) Brassinosteriods: a new class of plant hormones. Academic Press, San Diago, CA, pp. 456

Kim, Y.S., Nosaka, K., Downs, D.M., Kwak, J.M., Park, D., Chung, I.K. and Nam, H.G. (1998) A *Brassica* cDNA clone encoding a bifunctional hydroxymethylpyrimidine kinase/thiamin-phosphate pyrophosphorylase involved in thiamin biosynthesis. Plant Mol. Biol. 37: 955–966

Kobayashi, M., Snagasawa, T. and Yamada, H. (1992) Enzymatic synthesis of acrylamide: a success story not yet over. Trends Biotechnology 10: 402–408

Koga, J. (1995) Structure and function of indolepyruvate decarboxylase, a key enzyme in indole-3-acetic acid accumulation. Biochim Biophys Acta 1249: 1–13

Koga, J., Adachi, T. and Hidaka, H. (1991a) Molecular cloning of the gene for indolepyruvate decarboxylase from *Enterobacter cloacae*. Mol. Gen. Genet. 226: 10–16

Koga, J., Adachi, T. and Hidaka, H. (1991b) Molecular cloning of the gene for indolepyruvate decarboxylase, a novel enzyme for indole-3-acetic acid biosynthesis in *Enterobacter cloacae.* Agric. Biol. Chem. 55: 701–706

Koga, J., Adachi, T. and Hidaka, H. (1992) Purification and characterization of indolepyruvate decarboxylase. A novel enzyme for indole-3-acetic acid biosynthesis in *Enterobacter cloacae*. J. Biol. Chem. 267: 15823–15828

Koshiba, T., Kamiya, Y. and Lino, M. (1995) Biosynthesis of indole-3-acetic acid from L-tryptophan in coleoptile tips of maize (*Zea mays* L.). Plant Cell Physiology 36: 1503–1510

Lacan, G., Magnus, V., Simaga, S., Iskric, S. and Hall, P.J. (1985) Metabolism of tryptophol in higher and lower plants. Plant Physiology 78: 447–454

Lakaye, B., Wirtzfeld, B., Wins, P., Grisar, T. and Bettendorff, L. (2004) Thiamine triphosphate, a new signal required for optimal growth of *Escherichia coli* during amino acid starvation. J. Biol. Chem. 279: 17142–17147

Lawhorn, B.G., Gerdes, S.Y. and Begley, T.P. (2004a) A genetic screen for the identification of thiamin metabolic genes. J. Biol. Chem. 279: 43555–43559

Lawhorn, B.G., Mehl, R.A. and Begley, T.P. (2004b) Biosynthesis of the thiamin pyrimidine: the reconstitution of a remarkable rearrangement reaction. Org. Biomol. Chem. 2: 2538–2546

Lee, Y. and Duggleby, R.G. (2001) Identification of the regulatory subunit of *Arabidopsis thaliana* acetohydroxyacid synthase and reconstitution with its catalytic subunit. Biochemistry 40: 6836–6844

Letham, D.S. (1994) Cytokinins as phytohormones – sites of biosynthesis, translocation and function of translocated cytokinin. In: Cytokinins: Chemistry, Activity and Function. Mok D.W.S., Mok M.C., eds. Boca Raton, FL: CRC Press, pp. 57–80

Ludwig-Müller, J. and Cohen, J.D. (2002) Identification and quantification of three active auxins in different tissues of *Tropaeolum majus*. Physiologia Plantarum 115: 320–329

Ludwig-Müller, J. and Hilgenberg, W. (1990) Conversion of indole-3-acetaldoxime to indole-3-acetonitrile by plasma membranes from Chinese cabbage. Physiologia Plantarum 79: 311–318

Macháčkova, I., Chvojka, L., Našinec, V. and Zmrhal, Z. (1981) The effect of phenylacetic acid on ethylene formation in wheat seedlings. Biologia Plantarum 23: 116–119

Machado, C.R., de Oliveira, R.L., Boiteux, S., Praekelt, U.M., Meacock, P.A. and Menck, C.F. (1996) Thi1, a thiamine biosynthetic gene in *Arabidopsis thaliana*, complements bacterial defects in DNA repair. Plant Mol. Biol. 31: 585–593

Magnus, V., Iakric, S., and Kveder, S. (1973) The formation of tryptophol glucoside in the tryptamine metabolism of pea seedlings. Planta 110: 57–62

Mahadevan, S. (1963) Conversion of 3-indoleacetaldoxime to 3-indoleacetonitrile by plants. Archives of Biochemistry 100: 557–558

Makarchikov, A.F., Brans, A. and Bettendorff, L. (2007) Thiamine diphosphate adenylyl transferase from *E. coli*: functional characterization of the enzyme synthesizing adenosine thiamine triphosphate. BMC Biochem. 8: 17–24

Makarchikov, A.F., Lakaye, B., Gulyai, I.E., Czerniecki, J., Coumans, B., Wins, P., Grisar, T. and Bettendorff, L. (2003) Thiamine triphosphate and thiamine triphosphatase activities: from bacteria to mammals. Cell Mol. Life Sci. 60: 1477–1488

Mandal, M., Boese, B., Barrick, J.E., Winkler, W.C. and Breaker, R.R. (2003) Metabolite-sensing riboswitches control fundamental biochemical pathways in bacteria. Cell 113: 577–586

McCourt, J.A. and Duggleby, R.G. (2006) Acetohydroxyacid synthase and its role in the biosynthetic pathway for branched-chain amino acids. Amino Acids 31: 173–210

McCourt, J.A., Pang, S.S., King-Scott, J., Guddat, L.W. and Duggleby R.G. (2006) Herbicide-binding sites revealed in the structure of plant acetohydroxyacid synthase. Proc. Natl. Acad. Sci. USA 103: 569–573

Mendel, S., Elkayam, T., Sella, C., Vinogradov, V., Vyazmensky, M., Chipman, D.M. and Barak, Z. (2001) Acetohydroxyacid synthase: a proposed structure for regulatory subunits supported by evidence from mutagenesis. J. Mol. Biol. 307: 465–477

Michalczuk, L., Ribnicky, D.M., Cooke, T.J. and Cohen J.D. (1992) Regulation of indole-3-acetic acid biosynthetic pathways in carrot cell cultures. Plant Physiology 100: 1346–1353

Mikkelsen, M.D., Hansen, C.H., Wittstock, U. and Halkier, B.A. (2000) Cytochrome P450 CYP79B2 from *Arabidopsis* catalyzes the conversion of tryptophan to indole-3-acetaldoxime, a precursor of indole glucosinolates and indole-3-acetic acid. J. Biol. Chem. 275: 33712–33717

Miranda-Rios, J., Navarro, M. and Soberon, M. (2001) A conserved RNA structure (thi box) is involved in regulation of thiamin biosynthetic gene expression in bacteria. Proc. Natl. Acad. Sci. USA 98: 9736–9741

Muller, Y.A., Lindqvist, Y., Furey, W., Schulz, G.E., Jordan, F. and Schneider, G. (1993) A thiamin diphosphate binding fold revealed by comparison of the crystal structures of transketolase, pyruvate oxidase and pyruvate decarboxylase. Structure 1: 95–103

Narumiya, S., Takai, K., Tokuyama, T., Noda, Y., Ushiro, H. and Hayaishi, O. (1979) A new metabolic pathway of tryptophan initiated by tryptophan side chain oxidase. J. Biol. Chem. 254: 7007–7015

Nemhauser, J.L., Mockler, T.C. and Chory, J. (2004) Interdependency of brassinosteroid and auxin signaling in *Arabidopsis*. PLoS Biol 2(9): e258

Nghiêm, H.O., Bettendorff, L. and Changeux, J.P. (2000) Specific phosphorylation of *Torpedo* 43K rapsyn by endogenous kinase(s) with thiamine triphosphate as the phosphate donor. FASEB J. 14: 543–554

Ngo, P., Ozga, J.A. and Reinecke, D.M. (2002) Specificity of auxin regulation of gibberellin 20-oxidase gene expression in pea pericarp. Plant Molecular Biology 49: 439–448

Nishimura, H., Kawasaki, Y., Nosaka, K., Kanek, Y. and Iwashima, A. (1991) Constitutive thiamine metabolism mutation, *thi80*, causing reduced thiamine pyrophosphokinase activity in *Saccharomyces cerevisiae*. J. Bacteriol. 173: 2716–2719

Nordström, A., Tarkowski, P., Tarkowska D., Norbaek, R., rister Åstot, C., Dolezal, K. and Sandberg, G. (2004) Auxin regulation of cytokinin biosynthesis in *Arabidopsis thaliana*: A factor of potential importance for auxin-cytokinin-regulated development. Proc. Natl. Acad. Sci. USA 101 (21): 8039–8044

Normanly, J., Cohen, J.D. and Fink, G.R. (1993) *Arabidopsis thaliana* auxotrophs reveal a tryptophan-independent biosynthetic pathway for indole-3-acetic acid. Proc. Natl. Acad. Sci. USA 90: 10355–10359

Normanly, J., Grisafi, P., Fink, G.R. and Bartel, B. (1997) Arabidopsis mutants resistant to the auxin effects of indole-3-acetonitrile are defective in the nitrilase encoded by the NIT1 gene. The Plant Cell 9: 1781-1790

Normanly, J., Slovin, J.P. and Cohen, J.D. (1995) Rethinking auxin biosynthesis and metabolism. Plant Physiology 107: 323–329

Normanly, J., Slovin, J.P. and Cohen, J.D. (2005) Auxin biosynthesis and metabolism. In: Plant Hormones: Biosynthesis, Signal Transduction, Action! (3rd edition). P.J. Davies, ed. Kluwer Academic Publ., Dordrecht, pp. 36–62

Nosaka, K. (2006) Recent progress in understanding thiamin biosynthesis and its genetic regulation in *Saccharomyces cerevisiae*. Appl Microbiol Biotechnol. 72: 30–40

O'Donnell, P.J. Schmelz, E.A., Moussatche, P., Lund, S.T., Jones, J.B. and Klee, H.J. (2003) Susceptible to intolerance – a range of hormonal actions in a susceptible *Arabidopsis* pathogen response. Plant Journal 33: 245–257

Ogawa, T., Kawahigashi, H., Toki, S. and Handa, H. (2008) Efficient transformation of wheat by using a mutated rice acetolactate synthase gene as a selectable marker. Plant Cell Rep. 27: 1325–1331

Okada, K., Ueda, J., Komaki, M.K., Bell, C.J. and Shimura, Y. (1991) Requirement of the auxin polar transport system in early stages of *Arabidopsis* floral bud formation. The Plant Cell 3: 677–684

Östin, A., Ilić, N. and Cohen, J.D. (1999) An *in vitro* system from maize seedling for tryptophan-independent indole-3-acetic biosynthesis. Plant physiology 119: 173–178

Ouyang, J., Shao, X. and Li, J. (2001) Indole-3-glycerol phosphate, a branchpoint of indole-3-acetic acid biosynthesis from the tryptophan biosynthetic pathway in *Arabidopsis thaliana*. Plant Journal 24: 327–334

Ozga, J.A. and Reinecke, D.M. (2003) Hormonal interactions in fruit development. Journal of Plant Growth Regulation 22: 73–81

Patten, C.L. and Glick, B.R. (1996) Bacterial biosynthesis of indole-3-acetic acid. Can. J. Microbiol. 42: 207–220

Pincus, J.H., Cooper, J.R., Murphy, J.V., Rabe, E.F., Lonsdale, D. and Dunn, H.G. (1973) Thiamine derivatives in subacute necrotizing encephalomyelopathy. Pediatrics 51: 716–721

Pless, T., Boettger, M., Hedden, P. and Graebe, J. (1984) Occurrence of 4-Cl-indoleacetic acid in broad beans and correlation of its levels with seed development. Plant Physiology 74 (2): 320–323

Pollmann, S., Müller, A., Piotrowski, M. and Weiler, E.W. (2002) Occurrence and formation of indole-3-acetamide in *Arabidopsis thaliana*. Planta 216: 155–161

Pollmann, S., Neu, D. and Weiler, E.W. (2003) Molecular cloning and characterization of an amidase from *Arabidopsis thaliana* capable of converting indole-3-acetamide into the plant growth hormone, indole-3-acetic acid. Phytochemistry 62(3): 293–300

Rigaud, J. (1970) L'acide inolyl-3-lactique et son metabolisme chez Rhizohium. Arch. Mikrobiol. 72: 293–307

Rapparini, F., Cohen, J.D. and Slovin, J.P. (1999) Indole-3-acetic acid biosynthesis in *Lemna gibba* studied using stable isotope labeled anthranilate and tryptophan. Plant Growth Regulation 27: 139–144

Rapparini, F., Tam, Y., Cohen, J.D., and Slovin, J.P. (2002) IAA metabolism in *Lemna gibba* undergoes dynamic changes in response to growth temperature. Plant Physiology 128: 1410–1416

Rayle, D.L. and Cleland, R.E. (1992) The acid growth theory of auxin-induced cell elongation is alive and well. Plant Physiology 99: 1271–1274

Rayle, D.L. and Purves, W.K. (1967) Isolation and identification of indole-3-ethanol (tryptophol) from cucumber seedlings. Plant Physiology 42: 520–524

Reinecke, D.M. (1999) 4-Chloroindole-3-acetic acid and plant growth. Plant Growth Regulation 27: 3–13

Reinecke, D.M. and Bandurski, R.S. (1983) Oxindole-3-acetic acid, an indole-3-acetic acid catabolite in *Zea mays*. Plant Physiology 86: 868–872

Roje, S. (2007) Vitamin B biosynthesis in plants. Phytochemistry 68: 1904–1921

Ross, J.J., O'Neill, D.P., Wolbang, C.M., Symons, G.M. and Reid, J.B. (2001) Auxin-gibberellin interactions and their role in plant growth. Journal of Plant Growth Regulation 20: 336–353

Sandberg, G., Ernstsen, A. and Hamnede, M. (2006) Dynamics of indole-3-acetic acid and indole-3-ethanol during development and germination of *Pinus sylvestris* seeds. Physiologia Plantarum 71: 411–418

Schaaff, I., Green, J.B.A., Gozalbo, D. and Hohmann, S. (1989) A deletion of the PDC1 gene for pyruvate decarboxylase of yeast causes a different phenotype than previously isolated point mutations. Curr. Genet. 15: 75–81

Schmidt, R.C., Müller, A., Hain, R., Bartling, D. and Weiler, E.W. (1996) Transgenic tobacco plants expressing the *Arabidopsis thaliana* nitrilase II enzyme. Plant Journal 9: 683–691

Seo, M., Akaba, S., Oritani, T., Delarue, M., Bellini, C., Caboche, M. and Koshiba, T. (1998) Higher activity of an aldehyde oxidase in the auxin-overproducing superroot1 mutant of *Arabidopsis thaliana*. Plant Physiology 116: 687–693

Settembre, E., Begley, T.P. and Ealick, S.E. (2003) Structural biology of enzymes of the thiamin biosynthesis pathway. Current Opinion in Structural Biology 13: 739–747

Shaner, D.L. and O'Connor, S.L. (1991) The Imidazolinone Herbicides. Boca Raton, FL: CRC., pp. 290

Sherman, T.D., Vaughn, K.C. and Duke, S.O. (1996) Mechanisms of action and resistance to herbicides. In Herbicide-Resistant Crops - Agricultural, Environmental, Economic, Regulatory, and Technical Aspects, Edited by Duke, S.O., Lewis Publishers, Chelsea, MI, pp. 13–35

Singh, B., Szamosi, I., Hand, J.M. and Misra, R. (1992) *Arabidopsis* acetohydroxyacid synthase expressed in *Escherichia coli* is insensitive to the feedback inhibitors. Plant Physiol. 99: 812–816

Shininger, T.L. (1979) The control of vascular development. Annu. Rev. Plant Physiol. 30: 313-337

Slovin, J.P., Bandurski, R.S. and Cohen, J.D. (1999) Auxin, in biochemistry and molecular biology of plant hormones, eds. Hooykaas, P.J.J., Hall, M.A. and Libbenga, K.R. (Elsevier, Amsterdam), pp. 115–140

Songstad, D.D., De Luca, V., Brisson, N., Kurz, W.G.W. and Nessler, C.L. (1990) High levels of tryptamine accumulation in transgenic tobacco expressing tryptophan decarboxylase. Plant Physiology 94: 1410–1413

Sprunck, P., Jacobsen, H.-J. and Reinard, T. (1995) Indole-3-lactic acid is a weak auxin analogue but not an anti-auxin. Journal of Plant Growth Regulation 14: 191–197

Stepanova, A.N., Robertson-Hoyt, J., Yun, J., Benavente, L.M., Xie, D.-Y., Doležal, K., Schlereth, A., Jürgens, G. and Alonso, J.M. (2008). *TAA1*-mediated auxin biosynthesis is essential for hormone crosstalk and plant development. Cell 133: 177–191

Stetter, J. (1994) Herbicides Inhibiting Branched Chain Amino Acid Biosynthesis: Recent Developments. New York: Springer-Verlag, pp. 219

Sudarsan, N., Barrick, J.E. and Breaker, R.R. (2003) Metabolite-binding RNA domains are present in the genes of eukaryotes. RNA 9 (6): 644–647

Sugawara, S., Hishiyama, S., Jikumaru, Y., Hanada, A., Nishimura, T., Koshiba, T., Zhao, Y., Kamiya, Y. and Kasahara, H. (2009) Biochemical analyses of indole-3-acetaldoxime dependent auxin biosynthesis in *Arabidopsis*. Proc. Natl. Acad. Sci. USA 106: 5430–5435

Sun, J., Xu, Y., Ye, S., Jiang, H., Chen, Q., Liu, F., Zhou, W., Chen, R., Li, X., Tietz, O., Wu, X., Cohen, J.D., Palme, K. and Li, C. (2009) Arabidopsis ASA1 is important for jasmonate-mediated regulation of auxin biosynthesis and transport during lateral root formation. Plant Cell 21: 1495–1511

Sztein, A.E., Cohen, J.D. and Cooke, T.J. (2000) Evolutionary patterns in the auxin metabolism of green plants. Int. J. Plant Sci. 161: 849–859

Sztein, A.E., Ilić, N., Cohen J.D. and Cooke T.J. (2002) Indole-3-acetic biosynthesis in isolated axes from germinating bean seeds: the effect of wounding on the biosynthetic pathway. Plant Growth Regulation 36: 201–207

Taiz, L. and Zeiger, E. (1998) Plant Physiology, 2nd ed., Sinauer Associates, Inc., Publishers, Sunderland, Masachusetts, pp. 543–575

Tam, Y.Y. and Normanly, J. (1998) Determination of indole-3-pyruvic acid levels in *Arabidopsis thaliana* by gas chromatography-selected ion monitoring-mass spectrometry. Journal of Chromatography A 800: 101–108

Tao, Y., Ferrer J.-L, Ljung, K., Pojer, F., Hong, F., Long, J.A., Li, L., Moreno, J.E., Bowman, M.E., Ivans, L.J., Cheng Y., Lim, J., Zhao, Y., Balleré, C.L., Sandberg, G., Noel, J.P. and Chory, J. (2008) Rapid synthesis of auxin via a new tryptophan-dependent pathway is required for shade avoidance in plants. Cell 133: 164–176

Thimann, K.V. and Mahadevan, S. (1964) Nitrilase. I. Occurrence, preparation and general properties of the enzyme. Arch. Biochem. Biophys. 105: 133–141

Thimann, K.V. and Skoog, F. (1934) On the inhibition of bud development and other function of growth substance in *Vicia faba*. Proc. R. Soc. Lond (Biol) 114: 317–339

Thore, S., Leibundgut, M. and Ban, N. (2006) Structure of the eukaryotic thiamine pyrophosphate riboswitch with its regulatory ligand. Science 312: 1208–1211

Todd, A.E., Orengo, C.A. and Thornton, J.M. (2001) Evolution of function in protein superfamilies, from a structural perspective. J. Mol. Biol. 307: 1113–1143

Tourneur, C., Jouanin, L. and Vaucheret, H. (1993) Overexpression of acetolactate synthase confers resistance to valine in transformed tobacco. Plant Sci. 88: 159–168

Tranel, P.J. and Wright, T.R. (2002) Resistance of weeds to ALS-inhibiting herbicides: what have we learned? Weed Science 50: 700–712

Trinchant, J.-C. and Rigaud, J. (1974) Lactate dehydrogenase from *Rhizobium*. Purification and role in indole metabolism. Physiologia Plantarum 32: 394–399

Tuominen, H., Östin, A., Sandberg, G. and Sundberg, B. (1994) A novel metabolic pathway for indole-3-acetic acid in apical shoots of *Populus tremula* (L.) X *Populus tremuloides* (Michx.). Plant Physiology 106: 1511–1520

van Huizen, R., Ozga, J.A. and reinecke, D.M. (1997) Seed and hormonal regulation of gibberellin 20-oxidase expression in pea pericarp. Plant Physiology 115: 123–128

Vickery, L.E. and Purves, W.K. (1972) Isolation of indole-3-ethanol oxidase from cucumber seedlings. Plant Physiology 49: 716–721

Vinogradov, V., Vyazmensky, M., Engel, S., Belenky, I., Kaplun, A., Kryukov, O., Barak, Z. and Chipman D.M. (2006) Acetohydroxyacid synthase isozyme I from *Escherichia coli* has unique catalytic and regulatory properties. Biochimica et Biophysica Acta (BBA) - General Subjects 1760 (3): 356–363

Wang, G., Ding, X., Yuan, M., Qiu, D., Li, X., Xu, C. and Wang, S. (2006) Dual function of rice OsDR8 gene in disease resistance and thiamine accumulation. Plant Mol. Biol. 60: 437–449

West, A.H. and Stock, A.M. (2001) Histidine kinases and response regulator proteins in two-component signaling systems. Trends Biochem. Sci. 26: 369–376

Whaley, C.M., Wilson, H.P. and Westwood, J.H. (2007) A new mutation in plant ALS confers resistance to five classes of ALS-inhibiting herbicides. Weed Science 55: 83–90

Woodward, A.W. and Bartel, B. (2005) Auxin: regulation, action, and interaction. Annals of Botany 95: 707–735

Wright, A.D. and Neuffer, M.G. (1989) Organge pericarp in maize: filial expression in a maternal tissue. Journal of Heredity 80(3): 229–233

Wright, A.D., Sampson, M.B., Neuffer, M.G., Michalczuk, L., Slovin, J.P. and Cohen, J.D. (1991) Indole-3-acetic acid biosynthesis in the mutant maize orange pericarp, a tryptophan auxotroph. Science 254: 998–1000

Yamamoto, Y., Kamiya, N., Morinaka, Y., Matsuoka, M. and Sazuka, T. (2007) Auxin biosynthesis by the *YUCCA* genes in rice. Plant Physiology 143(3): 1362–1371

Yang, T., Law, D.M. and Davies, P.J. (1993) Magnitude and kinetics of stem elongation induced by exogenous indole-3-acetic acid in intact light-grown pea seedlings. Plant Physiology 102: 717–724

Yu, Q., Han, H. and Powles, S.B. (2008) Mutations of the ALS gene endowing resistance to ALS-inhibiting herbicides in *Lolium rigidum* populations. Pest Manag. Sci. 64: 1229–1236

Zhao, Y., Christensen, S.K., Fankhauser, C., Cashman, J.R., Cohen, J.D., Weigel, D. and Chory, J. (2001) A role for flavin monooxygenase-like enzymes in auxin biosynthesis. Science 291: 306–309

Zhu, J.S. and Scott, G.K. (1995) Purification, characterization and developmental expression of indole-3-ethanol oxidase from seeds of *Phaseolus vulgaris*. Biochemistry and molecular biology international 35: 423–432

**1.7 Figures**

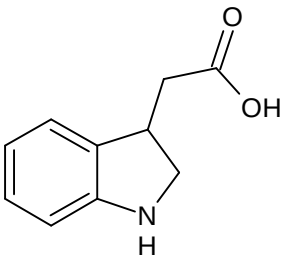


Indole-3-acetic acid (IAA)

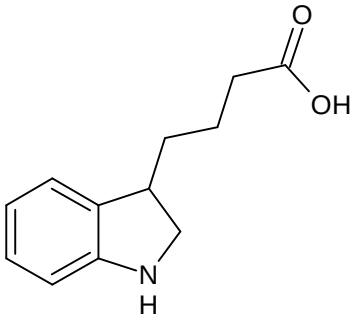


Indole-3-butyric acid (IBA)

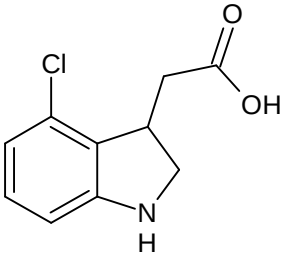


4-Chloroindole-3-acetic acid (4-Cl-IAA)

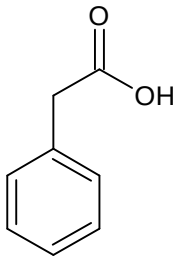


Phenylacetic acid (PAA)

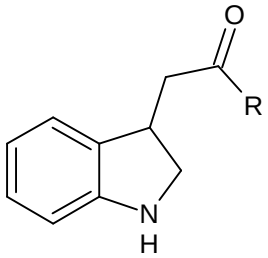


IAA conjugates

Figure 1.1 The chemical structures of naturally occurring auxins in plants. Naturally occurring auxins include free acids such as indole-3-acetic acid (IAA), indole-3-butyric acid (IBA), phenylacetic acid (PAA), 4-chloroindole-3-acetic acid (4-Cl-IAA), and IAA conjugates in which IAA is conjugated to a sugar, amino acid, or peptide. R can be a sugar, amino acid, or peptide.

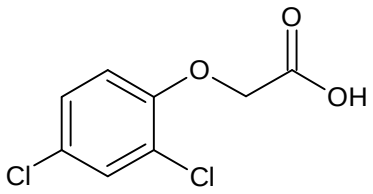


2,4-Dichlorophenoxyacetic acid (2,4-D)

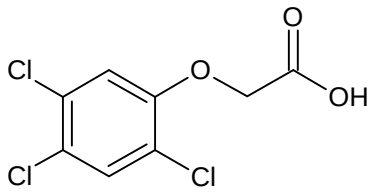


2,4,5-Trichlorophenoxyacetic acid (2,4,5-T)

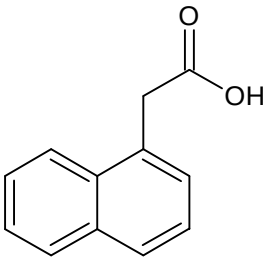


α-Naphthalene acetic acid (NAA)

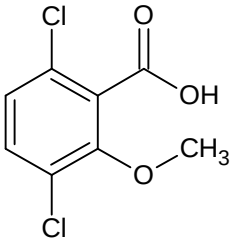


2-Methoxy-3,6-dichlorobenzoic acid (Dicamba)

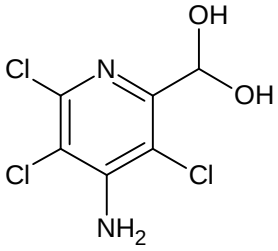


4-Amino-3,5,6-trichloropicolinic acid (Tordon or picloram)

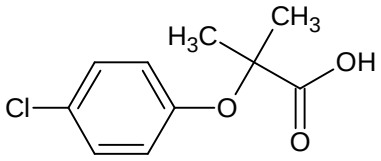


α-(p-Chlorophenoxy)isobutyric acid (PCIB, an antiauxin)

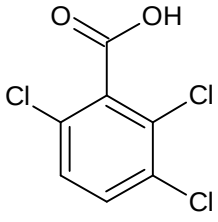


2,3,6-Trichlorobenzoic acid

Figure 1.2 The chemical structures of some synthetic auxins. Most of these synthetic auxins are used as herbicides in agriculture. 2,4-D and NAA are used in tissue culture.

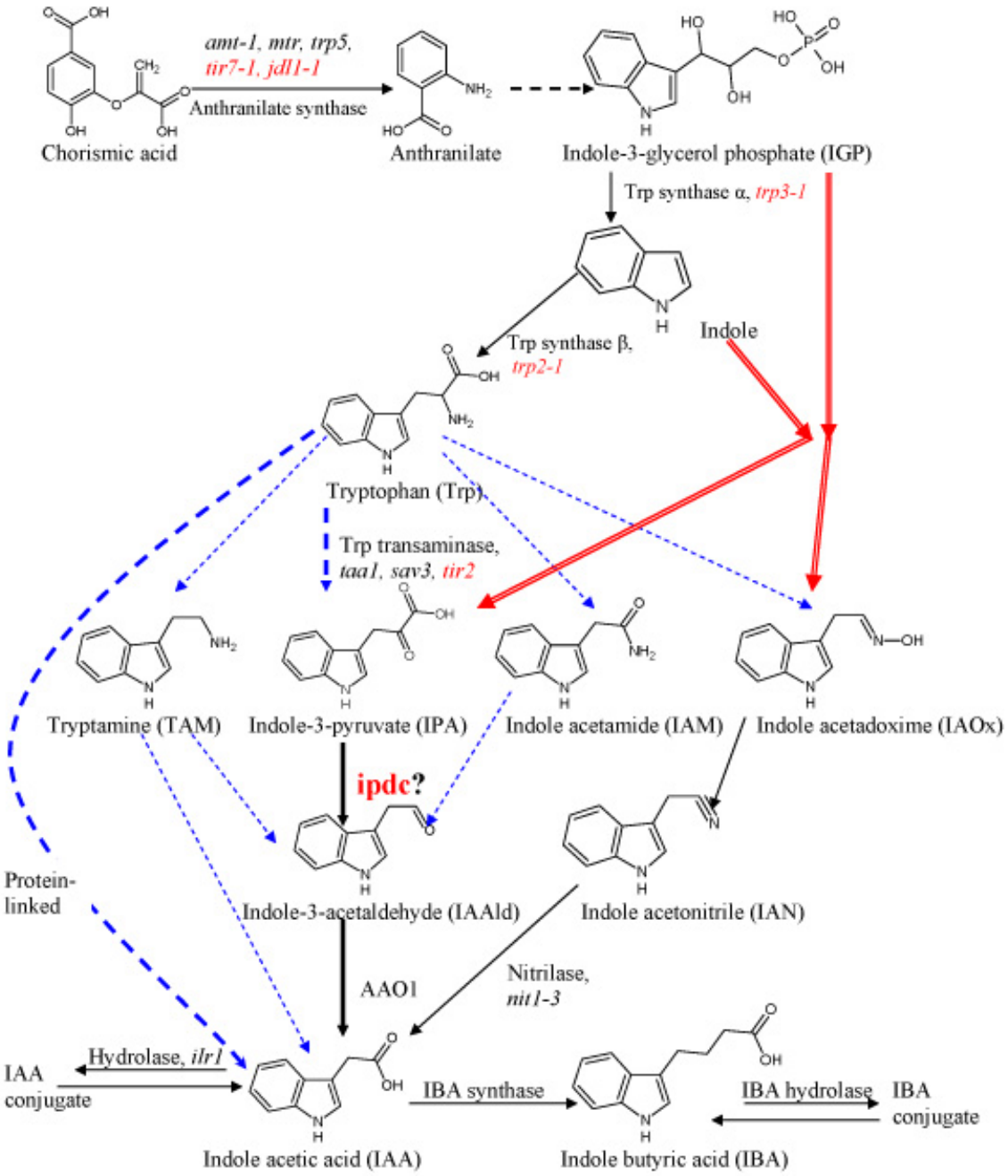


Figure 1.3 Multiple pathways of auxin biosynthesis (after Bartel, 1997). Red arrows indicate specific tryptophan independent pathways, blue arrows indicate specific tryptophan dependent pathways, and black arrows show steps common to both tryptophan dependent and independent pathways.

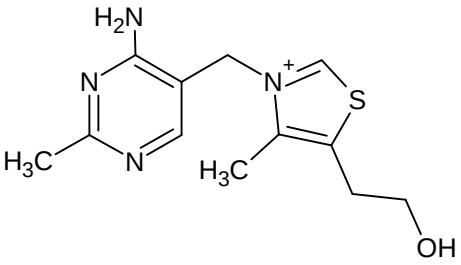

Thiamine

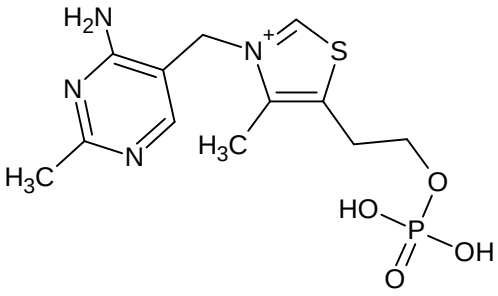

Thiamine monophosphate (TMP)

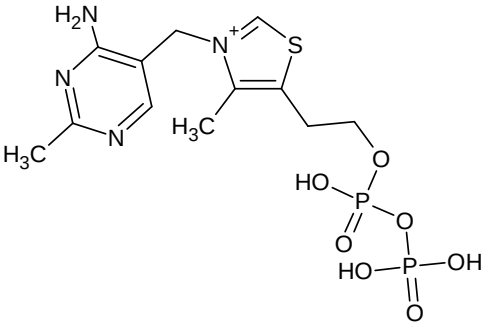

Thiamine pyrophosphate (TPP)

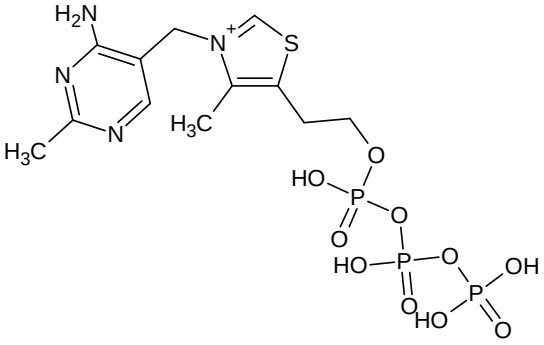

Thiamine triphosphate (TTP)

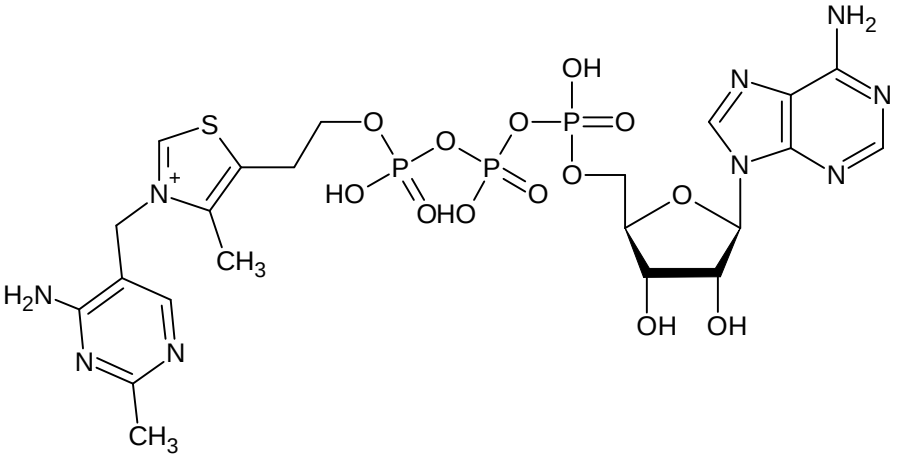

Adenosine thiamine triphosphate (ATTP or TATP)

Figure 1.4 Naturally occurring thiamine and its esters.

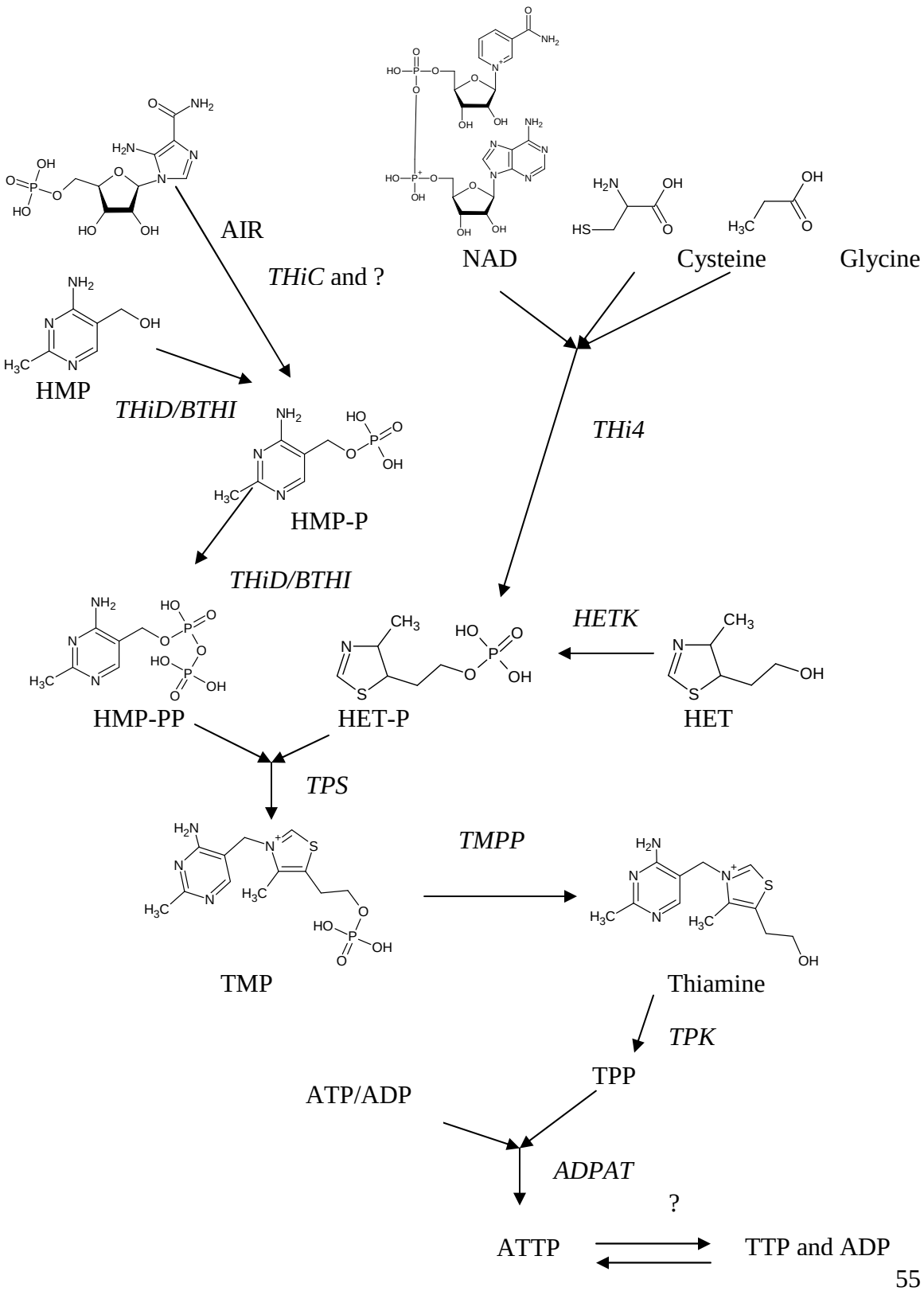
AIR
NAD
Cysteine
Glycine
THiC and ?
HMP
THiD/BTHI
THi4
HMP-P
THiD/BTHI
HETK
HMP-PP
HET-P
HET
TPS
TMPP
TMP
Thiamine
TPK
TPP
ATP/ADP
ADPAT
?
ATTP
TTP and ADP

Figure 1.5 Proposed biosynthetic pathways for thiamine and its derivatives in plants. Genes are represented in italics. *THI4/ThI1*, thiazole synthase; *HMPK*, hydroxymethylpyrimidine kinase; *HETK*, methylhydroxyethylthiazole kinase; *TPS*, thiamine phosphate synthase; *TMPP*, thiamine phosphate phosphatase; *TPK*, thiamine pyrophosphate kinase; ?, unidentified genes; *ADPAT*, thiamine diphosphate adenylyl transferase (reviewed in Settembre et al., 2003; Lawhorn et al., 2004a; Kim et al., 1998; Chatterjee et al., 2006; Chabregas et al., 2001; Makarchikov, et al., 2007; Jordan, 2007). P, phosphate group; PP, diphosphate; AIR, 5-aminoimidazole ribonucleotide; NAD, Nicotinamide adenine dinucleotide; HET, 4-methyl-5-β-hydroxyethylthiazole; HMP, 2-methyl-4-amino-5-hydroxymethylpyrimidine; TMP, thiamine monophosphate; TPP, thiamine pyrophosphate; TTP, thiamine triphosphate; ATP, adenosine-5'-triphosphate; ADP, adenosine-5'-diphosphate; ATTP, adenosine thiamine triphosphate;

# Chapter 2

## *PDC2* from *Arabidopis* has pyruvate decarboxylase activity but lacks significant activity toward indole-3-pyruvate

## 2.1 Introduction

Pyruvate is a key metabolite at the branch point between anaerobic and aerobic respiratory pathways. Pyruvate decarboxylase (PDC, EC 4.1.1.1) is a carboxy-lyase or carbon-carbon lyase, which converts, by decarboxylation, pyruvate into acetaldehyde, and then alcohol dehydrogenase (ADH, EC 1.1.1.1) reduces acetaldehyde into ethanol (Figure 2.1). PDC is particularly important under anaerobic stress conditions (or anoxia), which occur with events such as flooding, when plant roots cannot get enough oxygen for normal respiratory metabolism and must seek alternative means for energy production. Because of the central role the reactions catalyzed by PDC and related enzymes play in oxygen-stress responses, the enzymes remain under active investigation in reference species as well as in crop plants, including major studies in maize, pea, barley, and rice (Kürsteiner et al., 2003; Gass et al., 2005). Several *PDC* genes from crop species, such as sweet potato (Ōba and Uritani, 1975), wheat (Singer, 1955), pea (Mücke et al., 1995), tobacco (Bucher et al., 1995), and petunia (Gass et al., 2005), have been described. The *PDC* genes in all species studied were shown to be present as a small gene family (Peschke and Sachs, 1993; Rivoal et al., 1997; Kürsteiner et al., 2003). In *Arabidopsis*, *PDC* genes are a family comprised of 4 members (*PDC1*, *PDC2*, *PDC3*, and *PDC4*; Kürsteiner et al., 2003). *PDC1* is dramatically induced under anoxia for 3 hours; however, the expression of *PDC2*, *PDC3*, and *PDC4* were found to be undetectable even under anoxia in *Arabidopsis* (Kürsteiner et al., 2003). Overexpression of *PDC*2 in *Arabidopsis* has been shown to increase hairy root tolerance to hypoxia by inducing a higher PDC activity during hypoxia (Shiao et al., 2002). However, knowledge in this

area is still at an early stage. Biochemical characterization of PDC enzymes, or even studies to confirm biochemically the number of functional *PDC* genes, has not been extensively pursued.

A closely related activity to PDC is the enzyme that acts on indole-3-pyruvate, indolepyruvate decarboxylase (IPDC; EC 4.1.1.74; 3-(indole-3-yl)pyruvate carboxy-lyase [(2-indole-3-yl)acetaldehyde-forming]; Figure 2.2). Some of the very earliest proposed pathways for auxin (IAA) biogenesis hypothesized that this enzyme activity was a key step in the conversion of tryptophan to IAA (Reinert, 1954; Gordon 1956), and recent studies on mutants of Arabidopsis impaired in tissue specific responses to ethylene or shade-avoidance responses have heightened interest in this reaction (Reviewed in Palme and Nagy, 2008). In spite of this long interest and recent awareness, we still lack critical information about this enzyme, and it remains uncertain if a functional IPDC activity is actually present in plants. The situation is made more complex by the fact that it has been demonstrated that, in microbes, PDC and IPDC are bi-functional activities of the same proteins (Koga et al., 1992). Microbial enzymes that are primarily either a PDC or an IPDC protein display activities of varying levels toward both pyruvate and indole-3-pyruvate. Because microbes primarily produce IAA as part of an infection or synergism strategy (Dullaart, 1970; Glick, et al., 1999), this promiscuous activity toward two substrates may have few significant regulatory consequences. However, a bifunctional activity in plants could be envisioned to either link primary and signaling metabolic pathways in novel ways or it might be expected to result in the unregulated production of a hormonal signal with direct developmental consequences. To determine the

relationship of PDC and IPDC in plants, we have examined the substrate requirements for a major PDC in *Arabidopsis*. This is the first report that a plant PDC, *At*PDC2, does not have any measurable IPDC activity and thus is uniquely mono-functional.

## 2.2. Results

### 2.2.1 Homology of PDC1 from *Zymomonas mobilis* to putative PDCs in *Arabidopsis* by genomic sequence analysis

A search with the BLASTP program of the *Arabidopsis* protein database (http://www.ncbi.nlm.nih.gov/blast/Blast.cgi?PAGE=Proteins&PROGRAM=blastp&BLAST_PROGRAMS=blastp) showed that the PDC of *Zymomonas mobilis* (accession number gi: 118391) was homologous to four putative *PDC* genes in *Arabidopsis*. The amino acid sequence identity is 41%-44% and similarity is 61%-62%. The amino acid sequences of these four putative PDC sequences (*At*PDC1 or *At*4g33070, accession number gi: 15234062; *At*PDC2 or *At*5g54960, accession number gi: 15240423; *At*PDC3 or *At*5g01330, accession number gi: 15240952; and *At*PDC4 or *At*5g01320, accession number gi: 15240950) were aligned by the ClustalW program at NPS@ Network Protein Sequence Analysis (Combet et al., 2000). Protein sequence alignment showed that the PDC protein sequences are highly conserved except for the N-terminal region (see supplemental Figure S2.1). The alignment clearly demonstrated that several regions, which include the catalytic regions and the substrate binding sites, are highly conserved. *AtPDC2* encodes a protein with levels of amino acid sequence identity of 82%, 80%, and 81% to *At*PDC1, *At*PDC3, and *At*PDC4, respectively. For *At*PDC1, the analysis shows that it is 88% and 87% identical in amino acid sequence to *At*PDC3 and *At*PDC4, respectively. Among the four *At*PDC proteins, *At*PDC3 and *At*PDC4 share the highest degree of identity in sequence at 92%.

All the four putative PDC genes are highly conserved in the amino acid residues of the catalytic center of PDC and the $Mg^{2+}$ binding sites found in all species (Hawkins et al., 1989; Dyda et al., 1993). They also all have the TPP-enzyme motif, PXXXXXXXXGD (P and GD were separated by 8 amino acids), that is characteristic for the TPP binding site (see supplemental Figure S2.2), as would be expected for this class of enzymes. The sequence analysis using HmmerPfam (http://www.molgen.mpg.de/~service/scisoft/gcg/gcg10/hmmerpfam.html), Structural Classification of Proteins (SCOP; http://scop.mrc-lmb.cam.ac.uk/scop/), and Block (http://blocks.fhcrc.org/blocks/) confirmed that this conclusion.

Both *At*PDC1 and *At*PDC2 have the same number of amino acids, 607, while *At*PDC3 and *At*PDC4 have 592 and 603, respectively. Except for the divergence at the 5' coding area discussed above, the other parts of the sequence represent a nearly identical primary sequence. Interesting, *PDC2* is the only intron-free gene in this family while the other three genes have four introns. Among the three genes, the first exon and third exon are larger than other exons (Figure 2.3). From this analysis, *PDC3* and *PDC4* may be more closely related to each other and the intron-free *PDC2* may be more distantly related relative to the others.

### 2.2.2 Phylogenetic tree analysis

Taking into account the *PDC*s' catalytic center and the cofactor's binding sites in the C-terminal (158 amino acids) regions, which are highly conserved among all species, reference sequences from the NCBI were used to evaluate the genetic distance of the C-

terminal regions of all the known plant *PDC*s and *PDC* of *Zymomonas mobilis* by using the Jones-Taylor-Thornton model after the ClustalW2 alignment (Jones et al, 1992). A phylogenetic tree was generated using the Neighbor-Joining method to recalculate the genetic distance (Saitou and Nei, 1987; Figure 2.4). All *PDC*s from plants have a very close genetic distance. In general, *PDC*s of the same species have a closer relationship than that from other species. In *Arabidopsis*, *PDC*s are mostly grouped together and the tree indicated that *AtPDC2* is distinct relative to the other three *PDCs*. *PhPDC2* and *NtPDC2*, pollen specific *PDCs* in petunia and tobacco, respectively, have a much closer relationship with *AtPDC2* than they do to the other *PDC*s in *Arabidopsis*. This suggests *AtPDC2* may be a candidate gene that should be examined for pollen specific expression. The analysis also showed that there are two groups of *PDC*s in maize and rice and that *ZmPDC1* and *OsPDC1* are closely related to each other and their genetic distances are close compared to the other *PDC*s of maize and rice.

### 2.2.3 Microarray data analysis

Genevestigator, a useful web based database, allows for the facile query of Affymetrix GeneChip data [webpage of www.genevestigator.ethz.ch (Zimmermann et al., 2004)]. This type of analysis shows expression patterns of individual or groups of genes throughout chosen environmental conditions, different growth stages, or specific organs (Zimmermann, 2004). Upon investigation of the transcription level of all *PDC* genes using Genevestigator, the expression level could be determined by the Meta profile analysis for each individual *PDC* gene except for the pairs of *AtPDC3/AtPDC4*, which

share high sequence homology. The *PDC* gene family shows a broad pattern of expression across many developmental stages (Figure 2.5). Genes *AtPDC3/AtPDC4* had a very low level of expression throughout the life cycle; however, *AtPDC2* was expressed uniformly at a quite abundant level, although the levels changed somewhat across developmental stages. Interestingly, *AtPDC1* had a very low level of expression from bolting through the flowering stage, but it had a high expression level in organs such as seeds, siliques, and leaves. The expression level of all the *PDC* genes was induced under hypoxia and anoxia (Figure 2.6). Hypoxia and anoxia increased the expression of *AtPDC3/AtPDC4* from 70% to 120%; however, the expression of *AtPDC1* and *AtPDC2* were greatly induced, in some cases by more than 8 fold.

Cold acclimation helps plants increase their tolerance to freezing due to the induction of PDC and the subsequent elevated level of ethanol. However, details about which PDCs are induced under these conditions are only now becoming available. The transcription of different members of the *PDC* gene family is known to be differentially expressed during cold treatment. *AtPDC1,* for example, was not detectable in shoots, but was at very high levels in roots (Figure 2.7A and 2.7B). In contrast, *AtPDC2* had a much lower expression level in both roots and shoots (Figure 2.8A and 2.8B). Additional microarray data on expression levels in specific tissues is available from the website hosted by the Ward lab at http://wardlab.cbs.umn.edu/arabidopsis/. In response to cold stress, the expression of specific *PDC* gene family members displays dramatic differences. The expression of *AtPDC3/AtPDC4* was undetectable while the mRNA levels of *AtPDC1* and *AtPDC2* did not increase under short periods of cold treatment

(4°C; less than 6 hours), but increased by at least two-fold under cold treatment for 12 hours or 24 hours (Figure 2.7A and 2.7B). Interestingly, the expression of the *AtPDC1* gene was imperceptible during short periods of cold stress, but it could be induced dramatically following a six-hour or longer period of stress in shoots (Figure 2.7A). Using the *Arabidopsis* 22k ATH1 microarray dataset (from AT-176, AT-220, and AT-221), it was possible to investigate with Genevestigator the RNA blot signal values of the *PDC* gene family under a 24-hour cold stress. The results were similar to that obtained with a shorter exposure, and *AtPDC1* was induced greatly in response to cold treatment, while *AtPDC2* and *AtPDC3/AtPDC4* were only induced slightly (Figure 2.9).

### 2.2.4 Cloning and expression of recombinant protein in *E. coli*.

The *AtPDC*2 gene was cloned into the *E. coli* expression vector pCRT7/NT-TOPO® TA (Invitrogen, Life Technologies Corp., Carlsbad, CA) by using PCR from a stress cDNA library (LeClere and Bartel, 2001). The sequence was found to correspond to GenBank™ entry NM_124878, but was changed in one position (405, C → T). This deviation is a silent mutation, which happens in the third position of the proline 135 codon. The gene was amplified by PCR from Columbia wild type genomic DNA and when it was sequenced it confirmed that the position of 405 is T instead of C. This suggests the base change of C → T at the position of 405 could reflect a true polymorphism and not an artifact from cloning. Recombinant proteins with a His-tag encoded in the expressed gene were produced by cloning the putative *Arabidopsis PDC* genes in an expression system, pCRT7/NT-TOPO, in *E. coli*. Although the total

recombinant protein increased along with time, the soluble target protein did not increase concomitantly and most protein formed in inclusion bodies. We could not increase the proportion of soluble protein even when different vectors (Novagen's pET32, Invitrogen's pTrcHis-TOPO, or pCRT7/NT-TOPO), competent cells, Isopropyl-β-D-thiogalactopyranoside (IPTG) concentrations, media, and temperature regimes were used (data not shown).

### 2.2.5 Enzyme assay with recombinant protein

#### 2.2.5.1 The molecular weight of PDC

The calculated subunit molecular mass for the *At*PDC proteins is approximately 65 KDa. This was confirmed by mobility on SDS-PAGE analysis (Figure. 2.10) and native electrophoresis was employed to check the molecular weight of the holo-enzyme. A band of ~240 kDa was observed (data not shown) and this supports the expected result for the *At*PDC2 enzyme as a tetramer, which is the same as has been reported in sweet potato (Ōba and Uritani, 1975).

#### 2.2.5.2 Time course of product formation

PDC activity was measured spectrophotometrically using a coupled system with ADH and NADH (ter Schure et al., 1998; Figure 2.2). In initial studies a lag phase was observed before the enzyme reached its maximum rate (data not shown). We excluded the possibility of the lag phase being produced by the coupled system since excess amounts of ADH did not increase the overall activity. Therefore, the rate limiting step is

not the ADH coupled reaction, but it is likely the PDC itself (Figure 2.11). This residual lag time for the reaction obtaining its maximal rate is well documented to be due to substrate activation [the enzymes are inactive in the absence of substrate and are activated only upon addition of the substrate to the enzyme bound TPP that in turn stabilizes the enzyme dimer (Lu et al., 2001)], as has been described for microbial PDC enzymes (Hübner et al., 1978; Baburina et al., 1994; reviewed in König, 1998) as well as the PDC from *Pisum sativum* (Dietrich and König, 1997).

#### 2.2.5.3 The effect of buffer on recombinant activity

A number of inhibitors of pyruvate decarboxylase including glyoxylate were identified based on their inhibitory effect on the activity of the enzyme from brewer's yeast (Flatau et al., 1988). Glyoxylate formed a noncleavable bond with the catalytic center of TPP, thus inhibiting enzymatic activity of PDC. In addition, high concentration of TPP (75 mM) also completely inhibited the activity of PDC enzyme (Wang et al., 2004). There were prior reports indicating that 25 mM phosphate inhibits the activity (Lee and Langston-Unkefer, 1985). However, a lower concentration of phosphate did not appear to inhibit PDC activity, as no significant difference was seen when we compared 10 mM sodium phosphate with 20 mM imidazole buffer. Similar results were seen when comparing the effects of a number of inorganic salts (Wang et al., 2004).

#### 2.2.5.4 The effect of $Mg^{2+}$ and TPP on PDC activity

Another potential reason that would explain the observed lag phase could be the rate of binding between the enzyme and substrate. Similar results with an observed lag-phase had been reported for the PDC of yeast and wheat germ (Schellenberger 1967; Kenworthy and Davies, 1976). Increasing the TPP concentrations to 0.6 mM typically increased the overall PDC activity (Figure 2.12A). PDC activity with 0.6 mM TPP is twice as fast as PDC activity measured in the absence of added TPP. The end groups of TPP are associated with the α-domain or γ-domain, respectively to form a tightly bound dimer or tetramer (Dyda et al., 1993). Therefore, TPP might change the association between PDC molecules to dimerize and form tetramers, thus affecting PDC activity. Therefore, a better understanding of the rates of binding between enzyme and TPP and self-association would be important factors to consider. The $K_m$ of TPP binding to *At*PDC2 was found to be 0.25 mM (Figure 2.12B).

#### 2.2.5.5 Optimal pH, optimal temperature, and thermostability for *At*PDC2 activity

The effect of pH on PDC activity was analyzed using phosphate/citrate buffer (pH adjusted by varying the mixture of 20 mM dibasic sodium phosphate and 10 mM citric acid; after Pearse, 1980). As shown in Figure 2.13A, the recombinant *At*PDC2 protein displayed a relatively broad pH activity profile; *At*PDC2 showed highest activity at a pH between 5.5 and 7.0, and the broad pH optimum peaked at 6.2. Above pH 8.0 or below pH 4.0, the enzyme was essentially inactive. This pH range is consistent with the expected cytoplasmic pH during anoxia, when PDC activity is expected to be maximized (Roberts et al., 1982). The pH effect with *At*PDC2 shows quite different slopes between

above and below the optimal pH point (Figure 2.13A), as had been shown for PDCs from yeast and maize (Jordan et al., 1978; Lee and Langston-Unkefer, 1985).

The effect of temperature on *At*PDC2 was similar to that of pH. In general, PDC activity escalated as the temperature increased when only modest changes were made. *At*PDC2 had an optimal temperature of 55°C at pH 6.3 (Figure 2.13B). This is consistent with the prior observations that the optimal temperature of plant PDC is above 45°C (Singer, 1955). The activity decreased as the temperature increased to 60°C.

After storage at -80°C for 2 months, the enzyme retained at least 95% of its activity. In contrast, we observed that freezing at -20°C over several cycles caused considerable inactivation (80% or higher decrease; data not shown). To check the thermostability under modest conditions, the enzyme reaction was measured at pH 6.3 for a period from 0 hour to 24 hours at 30°C. We found during the first half hour, *At*PDC2 reached its highest activity. The reaction rate remained essentially the same in 1 - 4 hours, and it lost just 20% of its activity after 24 hours (Figure 2.13C). The reason for less activity at 0 hour is likely simply due to the addition of the cold protein sample that had been stored at 4°C. In general, it must be concluded that the expressed *At*PDC2 is relatively stable to standard laboratory manipulations.

#### 2.2.5.6 Kinetic characterization of *At*PDC2

It had been demonstrated that PDC and IPDC are bi-functional properties of the same enzyme proteins for those isolated from microbes (Koga et al., 1992). Microbial enzymes

were named for their preferred substrates as either PDC or IPDC and all display activities toward both substrates to varying degrees. The $K_m$ for *At*PDC2 is 3.5 mM for pyruvate (Figure 2.14A and 2.14B); however initial attempts to measure IPDC activity were unsuccessful. To clarify the situation with regard to IPDC activity, a more specific and sensitive assay was required.

### 2.2.5.7 Development of a gas chromatography-mass spectrometry based assay for IPDC activity

Indolepyruvate and indoleacetaldehyde are both easily converted by oxidative reactions to products that we have found interfere with traditional assays of IPDC activity, even those based on separation techniques including HPLC. Thus, when employing such methods we obtained ambiguous results that were compounded by the relatively low activity being measured. This necessitated the development of a method with high sensitivity and exacting chemical reliability to allow the indolic substrate and product(s) to be accurately identified and quantitatively determined. The enzyme reaction was started by adding purified recombinant *At*PDC2 into the equilibrated indolepyruvate solution at 30ºC. IAAld produced in the reaction was extracted by partitioning against ethyl acetate along with an internal standard, indole carboxaldehyde. IAAld and indole carboxaldehyde were moved into the ethyl acetate phase. Water in the decanted ethyl acetate was removed by dehydration over anhydrous sodium sulfate and the samples were analyzed by SIM-GC-MS. The quantification was based on the ratio of the peak area of IAAld ($M^+$ = 130 *m*/*z*) and that of the internal standard ($M^+$ = 144 *m*/*z*) as matched to the

calibration curve (Figure 2.15). IAAld produced by spontaneous degradation was subtracted based on the same time point obtained for the denatured enzyme protein.

To construct a calibration plot for IAAld, the abundances of different levels of indole carboxaldehyde were determined, and it was found that 0.6 ng indole carboxaldehyde showed a significantly strong signal for calibration (data not shown). Next, a series of samples were prepared with different levels of IAAld, and then each of the samples was mixed with 0.6 ng indole carboxaldehyde, and the integrated peak abundances after SIM-GC-MS were calculated and graphed (Figure 2.16). The calibration plot for IAAld was linear in the range of 0 – 3 ng ($y = 1.0305x - 0.2754$ when x = log (IAAld) and y = log (abundance of IAAld/abundance of indole carboxaldehyde); $R^2 = 0.9912$). Since a fixed amount of indole carboxaldehyde was used (0.6 ng), IAAld quantification was based on the ratio of the integrated peak area of IAAld ($M^+ = 130$ *m*/*z*) and the internal standard ($M^+ = 144$ *m*/*z*) as matched to the calibration plot.

#### 2.2.5.8 IPDC activity of recombinant *At*PDC2

No detectable IPDC activity for *At*PDC2 was found, suggesting that this plant enzyme, unlike the microbial enzyme, is mono-functional (Figure 2.17 and 2.18). In addition, the cloned and expressed *At*PDC1 and *At*PDC3 had no measurable activity of either PDC or IPDC (data not shown). This further supports the hypothesis that *At*PDC2 may be a unique *PDC* gene that encodes a mono-functional enzyme.

### 2.2.6 PDC and IPDC activity in *Arabidopsis* seedlings

#### 2.2.6.1 PDC activity in seedlings

Analysis of plant protein extracts confirmed that there was PDC activity in *Arabidopsis* seedlings (Figure 2.19). For further purification, it was critical to determine which fraction after ammonium sulfate precipitation contained the highest activity; thus total soluble protein extracted from *Arabidopsis* was precipitated by 0% – 25%, 25% – 35%, and 35% – 100% ammonium sulfate saturation, respectively. It was found that the 25% - 35% of ammonium sulfate fraction had the highest PDC activity, and this fraction had over a three-fold enrichment relative to the crude supernatant. In addition, the 0% – 25% and 35% – 100% ammonium sulfate fractions had less PDC activity when compared to the supernatant. Therefore, fractionation with 25% – 35% ammonium sulfate saturation can be used for partial PDC purification.

#### 2.2.6.2 IPDC activity in seedlings

After finding no IPDC activity from expressed PDC proteins, the GC-MS based IPDC assay was applied to proteins in plant extracts. As with the expressed proteins, it was possible to measure PDC activity but the proteins were devoid of measurable IPDC activity. However, diluted *Ec*IPDC (kindly provided by Dr. Jinichiro Koga, Meiji Seika Kasha, Ltd.) also failed to give measurable IAAld in the presence of plant protein extracts, suggesting rapid degradation of the product (data not shown).

Thus, the GC-MS based IPDC assay method was modified using a coupled reaction that rapidly converted IAAld to IAA using commercial ALDH (aldehyde dehydrogenase,

Sigma, Saint Louis, MO). IPDC activity was then observed for *Ec*IPDC-spiked plant extracts, even when the *Ec*IPDC was diluted 200 times relative to the plant extracts; however, even this system failed to detect IPDC activity for either the boiled control or the non-spiked plant extracts (Figure 2.20). The $T_{2h}$ plant extract had less IAA than the $T_0$ control, and this was likely due to a slow degradation of the trace IAA found in the substrate and the protein extracts during the incubation. This further confirmed the lack of significant IPDC activity in *Arabidopsis* PDC-related proteins.

### 2.2.7 Shade avoidance response (SAR)

Under simulated shade conditions, plants have longer hypocotyls and the longer hypocotyl has been ascribed to the resulting increase in auxin levels under these conditions (Figure 2.21A; Tao et al., 2008). Since a functional TAA1 was shown to be required to observe a SAR and the proposed product of activity of the TAA1 protein, an aminotransferase, is indole-3-pyruvate when tryptophan is the substrate, it was reasonable to propose that an IPDC would also be required for the pathway to be complete. Thus, as an additional test of the potential role of the PDC genes *in vivo*, it was important to determine if *pdc2* mutants gave the same SAR response as TAA1. Two *pdc2* mutants, CS875641, an exon insertion line and Salk066678, a 5' UTR insertion line were tested. Both *pdc2* mutants showed the same phenotype of SAR as the wild type plants. In addition, mutants of each of the other members of the *pdc* gene family also showed the same phenotype under SAR conditions as *pdc2* and the wild type plants (data not shown). Because an active IPDC was proposed as potentially the rate-limiting enzyme in the IPA

pathway (Tao et al., 2008), this would suggest that analysis of a mutation of this particular gene would be a particularly dramatic phenotypic test relative to the IPA pathway and the SAR. Thus, these findings bring into question both the shade induction of the IPA pathway as well as the role of the homologous PDC gene family in that pathway. Although we can not fully exclude other mechanisms, such as possible protein modifications, or association of PDCs into new complexes, or the existence of an active IPDC with limited homology to the known PDC/IPDC family and physical properties that make it undetectable in the protein extracts we tested, these possibilities seem unlikely. Therefore, if shade does induce an IPA pathway in *Arabidopsis*, it does not appear to involve any of the enzymes identified by sequence homology to be members of the PDC family.

## 2.3 Summary and Discussion

Four putative *PDC* genes were found in *Arabidopsis* by a sequence homology search. The putative *PDC* genes have been cloned into *E. coli* using cDNA clones or from an *Arabidopsis* cDNA library. Bacterially expressed *At*PDC2 was shown to be a functional PDC with a $K_m$ of 3.5 mM. *At*PDC2 however does not appear to have any measurable IPDC activity and thus is uniquely mono-functional in contrast to the better studied PDCs in microbes which all have bi-functional activity toward both indole-3-pyruvate and pyruvate substrates.

There was no significant IPDC activity in proteins expressed from *Arabidopsis* genes assayed by a new GC-MS based method. IPDC activity was also not observed in *Arabidopsis* protein extracts, although extracts spiked with *Ec*IPDC showed substantial activity. While the microbial gene produced a bi-functional PDC (a protein that had both IPDC and PDC activities) the enzyme produced from the only *Arabidopsis* gene with PDC activity was mono-functional and lacked measureable IPDC activity. In addition, shade did not appear to induce the IPA pathway *in vivo* based on the wild type shade response of mutants in each of the PDCs. These findings bring into question the physiological significance of the IPA pathway as proposed, although we cannot fully exclude all potential mechanisms of activation, redundancy of *in vivo* function or of an IPDC without significant sequence homology as well as significantly different physical properties to the known PDCs.

## 2.4 Experimental procedures

### *2.4.1 Construction of the phylogenetic tree*

All known PDC protein sequences from different plant species, including all four annotated PDC sequences of *Arabidopsis*, retrieved from NCBI databases were used for the construction of a phylogenetic tree. Alignments of full protein sequences were performed using ClustalW2 at the homepage URL:

http://www.ebi.ac.uk/Tools/clustalw2/index.html (Lakin et al., 2007). The guide tree obtained from ClustalW2 was viewed and saved by TreeView (Page, 1996). The alignment created by ClustalW2 was edited by BioEdit (version 7.0.9; Hall, 1999), a biological sequence alignment editor. Genetic distance for the sequences was calculated with the Prodist program using the Jones-Taylor-Thornton model (Jones et al, 1992) and was reestablished with the Neighbor program, using the Neighbor-Joining method (Saitou and Nei, 1987). The phylogenetic tree was created with Drawgram. Prodist, Neighbor, and Drawgram programs are contained in the PHYLIP software package (version 3.68; Felsenstein, 1993), and operations were performed based on the multiple alignments using the protein C-terminus (158 amino acids) sequences.

### *2.4.2 Microarray data analysis by Genevestigator*

The Meta profile analysis tools of the Genevestigator software was queried with the AGI (*Arabidopsis* Genome Initiative) codes of all *PDC* genes (Zimmermann, 2004). The microarray analyses at various developmental stages were performed using 3110 publicly available ATH1 22k microarray datasets. The expression level at different stages was determined by different number datasets based on availability.

The transcription expression of *PDC* under hypoxia and anoxia was determined by searching results compiled from *Arabidopsis* 22k ATH1 microarray experiments. These experiments include AT-158 from Perata's lab: Effects of anoxia (less than10 $\mu gmL^{-1}$ $O_2$ achieved by Anaerobic System model 1025; Forma Scientific, Marietta, OH) and 90 mM sucrose on seedling growth (Loreti et al., 2005), and AT-171 from Beiley-Serres' Lab: Change in transcript abundance and association with large polysomes in response to hypoxia stress in sealed Lucite chambers (Baxter-Burrell, et al., 2003; Branco-Price et al., 2005). Northern signal values were obtained from the website source decoded with Image J, a Java-based image processing program developed at the National Institutes of Health (Collins, 2007). Anoxia treatment had four replicate datasets, and all other treatments had two replicate datasets (see more microarray conditions at Gonzali et al., 2005; Branco-Price et al., 2005).

Data for the cold stress (4°C) time course from AtGenExpress, provided to the database by the Kudla lab, was analyzed (Kilian et al., 2007). Shoot and root tissue of 18-day-old seedlings had been treated and collected separately at the following time points: 0.5 hour, 1 hour, 3 hours, 6 hours, 12 hours, and 24 hours. More detailed information about the experiment that was done to obtain the public dataset is available from the website at:

http://arabidopsis.org/servlets/TairObject?type=expression_set_full&id=1007966553.

The transcription expression of *PDC* in relation to the cold response (4°C) was investigated by using public datasets obtained with the *Arabidopsis* 22k ATH1 microarray: AT-176 from Fowler's lab: response to CBF2 and ZAT12 expression and

response to cold in plate and soil grown plants (Vogel et al., 2005); AT-221 from Thomashow's lab: response to cold, plate grown plants (Vogel et al., 2005); AT-220 from Zhu's lab: ICE1 regulation of the *Arabidopsis* cold-responsive transcription (Lee et al., 2005). Northern data from above three teams decoded by Image J were used to calculate the difference between control and 24-hour 4°C treatment.

*2.4.3 Cloning of AtPDC2*

*AtPDC2* was amplified from a stress cDNA library (kindly provided by B. Bartel; LeClere and Bartel, 2001) by PCR using *Pfu* polymerase (Stratagene, La Jolla, CA). The primers were designed based on GenBank/EMBL database sequence available for NM_124878 (AT5G54960), and they were ATGGACACTAAGATCGGATC and CTACTGCGGATTTGGGGGA. The PCR products were cloned directly into the pCRT7/NT vector (Invitrogen). The resulting construct was sequenced using the T7 promoter primer: TAATACGACTCACTATAGGGA and the T7 reverse primer: GCTAGTTATTGCTCAGCGGTG at the DNA sequencing and analysis facility of the BioMedical Genomics Center, University of Minnesota. We constructed *E. cloacae IPDC* from the plasmid pIP362 (kindly provided by J. Koga, Meiji Seika Kaisha Ltd, Japan) into the above expression system as a positive control, since it has both enzymatic activities of IPDC and PDC. The primers used for this *IPDC/PDC* were: ATGCGAACCCCATACTGCGT and TCAGGCGTTATTACACGCT.

*2.4.4 Expression and Purification of the AtPDC and EcIPDC Proteins*

*E. coli* BL21 (DE3) Star™ (Invitrogen) was used for transformation of the pCRT7/NT-derived expression constructs of *AtPDC and EcIPDC*. They were

subsequently grown overnight in LB medium (Luria-Bertani medium) containing 75 µg/ml of ampicillin at 37°C. 0.5 mM IPTG was added when the cells reached an optical density (OD) of approximately 0.6 at 595 nm. After 5 h of induction, the transformants were harvested by centrifugation for 15 min at 5000 x *g* in a refrigerated (4°C) Sorvall RC-5 centrifuge. The cell pellets were resuspended in CelLytic B Plus working solution (Sigma). The cells were lysed by sonication at the 40% setting (Vibra-Cell™, Sonics & Materials, Inc., Newtown, CT) for 30 second and then centrifuged at 6000 x *g* for 15 min. The supernatant containing the soluble cell extract was applied to a HIS-Select™ Nickel Affinity Gel (Sigma). The N-terminal His-tagged *At*PDC and *Ec*IPDC proteins were purified according to the manufacturer's (Sigma) recommendations. The sizes and purity of the recombinant proteins were assessed by SDS-PAGE (sodium dodecyl sulfate polyacrylamide gel electrophoresis). Proteins were also detected by immunoblot (Western) analysis using an anti-polyhistidine antibody (Invitrogen).

*2.4.5 PDC enzyme activity assay*

The PDC assay was performed spectrophotometrically at 340 nm to determine the rate of acetaldehyde formation as shown by the concomitant rate of oxidation of NADH in a coupled reaction with yeast alcohol dehydrogenase (ADH; Sigma) as determined using a diode array UV spectrophotometer (Agilent model 8453; Waldbronn, Germany). The kinetic software mode in the Chemstation software (Agilent) was used to measure $A_{340}$ every 5 seconds, and then zero order conditions were used to calculate the rate of NADH change. The molar extinction coefficient ($\varepsilon_{340}$) of NADH was taken as 6290 $M^{-1}$ $cm^{-1}$ (Budavari et al., 1996). The purified protein was added to the reaction mixture

without pyruvate and pre-incubated for 5 min at 30°C, and the reaction was initiated by the addition of the substrate. The standard enzyme assay was performed at 30°C in the following buffers: 10 mM potassium phosphate (pH 6.5), 40 mM imidazole (pH 6.5), and 20 mM phosphate/10 mM citrate buffer (pH 6.5; Pearse, 1980). In addition, all assay mixtures included 0.1 mM thiamine diphosphate (TPP), 5 mM $MgCl_2$, 150 µM NADH, and yeast alcohol dehydrogenase (ADH, 2 IU/mL) unless otherwise described. All reactions were started by the addition of 20 mM pyruvate except for determination of Km which was started by adding 0.2 mM, 0.5 mM, 1 mM, 1.5 mM, 2 mM, 3 mM, 4 mM, 6 mM, 8 mM, 10 mM, 15 mM, 20 mM, or 30 mM pyruvate, respectively. One unit of enzyme activity was defined as 1 mg of protein catalyzing the decarboxylation of 1 µmol of pyruvate per min. The initial *At*PDC2 activity was 0.3 units per mg of protein. The activities and the $K_m$ calculations were based on three or more replicate analyses.

2.4.6 *Influence of temperature and pH on PDC activity*

The effect of pH on *At*PDC was determined by incubating the reaction mixture at different pH values ranging from 4.0 to 8.0 in the phosphate/citrate buffer solutions. The different pH values were achieved by changing the ratio of stock solutions of 20 mM dibasic sodium phosphate to 10 mM citric acid (Pearse, 1980). The optimum temperature for PDC activity was determined by performing the assay at different temperatures ranging from 24 to 60 °C at the optimal pH value (pH = 6.3). To check thermostability under moderate conditions, the enzyme reaction was performed at pH 6.3 following incubation for 0 hour to 24 hours at 30°C. The effect of TPP concentration was measured essentially the same way as described for analysis of pH, at pH 6.3 and 30°C.

*2.4.7 Analysis of IPDC activity by GC-MS*

Indole-3-pyruvate (0.4 mM) was preincubated in 10 mM $KH_2PO_4$ with 5 mM $MgCl_2$ and 0.25 mM TPP at room temperature (21ºC) for 20 min. The incubation volume was 300 μL, and 2 mg purified recombinant protein in 10 μL was added to start the reaction at 30ºC. At each time point of 0 min, 10 min, and 25 min, 100 μL reaction mixture was transferred into a tube with an equal volume of acetonitrile and then the reaction was stopped. The mixture was extracted with 200 μL of ethyl acetate with 180 ng indole carboxaldehyde (internal standard). The ethyl acetate phase was dehydrated with anhydrous sodium sulfate at 4ºC for 1 hour. The samples were injected using the splitless mode into a 5890A gas chromatograph coupled to a model 5970 quadruple mass spectrometer (Hewlett Packard, Palo Alto, CA) equipped with a 30 m, 0.25 mm internal diameter capillary column (HP-5MS; Hewlett Packard) with a crosslinked 0.25 μm film of 5% phenylmethylsiloxane. The injection port temperature was 280°C, and helium at 1 ml/min was used as the carrier gas. The column temperature, maintained at 70°C during the first 2 min, was increased by 20°C $min^{-1}$ to 280°C, and then finally was held for 5 min. The maximum sensitivity was achieved by using the selective ion monitoring (SIM) mode. In the SIM mode, the first peak to elute was IAAld ($M^+$ = 159 *m*/*z* and a stronger quinolinium fragment at $M^+ - 29$ = 130 *m*/*z*) and the second peak was indole carboxaldehyde ($M^+$ = 144 *m*/*z*, with a base peak at $M^+ - 29$ = 116 *m*/*z*). Retention time and electron impact ionization mass data for the reaction product was confirmed with an authentic standard. The quantification was based on the ratio of the peak area of IAAld ($M^+$ = 130 *m*/*z*) and internal standard ($M^+$ = 144 *m*/*z*) as matched to the calibration curve

based on combinations of a series of different levels of IAAld with 0.6 ng indole carboxaldehyde.

*2.4.8 Partial purification of PDC in Arabidopsis*

The plant material used was 30-day-old seedlings planted and grown in a growth chamber under continuous light (70 $\mu mol \cdot m^{-2} \cdot s^{-1}$, provided by cool white fluorescent tubes). Approximately 30 mL of medium containing half strength Murashige and Skoog salts (Caisson Laboratories, Inc., North Logan, UT), 1% sucrose, 0.5 g/L MES (2-(*N*-morpholino)-ethanesulfonic acid, Sigma) and 0.5% phytagel (Sigma), pH 5.7, was poured into each square Petri-dish (100 x 100 x 15 mm) and 19 seeds were placed in a line, 1 cm from the top edge. The Petri dishes were incubated vertically at 22°C. One g of freshly harvested seedlings was ground completely using a mortar and pestle pre-chilled on ice at 4°C. The sample was homogenized with 1.5 vol of 50 mM Tris buffer (pH 7.2) containing 150 mM NaCl, 0.2 mM DTT, 10% glycerol, 1% (wt/vol) polyvinylpolypyrrolidone, and protease inhibitor (cocktail set VI; Calbiochem, San Diego, CA), and then the sample was centrifuged at 1000 x g for 5 min. The supernatant was strained through Miracloth (Calbiochem) into a new centrifuge microtube and centrifuged at 10000 x g for 15 min. Protein was precipitated from the soluble extract by ammonium sulfate fractionation, and the ammonium sulfate concentration was calculated from a website calculator: http://www.encorbio.com/protocols/AM-SO4.htm. The protein fraction that precipitated between 0% and 25% saturation was collected by centrifugation at 10000 x g for 10 min. This material was then resuspended in a minimum volume of 10 mM Tris/Mes buffer (pH 6.5). The supernatant was further precipitated in 30% and 100%

saturated ammonium sulfate as above. All steps were carried out at 0°C to 4°C. Protein concentrations were determined using the Coomassie (Bradford) Protein Assay Kit (Pierce, Rockford, IL).

2.4.9 *Plant extract IPDC enzyme assay*

The plant material used was 3-week-old seedlings planted and grown as described previously. The sample was homogenized with 2 vol of 100 mM potassium phosphate buffer (pH 7.2) containing 25 mM sodium metabisulfite, 1 mM DTT, 5% glycerol, 1% (wt/vol) polyvinylpolypyrrolidone, and protease inhibitor (Cocktail set VI, Calbiochem) for 20 min, and then the sample was centrifuged at 10000 x g for 5 min. Plant total native protein was precipitated in 65% ammonium sulfate saturation and collected by centrifugation at 10000 x g for 10 min. This material was then resuspended in a minimum volume of IPDC assay buffer (15 mM sodium phosphate with 5 mM $MgCl_2$ and 0.3 mM TPP buffer, pH 6.5). The insoluble portion was removed by centrifugation and the supernatant was dialyzed against PBS buffer (phosphate buffered saline, pH 7.4) by using a Slide-A-Lyzer MINI Dialysis Unit (3.5K MWCO; Pierce). Protein concentrations were measured using the Coomassie (Bradford) Protein Assay Kit (Pierce).

For the IPDC assay, plant extract was incubated with 0.4 units of ALDH and 2 mM NAD (nicotinamide adenine dinucleotide) in 125 µL IPDC assay buffer at 30°C for 15 min. The reaction was started by the addition of 250 µL of 0.4 mM indole-3-pyruvate in IPDC assay buffer, followed by 2 hr incubation at 30°C. 100 µL of the reaction mixture

($T_0$ and $T_{2h}$) was stopped by the addition of 150 µL isopropanol. After adding 40 ng of [$^{13}C_6$] IAA as internal standard, each reaction was extracted, purified, methylated and then analyzed by using selected ion monitoring gas chromatography-mass spectrometry (GC-SIM-MS) as described (Barkawi et al., 2008; Appendix 1 of this thesis). *Ec*IPDC and PBS buffer were used as positive and negative controls, respectively. Three biological replicates were analyzed for each enzyme reaction.

2.4.10 *SAR of pdc2 mutants*

Seeds were planted on medium as described above. Seedlings were grown at 22°C under light of photosynthetically active radiation (PAR) 50 $\mu E \cdot m^{-2} \cdot s^{-1}$ and R:FR = 11.8 (4 HID metal Halide (MH) lamps supplemented with 6 red light fluorescent tubes; Engelen-Eigles et al., 2006). Five-day-old seedlings were transferred to simulated foliar shade conditions (PAR 20 $\mu E \cdot m^{-2} \cdot s^{-1}$ and R:FR = 0.68; 3 HID metal Halide (MH) lamps and 6 far-red light fluorescent tubes with 50% cloth; Engelen-Eigles et al., 2006) and control condition (PAR 20 $\mu E \cdot m^{-2} \cdot s^{-1}$ and R:FR = 11.8; 4 HID metal Halide bulbs and 6 red light fluorescent tubes with 50% cloth) for three more days, and then the lengths of the hypocotyl of the seedlings were measured. T-DNA insertion lines of mutant pdc2 (CS875641 and Salk066678) were from the ABRC (Arabidopsis Biological Resource Center) seed collection.

## 2.5 References


Baburina, I., Gao, Y., Hu, Z., Jordan, F., Hohmann, S. and Furey, W. (1994) Substrate activation of brewers' yeast pyruvate decarboxylase is abolished by mutation of cysteine 221 to serine. Biochemistry 33: 5630–5635

Barkawi, L.S., Tam, Y., Tillman, J.A., Pederson, B., Calio, J. Al-Amier, H., Emerick, M., Normanly, J. and Cohen J.D. (2008). A high-throughput method for the quantitative analysis of indole-3-acetic acid and other auxins from plant tissue. Analytical Biochemistry 372: 177–188

Baxter-Burrell, A., Chang, R., Springer, P. and Bailey-Serres, J. (2003) Gene and enhancer trap transposable elements reveal oxygen deprivation regulated genes and their complex patterns of expression in *Arabidopsis*. Annals of Botany 91: 129–141

Branco-Price, C., Kawaguchi, R., Ferreira, R.B. and Bailey-Serres, J. (2005) Genome-wide analysis of transcript abundance and translation in *Arabidopsis* seedlings subjected to oxygen deprivation. Annals of Botany 96(4): 647–660

Bucher, M., Brander, K.A., Sbicego, S., Mandel, T. and Kuhlemeier, C. (1995) Aerobic fermentation in tobacco pollen. Plant Mol. Biol. 28(4): 739–750

Budavari, S., O'Neil, M.J., Smith, A., Heckelman, P.E. and Kinneary, J.F. (1996) The Merck Index: an encyclopedia of chemicals, drugs, and biologicals. 12$^{th}$ edition, Merck Research Laboratories, Whitehouse Station, NJ, pp. 1088, #6429

Collins, T.J. (2007) ImageJ for microscopy. BioTechniques 43 (1 Suppl): 25–30

Combet C., Blanchet, C., Geourjon, C. and Deléage, G. (2000) NPS@: network protein sequence analysis. Trends Biochem Sci. 25(3): 147–150

Dietrich, A. and König, S. Substrate activation behaviour of pyruvate decarboxylase from *Pisum sativum* cv. Miko. FEBS Letters 400: 42–44

Dullaart, J. (1970) The Auxin Content of Root Nodules and Roots of *Alnus glutinosa* (L.) Vill.. Journal of Experimental Botany 21(4): 975–984

Dyda, F., Furey, W., Swaminathan, S., Sax, M., Farrenkopf, B. and Jordan, F. (1993) Catalytic centers in the thiamin diphosphate dependent enzyme pyruvate decarboxylase at 2.4-Å resolution. Biochemistry 32 (24): 6165–6170

Engelen-Eigles, G., Holden, G., Cohen, J.D. and Gardner, G. (2006**)** The effect of temperature, photoperiod, and light quality on gluconasturtiin concentration in watercress (*Nasturtium officinale* R. Br.). Journal of Agricultural and Food Chemistry 54 (2): 328**–**334

Felsenstein, J. (1993) PHYLIP (phylogeny inference package). Version 3.68. Department of Genetics, University of Washington, Seattle, Washington. Available from http://evolution.genetics.washington.edu/phylip.html

Flatau, S., Fischer, G., Kleinpeter, E. and Schellenberger, A. (1988) $^{31}$P NMR investigations on free and enzyme bound thiamine pyrophosphate. FEBS Letter 233: 379–382

Gass, N., Glagotskaia, T., Mellema, S., Stuurman, J. Barone, M., Mandel T., Roessner-Tunali, U. and Kuhlemeier, C. (2005) Pyruvate decarboxylase provides growing pollen tubes with a competitive advantage in petunia. The Plant Cell 17: 2355–2368

Glick, B.R., Patten, C.L., Holguin, G. and Penrose, D.M. (1999) Auxin production. In: Biochemical and genetic mechanisms used by plant growth-promoting bacteria. Imperial College Press, London, pp. 86–133

Gonzali, S., Loreti, E., Novi, G., Poggi, A., Alpi, A. and Perata, P. (2005) The use of microarrays to study the anaerobic response in *Arabidopsis*. Annals of Botany 96(4): 661–668

Gordon, S.A. (1956) The biogenesis of natural auxins. In: RL Wain and F Wightman (eds), The chemistry and mode of action of plant growth substances. Butterworths, London, pp. 65–75

Hall, T.A. (1999) BioEdit: a user-friendly biological sequence alignment editor and analysis program for Windows 95/98/NT. Nucleic Acids Symposium Series 41: 95–98

Hawkins, C.F., Borges, A. and Perham, R.N. (1989) A common structural motif in thiamin pyrophosphate-binding enzymes. FEBS Letter 255(1): 77–82

Hübner, G., Weidhase, R. and Schellenberger, A. (1978) The mechanism of substrate activation of pyruvate decarboxylase: A first approach. Eur. J. Biochemistry 92: 175–181

Jones, D.T., Taylor, W.R. and Thornton, J.M. (1992) The rapid generation of mutation data matrices from protein sequences. Comput. Appl. Biosci. 8: 275–282

Jordan, F., Kuo, D.J. and Monse, E.U. (1978) A pH-rate determination of the activity-pH profile of enzymes. Application to yeast pyruvate decarboxylase demonstrating the existence of multiple ionizable groups. Anal. Biochem. 86(1): 298–302

Kenworthy, P. and Davies, D.D. (1976) Kinetic aspects of regulation of pyruvic decarboxylase. Phytochemistry 15: 279–282

Kilian, J., Whitehead, D., Horak, J., Wanke, D., Weinl, S., Batistic, O., D'Angelo, C., Bornberg-Bauer, E., Kudla, J. and Harter, K. (2007) The AtGenExpress global stress

expression data set: protocols, evaluation and model data analysis of UV-B light, drought and cold stress responses. Plant J. 50: 347–363

Koga, J., Adachi T. and Hidaka H. (1992) Purification and characterization of indolepyruvate decarboxylase. A novel enzyme for indole-3-acetic acid biosynthesis in Enterobacter cloacae. J. Biol. Chem. 267 (22): 15823–15828

König, S. (1998) Subunit structure, function and organisation of pyruvate decarboxylases from various organisms. Biochim Biophys Acta - Protein Struc. and Mol. Enz. 1385: 271–286

Kürsteiner, O., Dupuis, I. and Kuhlemeier, C. (2003) The pyruvate decarboxylase1 gene of *Arabidopsis* is required during anoxia but not other environmental stresses. Plant Physiology 132: 968–978

Larkin, M.A., Blackshields, G., Brown, N.P., Chenna, R., McGettigan, P.A., McWilliam, H., Valentin, F., Wallace, I.M., Wilm, A., Lopez, R., Thompson, J.D., Gibson, T.J. and Higgins, D.G. (2007) ClustalW2 and ClustalX version 2. Bioinformatics 23(21): 2947–2948

LeClere, S. and Bartel, B. (2001). A library of *Arabidopsis* 35S-cDNA lines for identifying novel mutants. Plant Mol. Biol. 46: 695–703

Lee, B.H., Henderson, D.A. and Zhu, J.K. (2005) The *Arabidopsis* cold-responsive transcriptome and its regulation by ICE1. Plant Cell 17: 3155–3175

Lee, T.C. and Langston-Unkefer, P.J. (1985) Pyruvate decarboxylase from *Zea mays L*. I. Purification and partial characterization from mature kernels and anaerobically treated roots. Plant Physiol. 79: 242–247

Loreti, E., Poggi, A., Novi, G., Alpi, A. and Perata, P. (2005) A genome-wide analysis of the effects of sucrose on gene expression in *Arabidopsis* seedlings under anoxia. Plant Physiol. 137(3): 1130–1138

Lu, G., Dobritzsch, D., Baumann, S., Schneider, G. and König, S. The structural basis of substrate activation in yeast pyruvate decarboxylase. A crystallographic and kinetic study. Eur. J. Biochem. 267: 861-868

Mücke, U., König, S. and Hübner, G. 1995. Purification and characterization of pyruvate decarboxylase from pea seeds (Pisum sativum cv. Miko). Biol. Chem. Hoppe-Seyler 376: 111–117

Ōba, K. and Uritani, I. (1975) Purification and characterization of pyruvate decarboxylase from sweet potato roots. J. Biochem. 77(6): 1205–1213

Page, R.D.M. (1996) TREEVIEW: An application to display phylogenetic trees on personal computers. Computer Applications in the Biosciences 12(4): 357–358

Palme, K. and Nagy, F. (2008) A new gene for auxin synthesis. Cell 133: 31–32

Pearse, A.G.E. (1980) Histochemistry, theoretical and applied, 4th edition. Vol. 1. Preparative and optical technology. Edinburgh: Churchill-Livingstone.

Peschke, V.M. and Sachs, M.M. (1993) Multiple pyruvate decarboxylase genes in maize are induced by hypoxia. Mol. Gen. Genet. 240: 206–212

Reinert J 1954 Wachstum. Fortschr. Bot. 16: 330-340

Rivoal, J., Thind, S., Pradet, A. and Ricard, B. (1997) Differential induction of pyruvate decarboxylase subunits and transcripts in anoxic rice seedlings. Plant Physiol. 114(3): 1021–1029

Roberts, J.K.M., Wemmer, D., Ray, P.M. and Jardetzky, O. (1982) Regulation of cytoplasmic and vacuolar pH in maize root tips under different experimental conditions. Plant Physiol. 69 (6): 1344–1347

Saitou, N. and Nei, M. (1987) The neighbor-joining method: a new method for reconstructing phylogenetic trees. Mol. Biol. Evol. 4: 406–425

Schellenberger, A. (1967) Structure and mechanism of action of the active center of yeast pyruvate decarboxylase. Angew. Chem. Int. Ed. Engl. 6(12): 1024–1035

Shiao, T.L., Ellis, M.H., Dolferus, R., Dennis, E.S. and Doran, P.M. (2002) Overexpression of alcohol dehydrogenase or pyruvate decarboxylase improves growth of hairy roots at reduced oxygen concentrations. Biotechnol Bioeng 77(4): 455–461

Singer T.P. (1955) α-Carboxylase from wheat germ. Methods Enzymol. 1: 465–470

ter Schure, E.G., Flikweert, M.T. van Dijken, J.P., Pronk J.T. and Verrips, C.T. (1998) Pyruvate decarboxylase catalyzes decarboxylation of branched-chain 2-oxo acids but is not essential for fusel alcohol production by Saccharomyces cerevisiae. Appl. Environ. Microbiol. 64(4): 1303–1307

Vogel, J.T., Zarka, D.G., Van Buskirk, H.A., Fowler, S.G. and Thomashow, M.F. (2005) Roles of the CBF2 and ZAT12 transcription factors in configuring the low temperature transcriptome of *Arabidopsis*. Plant J. 41: 195–211

Wang, Q., He, P., Lu, D., Shen, A. and Jiang, N. (2004) Purification, characterization, cloning and expression of pyruvate decarboxylase from *Torulopsis glabrata* IFO005. J. Biochem. 136(4): 447-455

Zimmermann, P., Hirsch-Hoffmann, M., Hennig, L. and Gruissem W. (2004) GENEVESTIGATOR, *Arabidopsis* microarray database and analysis toolbox. Plant Physiol. 136: 2621–2632

## 2.6. Figures

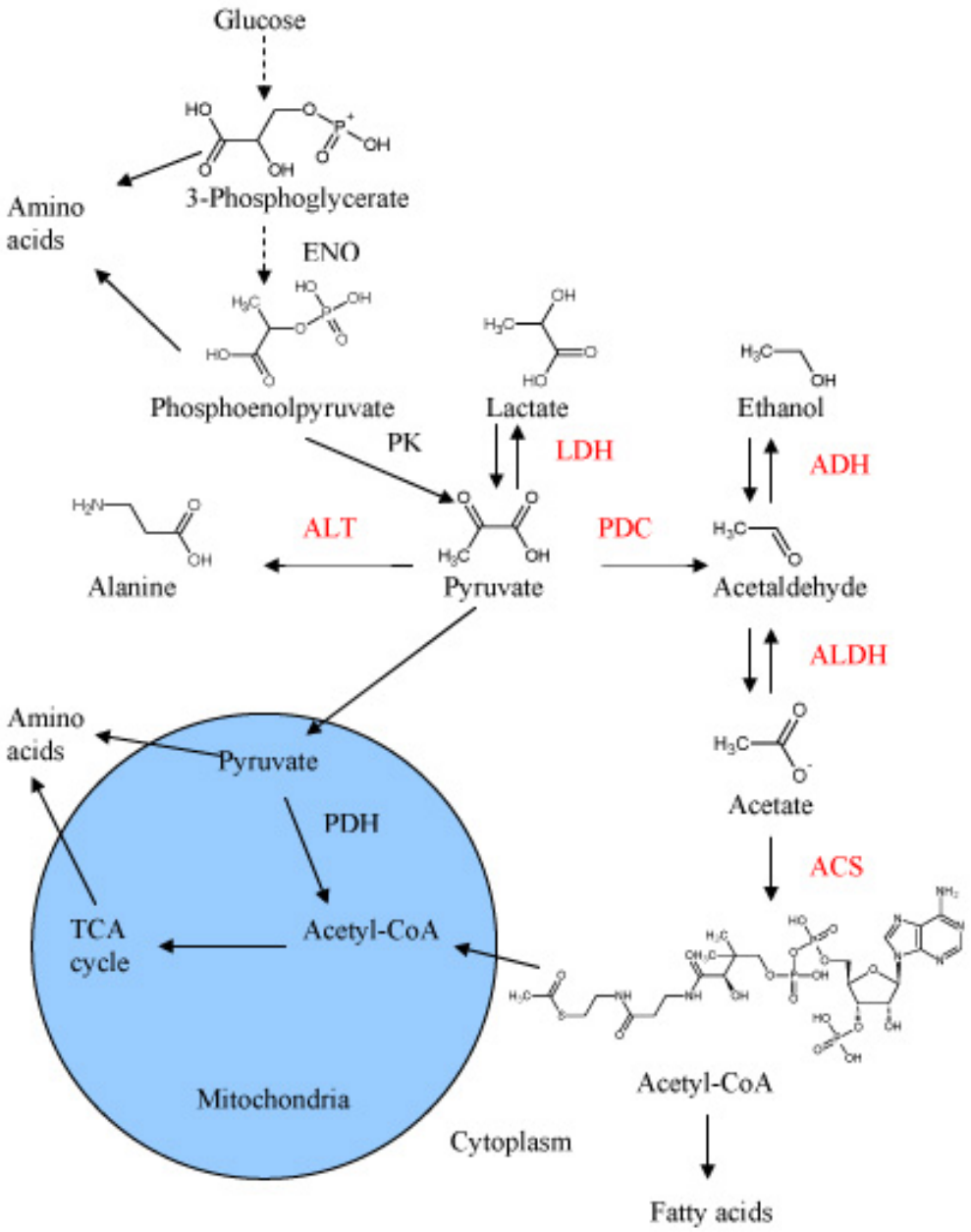


Figure 2.1. Schematic representation of pyruvate metabolism in the cytoplasm. Under aerobic conditions, pyruvate is utilized in the mitochondria (marked as a blue shaded area) and converted into acetyl-CoA. Acetyl-CoA goes on to form lactate, ethanol, or acetate under anaerobic conditions. The anaerobic stress protein (ASPs) enzymes are indicated in red and are proposed as being involved with anaerobic metabolism. PDC, pyruvate decarboxylase; ALT, Alanine transaminase; ENO: enolase; PK, pyruvate kinase; LDH, lactate dehydrogenase; ACS, acetyl-CoA synthetase; ADH, alcohol dehydrogenase; ALDH, aldehyde dehydrogenase.

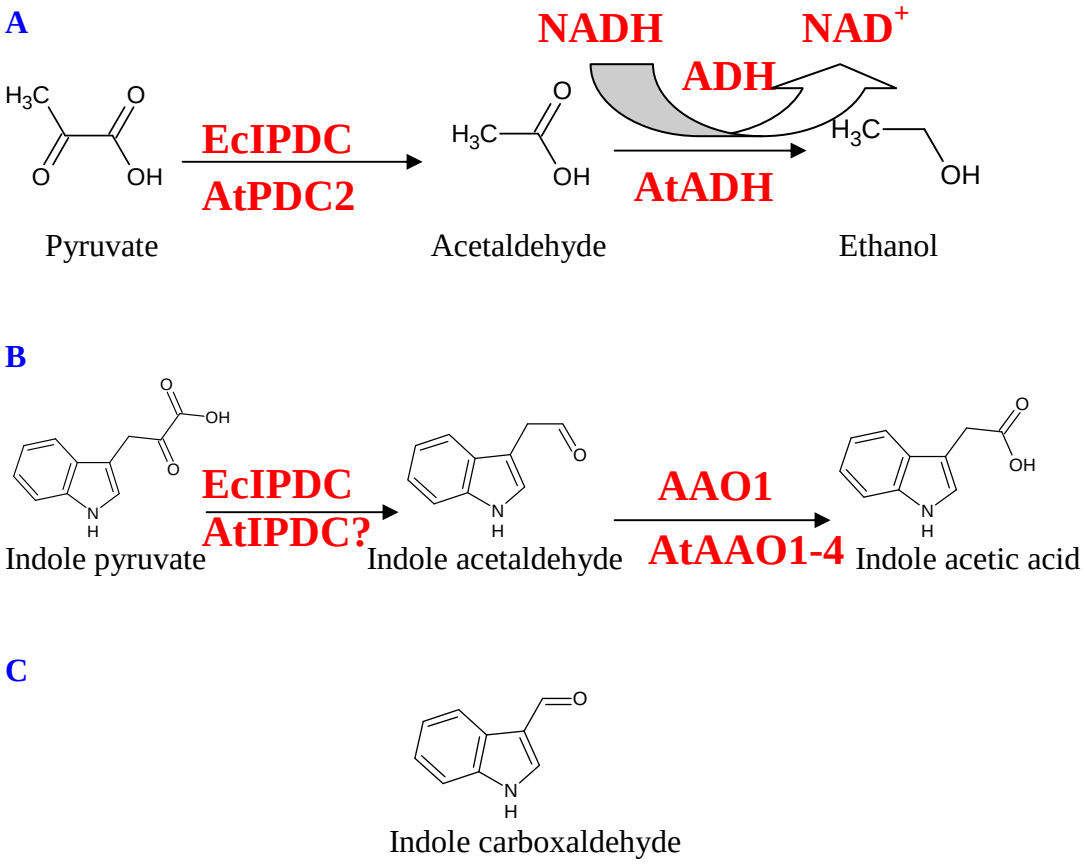


Figure 2.2. Comparison of the assays for enzymatic activity for IPDC and PDC. A: PDC activity was measured by the decrease of NADH in a coupled system. In *Arabidopsis*, this pathway is regulated *in vivo* by *At*PDC2 and *At*ADC (alcohol dehydrogenase). Bacterial *Ec*IPDC as well as *At*PDC2 showed high PDC activity in this assay. B: Bacterial IPDC could be measured in the expressed protein by the formation of indole acetaldehyde; however, this did not work with plant protein extracts due to the rapid degradation of the product. In an attempt to measured IPDC activity by plant enzymes, a coupled reaction was developed to measure this activity by the production of IAA. *Ec*IPDC had IPDC activity when assayed alone or when added to plant extracts. However, no IPDC was detected in plant extracts with this coupled reaction and GC-MS detection. Thus, an active IPDC for *Arabidopsis* remains an unknown. C: Indole carboxaldehyde was the internal standard used to measure indoleacetaldehyde by the GC-MS based method when production of indole acetaldehyde was being assayed from the *E. coli* expressed proteins.

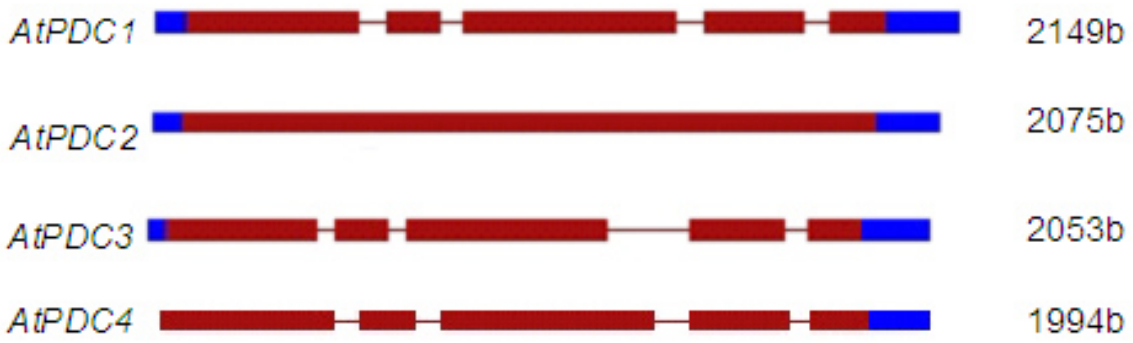


Figure 2.3. The structure of each *PDC* gene in *Arabidopsis*. Blue solid rectangle, red solid rectangle, and red line indicate untranslated region (UTR), exon, and intron, respectively. *AtPDC2* is an intron free gene while *AtPDC1*, *AtPDC3* and *AtPDC4* have five exons and four introns.

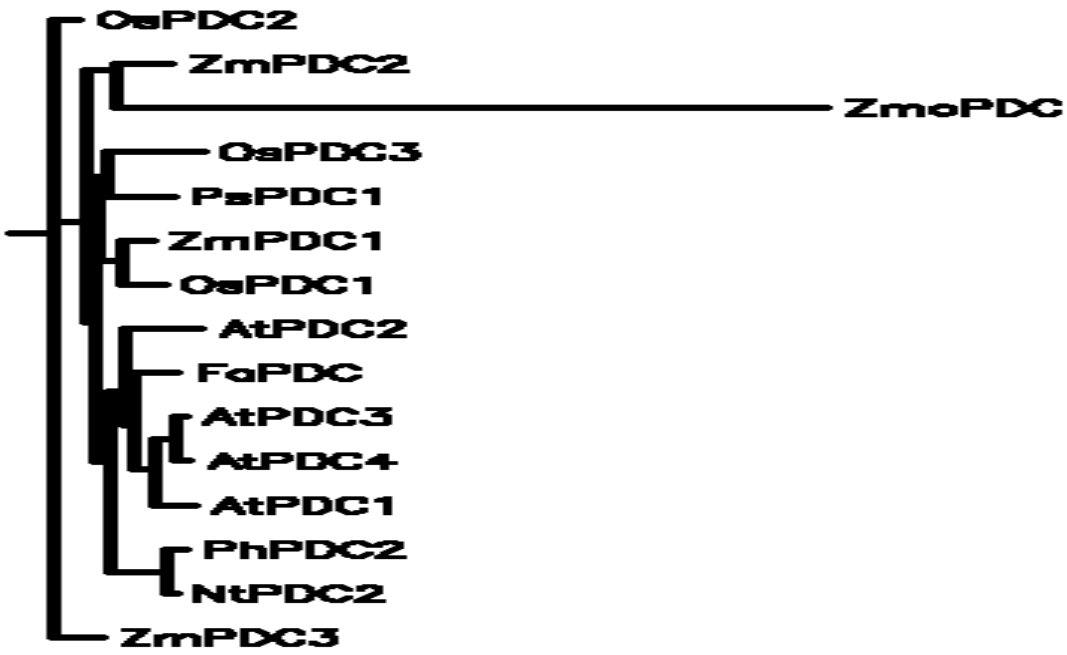


Figure 2.4. Evolutionary tree of the C-terminal (158 amino acids) region of the known *PDC* gene family product in plants using Neighbor joining (a distance method) of Phylip. Branch length was automatically rescaled. PDCs used in the phylogenetic tree are the following: *Zm*PDC1 (gi:162462437), *Zm*PDC2 (gi: 162458702), *Zm*PDC3 (gi: 162457852) from *Zea mays*; *Os*PDC1 (gi:115464407), *Os*PDC2 (gi: 115452421), *Os*PDC3 (gi: 115474257) from *Oryza sativa*; (*At*PDC1 (gi:15234062), *At*PDC2 (gi:15240423); *At*PDC3(gi:15240952); *At*PDC4 (gi:15240950) from *Arabidopsis thaliana*; *Ps*PDC1 (gi:1706326) from *Pisum sativum*; *Ph*PDC2 (gi: 60656563) from *Petunia hybrida*; *Nt*PDC2 (gi: 1706330) from *Nicotiana tabacum*; *Fa*PDC(gi: 10121330) from *Fragaria ananassa*. *Zom*PDC (gi: 118391) of *Zymomonas mobilis*.

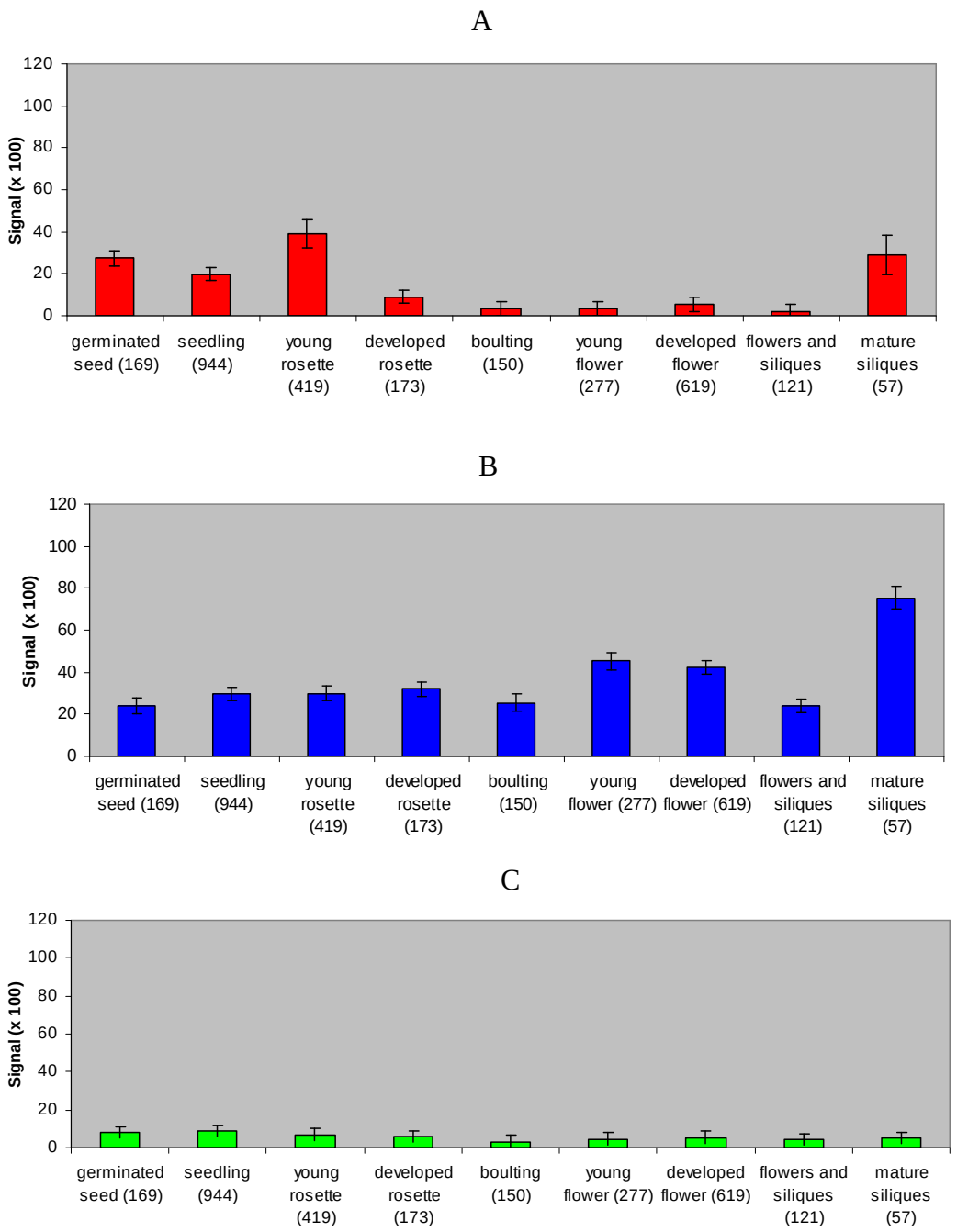


Figure 2.5. The level of *PDC* gene expression at different developmental stages. The Meta profile analysis tool of the Genevestigator software was queried with the AGI codes of all *PDC* genes from 3110 publicly available ATH1 22k microarray datasets. (A), gene expression of AT4G33070 (*AtPDC1*); (B), gene expression of AT5G54960 (*AtPDC2*); (C), gene expression of AT5G01330 (*AtPDC3*). Because of almost identical sequence, the expression of *AtPDC3* and *AtPDC4* are likely both reported for the data given for the *AtPDC3* gene. The numbers in parentheses indicate the datasets used.

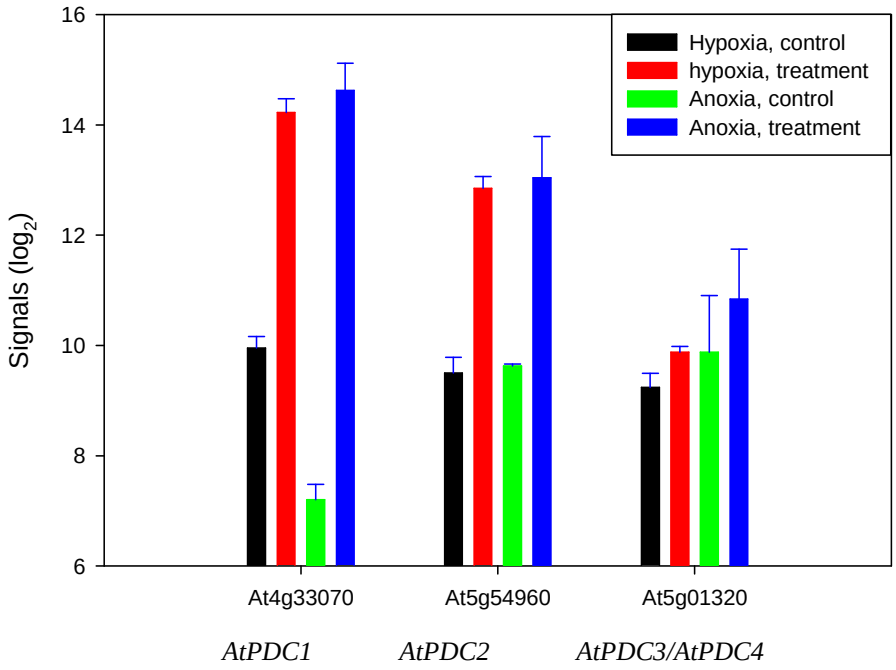


Figure 2.6. Expression in *Arabidopsis* seedlings of *PDC* genes as determined using Genevestigator from data derived following hypoxia and anoxia. The transcription expression of *PDC* was determined by searching results compiled from *Arabidopsis* 22k ATH1 microarray experiments. These experiments include AT-158 from the Perata lab: Effects of anoxia (less than 10 µg $mL^{-1}$ $O_2$ achieved by Anaerobic System model 1025; Forma Scientific, Marietta, OH) and 90 mM sucrose on seedling growth (Loreti et al., 2005) and AT-171 from the Beiley-Serres Lab: change in transcript abundance and association with large polysomes in response to hypoxia stress; Branco-Price et al., 2005). The Meta profile analysis tool of the Genevestigator software was queried with the AGI codes of all *PDC* genes. Genevestigator northern signal values were obtained from the website source (Zimmermann, 2004). Error bars show standard error of the mean (SEM). Anoxia treatment has four replicates and all other treatment have two replicates. AT5G33070, AT5G54960, and AT5G01320 corespond to *AtPDC1*, *AtPDC2*, and *AtPDC3/AtPDC4*, respectively.

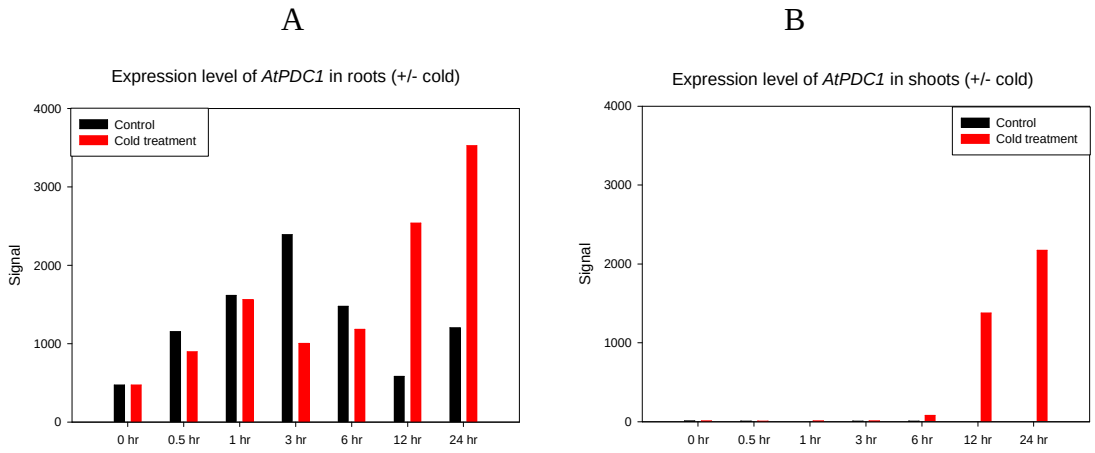


Figure 2.7. Time course of expression of the At4g33070 (*AtPDC1*) gene in roots and shoots. Data from a cold stress time course were obtained from AtGenExpress, as provided by the Kudla lab, and were analyzed (Kilian et al., 2007). Shoot and root tissue of 18-day-old seedlings had been treated at 4ºC and then collected separately at the following time points: 0 hr, 0.5 hr, 1 hr, 3 hr, 6 hr, 12 hr, and 24 hr. Each treatment had two replicates. A: expression in roots; B: expression in shoots.

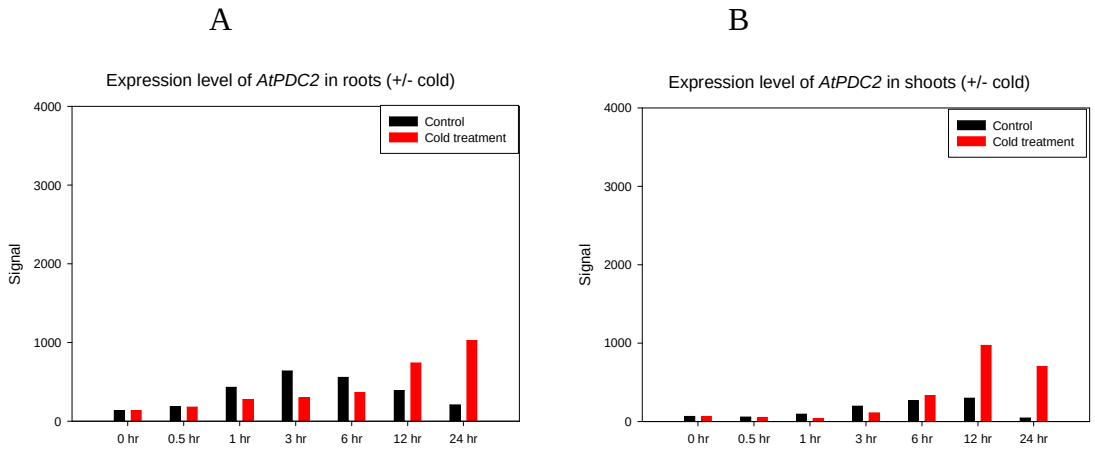


Figure 2.8. Time course of expression of the At5g54960 (*AtPDC2*) gene in roots and shoots. Data for the cold stress time course were from AtGenExpress, as provided by the Kudla lab, and were analyzed (Kilian et al., 2007). Shoot and root tissue of 18-day-old seedlings had been treated (4ºC) and were collected separately at the following time points: 0 hr, 0.5 hr, 1 hr, 3 hr, 6 hr, 12 hr, and 24 hr. Each treatment had two replicates. A: expression in roots; B: expression in shoots.

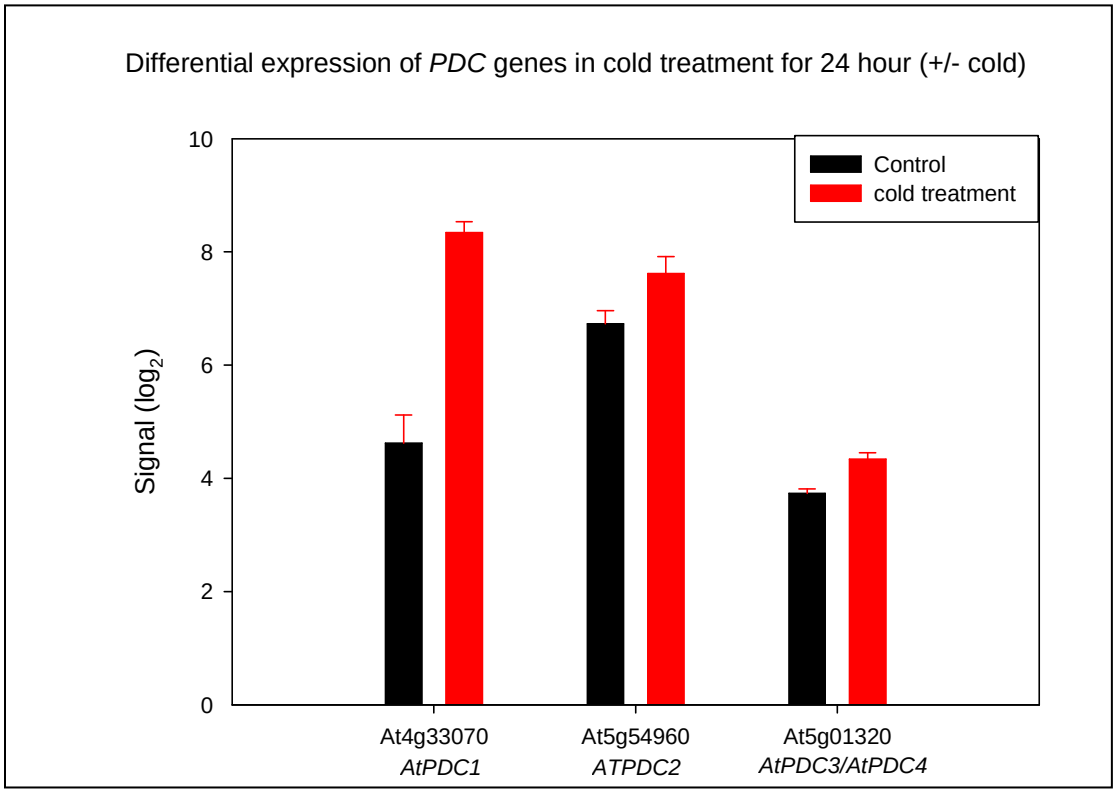


Figure 2.9. Expression in *Arabidopsis* seedlings of *PDC* genes as determined using Genevestigator from data derived following cold stress (4°C). Genevestigator stimulus signal values were obtained from the website source (Zimmermann, 2004). The transcription expression of *PDC* in the cold response was investigated by using the *Arabidopsis* 22k ATH1 microarray dataset (control and 24-hour treatment): AT-176 from the Fowler lab: response to CBF2 and ZAT12 expression and response to cold in plate and soil grown plants (Vogel et al., 2005); AT-221 from the Thomashow lab: response to cold, plate grown plants (Vogel et al., 2005); AT-220 from the Zhu lab: ICE1 regulation of the *Arabidopsis* cold-responsive transcription (Lee et al., 2005). The Meta profile analysis tool of the Genevestigator software was queried with the AGI codes of all *PDC* genes. Five pairs of northern datasets decoded by Image J were used to calculate the difference between control and 24-hour 4°C treatments, and each treatment had two replicates. Error bars show SEM.

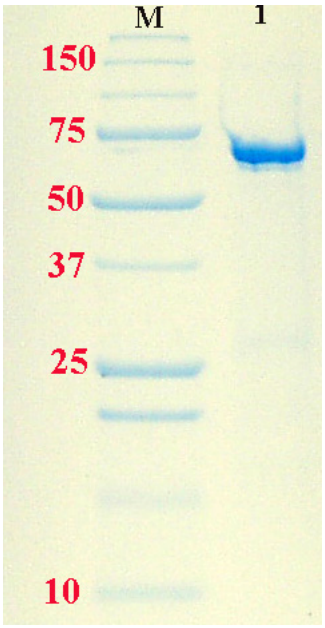


Figure 2.10. 4-15% SDS-PAGE gel (sodium dodecyl sulfate polyacrylamide gel electrophoresis) of purified recombinant AtPDC2 stained with Gelcode Blue Stain Reagent (Pierce, Rockford, IL). Lane M indicates Precision Plus Protein All Blue Standards (Bio-Rad, Hercules, CA) with their sizes listed in kilodaltons (left) and lane 1 shows purified recombinant AtPDC2.

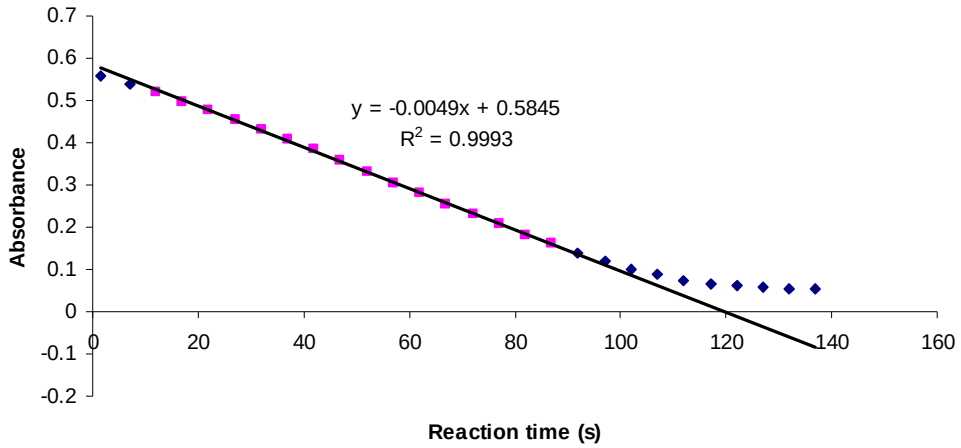


Figure 2.11. PDC enzyme activity was measured by the slope of the decrease in NADH concentration ($\Delta A_{340}$). The assay mixture contained 0.2 mM TPP, 5 mM $Mg^{2+}$, 10 mM sodium phosphate (pH 6.2), 150 µM NADH and 2 units of ADH. Data was recorded automatically at 5 second intervals using the kinetic mode on the Agilent 8453 diode array spectrophotometer system. The slope using data in pink shows the measured enzyme activity rate, and the lag due to substrate activation is shown by the blue time points in the first 10 minutes.

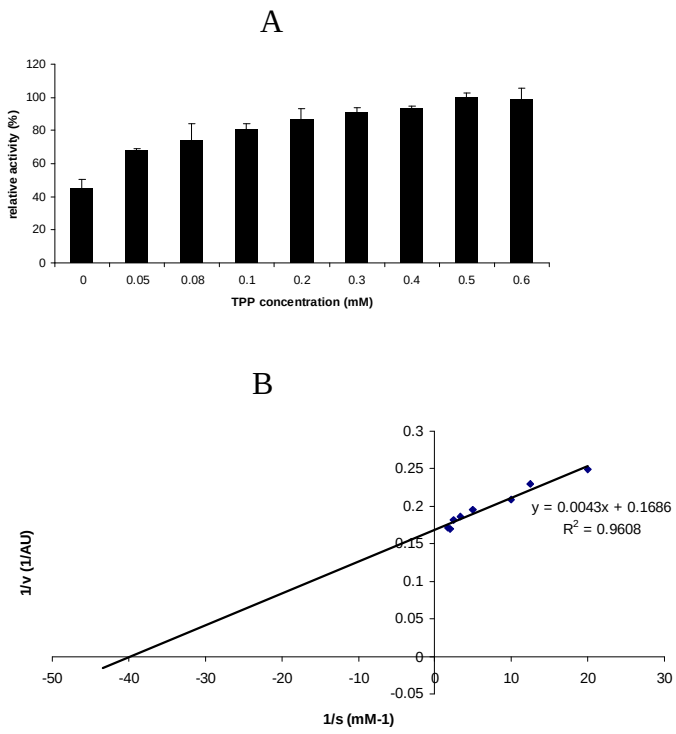


Figure 2.12. Effect of TPP concentration on the PDC activity of *At*PDC2. The data are shown as the binding of *At*PDC2 to different concentrations of TPP in the presence of 25 mM pyruvate (A; PDC activity is 100% when TPP is 0.3 mM) and Lineweaver-Burk double reciprocal plot (B).

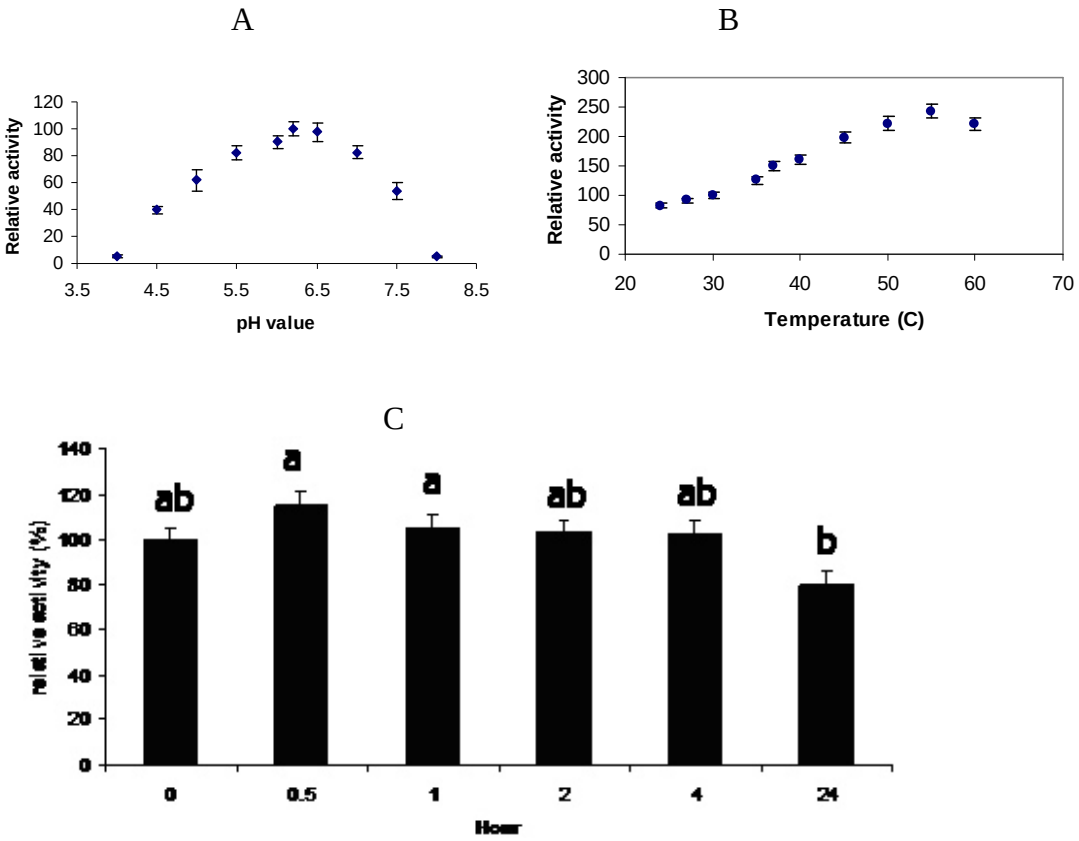


Figure 2.13. Optimal pH, temperature, and thermostability for PDC2 activity. A, the influence of pH on activity of *At*PDC2; B, the effect of temperature on activity of *At*PDC2 (pH 6.3); C, the thermostability of *At*PDC2 at 30°C (pH 6.3). Letters over the bars in C indicate the results form an analysis of variance (*ANOVA*) followed by a Tukey's Post-Hoc test (using the SPSS software package; SPSS Inc., Chicago, IL) that was performed on the enzyme thermostability data. Samples with different letters are significantly different at $P < 0.05$; error bars represent SEM.

A B

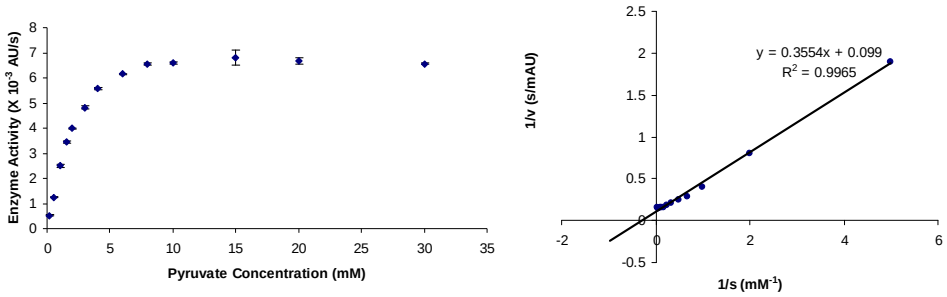


Figure 2.14. $K_m$ *At*PDC2 and binding of TPP and *At*PDC2. The buffer used was 10 mM sodium phosphate (pH 6.2) at 30°C. A, *At*PDC2 activity of pyruvate substrate concentration curve; B, Lineweaver-Burk plot of *At*PDC2 activity.

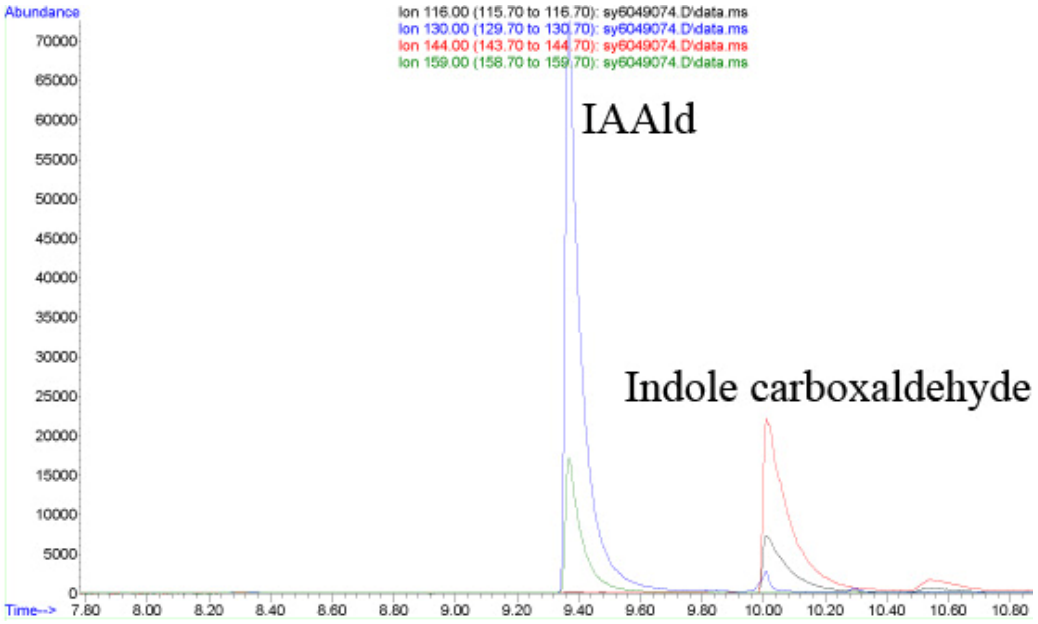


Figure 2.15. Representative ion chromatogram for the products of the IPDC assay reaction analyzed by GC-SIM-MS. The peaks shown on the left are from IAAld, which has a molecular ion ($M^+ = m/z$ 159, green) and a stronger quinolinium fragment ($M^+ - 29 = m/z$ 130, blue) and the peaks shown on the right are from indole carboxaldehyde, which has molecular ion ($M^+ = m/z$ 144, red) and a base peak ($M^+ - 29 = m/z$ 116, black).

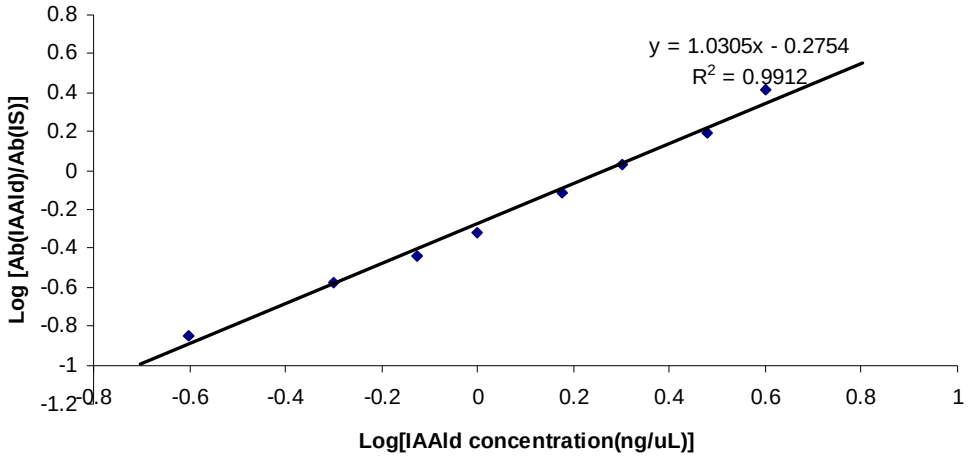


Figure 2.16. Standard concentration plot for calibration of the IPDC enzyme (*Ec*IPDC) assay. The calibration plot of IAAld was linear in the range of 0 – 3 ng. Axes X and Y stand for the log value of IAAld concentration (ng/µL) and of the ratio of abundance of IAAld to abundance of indole carboxaldehyde, respectively.

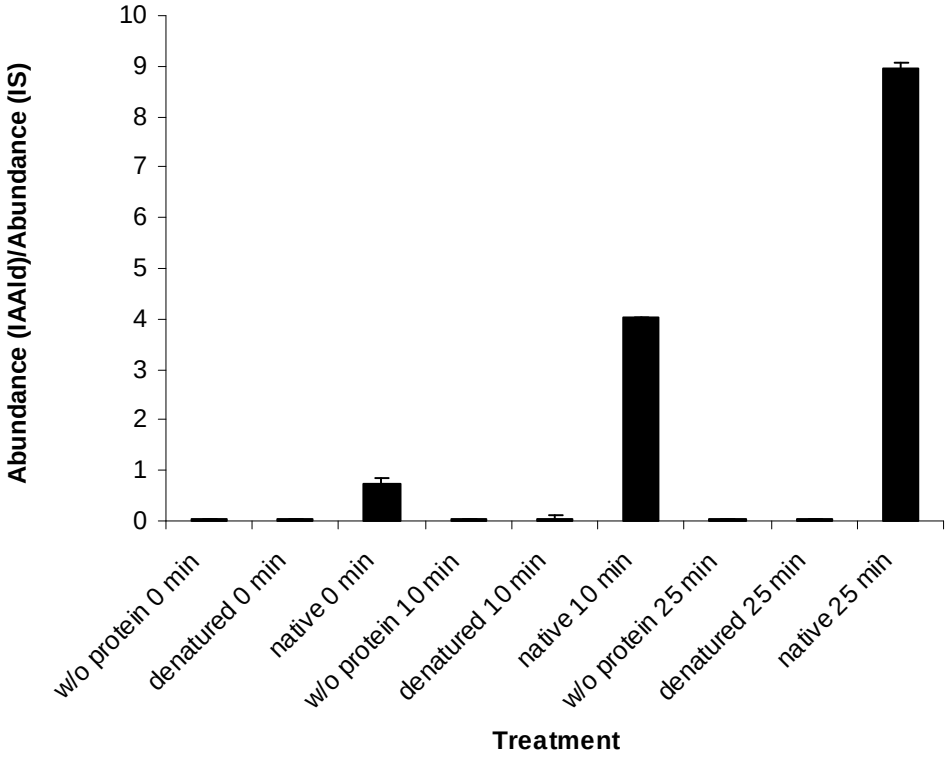


Figure 2.17. IPDC activity of *Ec*IPDC at different time points as determined by GC-MS. Enzyme reaction mixtures were incubated at 30ºC for 0 min, 10 min, and 25 min, respectively, and then reactions were stopped by adding an equal volume of acetonitrile. Enzyme assays had, as controls, sets using heat denatured protein and sets without protein. The quantification was based on the ratio of the peak area of IAAld ($M^+$ = 130 *m*/*z*) and the internal standard ($M^+$ = 144 *m*/*z*) and compared to the calibration plot. Each treatment had three replicates and error bars represent SEM. The error bar of treatment 'native 10 min' was too small to see.

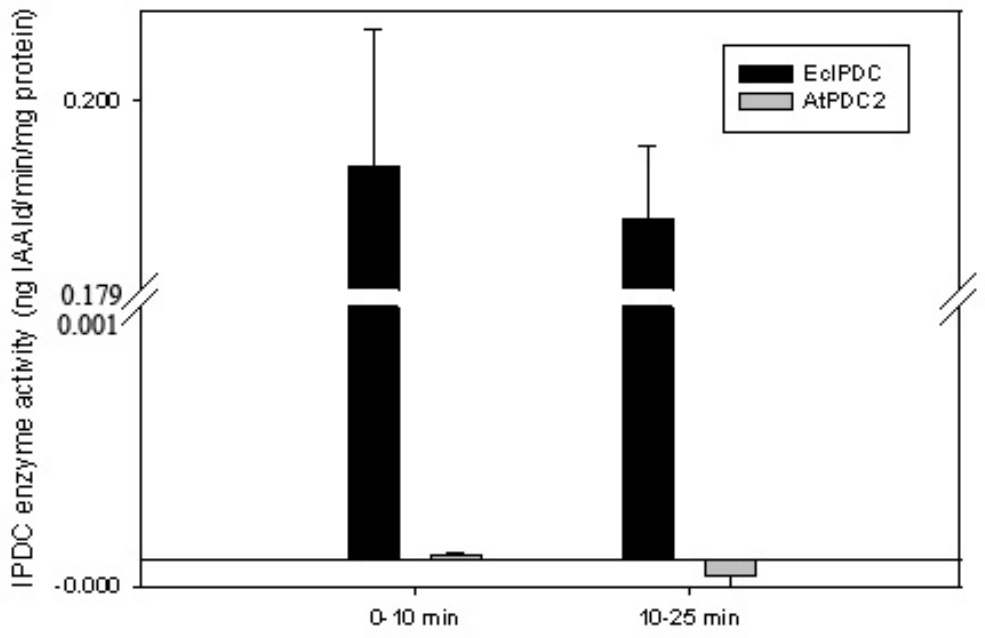


Figure 2.18. IPDC activities for *Ec*IPDC and *At*PDC2 as determined by GC-MS. Black and grey bars show the average rate of *Ec*IPDC and AtPDC2, respectively. Break starts from 0.001 to 0.179.

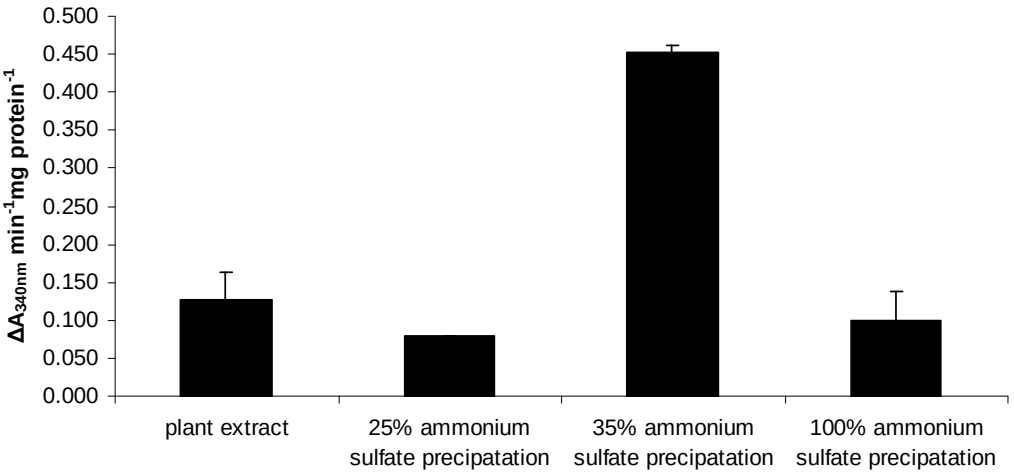


Figure 2.19. Enzyme activity of PDC precipitated by different ammonium sulfate concentrations from protein extracts of *Arabidopsis*. Each treatment had three replicates and error bars represent SEM.

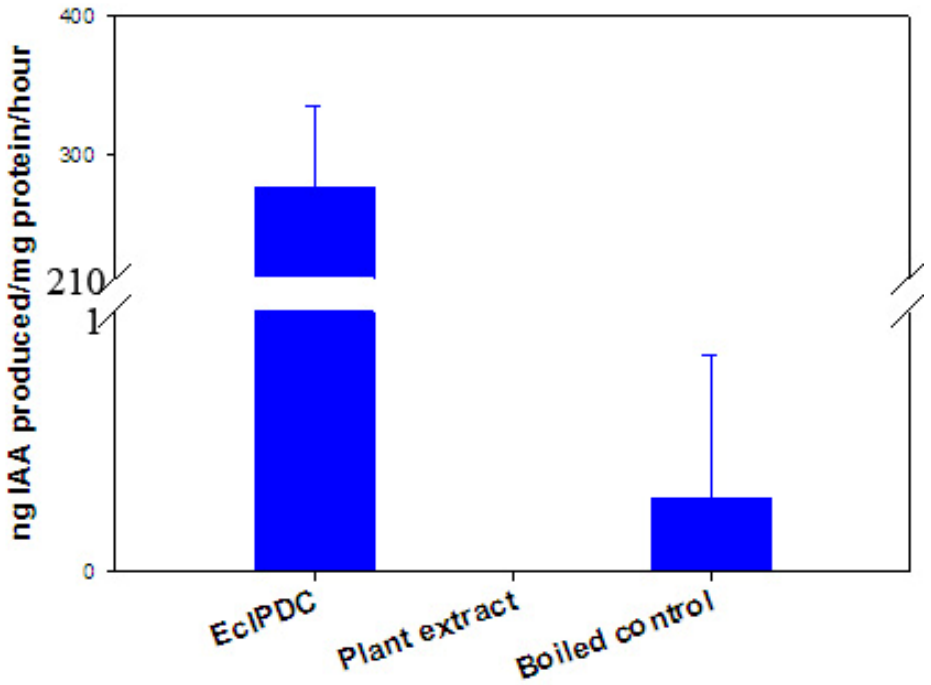


Figure 2.20. IPDC activity for *Ec*IPDC and plant extract as determined by GC-MS using a linked enzyme reaction. Break was from 1 to 210. Note, the $T_{2h}$ plant extract had less IAA than the $T_0$ control, likely due to a slow degradation of the trace IAA found in the substrate and the protein extract during the incubation.

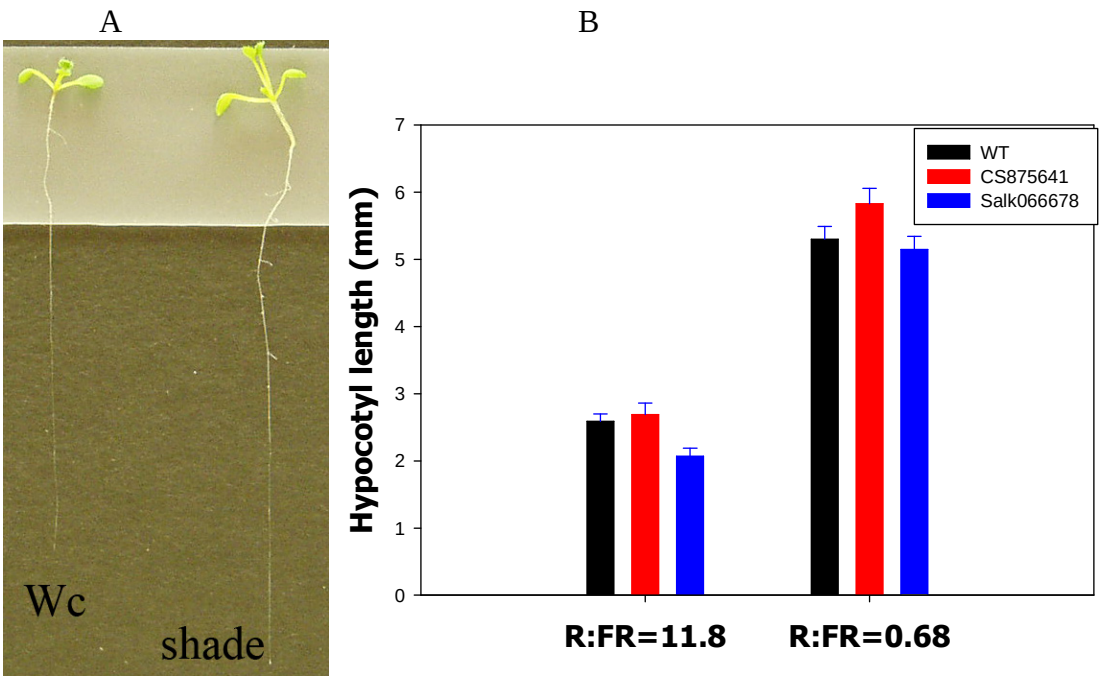


Figure 2.21. Under simulated shade conditions, plants had longer hypocotyls. The PAR for both simulated foliar shade and control was 20 $\mu E \cdot m^{-2} \cdot s^{-1}$. A, Col-0 phenotype with shade treatment; B, Shade avoidance response of Col-0 and *pdc2* mutants.

**Supplemental Figures:**

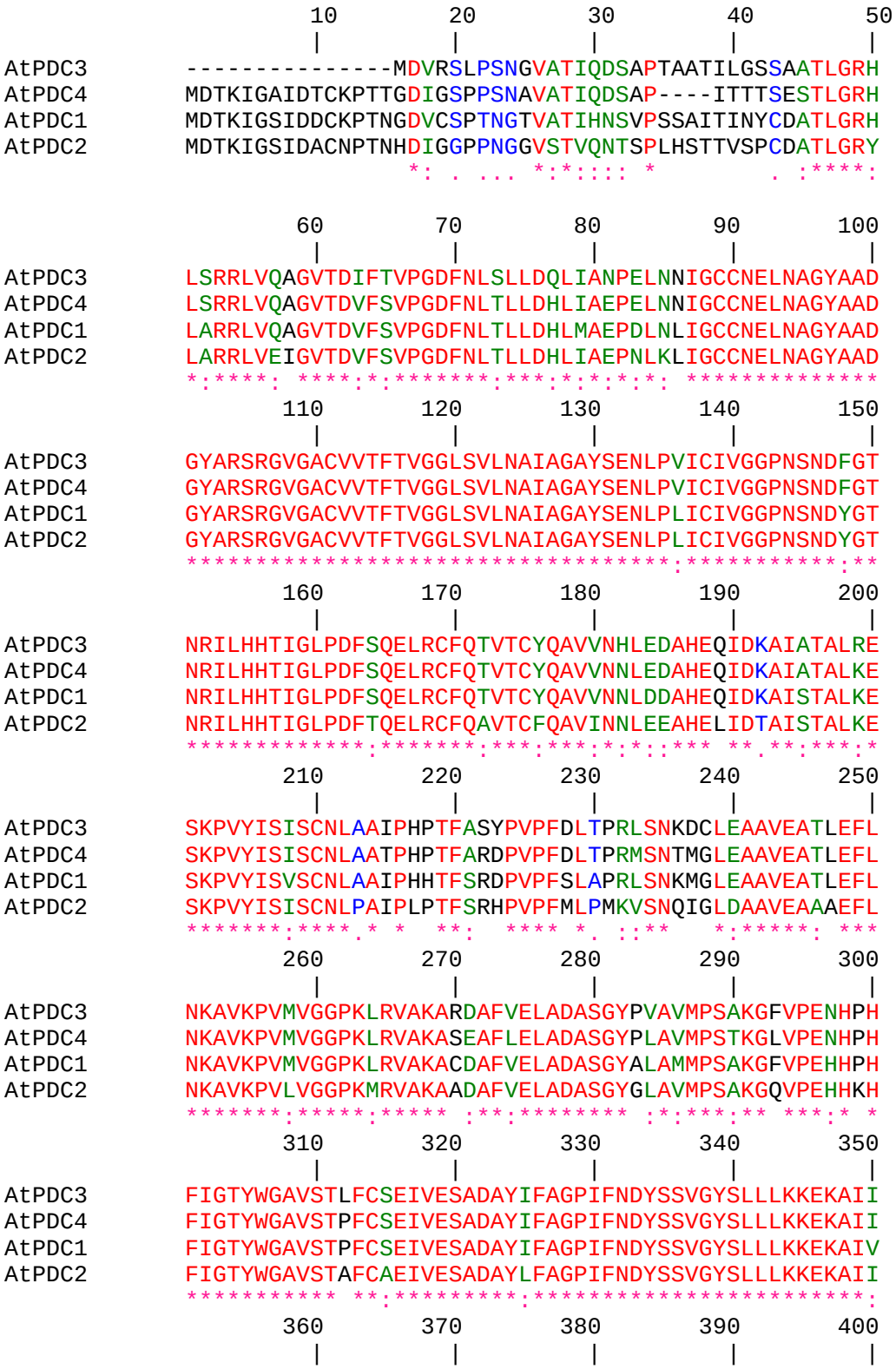

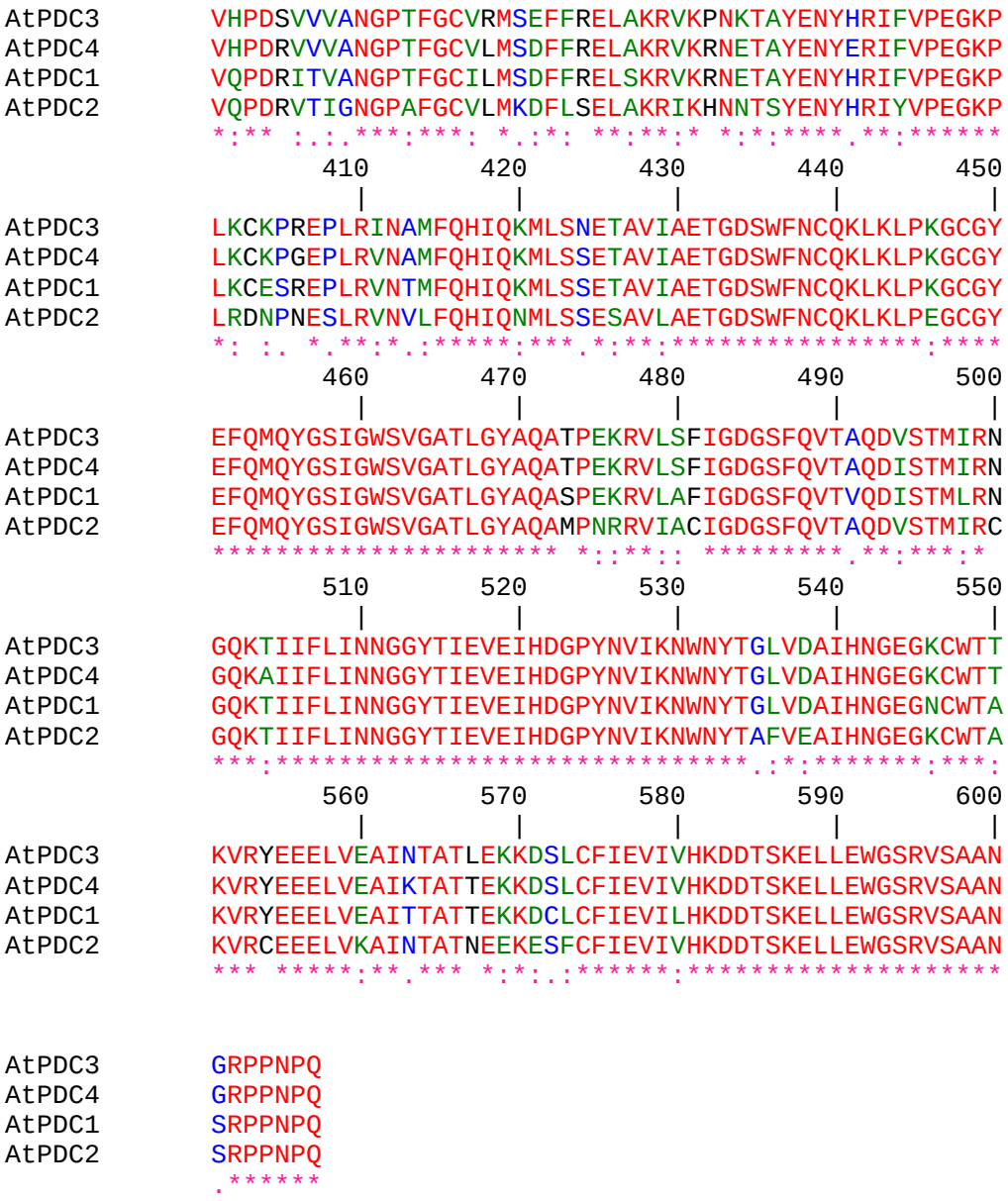


Figure S2.1. Comparison of the amino acid sequences of each *PDC* gene product (*At*PDC1, accession number gi:15234062; *At*PDC2, accession number gi:15240423; *At*PDC3, accession number gi:15240952; *At*PDC4, accession number gi:15240950) from *Arabidopsis*. The ClustalW program (NPS@) was used to align the sequences. Numbering corresponds to the location of amino acid residues in the *At*PDC2 protein. In alignment, "-" stands for a gap and "*", ":", "." and " " indicates amino acids that show identity, or are strongly similar, weakly similar, or different, respectively.

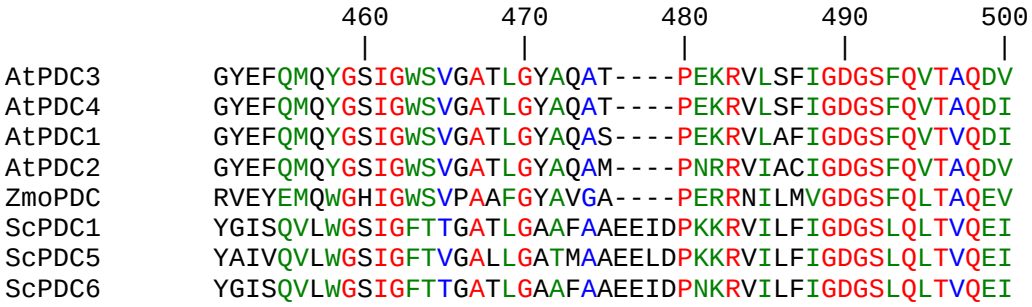


Figure S2.2. Sequences alignments of four PDCs from microbes and putative PDCs from *Arabidopsis*. The ClustalW program (NPS@: Network Protein Sequence Analysis) was used to align the sequences. Numbering corresponds to the location of amino acid residues in the *At*PDC3 protein. (*At*PDC1, accession number gi: 15234062; *At*PDC2, accession number gi: 15240423; *At*PDC3, accession number gi: 15240952; *At*PDC4, accession number gi: 15240950, *Zmo*PDC of Zymomonas mobilis, accession number gi: 118391).

# Chapter 3

## The pyruvate decarboxylase and/or indole pyruvate decarboxylase gene family in *Arabidopsis*

## 3.1 Introduction

Thiamine pyrophosphate (TPP), a major biologically active phosphorylated derivative of thiamine, is a cofactor in many important enzymes in all living systems. TPP and divalent cations such as $Mg^{2+}$ are required for the activity of the enzymes of the TPP-dependent family in microbes. The members of this family include pyruvate decarboxylase (PDC), indole pyruvate decarboxylase (indole-3-pyruvic acid decarboxylase or indolepyruvate decarboxylase, IPDC), and acetohydroxy acid synthase (AHAS, also referred to acetolactate synthase, *ALS*; reviewed in Hohmann and Meacock, 1998). It was found that the amino acids at the catalytic center of PDC and at the $Mg^{2+}$ binding sites are highly conserved in all species studied to date (Hawkins et al., 1989; Dyda, et al., 1993). In addition, those enzymes share a conserved pyrophosphate domain, a pyrimidine domain, and a structure where TPP is tightly bound to the interface of both domains, thus forming tight dimers or even tetramers (Dyda, et al., 1993; Costelloe, et al., 2008).

Auxins, an essential group of phytohormones, are involved in plant viability at essentially every stage of a plant's life cycle. Auxin levels and the metabolic events that control auxin levels are strictly regulated by complex biochemical mechanisms, including redundant pathways for biosynthesis, conjugation and conjugate hydrolysis, transport, and degradation (Cohen and Gray, 2006). Not only are these processes regulated by plant developmental signals but the control mechanisms are also responsive to biotic or non-biotic stress, and even environmental factors such as light and temperature. The indole-3-

pyruvate (or indole pyruvic acid, IPA) pathway, one of the tryptophan-dependent pathways, has often been proposed as the main auxin biosynthetic pathway (Costacurta and Vanderleyden, 1995; Taiz and Zeiger, 1998). More recently, based on several different lines of physiological responses, it has been proposed that TAA1, a gene encoding a protein with aminotransferase activity *in vitro*, is potentially the first step of the IPA pathway (Stepanova et al., 2008; Yamada et al., 2009). However, it was also suggested that it may not be the key rate-limiting enzyme in tryptophan-dependent IAA biosynthesis based on the fact that no auxin overproduction phenotype or longer hypocotyl under simulated foliar shade conditions was found for TAA1 over-expression lines (Tao et al., 2008). The second proposed step in the IPA pathway, IPA to IAAld, is thought to be catalyzed by an IPDC. In microbial IAA biosynthesis, this is the rate-limiting enzyme in the IPA biosynthetic pathway, as first described in *Enterobacter cloacae* (Koga, 1995). However, a functional IPDC has not yet been found in plants. There are a few candidate orthologues of the *E. cloacae* IPDC (EcIPDC) gene present in *Arabidopsis* as shown by sequence analysis. These genes are four *PDC/IPDC* genes, one *PDC*-like gene, and one *AHAS* (see Chapter 2). It was not possible to detect, in *Arabidopsis* protein extracts, measurable IPDC activity even when using a newly developed, sensitive, and highly reliable gas chromatography-mass spectrometry based assay. This finding likely excludes an expected role in IAA biosynthesis for these gene products; nevertheless, the other potential phenotypes of PDC family genes were investigated in this chapter in order to determine if the observed phenotypes confirm the *in vitro* analysis.

## 3.2 Results and Discussion

### 3.2.1 Homologs of known bacterial IPDC in *Arabidopsis*

A search with the BLASTP programs in *Arabidopsis* protein databases showed that the IPDC of *Enterobacter cloacae* (*EcIPDC*, accession number gi:118333) was homologous to six putative *PDC*-like family genes, which were named as *AtPDC*1, *AtPDC*2, *AtPDC3*, *AtPDC*4, *AtPDC*-like, and *AtAHAS*. The whole protein sequence identity and similarity between *Ec*IPDC and *At*PDC1-4 are 31%-33% and 49%-50%, respectively. The identity and similarity between *Ec*IPDC and *At*PDC-like are 23% and 38%, respectively, while the identity and similarity between *Ec*IPDC and *At*AHAS are 23% and 40%, respectively. *Ec*IPDC and these six amino acid sequences of the PDC-like family (*At*PDC1, At5g33070, accession number gi: 15234062; *At*PDC2, At5g54960, accession number gi: 15240423; *At*PDC3, At5g01330, accession number gi: 15240952; *At*PDC4, At5g01320, accession number gi: 15240950; *At*AHAS, At3g48560, accession number gi: 58331777; *At*PDC-like, At5g17380, accession number gi: 15237954) were aligned by the ClustalW program at NPS@ Network Protein Sequence Analysis (Combet, et al., 2000). Protein sequence alignment shows that C-terminal domain sequences are highly conserved and they have the TPP-enzyme motif, PXXXXXXXXGD (P and GD were separated by 8 amino acids), for the TPP binding site, as would be expected for this class of enzymes (Figure 3.1; Chapter 2). *AtPDC2*, a real *PDC* gene, encodes a protein with levels of amino acid sequence identity of 82%, 80%, 81%, 39%, and 39% to AtPDC1, AtPDC3, AtPDC4, *AtPDC*-like, and *At*AHAS respectively.

Similar searches with the BLASTP programs analyzing the *Arabidopsis* protein databases showed that the typical "AHAS" of *Escherichia coli* strain K-12 sub-strain W3110 (*Ec*AHASIII, accession number gi: 89106961) was also homologous to products of these six homologous genes in *Arabidopsis*. Among them, *At*AHAS has the highest homology with an identity of 40% and a similarity of 60%. *At*PDC-like has the second highest homology with an identity of 26% and a similarity of 44%. The homology between bacterial AHASIII and *At*PDC1-4 is low with identity of 20% and similarity of 40%. The C-terminal amino acid sequences of bacterial AHAS and PDC candidates from *Arabidopsis* were conserved (Figure 3.2).

### 3.2.2 Structure of PDC family genes in *Arabidopsis*

*AtPDC1* is on chromosome 4 and *AtAHAS* is on chromosome 3, whereas *AtPDC2*, *AtPDC3*, *AtPDC4*, and *AtPDC*-like are all on chromosome 5. *AtPDC3* and *AtPDC4* are aligned next to each other. *AtPDC1* and *AtPDC2* both have the same number of amino acids, 607, while *AtPDC3, AtPDC4, AtAHAS*, and *AtPDC*-like have 592, 603, 670, and 572 amino acids, respectively. Coincidently, the activity of *AtPDC2* and *AtAHAS*, the only intron-free genes in this family, have been identified (Chapter 2; Roux et al., 2005), while the functions of the other family members have yet to be clearly shown. *AtPDC*-like has one intron while *AtPDC1, AtPDC3*, and *AtPDC4* have four introns (Figure 3.3). The size and order of exons of *AtPDC1, AtPDC3*, and *AtPDC4* are quite similar. For example, the first exon and third exon are larger than the other exons (Figure 3.3).

### 3.2.3 Subcellular localization prediction for PDC family genes

Predictions of protein localization were performed using the web programs Predotar, PSORT, and TargetP (Small et al., 2004; Emanuelsson et al., 2007; Nakai and Kanehisa, 1991). Predotar (Prediction of Organelle Targeting sequences) is a neural network-based program capable of identifying plastid transit peptides (as well as signal peptide sequences) amongst eukaryotic genome sequences (Small et al., 2004). TargetP, a subcellular predictor, relies on the detection of an N-terminal transit sequence using neural networks for pattern recognition (Emanuelsson et al., 2007). PSORT analyzes the input sequence and its source origin by applying the designed algorithms for various sequence features of known protein sorting signals (Nakai and Kanehisa, 1991). AtAHAS showed a high probability of chloroplast localization (scores of 0.95–0.976 on a scale of 0-1.0 by the three web programs shown in Table 3.1), while AtPDC1, AtPDC2, AtPDC4, and AtPDC-like did not appear to be plastid-localized proteins. Interestingly, a transit peptide was predicted by TargetP, but not by Predptar and PSORT for AtPDC3. Of course, each program can yield either false positives or false negatives, and such contradictions among programs need to be resolved experimentally. Even though TargetP performed very well on prediction of mitochondrial and plastid transit peptides and secretory pathway signal peptides, the success rate on test sets was 85% (Emanuelsson et al., 2000). Therefore, more investigation will be required to resolve the difference and to confirm the specific subcellular localizations of these gene products.

### 3.2.4 Phylogenetic tree analysis

A phylogenetic tree was generated using the TPP binding domain of 27 AHAS protein sequences including the 6 candidate sequences of *Arabidopsis*. The tree indicated

that microbial AHASs were grouped together, and they were quite different from plant AHASs. In addition, *At*AHAS was distinct from other PDC proteins in *Arabidopsis* (Figure 3.4). AtAHAS appeared to have evolved in parallel to AHAS of *B. napus* (Bekkaoui et al., 1991). This confirmed that *AtAHAS* is a unique *AHAS* gene in *Arabidopsis* although *AHAS* was shown to be a family of five genes in *Brassica napus* (Ouellet et al., 1992).

A similar tree was generated using the TPP binding domain, a significant structural feature of all known IPDC proteins including the six candidate sequences of *Arabidopsis* (Figure 3.5). The tree showed that AtPDC1-4 were significantly different from the reference microbial IPDC sequences.

### 3.2.5 Microarray data analysis

To investigate differential gene expression of PDC family genes, 4070 ATH1 22k microarray datasets were queried by the Genevestigator software. These results showed that the *PDC* gene family had a different pattern of expression through sequential developmental stages (Figure 3.6). Throughout the entire life cycle, At5g01330 (*AtPDC3*)/At5g01320 (*AtPDC4*) had very low expression while At3G48560 (*AtAHAS*) showed especially high expression. The difference might be related to AtAHAS being a chloroplast localized gene product since chloroplast proteins are among the most abundant cellular proteins. At5G17380 (*AtPDC*-like) and At5g54960 (*AtPDC2*) had very similar expression patterns, which were characterized by maintenance at an abundant expression level relative to the other genes in the family. Interesting, At4g33070

(*AtPDC1*) has a very low level of expression from bolting through the flowering stage, but has a higher level of expression at earlier and later stages.

### 3.2.6 Shade avoidance response (SAR)

The IPA pathway, where tryptophan is converted to IPA followed by decarboxylation to IAAld by IPDC and then oxidized to IAA, had been shown to be one of the main auxin biosynthetic pathways in microbes (Taiz and Zeiger, 1998), and its presence is often found in beneficial plant-associated bacteria (Glick et al. 1999). Based largely on physiological evidence obtained while studying simulated foliar shade (low ratio of red light to far-red light, R:FR) and shade-induced increases in growth of *Arabidopsis* lines, IPDC was postulated to be a potential rate-limiting enzyme in the IPA pathway (Tao et al., 2008). Under low R:FR, CS836803 (a *taa1* mutant defective in a gene encoding an aminotransferase) had the same short hypocotyl phenotype as control (high R:FR) treatment (Figure 3.7; Tao et al., 2008). This finding seemed to confirm that a functional TAA1 was required in order to observe a shade avoidance response (SAR). Based on the hypothesis put forward by Tao et al. (2008), it would be expected then that a mutation of a functional IPDC, if it existed, would have a similar phenotype relative to the SAR as was shown by *taa1*. Mutants of *AtPDC2*, a unique mono-functional *PDC*, showed the same SAR phenotype as WT plants (Chapter 2). This provides genetic evidence that adds support to the *in vitro* analysis that showed no IPDC activity for AtPDC2, provided that the original hypothesis relative to *taa1* and SAR was correct. To investigate if other PDCs were involved in SAR, possibly by acting as an

IPDC that was not detected by our methods, all *pdc* mutants were treated under foliar shade conditions. Mutants of the other members of the *PDC* family genes also showed the same phenotype under SAR conditions as *pdc2* and the wild type plants (Figure 3.7). This observation, coupled with the finding that there was not measurable IPDC activity even in *Arabidopsis* total protein extracts (Chapter 2), suggests that none of the enzymes identified by sequence homology to proteins encoded by the *PDC* family of genes are functionally involved in the SAR and brings into question the relationship between shade avoidance and any IPA-like IAA biosynthetic pathway in *Arabidopsis*.

### 3.2.7 Herbicide resistance assay

The relationship between the *Arabidopsis AHAS* and *PDC* family genes suggested experiments to investigate the inhibition of AHAS-type herbicides on *Arabidopsis* in order to suggest a possible function of one or more members of this gene family. Specifically, if any members of this gene family were functionally involved in the biosynthetic pathway for the branched-chain amino acids, one would expect that a deletion mutation in that gene would alter the response to the herbicide (Zheng et al., 2005). Seedlings of Col-0 and all *pdc* mutants were sprayed with different concentrations of Telar DF (chlorsulfuron; DuPont, DL) and Raptor (ammonium of imazamox; BASF, NC). In the case of Telar treatment, a concentration of 60 µM (301 µg $m^{-2}$) killed 100% of the seedlings while a concentration of 3.8 µM (18.9 µg $m^{-2}$) killed around 80% of the seedlings (Figure 3.8A and 3.8B). This result was consistent with a previous report (Jander et al., 2003). A similar result was observed in the case of Raptor treatment: a concentration of 21 mM (15.76 µg $m^{-2}$) killed 100% of the seedlings while a

concentration of 2.34 mM (1.75 µg $m^{-2}$) killed around 70% of the seedlings (data not shown). To determine the $I_{50}$ (herbicide concentration giving 50% inhibition) concentration of chlorsulfuron and imazamox for *Arabidopsis*, seven-day-old seedlings planted on agar plates were transferred onto a range of herbicide concentrations. Root growth inhibition was observed one day after treatment, while leaves turned yellow in four days and shoot growth inhibition was observed in five to six days. The $I_{50}$ for chlorsulfuron in *Arabidopsis* was estimated in the range of 1 nM to 10 nM while the $I_{50}$ of imazamox was around 10 fold higher than the $I_{50}$ of chlorsulfuron (Figure 3.9A, 3.9B, and 3.9C). Therefore, chlorsulfuron was more active than imazamox for *Arabidopsis*. Considering the similar biological effect caused by chlorsulfuron and imazamox (McCourt et al., 2006), imazamox was used for a more detailed analysis of the $I_{50}$ for inhibition using a greater number of concentration levels. The $I_{50}$ of imazamox for *Arabidopsis* was shown to be 11.8 nM (Figure 3.9D).

All *pdc*-family mutants, including the two *ahas* mutants, did not show any resistance or enhanced sensitivity to chlorsulfuron (data not shown). Similarly, no detectable resistance or increase in sensitivity to imazamox was shown by all the *pdc* mutants (data not shown).

### 3.3 Summary

Among all six *PDC* genes studied, *AtPDC2* is the only structural *PDC* gene found in *Arabidopsis*. No detectable IPDC or PDC enzyme activity was observed in the other *PDC* genes. While this result may seem unusual, it is in fact not dissimilar to the situation observed in yeast, where *PDC1*, *PDC5*, and the weakly expressed *PDC6* are structural genes, while the function of *PDC2* is unknown and expression of the functionally inactive *PDC3* and *PDC4* genes reduce PDC activity and alter glucose fermentation rates accordingly (Hohmann and Cederberg, 1990; Hohmann, 1991). Since the activity of PDC enzymes has been shown to function via formation of a shared active site between dimers (Sergienko and Jordan, 2002), the formation of heterodimers between active and inactive or less active protein pairs appears in yeast to be a mechanism for modulation of overall PDC activity. Such a mechanism for regulation of activity in yeast would in part account for the observation that a *pdc1* deletion mutation had a distinctly different phenotype from the catalytically inactive *pdc1-8* point mutation (Schmitt and Zimmermann, 1982; Schaaff et al., 1989; Hohmann and Cederberg, 1990). Yeast and bacterial PDCs are typically found as tetramers that can dissociate into fully functional dimers after exposure to elevated pH. PDCs of plant origin are known to form aggregate structures from tetramers to complexes as large as 1 MDa (König, 1998), suggesting an essentially endless number of associations composed of hetero- and homo-dimer pairs. In addition, for the PDCs in yeast, it has been shown that deletion of the more strongly expressed *PDC1* gene stimulates the activity of the promoters of both *PDC1* and *PDC5* structural genes. The repressive effect of protein expression on *PDC* transcription also

seems to be independent of the catalytic activity (Eberhardt et al., 1999). This phenomenon is called PDC autoregulation (Hohmann and Cederberg, 1990). While we do not as yet know the proteins that make up the dimer pairs in *Arabidopsis* nor do we know if regulatory responses similar to PDC autoregulation occur with plant *PDC* and *PDC-like* genes, the presence of genes encoding proteins that show no activity, presumably when assayed as homodimers, suggests that a similar mechanism to that proposed for yeast might be possible in *Arabidopsis* as well. This possibility should be explored in future studies and the methods established in this study should allow detailed future investigations on this aspect of PDC regulation in plant systems.

All *Arabidopis PDC* T-DNA insertion mutants were found to share the same responsive phenotype to shade avoidance as did wild-type plants. This result appears to confirm our *in vitro* studies that could not detect IPDC in *Arabidopsis* gene products expressed in *E. coli* nor in enzyme extracts from plant material. It also suggests that the hypothesis that the *TAA1* gene product produces IPA that is acted upon by an IPDC needs to be reexamined.

None of the *pdc* mutants showed a change in resistance to chlorsulfuron or imazamox herbicides, and this result suggests that although related by sequence to the *AHAS* genes, the product of which is the established herbicide target, the gene products are not likely functioning as AHAS-like enzymes involved in branch chain amino acid biosynthesis. This result is also consistent with a hypothesis that the inactive *AtPDC* genes may play a role in PDC activity regulation in *Arabidopsis*.

## 3.4 Experimental procedures

### *3.4.1 Construction of phylogenetic trees*

All known IPDC protein sequences from different microbes and all candidates in *Arabidopsis* were retrieved, aligned, and edited using methods described in Chapter 2. The TPP binding module (for example, amino acid sequence of 385- 466 of *Ec*IPDC) was chosen to demonstrate the genetic distance using Seqboot, Protpars, Consensus, and Drawgram programs in the PHYLIP software package (version 3.68; Felsenstein, 1993).

Similarly, AHAS sequences with the TPP binding domain (for example, 193 amino acids from 391-583 in *B. napus*) were used to demonstrate the relationship of AHAS from different species.

### *3.4.2 Prediction of protein localization sites in cells*

An assortment of bioinformatic software is available to identify subcellular localization target sequences. Analyses of the deduced amino acid sequences of *PDC* gene family members were performed for possible subcellular localizations. The programs utilized for these studies included the web-site versions of: Predotar v.1.03 (http://urgi.versailles.inra.fr/predotar/predotar.html; Small et al. 2004), PSORT (http://psort.ims.u-tokyo.ac.jp/form.html; Nakai and Kanehisa 1991), and TargetP v.1.01 (http://www.cbs.dtu.dk/services/TargetP/; Emanuelson et al. 2007).

### *3.4.3 Microarray data analysis by Genevestigator*

The transcriptional expression data analysis for all six candidate *PDC* genes in plant tissues at different development stages were queried using the Genevestigator software as described in Chapter 2.

*3.4.4 Cloning of all PDC candidate genes*

Cloning of all *PDC* genes was the same as the method used for cloning of *AtPDC2* described in Chapter 2. *AtPDC1*, *AtPDC3*, *AtPDC-like*, and *AtAHAS* were cloned by PCR from cDNA clones U18426, U22953, U25039, and S69379, respectively, provided from the Arabidopsis Biological Resource Center (ABRC). The primers were: ATGGACACCAAAATCGGATCGA and CTACTGAGGATTGGGAGGAC for *AtPDC1*; ATGGACGTCCGAAGTCTACC and CTACTGAGGATTGGGAGGAC for *AtPDC3*; ATGGCGGATAAATCAGAAACCACTCCAC and TTAGTTCTTGTGCTGTAATCTCCCACTC for *AtPDC-like*; ATGGCGGCGGCAACAACAACAACAACAACATC and TCAGTATTTAATCCGGCCATC for AtAHAS. AtPDC4 was cloned from a cDNA stress library (kindly provided by B. Bartel, Rice University) by PCR using the primers ATGGACACCAAAATTGGAGC and CTACTGAGGATTGGGAGGACGA. The clones with insertion of PCR products were chosen for enzyme digestion. A specific pattern of enzyme digestion was used to select colonies for the correct orientation. Plasmid DNA was isolated from positive transformants and was further confirmed by sequencing. Finally, all PDC genes were over-expressed by induction of the expression of T7 RNA

polymerase with 0.5 mM IPTG (isopropyl β-D-1-thiogalactopyranoside). Recombinant proteins were purified using the methods described in Chapter 2.

*3.4.5 SAR of pdc mutants*

Seeds germination, growth conditions, and shade treatments were as described in Chapter 2. T-DNA insertion lines Salk090204, Salk087974, CS872403, Salk142717, Salk053813/Salk002944, and CS836803 were T-DNA insertion mutants of *pdc1*, *pdc3*, *pdc4*, *pdc-like*, *ahas*, and *taa1*, respectively. Their insertions were in exon areas except Salk053813 and Salk002944, whose insertions were in the 5' UTR (untranslated region). All T-DNA insertion lines including CS875641 and Salk066678 (T-DNA insertion lines of mutant *pdc2*) were from the ABRC seed collection.

*3.4.6 Test for herbicide resistance*

For analysis of seedling plants growing on soil, approximately 100 seeds of Col-0 or *pdc* mutants were planted in 9-cm plastic pots. Nine-day-old seedlings were sprayed with Telar® DF (chlorsulfuron, active ingredient 75%; DuPont, DL) and Raptor® (ammonium of imazamox, active ingredient 12.1%; BASF, NC) using a pressurized track sprayer equipped with a TP8004EVS nozzle (Spraying Systems Co., Wheaton, IL) at a boom height of 46 cm and 18.7 mL/$m^2$ carrier volume. Raptor® was applied at 1.75 µg $m^{-2}$ and 15.76 µg $m^{-2}$ while Telar® was applied at 18.9 µg $m^{-2}$ and 301 µg $m^{-2}$. One week after treatment, seedling viability was recorded following visual evaluation.

For analysis of seedlings growing in Petri plants on solid medium, seeds were planted on germination medium as shown in the Appendix. Seven-day-old seedlings were

transferred to the treatment medium supplemented with 0 - 1 µM chlorsulfuron [2-Chloro-N-[[4-methoxy-6-methyl-1.3.5-triazin-2-yl)amino]carbonyl]benzenesulfonamide; Chem Service Inc., West Chester, PA] or 0 - 10 µM imazamox [Raptor®/(RS)-2-(4-Isopropyl-4-methyl-5-oxo-2-imidazolin-2-yl)-5-methoxy-methylnicotinic acid; Chem Service Inc., West Chester, PA] and were allowed to grow for an additional 4 days. Primary root length was measured and the plates were photographed.

## 3.5 References


Bekkaoui, F., Condie, J.A., Neustaedter, D.A., Moloney, M.M. and Crosby, W.L. (1991) Isolation, structure and expression of a cDNA for acetolactate synthase from *Brassica napus*. Plant Mol. Biol. 16 (4): 741–744

Cohen, J.D. and Gray, W.M. (2006) Auxin metabolism and signaling. In: Hedden P, Thomas, S (eds), Plant Hormone Signaling (Annual Plant Reviews, Vol. 24). Blackwell Publishing, Oxford, pp. 37–66

Combet, C., Blanchet, C., Geourjon, C. and Deléage, G. (2000) NPS@: network protein sequence analysis. Trends Biochem. Sci. 25(3): 147–150

Costacurta, A., Keijers, V. and Vanderleyden, J. (1994) Molecular cloning and sequence analysis of an *Azospirillum brasilense* indole-3-pyruvate decarboxylase gene. Mol. Gen. Genet. 243: 463–472

Costelloe, S.J., Ward, J.M. and Dalby, P.A. (2008) Evolutionary analysis of the TPP-dependent enzyme family. J. Mol. Evol. 66: 36–49

Dyda, F., Furey, W., Swaminathan, S., Sax, M., Farrenkopf, B. and Jordan, F. (1993) Catalytic centers in the thiamin diphosphate dependent enzyme pyruvate decarboxylase at 2.4-ANG. resolution. *Biochemistry* 32 (24): 6165–6170

Eberhardt, I., Cederberg, H., Li, H., König S., Jordan F. and Hohmann, S. (1999) Autoregulation of yeast pyruvate decarboxylase gene expression requires the enzyme but not its catalytic activity. Eur. J. Biochem. 262: 191–201

Emanuelsson, O., Brunak, S., von Heijne, G. and Nielsen, H. (2007) Locating proteins in the cell using TargetP, SignalP, and related tools. Nature Protocols 2**:** 953–971

Emanuelsson, O., Nielsen H., Brunak, S. and von Heijne, G. (2000) Predicting subcellular localization of proteins based on their N-terminal amino acid sequence. J. Mol. Biol. 300: 1005–1016

Felsenstein, J. (1993) PHYLIP (phylogeny inference package). Version 3.68. Department of Genetics, University of Washington, Seattle, Washington. Available from http://evolution.genetics.washington.edu/phylip.html

Glick, B.R., Patten, C.L., Holguin, G. and Penrose, D.M. (1999) Biochemical and genetic mechanisms used by plant growth promoting bacteria. Imperial College Press, London, pp. 267

Hawkins, C.F., Borges, A. and Perham, R.N. (1989) A common structural motif in thiamin pyrophosphate-binding enzymes. FEBS Letter 255: 77–82

Hohmann, S. (1991) Characterization of *PDC6*, a third structural gene for pyruvate decarboxylase in *Saccharomyces cerevisiae*. J. Bacteriology 173: 7963–7969

Hohmann, S. and Cederberg, H. (1990) Autoregulation may control the expression of yeast pyruvate decarboxylase structural genes *PDC1* and *PDC5*. Eur. J Biochem 188: 615–621

Hohmann, S. and Meacock, P.A. (1998) Thiamin metabolism and thiamin diphosphate-dependent enzymes in the yeast *Saccharomyces cerevisiae*: genetic regulation. Biochim. Biophys. Acta 1385: 201–219

Jander, G., Baerson, S.R., Hudak, J.A., Gonzalez, K.A., Gruys, K.J. and Last, R.L. (2003) Ethylmethanesulfonate saturation mutagenesis in *Arabidopsis* to determine frequency of herbicide resistance. Plant Physiol. 131: 139–146

Koga J. (1995) Structure and function of indolepyruvate decarboxylase, a key enzyme in indole-3-acetic acid accumulation. Biochim. Biophys. Acta 1249: 1–13

König, S. (1998) Subunit structure, function and organisation of pyruvate decarboxylases from various organisms. Biochim. Biophys. Acta - Protein Struc. and Mol. Enz. 1385**:** 271–286

McCourt, J.A. Pang, S.S., King-Scott, J., Guddat, L.W. and Duggleby R.G. (2006) Herbicide-binding sites revealed in the structure of plant acetohydroxyacid synthase. Proc. Natl. Acad. Sci. 103(3): 569–573

Nakai, K. and Kanehisa, M. (1991) Expert system for predicting protein localization sites in gram-negative bacteria. PROTEINS: Structure, Function, and Genetics 11: 95–110

Ouellet, T., Rutledge, R.G. and Miki, B.L. (1992) Members of the acetohydroxy acid synthase multigene family of *Brassica napus* have divergent patterns of expression. Plant J. 2: 321–330

Roux, F., Matejicek, A., Gasquez, J. and Reboud, X. (2005) Dominance variation across six herbicides of the *Arabidopsis thaliana* csr1-1 and csr1-2 resistance alleles. Pest Manag. Sci. 61: 1089–1095

Schaaff, I., Green, J. B. A., Gozalbo, D. and Hohmann, S. (1989) A deletion of the PDC1 gene for pyruvate decarboxylase of yeast causes a different phenotype than previously isolated point mutations. Curr. Genet. 15: 75–81

Schmitt, H.D. and Zimmermann, F.K. (1982) Genetic analysis of the pyruvate decarboxylase reaction in yeast glycolysis. J. Bacteriology 151: 1146–1152

Sergienko, E.A. and Jordan, F. (2002) Yeast pyruvate decarboxylase tetramers can dissociate into dimers along two interfaces. Hybrids of low-activity D28A (or D28N) and E477Q variants, with substitution of adjacent active center acidic groups from different subunits, display restored activity. Biochemistry 41: 6164–6169

Small, I., Peeters, N., Legeai, F. and Lurin, C. (2004) Predotar: A tool for rapidly screening proteomes for N-terminal targeting sequences. Proteomics 4: 1581–1590

Stepanova, A., Robertson-Hoyt, J., Yun J., Benavente, L., Xie, D., Doležal, K., Schlereth, A., Jürgens, G. and Alonso J. (2008) TAA1-mediated auxin biosynthesis is essential for hormone crosstalk and plant development. Cell 133: 177–191

Taiz, L. and Zeiger, E. (1998) Plant Physiology, 2nd ed., Sinauer Associates, Inc., Publishers, Sunderland, Masachusetts, pp: 543–575

Tao, Y., Ferrer J.-L, Ljung, K., Pojer, F., Hong, F., Long, J. A., Li, L., Moreno, J. E., Bowman, M. E., Ivans, L. J., Cheng Y., Lim, J., Zhao, Y., Balleré, C. L., Sandberg, G., Noel, J. P., Chory, J. (2008) Rapid synthesis of auxin via a new tryptophan-dependent pathway is required for shade avoidance in plants. Cell 133: 164–176

Yamada, M., Greenham, K., Prigge, M.J., Jensen, P.J. and Estelle, M. The *TRANSPORT INHIBITOR RESPONSE2* (*TIR2*) gene is required for auxin synthesis and diverse aspects of plant development. Plant Physiology (Preview DOI:10.1104/pp.109.138859)

Zheng, D., Patzoldt, W.L. and Tranel P.J. (2005) Association of the W574L ALS substitution with resistance to cloransulam and imazamox in common ragweed (*Ambrosia artemisiifolia*). Weed Science 53(4): 424–430

### 3.6 Table

| Gene name | AGI code | Length (aa #) | Prediction tools* | | | Localization (cTP) |
|---|---|---|---|---|---|---|
| | | | Predotar | PSORT | TargetP | |
| *AtPDC1* | At4g33070 | 607 | 0 | 0.126 | 0.199 | No |
| *AtPDC2* | At5g54960 | 607 | 0 | 0.126 | 0.384 | No |
| *AtPDC3* | At5g01330 | 592 | 0.01 | 0.2 | 0.504 | ? |
| *AtPDC4* | At5g01320 | 603 | 0 | 0.126 | 0.433 | No |
| *AtPDC-like* | At5G17380 | 572 | 0.01 | 0.28 | 0.148 | No |
| *AtAHAS* | At3G48560 | 670 | 0.97 | 0.95 | 0.976 | Yes |

Table 3.1 List of predicted protein localizations for six PDC candidate genes. * These three scores show the probability of plastid localization as predicted by the respective programs. If the value is over 0.5, it is likely that the targeting site is the chloroplast and "Yes" will be given to cTP; otherwise, it will be "No". cTP = predicted chloroplast transit peptide; ? = unknown/could not be determined based on conflicting results among the three prediction programs.

### 3.7 Figures

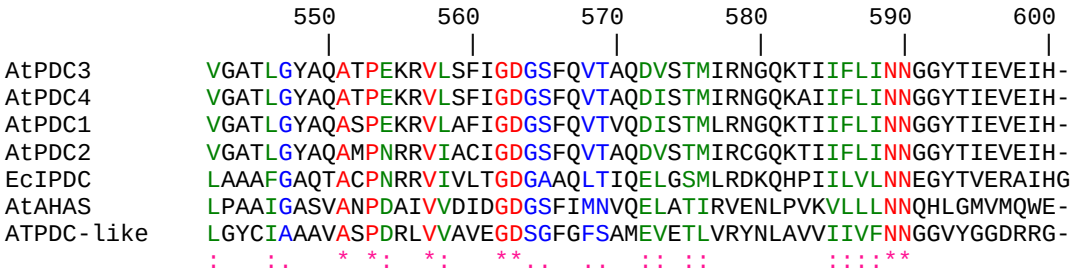


Figure 3.1. Sequence alignments of EcIPDC and homologous proteins from *Arabidopsis*. The ClustalW program (NPS@: Network Protein Sequence Analysis) was used to align the sequences. Numbering corresponds to the location of the specific amino acid residue in the *Ec*IPDC protein. (*At*PDC1, accession number gi: 15234062; *At*PDC2, accession number gi: 15240423; *At*PDC3, accession number gi: 15240952; *At*PDC4, accession number gi: 15240950, *Ec*IPDC of *Enterobacter cloacae*, accession number gi: 118333; *At*AHAS, accession number gi: 58331777; *At*PDC-like, accession number gi: 15237954).

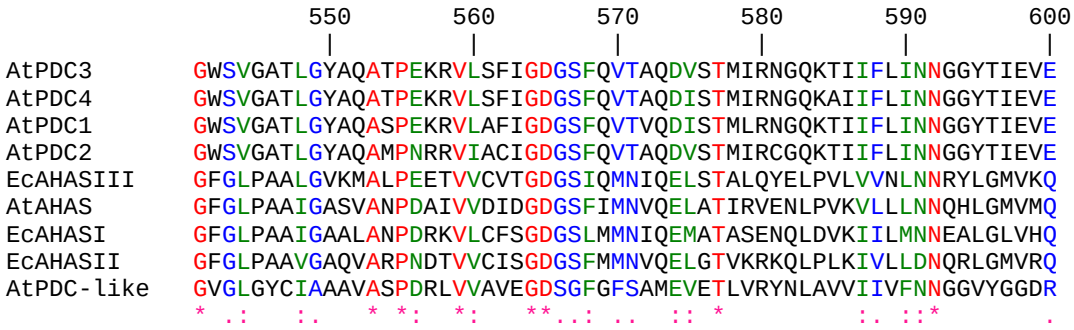


Figure 3.2. Sequence alignments of AHAS from *E. coli* and homologous proteins from *Arabidopsis*. The sequences were aligned by using the ClustalW program (NPS@: Network Protein Sequence Analysis). Numbering corresponds to the location of specific amino acid residues in the AHAS III of *E. coli*. Accession numbers for *At*PDC1, *At*PDC2, *At*PDC3, *At*PDC4, *At*AHAS, and *At*PDC-like are gi: 15234062, 15240423, 15240952, 15240950, 58331777, and 15237954, respectively and accession numbers for *E. coli* AHAS I, II, and III are gi: 89110341, 15833956, and 89106961, respectively.

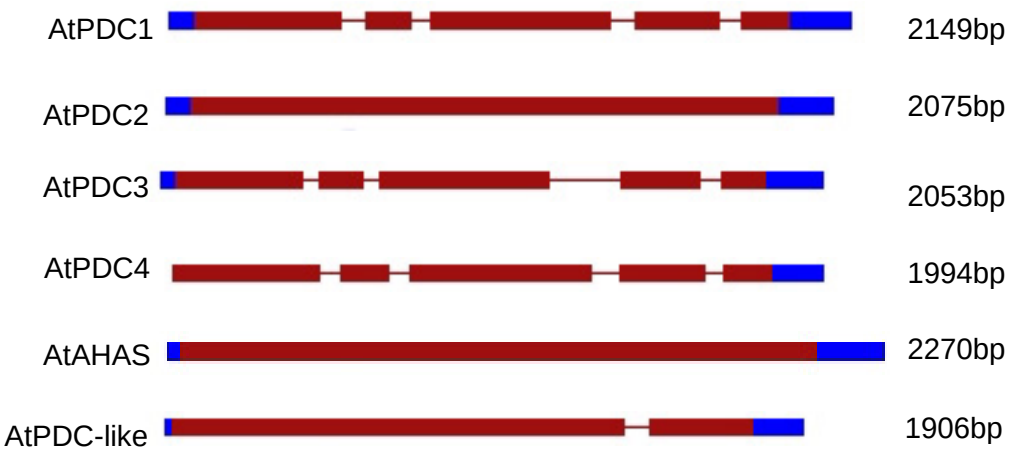


Figure 3.3. The structure of *PDC* candidate genes from *Arabidopsis*. Blue solid rectangle, red solid rectangle, and red line indicate UTR, exon, and intron, respectively. *AtPDC2* and *AtAHAS* are intron free genes while *AtPDC-like* has one intron and *AtPDC1*, *AtPDC3*, and *AtPDC4* each have four introns.

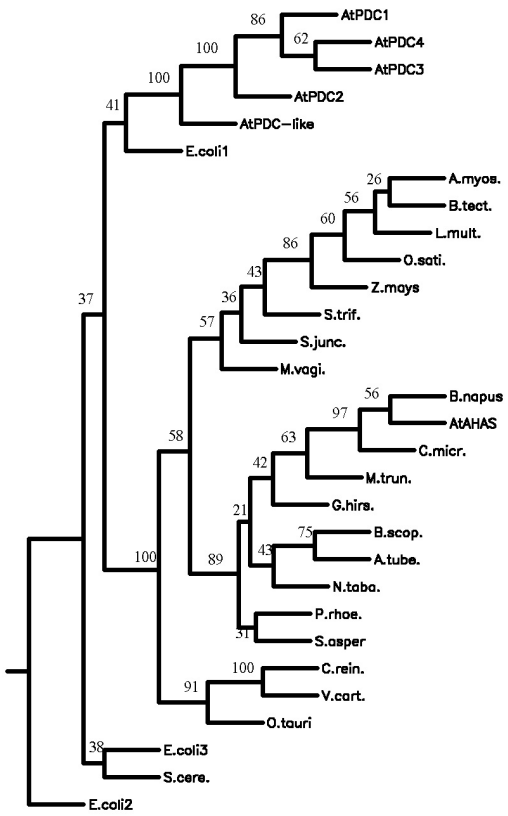


Figure 3.4. Phylogenetic tree showing similarity among AHAS genes. Sequences of AHAS genes are available from GenBank. Phylogenic relationships were calculated with SEQBOOT, PROTPARS, and CONSENSUS programs and created by DRAWGRAM from the PHYLIP software package. The bootstrapped values (out of a total of 100) are indicated on the branches to show the level of support of each node on the tree. Source names are shown as follows: S.cere, Saccharomyces cerevisiae (baker's yeast); V.cart., *Volvox carteri*; C.rein., *Chlamydomonas reinhardtii*; B.scop., *Bassia scoparia* (burningbush); O.sati., *Oryza sativa* (rice); A.myos., *Alopecurus myosuroides* (slender meadow foxtail); M.vagi., *Monochoria vaginalis* (heartshape false pickerelweed); S.junc., *Schoenoplectus juncoides* (rock bulrush); S.trif., *Sagittaria trifolia* (threeleaf arrowhead); B.tect., *Bromus tectorum* (cheatgrass); B.napus, *Brassica napus* (oilseed rape); M.trun., *Medicago truncatula* (annual medic, relative of alfalfa); A.tube., *Amaranthus tuberculatus* (roughfruit amaranth); P.rhoe., *Papaver rhoeas* (corn poppy); S.asper, *Sonchus asper* (spiny sowthistle); C.micr., *Camelina microcarpa* (littlepod false flax); L.mult., *Lolium multiflorum* (Italian ryegrass); O.tauri, *Ostreococcus tauri* (marine green alga; smallest-known free-living eukaryote); N.taba., *Nicotiana tabacum* (tobacco); Z.mays, *Zea mays* (maize, corn); G.hirs., *Gossypium hirsutum* (cotton); E.coli, *Escherichia coli*.

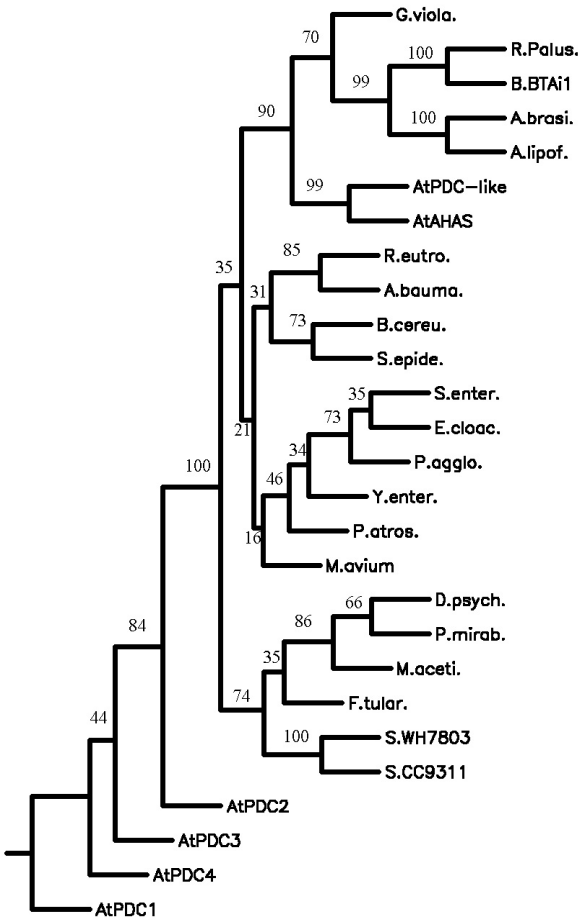


Figure 3.5. Phylogenetic tree showing similarity among microbial IPDC genes and the *Arabidopsis* genes used in this study. Sequences of specific IPDC genes are available from GenBank. Phylogenic relationships were calculated with SEQBOOT, PROTPARS, and CONSENSUS programs and created by DRAWGRAM in the PHYLIP software package. The bootstrapped values (out of a total of 100) are indicated on the branches to show the level of support of each node on the tree. Source names are shown as follows: Y.enter., *Yersinia enterocolitica*; P.atros., *Pectobacterium atrosepticum*; F.tular., *Francisella tularensis*; R.eutro, *Ralstonia eutropha*; B.BTAil, *Bradyrhizobium* sp. BTAi1; S.epide, *Staphylococcus epidermidis*; M.aceti., *Methanosarcina acetivorans*; R.palus., *Rhodopseudomonas palustris*; E.cloac., *Enterobacter cloacae*; A.brasi., *Azospirillum brasilense*; A.lipof., *Azospirillum lipoferum*; P.mirab., *Proteus mirabilis*; B.cereu., *Bacillus cereus*; P.agglo., *Pantoea agglomerans*; S.enter., *Salmonella enterica*; G.viola., *Gloeobacter violaceus*;S.CC9311, *Synechococcus* sp. CC9311; A.bauma., *Acinetobacter baumannii*; M.avium, *Mycobacterium avium*; S.WH7803, *Synechococcus* sp. WH 7803; D.psych., *Desulfotalea psychrophila*.

A

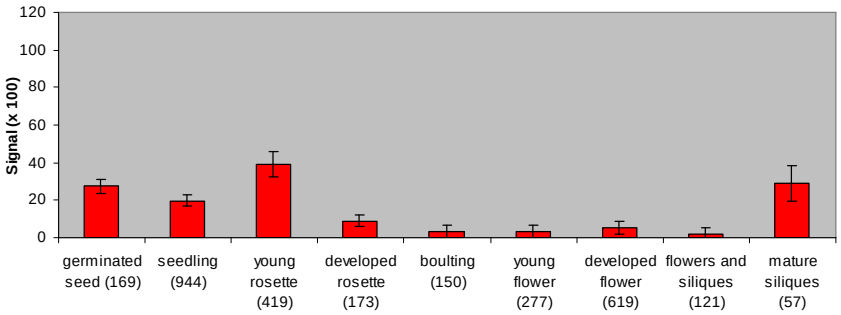
Signal (x 100)
120
100
80
60
40
20
0
germinated seed (169)
seedling (944)
young rosette (419)
developed rosette (173)
boulting (150)
young flower (277)
developed flower (619)
flowers and siliques (121)
mature siliques (57)

B

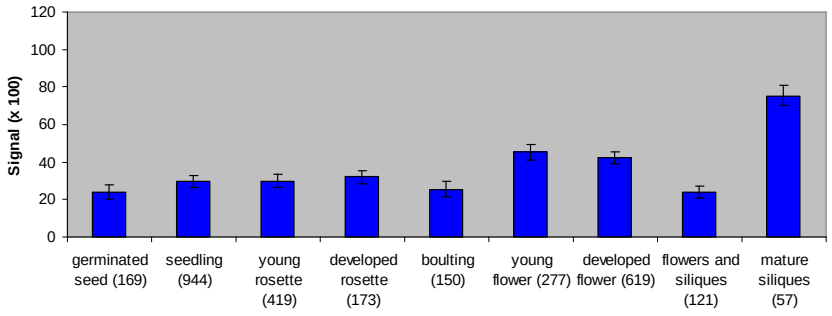
Signal (x 100)
120
100
80
60
40
20
0
germinated seed (169)
seedling (944)
young rosette (419)
developed rosette (173)
boulting (150)
young flower (277)
developed flower (619)
flowers and siliques (121)
mature siliques (57)

C

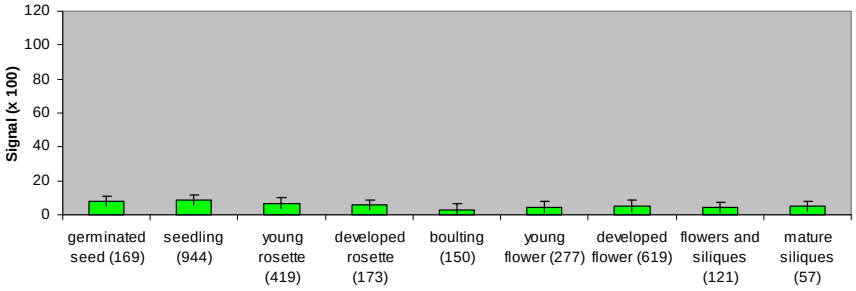
Signal (x 100)
120
100
80
60
40
20
0
germinated seed (169)
seedling (944)
young rosette (419)
developed rosette (173)
boulting (150)
young flower (277)
developed flower (619)
flowers and siliques (121)
mature siliques (57)

D

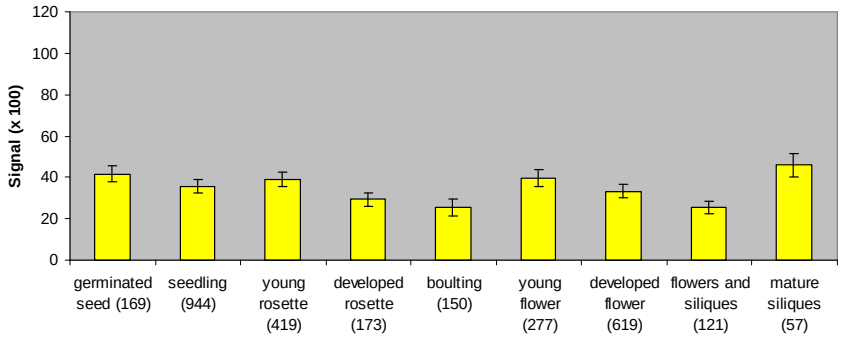
Signal (x 100)
120
100
80
60
40
20
0
germinated seed (169)
seedling (944)
young rosette (419)
developed rosette (173)
boulting (150)
young flower (277)
developed flower (619)
flowers and siliques (121)
mature siliques (57)

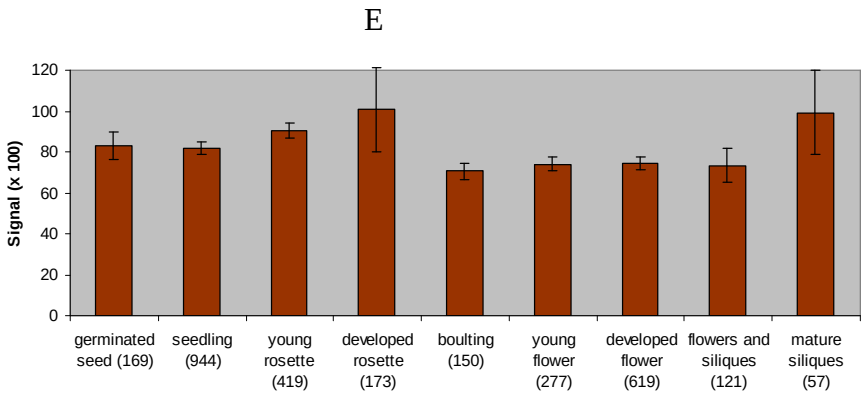


Figure 3.6. The differential expression of *PDC* genes at different stages of development in *Arabidopsis*. 4070 ATH1 22k microarray datasets were queried by the Genevestigator software. (A), gene expression of AT4G33070 (*AtPDC1*); (B), gene expression of AT5G54960 (*AtPDC2*); (C), gene expression of AT5G01330 (*AtPDC3*). Because of almost identical sequence, the expression of *AtPDC3* and *AtPDC4* are likely both reported for the data given for the *AtPDC3* gene. (D), gene expression of *AtPDC-like*; (E), gene expression of *AtAHAS*. The numbers in parentheses indicate the datasets used.

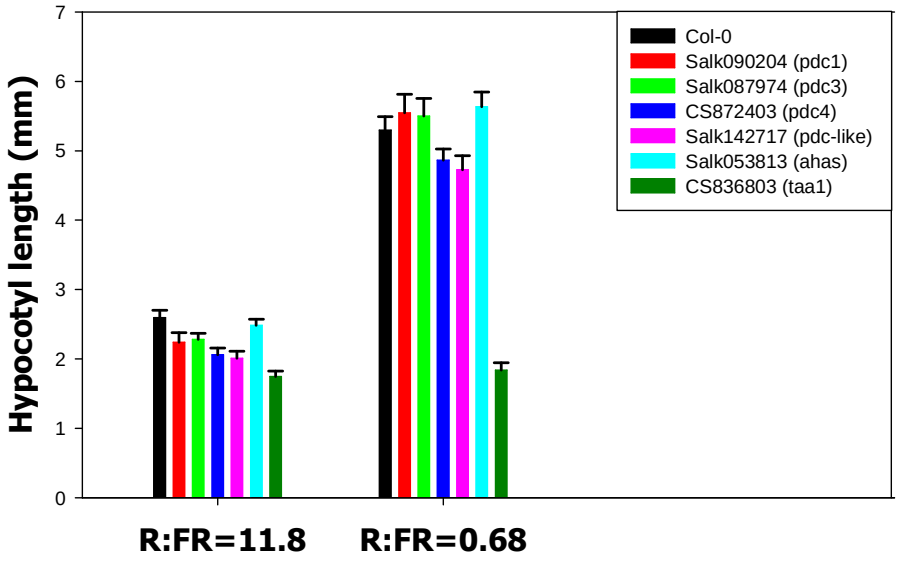


Figure 3.7. Under simulated foliar shade conditions [Red:Far Red (R:FR) ratio of 0.68], plants have longer hypocotyls. Seedlings were grown at 22°C under light of photosynthetically active radiation (PAR) of 50 $\mu E \cdot m^{-2} \cdot s^{-1}$ and R:FR = 11.8 for 5 d and then transferred to shade conditions (PAR 20 $\mu E \cdot m^{-2} \cdot s^{-1}$ and R:FR = 0.68) or control conditions (PAR 20 $\mu E \cdot m^{-2} \cdot s^{-1}$ and R:FR = 11.8) for another 3 days. T-DNA insertion lines are Salk090204 (*pdc1*), Salk087974 (*pdc3*), CS872403 (*pdc4*), Salk142717 (*pdc-1ike*), Salk053813 (*ahas*), and CS836803 (*taa1*). Their T-DNA insertions were in the exon areas except for Salk053813, whose insertion was in the 5' UTR. All insertion lines were from the ABRC (Arabidopsis Biological Resource Center) seed collection.

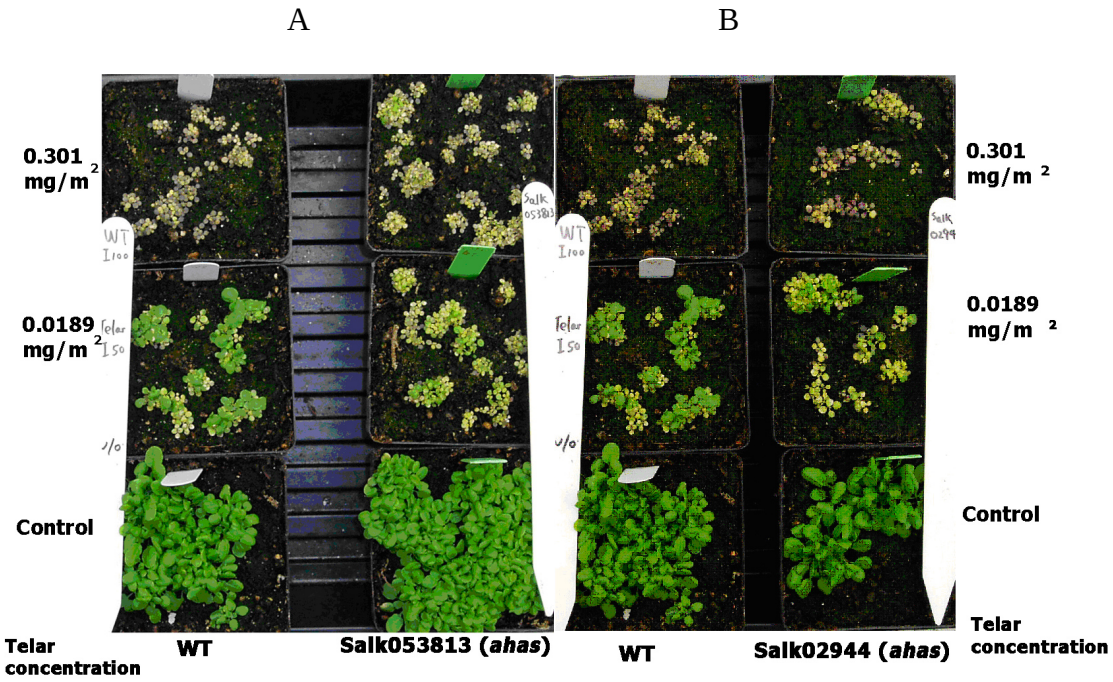


Figure 3.8. Nine-day-old seedlings of Col-0 and the *ahas* mutant were sprayed with 18.9 μg/m$^2$ and 301 μg/m$^2$ Telar®. Plants without treatment (bottom row of four pots) were used as the controls. A, Comparison between Col-0 and Salk053813 (*ahas*) under treatment; B, Comparison between Col-0 and Salk002944 (*ahas*) under treatment.

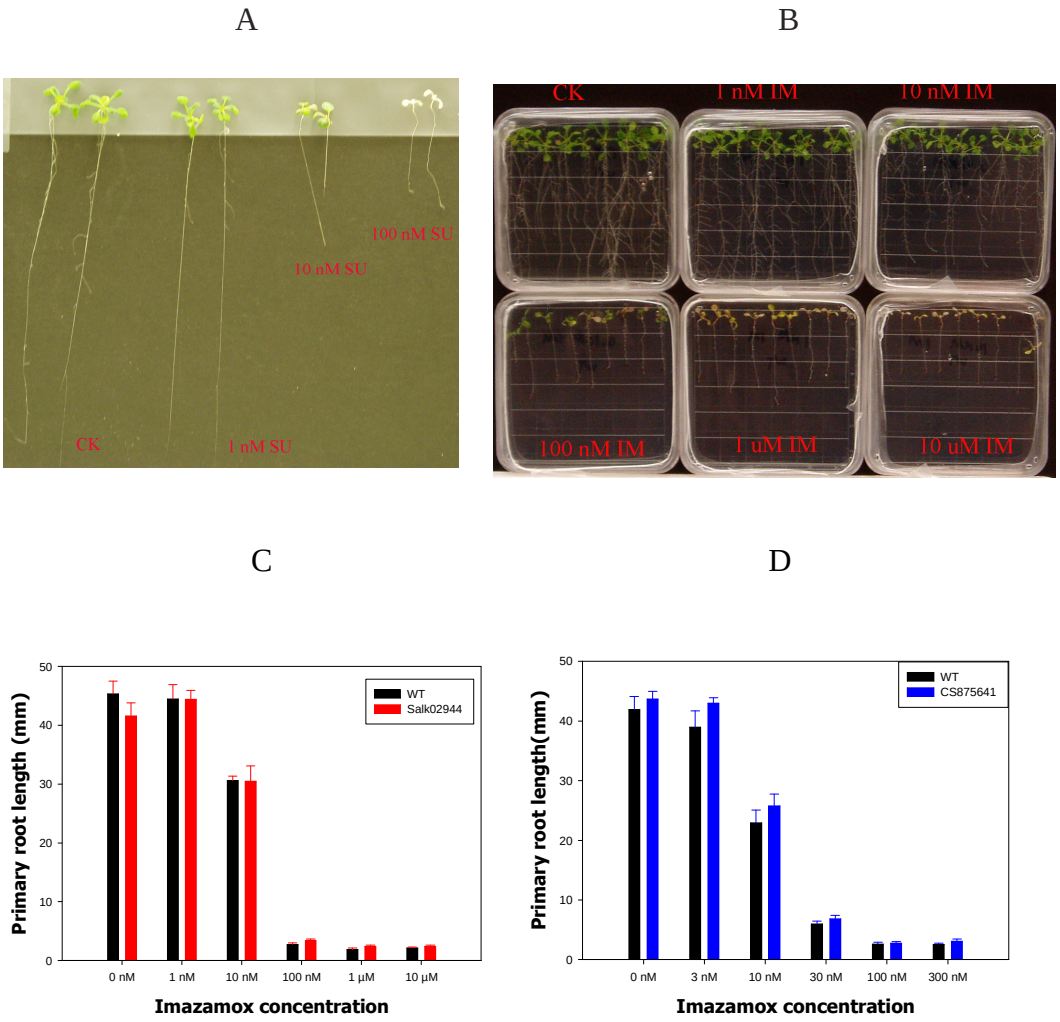


Figure 3.9. The inhibition of *Arabidopsis* growth by treatment with different concentrations of imazamox and chlorsulfuron. Seedlings were grown for 7 days on unsupplemented medium and then transferred to the treatment medium with the indicated concentration of herbicide for an additional 4 days.

A, Representative Col-0 seedlings after being treated with chlorsulfuron (SU) for four days.

B, Inhibition of *Arabidopsis* seedlings (Col-0) treated with imazamox (IM).

C, Primary root growth reduction of both wild-type (black bar) and Salk002944 (*ahas*, red bar) four days following 0–10 µM treatment with the herbicide. The primary root lengths were measured (n=9). Error bars indicate standard error of the mean **(**SEM).

D, Primary root growth reduction of both wild-type (black bar) and CS875641 (*pdc2*, see Chapter 2, blue bar) under 0–300 nM herbicide treatment. The length of the primary roots was measured (n > 8). Error bars indicate SEM.

# Summary and Future Directions

## 4.1 Summary of work and main conclusions

### 4.1.1 *At*PDC2 is a unique functional PDC of *Arabidopsis*

Pyruvate decarboxylase is a critical enzyme in plant metabolism that regulates energy production especially during periods of anaerobic stress. As shown in this work, *At*PDC2 has now been identified in Chapter 2 as a unique monofunctional PDC in *Arabidopsis,* and this result was confirmed by methods of molecular cloning, biochemical characterization, and GC-MS analysis of putative products. In Chapter 3 it was shown that proteins expressed from the genes with close homology to *AtPDC2* lacked both PDC and IPDC activity, and it was proposed that this might suggest a regulatory role for these proteins in modulation of PDC activity, similar to a mechanism found in yeast.

### 4.1.2 AtPDC2 has PDC activity but lacks significant activity toward indole-3-pyruvate

It had been demonstrated that PDC and IPDC are bi-functional activities of the same proteins in microbes. Enzymes that are primarily either a PDC or an IPDC protein display activities of varying levels of activity toward both substrates: pyruvate and indole-3-pyruvate. This has led to an unresolved question in plant metabolism since indole-3-pyruvate is thought to be a precursor to the signaling molecule indole-3-acetic acid and production of substantial levels of a signal regulator by a respiratory regulatory enzyme was difficult to reconcile with our understanding of hormonal signaling systems. However, in Chapter 2 it was shown that there was no significant IPDC activity in the

AtPDC2 protein expressed in *E. coli* although it was a fully functional PDC. In Chapter 3, data were presented that showed the proteins produced in *E. coli* for other *Arabidopsis* genes with close homology to PDCs, as well as *Arabidopsis* protein extracts, lacked measurable IPDC activity even when assayed by a sensitive and exacting GC-MS based method. These findings bring into question the role of the proposed IPA pathway to IAA in plants since without a functional IPDC activity; it is now not clear how such a process might proceed.

### 4.1.3 Enzymatic activity of IPDC is measured by GC-MS methods

Due to the fact that indolepyruvate and indoleacetaldehyde are both unstable in solution and during analytical procedures, it is difficult to accurately measure IPDC activity using traditional assays including those based on HPLC. In Chapter 2, indole carboxaldehyde was introduced as an internal standard in order to accurately measure the levels of indole acetaldehyde produced in the enzymatic assays by using GC-MS for detection. This provided an accurate quantitative assay with high assurance of product identity. Assays of plant-derived enzymes, however, produced no measurable IAAld even when spiked with active *Ec*IPDC protein. This appeared to be due to the aldehyde reacting with something in the plant extracts. Thus, in order to assay the products formed from proteins isolated from *Arabidopsis* plant extracts, the GC-MS based IPDC assay method was modified by using a coupled reaction that rapidly converted IAAld formed in the reaction to IAA by using a commercial aldehyde dehydrogenase (ALDH) and assaying the IAA formed by GC-MS after methylation. Both of these methods are highly

sensitive and accurate for the assay of IPDC activity, as determined by using a positive control, *Ec*IPDC.

Taken together, the results of this work represent the first comprehensive functional analysis of the PDC gene family in *Arabidopsis*. The results show that many of the preconceived ideas about these genes need to be reevaluated. Specifically, there appears to be only a single active PDC, AtPDC2, and it lacks IPDC activity. The other members of this family appear to be inactive and this suggests a regulatory function for these proteins. Finally, deletion mutants of each member of the PDC family all fail to give an altered shade avoidance response, providing genetic evidence that they are not functionally linked to the activity of the TAA1 gene.

### 4.2 Future directions

These experiments open up at least three directions for future studies. First, the disconnect between the relationship between TAA1 and IPDC should provide important guidance for additional studies of the shade avoidance response in plants. Second, the possibility of alternative reactions substituting for an active IPDC needs additional attention before the IPA pathway in *Arabidopsis* can be excluded. Finally, understanding the role of the inactive PDC proteins, potentially as regulatory proteins, need to be followed up in a plant system, and these data now make *Arabidopsis* the most advanced plant species in which to pursue such studies.

TAA1, an aminotransferase proposed to be linked to plant IPDC activity by catalysis of the step previous to a IPDC function in the IPA pathway, has recently been substantially studied in plants by at least three groups (Tao et al., 2008; Stepanova et al., 2008; Yamada et al., 2009). It was proposed that TAA1 might be involved in organ development and responses to ethylene, auxin transport inhibitors, and shade avoidance. However, a gene(s) encoding a functional IPDC enzyme, which is the rate-limiting step of the IPA pathway in microbes, has not been identified in plants. These present studies show that the genes most likely to be candidates for an IPDC lack such activity. Furthermore, every single gene T-DNA insertion mutant of these candidate genes identified by sequence homology did not show *taa1*-like phenotypes (Table 4.1). While it might be important to determine the shade avoidance phenotype of double, triple, or quadruple *pdc* insertion lines to assuage any doubts about functions of heterodimers, a more fruitful approach for future studies is to determine the metabolic fate of IPA in plants. As *Arabidopsis* has a wealth of novel indolic pathways, it is far from certain at this point that IPA serves as a precursor to IAA *in vivo*.

The dilemma faced by pollen during germination is to balance between rapid growth, a process of high energy consumption in competitive environments, while managing the conditions of an energy crisis such as hypoxia or even anoxia. Thus, pollen tube elongation may result in the redirection of energy metabolism to ethanolic fermentation, in which ethanol is produced during pyruvate assimilation by PDC and other enzymes. PDC2, the only PDC expressed in petunia pollen, is the rate-limiting enzyme in the PDH bypass pathway, which provides acetyl-CoA to maintain energy

production (Gass et al., 2005). The situation is more complex in other tissues, for example in roots during flooding. In order to better understand regulation of the functional activity of PDC, it will be critical to identify which genes are expressed during pollen germination as well as during other times of respiratory stress. The data in this thesis suggest that a fruitful area for future study is to examine the role of heterodimers in the regulation of activity of the functional enzyme. A combination of immunoaffinity approaches, coupled with analysis of the specific proteins, should help resolve some of these questions. In addition, more detailed expression analysis, perhaps by monitoring GFP localization following expression using PDC-GFP constructs driven by the promoter of each PDC would be helpful. In addition, gene expression of each PDC can be identified by real-time quantitative PCR. This method will be useful to confirm PDC autoregulation using *pdc* mutants and to detect which PDC is induced under different stress conditions such as cold, anoxia, or even pollen elongation. Finally, a technique used with yeast, where the promoters and structural genes are interchanged, might be useful to understand the relationship among the PDC genes in the family.

| Gene name | AGI code | Mutants (insertion position) | Overexpression lines |
|---|---|---|---|
| AtPDC1 | At4g33070 | Salk090204, exon | pBI1.4t-PDC1 |
| AtPDC2 | At5g54960 | Salk066678 (5' UTR)<br>CS875641 (exon)<br>Salk053097 (5' UTR) | pX7-PDC2 |
| AtPDC3 | At5g01330 | Salk087974 (exon) | pBI1.4t-PDC3 |
| APDC4 | At5g01320 | CS872403 (exon)<br>CS843662 (5' UTR) | pBI1.4t-PDC4 |
| AtPDC-like | At5G17380 | Salk142717 (exon) | N/A |
| AtAHAS | At3G48560 | Salk002944 (5' UTR)<br>Salk053813 (5' UTR) | N/A |
| EcIPDC | | | pX7-IPDC |

Table 4.1 A list of the T-DNA insertion lines and overexpression lines of PDC family genes used in this study. The T-DNA lines were obtained form sources detailed in each chapter and the overexpression lines were generated in these studies. UTR, untranslation region; N/A, homozygous lines are not available yet; pX7 is an estrogen-receptor-based chemically-inducible system (kindly provided by Dr. Nam-Hai Chua, The Rockefeller University); pBI1.4t, a plant transformation vector with modified CaMV 35S promoter (kindly provided by Dr. Fumi Katagiri, University of Minnesota).

## 5.1 Bibliography

Aloni, R. (1995) The induction of vascular tissue by auxin and cytokinin. In Plant Hormones and Their Role in Plant Growth Development, 2nd ed., P.J. Davies, ed., Kluwer, Dordrecht, Netherlands, pp. 531–546

Aloni, R., Langhans, M., Aloni, E. and Ullrich C.I. (2004) Role of cytokinin in the regulation of root gravitropism. Planta 220(1): 177–182

Alonso, J.M., et al. (2003). Genome-wide insertional mutagenesis of *Arabidopsis thaliana*. Science 301: 653–657

Alonso, J.M., Hirayama, T., Roman, G., Nourizadeh, S. and Ecker, J.R. (1999) EIN2, a bifunctional transducer of ethylene and stress responses in *Arabidopsis*. Science 284: 2148–2152

Anderson, P.C. and Georgeson, M. (1989) Herbicide-tolerant mutants of corn. Genome 31(2): 994–999

Baburina, I., Gao, Y., Hu, Z., Jordan, F., Hohmann, S. and Furey, W. (1994) Substrate activation of brewers' yeast pyruvate decarboxylase is abolished by mutation of cysteine 221 to serine. Biochemistry 33: 5630–5635

Baldi, B.G., Maher, B.R., Slovin, J.P. and Cohen, J.D. (1991) Stable isotope labeling, *in vivo*, of d- and l-tryptophan pools in *Lemna gibba* and the low incorporation of label into indole-3-acetic acid. Plant Physiology 95(4): 1203–1208

Bandurski, R.S., Cohen, J.D. and Slovin, J.P. (1995) Auxin biosynthesis and metabolism. In: Plant Hormones: Physiology, Biochemistry and Molecular Biology. P.J. Davies, ed. Kluwer Academic Publ., Dordrecht, pp. 35–57

Barkawi, L.S., Tam, Y.Y., Tillman, J.A., Pederson, B., Calio, J., Al-Amier, H., Emerick, M., Normanly, J. and Cohen, J.D. (2008) A high-throughput method for the quantitative analysis of indole-3-acetic acid and other auxins from plant tissue. Anal. Biochem. 372: 177–188

Bartel, B. (1997) Auxin biosynthesis. Annual Review of Plant Physiology and Plant Molecular Biology 48: 51–66

Bartel, B. and Fink, G.R. (1994) Differential regulation of an auxin-producing nitrilase gene family in Arabidopsis thaliana. Proc. Natl. Acad. Sci. USA 91: 6649–6653

Bartel, B., LeClere, S., Magidin, M. and Zolman, B.K. (2001) Inputs to the active indole-3-acetic acid pool: *de novo* synthesis, conjugate hydrolysis, and indole-3-butyric acid β-oxidation. Journal of Plant Growth Regulation 20: 198–216.

Baxter-Burrell, A., Chang, R., Springer, P. and Bailey-Serres, J. (2003) Gene and enhancer trap transposable elements reveal oxygen deprivation regulated genes and their complex patterns of expression in *Arabidopsis*. Annals of Botany 91: 129–141

Bechtold, N. and Pelletier, G. (1998). In planta Agrobacterium-mediated transformation of adult *Arabidopsis thaliana* plants by vacuum infiltration. Methods in Mol. Biol. 82: 259–266

Beemster, G. T. S., Fiorani, F. and Inzé, D. (2003) Cell cycle: the key to plant growth control? Trends Plant Sci. 8: 154–158

Bekkaoui, F., Condie, J.A., Neustaedter, D.A., Moloney, M.M. and Crosby, W.L. (1991) Isolation, structure and expression of a cDNA for acetolactate synthase from *Brassica napus*. Plant Mol. Biol. 16 (4): 741–744

Belanger, F.C., Leustek, T., Chu, B. and Kriz, A.L. (1995) Evidence for the thiamine biosynthetic pathway in higher-plant plastids and its developmental regulation. Plant Mol. Biol. 29: 809–821

Benková, E., Michniewicz, M., Sauer, M., Teichmann, T., Seifertova, D., Jurgens, G. and Friml, J. (2003) Local, efflux-dependent auxin gradients as a common module for plant organ formation. Cell 115: 591–602

Besseau, S., Hoffmann, L., Geoffroy, P., Lapierre, C., Pollet, B. and Legrand, M. (2007) Flavonoid accumulation in *Arabidopsis* repressed in lignin synthesis affects auxin transport and plant growth. Plant Cell 19: 148–162

Bettendorff, L., Wirtzfeld, B., Makarchikov, A.F., Mazzucchelli, G., Frédérich, M., Gigliobianco, T., Gangolf, M., De Pauw, E., Angenot, L. and Wins, P. (2007) Discovery of a natural thiamine adenine nucleotide. Nature Chemical Biology 3: 211–212

Bhalerao, R.P., Eklof, J., Ljung, K., Marchant, A., Bennett, M. and Sandberg, G. (2002) Shoot-derived auxin is essential for early lateral root emergence in *Arabidopsis* seedlings. Plant J. 29: 325–332

Blilou, I., Xu, J., Wildwater, M., Willemsen, V., Paponov, I., Friml, J., Heidstra, R., Aida, M., Palme, K. and Scheres, B. (2005) The PIN auxin efflux facilitator network controls growth and patterning in *Arabidopsis* roots. Nature 433: 39–44

Boiteux, A. and Hess, B. (1970) Allosteric properties of yeast pyruvate decarboxylase. FEBS Letter 9: 293–296

Bourquin, M. and Pilet, P.E. (1990) Effect of zeatin on the growth and indolyl-3-acetic acid and abscisic acid levels in maize roots. Physiologia Plantarum 80: 342–349

Branco-Price, C., Kawaguchi, R., Ferreira, R.B. and Bailey-Serres, J. (2005) Genome-wide analysis of transcript abundance and translation in *Arabidopsis* seedlings subjected to oxygen deprivation. Annals of Botany 96(4): 647–660

Brown, D.E., Rashotte, A.M., Murphy, A.S., Normanly, J., Tague, B.W., Peer, W.A., Taiz, L. and Muday, G.K. (2001) Flavonoids act as negative regulators of auxin transport in vivo in *Arabidopsis*. Plant Physiol. 126: 524–535

Browse, J. (2005) Jasmonate: an oxylipin signal with many roles in plants. Vitamins and Hormones 72: 431–456

Bucher, M., Brander, K.A., Sbicego, S., Mandel, T. and Kuhlemeier, C. (1995) Aerobic fermentation in tobacco pollen. Plant Mol. Biol. 28(4): 739–750

Budavari, S., O'Neil, M.J., Smith, A., Heckelman, P.E. and Kinneary, J.F. (1996) The Merck Index: an encyclopedia of chemicals, drugs, and biologicals. 12th edition, Merck Research Laboratories, Whitehouse Station, NJ, pp. 1088, #6429

Buer, C.S. and Muday, G.K. (2004). The transparent testa4 mutation prevents flavonoid synthesis and alters auxin transport and the response of Arabidopsis roots to gravity and light. Plant Cell 16: 1191–1205

Casimiro, I., Beeckman, T., Graham, N., Bhalerao, R., Zhang, H., Casero, P., Sandberg, G. and Bennett, M.J. (2003) Dissecting *Arabidopsis* lateral root development. Trends Plant Sci. 8: 165–171

Casimiro, I., Marchant, A., Bhalerao, R.P., Beeckman, T., Dhooge, S., Swarup, R., Graham, N., Inze, D., Sandberg, G., Casero, P.J. and Bennett, M. (2001) Auxin transport promotes *Arabidopsis* lateral root initiation. Plant Cell 13: 843–852

Celenza, J.L., Jr., Grisafi, P.L. and Fink, G.R. (1995) A pathway for lateral root formation in *Arabidopsis thaliana*. Genes Dev. 9: 2131–2142

Chabregas, S.M., Luche, D.D., Farias, L.P., Ribeiro, A.F., van Sluys, M.A., Menck, C.F.M. and Silva-Filho, M.C. (2001) Dual targeting properties of the N-terminal signal sequence of *Arabidopsis thaliana* THI1 protein to mitochondria and chloroplasts. Plant Mol. Biol. 46: 639–650

Chang, A.K. and Duggleby, R.G. (1997) Expression, purification and characterization of *Arabidopsis thaliana* acetohydroxyacid synthase. Biochem. J. 327: 161–169

Chang, A.K. and Duggleby, R.G. (1998) Herbicide-resistant forms of *Arabidopsis thaliana* acetohydroxyacid synthase: characterization of the catalytic properties and sensitivity to inhibitors of four defined mutants. Biochem. J. 333: 765–777

Chang, C., Kwok, S.F., Bleecker, A.B. and Meyerowitz, E.M. (1993) *Arabidopsis* ethylene-response gene ETR1: similarity of product to two-component regulators. Science 262: 539–544

Chatterjee, A., Jurgenson, C.T., Schroeder, F.C., Ealick, S.E. and Begley, T.P. (2006) Thiamin biosynthesis in eukaryotes: characterization of the enzyme-bound product of thiazole synthase from *Saccharomyces cerevisiae* and its implications in thiazole biosynthesis. Journal of the American Chemical Society 128: 7158–7159

Chatterjee, A., Jurgenson, C.T., Schroeder, F.C., Ealick, S.E. and Begley, T.P. (2007) Biosynthesis of thiamin thiazole in eukaryotes: conversion of NAD to an advanced intermediate. Journal of the American Chemical Society 129: 2914–2922

Cheah, M.T., Wachter, A., Sudarsan, N. and Breaker, R.R. (2007) Control of alternative RNA splicing and gene expression by eukaryotic riboswitches. Nature 447: 497–500

Cheng, Y., Dai, X. and Zhao, Y. (2006) Auxin biosynthesis by the YUCCA flavin monooxygenases controls the formation of floral organs and vascular tissues in *Arabidopsis*. Genes and Dev. 20: 1790–1799

Chipman, D.M, Duggleby, R.G. and Tittmann, K. (2005) Mechanisms of acetohydroxyacid synthases. Current Opinion in Chemical Biology 9: 475–481

Chipman, D.M., Barak, Z. and Schloss, J.V. (1998) Biosynthesis of 2-aceto-2-hydroxy acids: acetolactate synthases and acetohydroxyacid synthases. Biochim Biophys Acta 1385: 401–419

Ciesielski, T. (1872) Untersuchungen uber die Abwartskrummung der Wurzel. Beitraege zur Biologie der Pflanzen 1: 1–17

Cohen, J.D. and Gray, W.M. (2006) Auxin metabolism and signaling. In: Hedden P, Thomas, S (eds), Plant Hormone Signaling (Annual Plant Reviews, Vol. 24). Blackwell Publishing, Oxford, pp. 37–66

Cohen, J.D. and Meudt W.J. (1983) Investigations on the mechanism of the brassinosteroid response. I. Indole‐3‐acetic acid metabolism and transport. Plant Physiol. 72: 691‐694

Collins, T.J. (2007) ImageJ for microscopy. BioTechniques 43 (1 Suppl): 25–30

Colón-Carmona, A., You, R., Haimovitch-Gal, T. and Doerner, P. (1999) Technical advance: spatio-temporal analysis of mitotic activity with a labile cyclin-GUS fusion protein. Plant J. 20: 503–508

Combet C., Blanchet, C., Geourjon, C. and Deléage, G. (2000) NPS@: network protein sequence analysis. Trends Biochem Sci. 25(3): 147–150

Cooke, T.J., Poli, D.B., Sztein, A.E. and Cohen, J.D. (2002) Evolutionary patterns in auxin action. Plant Mol. Biol. 49: 319-338

Cooney, T.P. and Nonhebel, H.M. (1989) The measurement and mass spectral identification of indole-3-pyruvate from tomato shoots. Biochem. Biophys. Res. Commun. 162: 761–766

Cooney, T.P. and Nonhebel, H.M. (1991) Biosynthesis of indole-3-acetic acid in tomato shoots: measurement, mass spectral identification and incorporation of $^{2}H$ from $^{2}H_2O$ into indole-3-acetic acid, D- and L-tryptophan, indole-3-pyruvate and tryptamine. Planta 184: 368–376

Costacurta, A. and Vanderleylden, J. (1995) Synthesis of phytohormones by plant-associated bacteria. Crit. Rev. Microbiol. 21: 1–18

Costacurta, A., Keijers, V. and Vanderleyden, J. (1994) Molecular cloning and sequence analysis of an *Azospirillum brasilense* indole-3-pyruvate decarboxylase gene. Mol. Gen. Genet. 243: 463–472

Costelloe, S.J., Ward, J.M. and Dalby, P.A. (2008) Evolutionary analysis of the TPP-dependent enzyme family. J. Mol. Evol. 66: 36–49

Creelman, R.A. and Mullet, J.E. (1997) Biosynthesis and action of jasmonates in plants. Annu. Rev. Plant Physiol. Plant Mol. Biol. 48: 355–381

Croft, M.T., Moulin, M., Webb, M.E. and Smith, A.G. (2007) Thiamine biosynthesis in algae is regulated by riboswitches. Proc. Natl. Acad. Sci. USA 104: 20770–20775

Culler, A.H. (2007) Analysis of the tryptophan-dependent indole-3-acetic acid biosynthesis pathway in maize endosperm. PH.D. thesis, University of Minnesota, Twin Cities.

Dannenburg, W.N. and Liverman, J.L. (1957) Conversion of tryptophan-2-C14 to indoleacetic acid by watermelon tissue slices. Plant Physiology 32: 263–269

Davies, P. (2005) Regulatory factors in hormone action: level, location and signal transduction. In: Plant Hormones: Biosynthesis, Signal Transduction, Action! (3rd edition). Davies, P.J. ed. Kluwer Academic Publ., Dordrecht, pp. 16–35

Davies, R.T., Goetz, D.H., Lasswell, J., Anderson, M.N. and Bartel, B. (1999) IAR3 encodes an auxin conjugate hydrolase from *Arabidopsis*. Plant Cell 11: 365–376

De Smet, I., Tetsumura, T., De Rybel, B., Frey, N.F., Laplaze. L., Casimiro, I., Swarup, R., Naudts, M., Vanneste, S., Audenaert, D., Inzé, D., Bennett, M.J. and Beeckman, T. (2007) Auxin-dependent regulation of lateral root positioning in the basal meristem of *Arabidopsis*. Development 134: 681–690

De Smet, I., Vanneste, S., Inzé, D. and Beeckman, T. (2006) Lateral root initiation or the birth of a new meristem. Plant Mol. Biol. 60: 871-887

Desgagné-Penix, I. and Sponsel, V.M. (2008) Expression of gibberellin 20-oxidase1 (AtGA20ox1) in *Arabidopsis* seedlings with altered auxin status is regulated at multiple levels. J. Experimental Botany 59: 2057–2070

Desgagné-Penix, I., Eakanunkul, S., Coles, J.P., Phillips, A.L., Hedden, P. and Sponsel, V.M. (2005) The auxin transport inhibitor response 3 (*tir3*) allele of BIG and auxin transport inhibitors affect the gibberellin status of *Arabidopsis*. Plant J. 41: 231–242

Dharmasiri, S., Swarup, R., Mockaitis, K., Dharmasiri, N., Singh, S.K., Kowalchyk, M., Marchant, A., Mills, S., Sandberg, G., Bennett, M.J., and Estelle, M. (2006) AXR4 is required for localization of the auxin influx facilitator AUX1. Science 312: 1218-1220

Dietrich, A. and König, S. (1997) Substrate activation behaviour of pyruvate decarboxylase from *Pisum sativum* cv. Miko. FEBS Letters 400: 42–44

Dombrecht, B., Xue, G.P., Sprague, S.J., Kirkegaard, J.A., Ross, J.J., Reid, J.B., Fitt, G.P., Sewelam, N., Schenk, P.M., Manners, J.M. and Kazan, K. (2007) MYC2 differentially modulates diverse jasmonate-dependent functions in *Arabidopsis*. Plant Cell 19: 2225–2245

Dubrovsky, J.G., Rost, T.L., Colón-Carmona, A. and Doerner, P. (2001) Early primordium morphogenesis during lateral root initiation in *Arabidopsis thaliana*. Planta 214: 30–36

Dubrovsky, J.G., Sauer, M., Napsucialy-Mendivil, S., Ivanchenko, M.G., Friml, J., Shishkova, S., Celenza, J. and Benkova, E. (2008). Auxin acts as a local morphogenetic trigger to specify lateral root founder cells. Proc. Natl. Acad. Sci. USA 105: 8790–8794

Duggleby, R.G., McCourt, J.A. and Guddat, L.W. (2008) Structure and mechanism of inhibition of plant acetohydroxyacid synthase. Plant Physiology and Biochemistry 46: 309–324

Dullaart, J. (1970) The Auxin Content of Root Nodules and Roots of *Alnus glutinosa* (L.) Vill.. Journal of Experimental Botany 21(4): 975–984

Dunlap, J.R. and Robacker, K.M. (1990) Abscisic acid alters the metabolism of indole-3-acetic acid in senescing flowers of *Cucumis melo* L. Plant Physiology 94: 870–874

Dyda, F., Furey, W., Swaminathan, S., Sax, M., Farrenkopf, B. and Jordan, F. (1993) Catalytic centers in the thiamin diphosphate dependent enzyme pyruvate decarboxylase at 2.4-Å resolution. Biochemistry 32 (24): 6165–6170

Eberhardt, I., Cederberg, H., Li, H., König S., Jordan F. and Hohmann, S. (1999) Autoregulation of yeast pyruvate decarboxylase gene expression requires the enzyme but not its catalytic activity. Eur. J. Biochem. 262: 191–201

Eklöf, S., Astot, C., Sitbon, F., Moritz, T., Olsson, O. and Sandberg, G. (2000) Transgenic tobacco plants co-expressing Agrobacterium iaa and ipt genes have wild-type hormone levels but display both auxin- and cytokinin-overproducing phenotypes. Plant Journal 23: 279–284

Emanuelsson, O., Brunak, S., von Heijne, G. and Nielsen, H. (2007) Locating proteins in the cell using TargetP, SignalP, and related tools. Nature Protocols 2: 953–971

Emanuelsson, O., Nielsen H., Brunak, S. and von Heijne, G. (2000) Predicting subcellular localization of proteins based on their N-terminal amino acid sequence. J. Mol. Biol. 300: 1005–1016

Engelen-Eigles, G., Holden, G., Cohen, J.D. and Gardner, G. (2006) The effect of temperature, photoperiod, and light quality on gluconasturtiin concentration in watercress (*Nasturtium officinale* R. Br.). Journal of Agricultural and Food Chemistry 54 (2): 328–334

Engvild, K.C. (1996) Herbicidal activity of 4-chloroindoleacetic acid and other auxins on pea, barley and mustard. Physiologia Plantarum 96: 333–337

Epstein, E. and Lavee, S. (1984) Conversion of indole-3-butyric acid to indole-3-acetic acid by cuttings of grapevine (*Vitus vinifera*) and olive (*Olea europa*). Plant Cell Physiol. 25: 697–703

Epstein, E. and Ludwig-Müller, J. (1993) Indole-3-butyric acid in plants: occurrence, synthesis, metabolism and transport. Physiologia Plantarum 88: 382–389

Epstein, E., Chen, K‑H. and Cohen, J.D. (1989) Identification of indole‑3‑butyric acid as an endogenous constituent of maize kernels and leaves. Plant Growth Regulation 8: 215–223

Epstein, E., Cohen, J.D. and Slovin, J.P. (2002) The biosynthetic pathway for indole-3-acetic acid changes during tomato fruit development. Plant Growth Regulation 38: 15–20

Falco, S.C., Dumas, K.S. and Livak, K.J. (1985) Nucleotide sequence of the yeast *ILV2* gene which encodes acetolactate synthase. Nucleic Acids Res. 13: 4011–4027

Felsenstein, J. (1993) PHYLIP (phylogeny inference package). Version 3.68. Department of Genetics, University of Washington, Seattle, Washington. Available from http://evolution.genetics.washington.edu/phylip.html

Flatau, S., Fischer, G., Kleinpeter, E. and Schellenberger, A. (1998) 31P NMR investigations on free and enzyme bound thiamine pyrophosphate. FEBS Letter 233: 379–382

Flikweert, M.T. (1999) Physiological roles of pyruvate decarboxylase in *Saccharomyces cerevisiae*. PhD thesis, Delft University of Technology, Delft.

Friml J., Benková E., Blilou I., Wisniewska J., Hamann T., Ljung K., Woody S., Sandberg G., Scheres B., Jürgens G. and Palme K. (2002) AtPIN4 mediates sink-driven auxin gradients and root patterning in Arabidopsis. Cell 108: 661–673

Fukaki, H., Okushima, Y. and Tasaka, M. (2007) Auxin-mediated lateral root formation in higher plants. Int. Rev. Cytol. 256: 111–137

Fukaki, H., Tameda, S., Masuda, H. and Tasaka, M. (2002) Lateral root formation is blocked by a gain-of-function mutation in the SOLITARY-ROOT/IAA14 gene of *Arabidopsis*. Plant J. 29: 153–168

Fukaki, H. and Tasaka, M. (2009) Hormone interactions during lateral root formation. Plant Mol. Biol. 69: 383–396

Gallavotti, A., Barazesh, S., Malcomber, S., Hall, D., Jackson D., Schmidt, R.J. and McSteen, P. (2008) Sparse inflorescence1 encodes a monocot-specific YUCCA-like gene required for vegetative and reproductive development in maize. Proc. Natl. Acad. Sci. USA 105(39): 15196–15201

Gass, N., Glagotskaia, T., Mellema, S., Stuurman, J. Barone, M., Mandel T., Roessner-Tunali, U. and Kuhlemeier, C. (2005) Pyruvate decarboxylase provides growing pollen tubes with a competitive advantage in petunia. The Plant Cell 17: 2355–2368

Glick, B.R., Patten, C.L., Holguin, G. and Penrose, D.M. (1999) Auxin production. In: Biochemical and genetic mechanisms used by plant growth-promoting bacteria. Imperial College Press, London, pp. 86–133

Glick, B.R., Patten, C.L., Holguin, G. and Penrose, D.M. (1999) Biochemical and genetic mechanisms used by plant growth promoting bacteria. Imperial College Press, London, pp. 267

Gonzali, S., Loreti, E., Novi, G., Poggi, A., Alpi, A. and Perata, P. (2005) The use of microarrays to study the anaerobic response in *Arabidopsis*. Annals of Botany 96(4): 661–668

Gordon, S.A. (1956) The biogenesis of natural auxins. In: RL Wain and F Wightman (eds), The chemistry and mode of action of plant growth substances. Butterworths, London, pp. 65–75

Gray, W.M., Ostin, A., Sandberg, G., Romano, C.P. and Estelle, M. (1998) High temperature promotes auxin-mediated hypocotyl elongation in *Arabidopsis*. Proc. Natl. Acad. Sci. USA 95: 7197–7202

Green, J.M. (2007) Review of glyphosate and ALS-Inhibiting herbicide crop resistance and resistant weed management. Weed Technology 21: 547–558

Green, J.M., Hazel, C.B., Forney, D.R. and Pugh, L.M. (2008) New multiple-herbicide crop resistance and formulation technology to augment the utility of glyphosate. Pest Manag. Sci. 64: 332–339

Hall, T.A. (1999) BioEdit: a user-friendly biological sequence alignment editor and analysis program for Windows 95/98/NT. Nucleic Acids Symposium Series 41: 95–98

Harms, C.T., Armour, S.L., DiMaio, J.J., Middlesteadt, L.A., Murray, D., Negrotto, D.V., Thompson-Taylor, H., Weymann, K., Montoya, A.L., Shillito, R.D. and Jen, G.C. (1992) Herbicide resistance due to amplification of a mutant acetohydroxyacid synthase gene. Mol. Gen. Genet. 233: 427–435

Hattori, J., Rutledge, R., Labbé, H., Brown, D., Sunohara, G. and Miki, B. (1992) Multiple resistance to sulfonylureas and imidazolinones conferred by an acetohydroxyacid synthase gene with separate mutations for selective resistance. Mol. Gen. Genet. 232: 167–173

Hawkins, C.F., Borges, A. and Perham, R.N. (1989) A common structural motif in thiamin pyrophosphate-binding enzymes. FEBS Letter 255(1): 77–82

Heap, I. The international survey of herbicide resistant weeds. February 06, 2009. [Online available at http://www.weedscience.org/summary/MOASummary.asp]

Hill, C.M., Pang, S.S. and Duggleby, R.G. (1997) Purification of *Escherichia coli* acetohydroxyacid synthase isoenzyme II and reconstitution of active enzyme from its individual pure subunits. Biochem J. 327: 891–898

Himanen, K., Boucheron, E., Vanneste, S., de Almeida Engler, J., Inze, D. and Beeckman, T. (2002) Auxin-mediated cell cycle activation during early lateral root initiation. Plant Cell 14: 2339–2351

Hohmann, S. (1991) Characterization of PDC6, a third structural gene for pyruvate decarboxylase in *Saccharomyces cerevisiae*. J. Bacteriology 173: 7963–7969

Hohmann, S. and Cederberg, H. (1990) Autoregulation may control the expression of yeast pyruvate decarboxylase structural genes PDC1 and PDC5. Eur. J Biochem 188: 615–621

Hohmann, S. and Meacock, P.A. (1998) Thiamin metabolism and thiamin diphosphate-dependent enzymes in the yeast *Saccharomyces cerevisiae*: genetic regulation. Biochim. Biophys. Acta 1385: 201–219

Howe, G.A. and Jander, G. (2008) Plant immunity to insect herbivores. Annu. Rev. Plant Biol. 59: 41–66

Hübner, G., Weidhase, R. and Schellenberger, A. (1978) The mechanism of substrate activation of pyruvate decarboxylase: A first approach. Eur. J. Biochemistry 92: 175–181

Ishikawa, H. and Evans, M. L. (1995) Specialized zones of development in roots. Plant Physiol. 109: 725–727

Jacobs, W.P. (1952) The role of auxin in differentiation of xylem around a wound. American Journal of Botany 39: 301–309

Jander, G., Baerson, S.R., Hudak, J.A., Gonzalez, K.A., Gruys, K.J. and Last, R.L. (2003) Ethylmethanesulfonate saturation mutagenesis in *Arabidopsis* to determine frequency of herbicide resistance. Plant Physiol. 131: 139–146

Jefferson, R.A., Kavanagh, T.A. and Bevan, M.W. (1987) GUS fusions: beta-glucuronidase as a sensitive and versatile gene fusion marker in higher plants. EMBO J. 6: 3901–3907

Jones, D.T., Taylor, W.R. and Thornton, J.M. (1992) The rapid generation of mutation data matrices from protein sequences. Comput. Appl. Biosci. 8: 275–282

Jordan, F. (2007) Adenosine triphosphate and thiamine cross paths. Nature Chemical Biology 3: 202–203

Jordan, F., Kuo, D.J. and Monse, E.U. (1978) A pH-rate determination of the activity-pH profile of enzymes. Application to yeast pyruvate decarboxylase demonstrating the existence of multiple ionizable groups. Anal. Biochem. 86(1): 298–302

Joutel, A., Ducros, A., Alamowitch, S., Cruaud, C., Domenga, V., Maréchal, E., Vahedi, K., Chabriat, H., Bousser, M.G., and Tournier-Lasserve, E. (1996) A human homolog of bacterial acetolactate synthase genes maps within the CADASIL critical region. Genomics 38: 192–198

Kazan, K. and Manners, J.M. (2008) Jasmonate signaling: toward an integrated view. Plant Physiol. 146: 1459–1468

Kenworthy, P. and Davies, D.D. (1976) Kinetic aspects of regulation of pyruvic decarboxylase. Phytochemistry 15: 279–282

Khalifah, R.A., Lewis, L.N. and Coggins, C.W. (1963) New natural growth promoting substance in young Citrus fruit. Science 142: 399–400

Khripach, V.A., Zhabinskii, V.N. and de Groot, A.E. (1999) Brassinosteriods: a new class of plant hormones. Academic Press, San Diago, CA, pp. 456

Kilian, J., Whitehead, D., Horak, J., Wanke, D., Weinl, S., Batistic, O., D'Angelo, C., Bornberg-Bauer, E., Kudla, J. and Harter, K. (2007) The AtGenExpress global stress expression data set: protocols, evaluation and model data analysis of UV-B light, drought and cold stress responses. Plant J. 50: 347–363

Kim, Y.S., Nosaka, K., Downs, D.M., Kwak, J.M., Park, D., Chung, I.K. and Nam, H.G. (1998) A Brassica cDNA clone encoding a bifunctional hydroxymethylpyrimidine kinase/thiamin-phosphate pyrophosphorylase involved in thiamin biosynthesis. Plant Mol. Biol. 37: 955–966

Kobayashi, M., Snagasawa, T. and Yamada, H. (1992) Enzymatic synthesis of acrylamide: a success story not yet over. Trends Biotechnology 10: 402–408

Koga J. (1995) Structure and function of indolepyruvate decarboxylase, a key enzyme in indole-3-acetic acid accumulation. Biochim. Biophys. Acta 1249: 1–13

Koga, J., Adachi T. and Hidaka H. (1992) Purification and characterization of indolepyruvate decarboxylase. A novel enzyme for indole-3-acetic acid biosynthesis in *Enterobacter cloacae*. J. Biol. Chem. 267 (22): 15823–15828

Koga, J., Adachi, T. and Hidaka, H. (1991a) Molecular cloning of the gene for indolepyruvate decarboxylase from *Enterobacter cloacae*. Mol. Gen. Genet. 226: 10–16

Koga, J., Adachi, T. and Hidaka, H. (1991b) Molecular cloning of the gene for indolepyruvate decarboxylase, a novel enzyme for indole-3-acetic acid biosynthesis in *Enterobacter cloacae*. Agric. Biol. Chem. 55: 701–706

König, S. (1998) Subunit structure, function and organisation of pyruvate decarboxylases from various organisms. Biochim Biophys Acta - Protein Struc. and Mol. Enz. 1385: 271–286

Koshiba, T., Kamiya, Y. and Lino, M. (1995) Biosynthesis of indole-3-acetic acid from L-tryptophan in coleoptile tips of maize (*Zea mays* L.). Plant Cell Physiology 36: 1503–1510

Kürsteiner, O., Dupuis, I. and Kuhlemeier, C. (2003) The pyruvate decarboxylase1 gene of *Arabidopsis* is required during anoxia but not other environmental stresses. Plant Physiology 132: 968–978

Kutz, A., Muller, A., Hennig, P., Kaiser, W.M., Piotrowski, M. and Weiler, E.W. (2002) A role for nitrilase 3 in the regulation of root morphology in sulphur-starving *Arabidopsis thaliana*. Plant J. 30: 95–106

Lacan, G., Magnus, V., Simaga, S., Iskric, S. and Hall, P.J. (1985) Metabolism of tryptophol in higher and lower plants. Plant Physiology 78: 447–454

Lakaye, B., Wirtzfeld, B., Wins, P., Grisar, T. and Bettendorff, L. (2004) Thiamine triphosphate, a new signal required for optimal growth of *Escherichia coli* during amino acid starvation. J. Biol. Chem. 279: 17142–17147

Laplaze, L., Benkova, E., Casimiro, I., Maes, L., Vanneste, S., Swarup, R., Weijers, D., Calvo, V., Parizot, B., Herrera-Rodriguez, M.B., Offringa, R., Graham, N., Doumas, P., Friml, J., Bogusz, D., Beeckman, T. and Bennett, M. (2007) Cytokinins act directly on lateral root founder cells to inhibit root initiation. Plant Cell 19: 3889–3900

Larkin, M.A., Blackshields, G., Brown, N.P., Chenna, R., McGettigan, P.A., McWilliam, H., Valentin, F., Wallace, I.M., Wilm, A., Lopez, R., Thompson, J.D., Gibson, T.J. and Higgins, D.G. (2007) ClustalW2 and ClustalX version 2. Bioinformatics 23(21): 2947–2948

Lawhorn, B.G., Gerdes, S.Y. and Begley, T.P. (2004a) A genetic screen for the identification of thiamin metabolic genes. J. Biol. Chem. 279: 43555–43559

Lawhorn, B.G., Mehl, R.A. and Begley, T.P. (2004b) Biosynthesis of the thiamin pyrimidine: the reconstitution of a remarkable rearrangement reaction. Org. Biomol. Chem. 2: 2538–2546

LeClere, S. and Bartel, B. (2001). A library of *Arabidopsis* 35S-cDNA lines for identifying novel mutants. Plant Mol. Biol. 46: 695–703

Lee, B.H., Henderson, D.A. and Zhu, J.K. (2005) The *Arabidopsis* cold-responsive transcriptome and its regulation by ICE1. Plant Cell 17: 3155–3175

Lee, T.C. and Langston-Unkefer, P.J. (1985) Pyruvate decarboxylase from *Zea mays* L. I. Purification and partial characterization from mature kernels and anaerobically treated roots. Plant Physiol. 79: 242–247

Lee, Y. and Duggleby, R.G. (2001) Identification of the regulatory subunit of *Arabidopsis thaliana* acetohydroxyacid synthase and reconstitution with its catalytic subunit. Biochemistry 40: 6836–6844

Letham, D.S. (1994) Cytokinins as phytohormones – sites of biosynthesis, translocation and function of translocated cytokinin. In: Cytokinins: Chemistry, Activity and Function. Mok D.W.S., Mok M.C., eds. Boca Raton, FL: CRC Press, pp. 57–80

Leyser, O. (2005) Auxin distribution and plant pattern formation: how many angels can dance on the point of PIN? Cell 121: 819–822

Ljung, K., Hull, A.K., Celenza, J., Yamada, M., Estelle, M., Normanly, J. and Sandberg, G. (2005) Sites and regulation of auxin biosynthesis in *Arabidopsis* roots. Plant Cell 17: 1090–1104

Loreti, E., Poggi, A., Novi, G., Alpi, A. and Perata, P. (2005) A genome-wide analysis of the effects of sucrose on gene expression in *Arabidopsis* seedlings under anoxia. Plant Physiol. 137(3): 1130–1138

Lu, G., Dobritzsch, D., Baumann, S., Schneider, G. and König, S. (2000) The structural basis of substrate activation in yeast pyruvate decarboxylase. A crystallographic and kinetic study. Eur. J. Biochem. 267: 861–868

Ludwig-Müller, J. and Cohen, J.D. (2002) Identification and quantification of three active auxins in different tissues of *Tropaeolum majus*. Physiologia Plantarum 115: 320–329

Ludwig-Müller, J. and Hilgenberg, W. (1990) Conversion of indole-3-acetaldoxime to indole-3-acetonitrile by plasma membranes from Chinese cabbage. Physiologia Plantarum 79: 311–318

Lukowitz, W., Gillmor, C.S. and Scheible, W.R. (2000) Positional cloning in *Arabidopsis*. Why it feels good to have a genome initiative working for you. Plant Physiol. 123: 795–805

Macháčkova, I., Chvojka, L., Našinec, V. and Zmrhal, Z. (1981) The effect of phenylacetic acid on ethylene formation in wheat seedlings. Biologia Plantarum 23: 116–119

Machado, C.R., de Oliveira, R.L., Boiteux, S., Praekelt, U.M., Meacock, P.A. and Menck, C.F. (1996) Thi1, a thiamine biosynthetic gene in *Arabidopsis thaliana*, complements bacterial defects in DNA repair. Plant Mol. Biol. 31: 585–593

Magnus, V., Iakric, S., and Kveder, S. (1973) The formation of tryptophol glucoside in the tryptamine metabolism of pea seedlings. Planta 110: 57–62

Mahadevan, S. (1963) Conversion of 3-indoleacetaldoxime to 3-indoleacetonitrile by plants. Archives of Biochemistry 100: 557–558

Makarchikov, A.F., Brans, A. and Bettendorff, L. (2007) Thiamine diphosphate adenylyl transferase from E. coli: functional characterization of the enzyme synthesizing adenosine thiamine triphosphate. BMC Biochem. 8: 17–24

Makarchikov, A.F., Lakaye, B., Gulyai, I.E., Czerniecki, J., Coumans, B., Wins, P., Grisar, T. and Bettendorff, L. (2003) Thiamine triphosphate and thiamine triphosphatase activities: from bacteria to mammals. Cell Mol. Life Sci. 60: 1477–1488

Malamy, J.E. (2005) Intrinsic and environmental response pathways that regulate root system architecture. Plant Cell Environ. 28: 67–77

Malamy, J.E., and Benfey, P.N. (1997). Organization and cell differentiation in lateral roots of *Arabidopsis thaliana*. Development 124: 33–44

Mandal, M., Boese, B., Barrick, J.E., Winkler, W.C. and Breaker, R.R. (2003) Metabolite-sensing riboswitches control fundamental biochemical pathways in bacteria. Cell 113: 577–586

Marchant, A., Bhalerao, R., Casimiro, I., Eklof, J., Casero, P.J., Bennett, M. and Sandberg, G. (2002) AUX1 promotes lateral root formation by facilitating indole-3-acetic acid distribution between sink and source tissues in the *Arabidopsis* seedling. Plant Cell 14: 589–597

McCourt, J.A. and Duggleby, R.G. (2006) Acetohydroxyacid synthase and its role in the biosynthetic pathway for branched-chain amino acids. Amino Acids 31: 173–210

McCourt, J.A. Pang, S.S., King-Scott, J., Guddat, L.W. and Duggleby R.G. (2006) Herbicide-binding sites revealed in the structure of plant acetohydroxyacid synthase. Proc. Natl. Acad. Sci. 103(3): 569–573

Mendel, S., Elkayam, T., Sella, C., Vinogradov, V., Vyazmensky, M., Chipman, D.M. and Barak, Z. (2001) Acetohydroxyacid synthase: a proposed structure for regulatory subunits supported by evidence from mutagenesis. J. Mol. Biol. 307: 465–477

Michalczuk, L., Ribnicky, D.M., Cooke, T.J. and Cohen J.D. (1992) Regulation of indole-3-acetic acid biosynthetic pathways in carrot cell cultures. Plant Physiology 100: 1346–1353

Michniewicz, M., Zago, M.K., Abas, L., Weijers, D., Schweighofer, A., Meskiene, I., Heisler, M.G., Ohno, C., Zhang, J., Huang, F., Schwab, R., Weigel, D., Meyerowitz, E.M., Luschnig, C., Offringa, R. and Friml, J. (2007) Antagonistic regulation of PIN phosphorylation by PP2A and PINOID directs auxin flux. Cell 130: 1044–1056

Mikkelsen, M.D., Hansen, C.H., Wittstock, U. and Halkier, B.A. (2000) Cytochrome P450 CYP79B2 from *Arabidopsis* catalyzes the conversion of tryptophan to indole-3-acetaldoxime, a precursor of indole glucosinolates and indole-3-acetic acid. J. Biol. Chem. 275: 33712–33717

Miranda-Rios, J., Navarro, M. and Soberon, M. (2001) A conserved RNA structure (thi box) is involved in regulation of thiamin biosynthetic gene expression in bacteria. Proc. Natl. Acad. Sci. USA 98: 9736–9741

Mücke, U., König, S. and Hübner, G. 1995. Purification and characterization of pyruvate decarboxylase from pea seeds (*Pisum sativum* cv. Miko). Biol. Chem. Hoppe-Seyler 376: 111–117

Muller, Y.A., Lindqvist, Y., Furey, W., Schulz, G.E., Jordan, F. and Schneider, G. (1993) A thiamin diphosphate binding fold revealed by comparison of the crystal structures of transketolase, pyruvate oxidase and pyruvate decarboxylase. Structure 1: 95–103

Murashige, T. and Skoog, F. (1962) A revised medium for rapid growth and bioassays with tobacco tissue culture. Physiol. Plant 15: 473–497

Nakai, K. and Kanehisa, M. (1991) Expert system for predicting protein localization sites in gram-negative bacteria. PROTEINS: Structure, Function, and Genetics 11: 95–110

Narumiya, S., Takai, K., Tokuyama, T., Noda, Y., Ushiro, H. and Hayaishi, O. (1979) A new metabolic pathway of tryptophan initiated by tryptophan side chain oxidase. J. Biol. Chem. 254: 7007–7015

Nemhauser, J.L., Mockler, T.C. and Chory, J. (2004) Interdependency of brassinosteroid and auxin signaling in *Arabidopsis*. PLoS Biol 2(9): e258

Nghiêm, H.O., Bettendorff, L. and Changeux, J.P. (2000) Specific phosphorylation of Torpedo 43K rapsyn by endogenous kinase(s) with thiamine triphosphate as the phosphate donor. FASEB J. 14: 543–554

Ngo, P., Ozga, J.A. and Reinecke, D.M. (2002) Specificity of auxin regulation of gibberellin 20-oxidase gene expression in pea pericarp. Plant Molecular Biology 49: 439–448

Nibau, C., Gibbs, D.J. and Coates, J.C. (2008) Branching out in new directions: the control of root architecture by lateral root formation. New Phytol. 179: 595–614

Nishimura, H., Kawasaki, Y., Nosaka, K., Kanek, Y. and Iwashima, A. (1991) Constitutive thiamine metabolism mutation, thi80, causing reduced thiamine pyrophosphokinase activity in *Saccharomyces cerevisiae*. J. Bacteriol. 173: 2716–2719

Niyogi, K.K. and Fink, G.R. (1992) Two anthranilate synthase genes in *Arabidopsis*: defense-related regulation of the tryptophan pathway. Plant Cell 4: 721–733

Nordström, A., Tarkowski, P., Tarkowska D., Norbaek, R., rister Åstot, C., Dolezal, K. and Sandberg, G. (2004) Auxin regulation of cytokinin biosynthesis in *Arabidopsis thaliana*: A factor of potential importance for auxin-cytokinin-regulated development. Proc. Natl. Acad. Sci. USA 101 (21): 8039–8044

Normanly, J., Cohen, J.D. and Fink, G.R. (1993) *Arabidopsis thaliana* auxotrophs reveal a tryptophan-independent biosynthetic pathway for indole-3-acetic acid. Proc. Natl. Acad. Sci. USA 90: 10355–10359

Normanly, J., Grisafi, P., Fink, G.R. and Bartel, B. (1997) *Arabidopsis* mutants resistant to the auxin effects of indole-3-acetonitrile are defective in the nitrilase encoded by the NIT1 gene. The Plant Cell 9: 1781–1790

Normanly, J., Slovin, J.P. and Cohen, J.D. (1995) Rethinking auxin biosynthesis and metabolism. Plant Physiology 107: 323–329

Normanly, J., Slovin, J.P. and Cohen, J.D. (2005) Auxin biosynthesis and metabolism. In: Plant Hormones: Biosynthesis, Signal Transduction, Action! (3rd edition). P.J. Davies, ed. Kluwer Academic Publ., Dordrecht, pp. 36–62

Nosaka, K. (2006) Recent progress in understanding thiamin biosynthesis and its genetic regulation in *Saccharomyces cerevisiae*. Appl Microbiol Biotechnol. 72: 30–40

Ōba, K. and Uritani, I. (1975) Purification and characterization of pyruvate decarboxylase from sweet potato roots. J. Biochem. 77(6): 1205–1213

O'Donnell, P.J. Schmelz, E.A., Moussatche, P., Lund, S.T., Jones, J.B. and Klee, H.J. (2003) Susceptible to intolerance – a range of hormonal actions in a susceptible *Arabidopsis* pathogen response. Plant Journal 33: 245–257

Ogawa, T., Kawahigashi, H., Toki, S. and Handa, H. (2008) Efficient transformation of wheat by using a mutated rice acetolactate synthase gene as a selectable marker. Plant Cell Rep. 27: 1325–1331

Okada, K., Ueda, J., Komaki, M.K., Bell, C.J. and Shimura, Y. (1991) Requirement of the auxin polar transport system in early stages of Arabidopsis floral bud formation. The Plant Cell 3: 677–684

Okushima, Y., Overvoorde, P.J., Arima, K., Alonso, J.M., Chan, A., Chang, C., Ecker, J.R., Hughes, B., Lui, A., Nguyen, D., Onodera, C., Quach, H., Smith, A., Yu, G. and Theologis, A. (2005) Functional genomic analysis of the AUXIN RESPONSE FACTOR gene family members in *Arabidopsis thaliana*: unique and overlapping functions of ARF7 and ARF19. Plant Cell 17: 444–463

Östin, A., Ilić, N. and Cohen, J.D. (1999) An in vitro system from maize seedling for tryptophan-independent indole-3-acetic biosynthesis. Plant physiology 119: 173–178

Ottenschlager, I., Wolff, P., Wolverton, C., Bhalerao, R.P., Sandberg, G., Ishikawa, H., Evans, M. and Palme, K. (2003) Gravity-regulated differential auxin transport from columella to lateral root cap cells. Proc. Natl. Acad. Sci. USA 100: 2987–2991

Ouellet, T., Rutledge, R.G. and Miki, B.L. (1992) Members of the acetohydroxy acid synthase multigene family of *Brassica napus* have divergent patterns of expression. Plant J. 2: 321–330

Ouyang, J., Shao, X. and Li, J. (2001) Indole-3-glycerol phosphate, a branchpoint of indole-3-acetic acid biosynthesis from the tryptophan biosynthetic pathway in *Arabidopsis thaliana*. Plant Journal 24: 327–334

Ozga, J.A. and Reinecke, D.M. (2003) Hormonal interactions in fruit development. Journal of Plant Growth Regulation 22: 73–81

Page, R.D.M. (1996) TREEVIEW: An application to display phylogenetic trees on personal computers. Computer Applications in the Biosciences 12(4): 357–358

Palme, K. and Nagy, F. (2008) A new gene for auxin synthesis. Cell 133: 31–32

Patten, C.L. and Glick, B.R. (1996) Bacterial biosynthesis of indole-3-acetic acid. Can. J. Microbiol. 42: 207–220

Pearse, A.G.E. (1980) Histochemistry, theoretical and applied, 4th edition. Vol. 1. Preparative and optical technology. Edinburgh: Churchill-Livingstone.

Peer, W.A., Bandyopadhyay, A., Blakeslee, J.J., Makam, S.N., Chen, R.J., Masson, P.H. and Murphy, A.S. (2004) Variation in expression and protein localization of the PIN family of auxin efflux facilitator proteins in flavonoid mutants with altered auxin transport in *Arabidopsis thaliana*. Plant Cell 16: 1898–1911

Peschke, V.M. and Sachs, M.M. (1993) Multiple pyruvate decarboxylase genes in maize are induced by hypoxia. Mol. Gen. Genet. 240: 206–212

Pincus, J.H., Cooper, J.R., Murphy, J.V., Rabe, E.F., Lonsdale, D. and Dunn, H.G. (1973) Thiamine derivatives in subacute necrotizing encephalomyelopathy. Pediatrics 51: 716–721

Pless, T., Boettger, M., Hedden, P. and Graebe, J. (1984) Occurrence of 4-Cl-indoleacetic acid in broad beans and correlation of its levels with seed development. Plant Physiology 74 (2): 320–323

Pollmann, S., Müller, A., Piotrowski, M. and Weiler, E.W. (2002) Occurrence and formation of indole-3-acetamide in *Arabidopsis thaliana*. Planta 216: 155–161

Pollmann, S., Neu, D. and Weiler, E.W. (2003) Molecular cloning and characterization of an amidase from *Arabidopsis thaliana* capable of converting indole-3-acetamide into the plant growth hormone, indole-3-acetic acid. Phytochemistry 62(3): 293–300

Radwanski, E.R. and Last, R.L. (1995) Tryptophan biosynthesis and metabolism: biochemical and molecular genetics. Plant Cell 7: 921–934

Rahman, A., Amakawa, T., Goto, N. and Tsurumi, S. (2001) Auxin is a positive regulator for ethylene-mediated response in the growth of *Arabidopsis* roots. Plant Cell Physiol. 42: 301–307

Rapparini, F., Cohen, J.D. and Slovin, J.P. (1999) Indole-3-acetic acid biosynthesis in *Lemna gibba* studied using stable isotope labeled anthranilate and tryptophan. Plant Growth Regulation 27: 139–144

Rapparini, F., Tam, Y., Cohen, J.D. and Slovin, J.P. (2002) IAA metabolism in *Lemna gibba* undergoes dynamic changes in response to growth temperature. Plant Physiology 128: 1410–1416

Rayle, D.L. and Cleland, R.E. (1992) The acid growth theory of auxin-induced cell elongation is alive and well. Plant Physiology 99: 1271–1274

Rayle, D.L. and Purves, W.K. (1967) Isolation and identification of indole-3-ethanol (tryptophol) from cucumber seedlings. Plant Physiology 42: 520–524

Reinecke, D.M. (1999) 4-Chloroindole-3-acetic acid and plant growth. Plant Growth Regulation 27: 3–13

Reinecke, D.M. and Bandurski, R.S. (1983) Oxindole-3-acetic acid, an indole-3-acetic acid catabolite in *Zea mays*. Plant Physiology 86: 868–872

Reinert J 1954 Wachstum. Fortschr. Bot. 16: 330-340

Rigaud, J. (1970) L'acide inolyl-3-lactique et son metabolisme chez Rhizohium. Arch. Mikrobiol. 72: 293–307

Rivoal, J., Thind, S., Pradet, A. and Ricard, B. (1997) Differential induction of pyruvate decarboxylase subunits and transcripts in anoxic rice seedlings. Plant Physiol. 114(3): 1021–1029

Roberts, J.K.M., Wemmer, D., Ray, P.M. and Jardetzky, O. (1982) Regulation of cytoplasmic and vacuolar pH in maize root tips under different experimental conditions. Plant Physiol. 69 (6): 1344–1347

Roje, S. (2007) Vitamin B biosynthesis in plants. Phytochemistry 68: 1904–1921

Ross, J.J., O'Neill, D.P., Wolbang, C.M., Symons, G.M. and Reid, J.B. (2001) Auxin-gibberellin interactions and their role in plant growth. Journal of Plant Growth Regulation 20: 336–353

Roux, F., Matejicek, A., Gasquez, J. and Reboud, X. (2005) Dominance variation across six herbicides of the *Arabidopsis thaliana* csr1-1 and csr1-2 resistance alleles. Pest Manag. Sci. 61: 1089–1095

Ruegger, M., Dewey, E., Hobbie, L., Brown, D., Bernasconi, P., Turner, J., Muday, G., and Estelle, M. (1997). Reduced naphthylphthalamic acid binding in the *tir3* mutant of *Arabidopsis* is associated with a reduction in polar auxin transport and diverse morphological defects. Plant Cell 9: 745-757

Rutherford, R., Gallois, P. and Masson, P.H. (1998) Mutations in *Arabidopsis thaliana* genes involved in the tryptophan biosynthesis pathway affect root waving on tilted agar surfaces. Plant J. 16:145–154

Ruzicka, K., Ljung, K., Vanneste, S., Podhorska, R., Beeckman, T., Friml, J. and Benkova, E. (2007) Ethylene regulates root growth through effects on auxin biosynthesis and transport-dependent auxin distribution. Plant Cell 19: 2197–2212

Sabatini, S., Beis, D., Wolkenfelt, H., Murfett, J., Guilfoyle, T., Malamy, J., Benfey, P., Leyser, O., Bechtold, N., Weisbeek, P. and Scheres, B. (1999). An auxin-dependent distal organizer of pattern and polarity in the *Arabidopsis* root. Cell 99: 463–472

Saitou, N. and Nei, M. (1987) The neighbor-joining method: a new method for reconstructing phylogenetic trees. Mol. Biol. Evol. 4: 406–425

Sambrook, J., and Russell, D.W. (2001). Molecular cloning, 3rd edn. Cold Spring Harbor Laboratory Press, Cold Spring Harbor, New York

Sandberg, G., Ernstsen, A. and Hamnede, M. (2006) Dynamics of indole-3-acetic acid and indole-3-ethanol during development and germination of *Pinus sylvestris* seeds. Physiologia Plantarum 71: 411–418

Schaaff, I., Green, J. B. A., Gozalbo, D. and Hohmann, S. (1989) A deletion of the *PDC1* gene for pyruvate decarboxylase of yeast causes a different phenotype than previously isolated point mutations. Curr. Genet. 15: 75–81

Schellenberger, A. (1967) Structure and mechanism of action of the active center of yeast pyruvate decarboxylase. Angew. Chem. Int. Ed. Engl. 6(12): 1024–1035

Schmidt, R.C., Müller, A., Hain, R., Bartling, D. and Weiler, E.W. (1996) Transgenic tobacco plants expressing the *Arabidopsis thaliana* nitrilase II enzyme. Plant Journal 9: 683–691

Schmitt, H.D. and Zimmermann, F.K. (1982) Genetic analysis of the pyruvate decarboxylase reaction in yeast glycolysis. J. Bacteriology 151: 1146–1152

Seo, M., Akaba, S., Oritani, T., Delarue, M., Bellini, C., Caboche, M. and Koshiba, T. (1998) Higher activity of an aldehyde oxidase in the auxin-overproducing superroot1 mutant of *Arabidopsis thaliana*. Plant Physiology 116: 687–693

Sergienko, E.A. and Jordan, F. (2002) Yeast pyruvate decarboxylase tetramers can dissociate into dimers along two interfaces. Hybrids of low-activity D28A (or D28N) and E477Q variants, with substitution of adjacent active center acidic groups from different subunits, display restored activity. Biochemistry 41: 6164–6169

Settembre, E., Begley, T.P. and Ealick, S.E. (2003) Structural biology of enzymes of the thiamin biosynthesis pathway. Current Opinion in Structural Biology 13: 739–747

Shaner, D.L. and O'Connor, S.L. (1991) The Imidazolinone Herbicides. Boca Raton, FL: CRC., pp. 290

Sherman, T.D., Vaughn, K.C. and Duke, S.O. (1996) Mechanisms of action and resistance to herbicides. In Herbicide-Resistant Crops - Agricultural, Environmental, Economic, Regulatory, and Technical Aspects, Edited by Duke, S.O., Lewis Publishers, Chelsea, MI, pp. 13–35

Shiao, T.L., Ellis, M.H., Dolferus, R., Dennis, E.S. and Doran, P.M. (2002) Overexpression of alcohol dehydrogenase or pyruvate decarboxylase improves growth of hairy roots at reduced oxygen concentrations. Biotechnol Bioeng 77(4): 455–461

Shininger, T.L. (1979) The control of vascular development. Annu. Rev. Plant Physiol. 30: 313-337

Singer T.P. (1955) α-Carboxylase from wheat germ. Methods Enzymol. 1: 465–470

Singh, B., Szamosi, I., Hand, J.M. and Misra, R. (1992) *Arabidopsis* acetohydroxyacid synthase expressed in *Escherichia coli* is insensitive to the feedback inhibitors. Plant Physiol. 99: 812–816

Slovin, J.P., Bandurski, R.S. and Cohen, J.D. (1999) Auxin, in biochemistry and molecular biology of plant hormones, eds. Hooykaas, P.J.J., Hall, M.A. and Libbenga, K.R. (Elsevier, Amsterdam), pp. 115–140

Small, I., Peeters, N., Legeai, F. and Lurin, C. (2004) Predotar: A tool for rapidly screening proteomes for N-terminal targeting sequences. Proteomics 4: 1581–1590

Songstad, D.D., De Luca, V., Brisson, N., Kurz, W.G.W. and Nessler, C.L. (1990) High levels of tryptamine accumulation in transgenic tobacco expressing tryptophan decarboxylase. Plant Physiology 94: 1410–1413

Sprunck, P., Jacobsen, H.-J. and Reinard, T. (1995) Indole-3-lactic acid is a weak auxin analogue but not an anti-auxin. Journal of Plant Growth Regulation 14: 191–197

Staswick, P.E., Su, W. and Howell, S.H. (1992) Methyl jasmonate inhibition of root growth and induction of a leaf protein are decreased in an *Arabidopsis thaliana* mutant. Proc. Natl. Acad. Sci. USA 89: 6837–6840

Stepanova, A.N., Hoyt, J.M., Hamilton, A.A. and Alonso, J.M. (2005) A Link between ethylene and auxin uncovered by the characterization of two root-specific ethylene-insensitive mutants in *Arabidopsis*. Plant Cell 17: 2230–2242

Stepanova, A.N., Robertson-Hoyt, J., Yun, J., Benavente, L.M., Xie, D.-Y., Doležal, K., Schlereth, A., Jürgens, G. and Alonso, J.M. (2008). TAA1-mediated auxin biosynthesis is essential for hormone crosstalk and plant development. Cell 133: 177–191

Stetter, J. (1994) Herbicides Inhibiting Branched Chain Amino Acid Biosynthesis: Recent Developments. New York: Springer-Verlag, pp. 219

Sudarsan, N., Barrick, J.E. and Breaker, R.R. (2003) Metabolite-binding RNA domains are present in the genes of eukaryotes. RNA 9 (6): 644–647

Sugawara, S., Hishiyama, S., Jikumaru, Y., Hanada, A., Nishimura, T., Koshiba, T., Zhao, Y., Kamiya, Y. and Kasahara, H. (2009) Biochemical analyses of indole-3-acetaldoxime dependent auxin biosynthesis in *Arabidopsis*. Proc. Natl. Acad. Sci. USA 106: 5430–5435

Sun, J., Xu, Y., Ye, S., Jiang, H., Chen, Q., Liu, F., Zhou, W., Chen, R., Li, X., Tietz, O., Wu, X., Cohen, J.D., Palme, K. and Li, C. (2009) Arabidopsis ASA1 is important for jasmonate-mediated regulation of auxin biosynthesis and transport during lateral root formation. Plant Cell 21: 1495–1511

Swarup, K., Benkova, E., Swarup, R., Casimiro, I., Peret, B., Yang, Y., Parry, G., Nielsen, E., De Smet, I., Vanneste, S., Levesque, M.P., Carrier, D., James, N., Calvo, V., Ljung, K., Kramer, E., Roberts, R., Graham, N., Marillonnet, S., Patel, K., Jones, J.D., Taylor, C.G., Schachtman, D.P., May, S., Sandberg, G., Benfey, P., Friml, J., Kerr, I., Beeckman, T., Laplaze, L. and Bennett, M.J. (2008) The auxin influx carrier LAX3 promotes lateral root emergence. Nat. Cell Biol. 10: 946–954

Swarup, R., Friml, J., Marchant, A., Ljung, K., Sandberg, G., Palme, K. and Bennett, M. (2001) Localization of the auxin permease AUX1 suggests two functionally distinct hormone transport pathways operate in the *Arabidopsis* root apex. Genes Dev. 15: 2648–2653

Swarup, R., Kramer, E. M., Perry, P., Knox, K., Leyser, H. M. O., Haseloff, J., Beemster, G. T. S., Bhalerao, R. and Bennett, M. J. (2005) Root gravitropism requires lateral root cap and epidermal cells for transport and response to a mobile auxin signal. Nat. Cell Biol. 7: 1057–1065

Swarup, R., Perry, P., Hagenbeek, D., Van Der Straeten, D., Beemster, G.T., Sandberg, G., Bhalerao, R., Ljung, K. and Bennett, M.J. (2007) Ethylene upregulates auxin biosynthesis in *Arabidopsis* seedlings to enhance inhibition of root cell elongation. Plant Cell 19: 2186–2196

Sztein, A.E., Cohen, J.D. and Cooke, T.J. (2000) Evolutionary patterns in the auxin metabolism of green plants. Int. J. Plant Sci. 161: 849–859

Sztein, A.E., Ilić, N., Cohen J.D. and Cooke T.J. (2002) Indole-3-acetic biosynthesis in isolated axes from germinating bean seeds: the effect of wounding on the biosynthetic pathway. Plant Growth Regulation 36: 201–207

Taiz, L. and Zeiger, E. (1998) Plant Physiology, 2nd ed., Sinauer Associates, Inc., Publishers, Sunderland, Masachusetts, pp. 543–575

Tam, Y.Y. and Normanly, J. (1998) Determination of indole-3-pyruvic acid levels in *Arabidopsis thaliana* by gas chromatography-selected ion monitoring-mass spectrometry. Journal of Chromatography A 800: 101–108

Tanaka, H., Dhonukshe, P., Brewer, P.B. and Friml, J. (2006) Spatiotemporal asymmetric auxin distribution: a means to coordinate plant development. Cell Mol. Life Sci. 63: 2738-2754

Tao, Y., Ferrer J.-L, Ljung, K., Pojer, F., Hong, F., Long, J. A., Li, L., Moreno, J. E., Bowman, M. E., Ivans, L. J., Cheng Y., Lim, J., Zhao, Y., Balleré, C. L., Sandberg, G., Noel, J. P. and Chory, J. (2008) Rapid synthesis of auxin via a new tryptophan-dependent pathway is required for shade avoidance in plants. Cell 133: 164–176

ter Schure, E.G., Flikweert, M.T. van Dijken, J.P., Pronk J.T. and Verrips, C.T. (1998) Pyruvate decarboxylase catalyzes decarboxylation of branched-chain 2-oxo acids but is not essential for fusel alcohol production by *Saccharomyces cerevisiae*. Appl. Environ. Microbiol. 64(4): 1303–1307

Thimann, K.V. and Mahadevan, S. (1964) Nitrilase. I. Occurrence, preparation and general properties of the enzyme. Arch. Biochem. Biophys. 105: 133–141

Thimann, K.V. and Skoog, F. (1934) On the inhibition of bud development and other function of growth substance in *Vicia faba*. Proc. R. Soc. Lond (Biol) 114: 317–339

Thore, S., Leibundgut, M. and Ban, N. (2006) Structure of the eukaryotic thiamine pyrophosphate riboswitch with its regulatory ligand. Science 312: 1208–1211

Tiryaki, I. and Staswick, P.E. (2002) An *Arabidopsis* mutant defective in jasmonate response is allelic to the auxin-signaling mutant axr1. Plant Physiol. 130: 887–894.

Todd, A.E., Orengo, C.A. and Thornton, J.M. (2001) Evolution of function in protein superfamilies, from a structural perspective. J. Mol. Biol. 307: 1113–1143

Tourneur, C., Jouanin, L. and Vaucheret, H. (1993) Overexpression of acetolactate synthase confers resistance to valine in transformed tobacco. Plant Sci. 88: 159–168

Tranel, P.J. and Wright, T.R. (2002) Resistance of weeds to ALS-inhibiting herbicides: what have we learned? Weed Science 50: 700–712

Trinchant, J.-C. and Rigaud, J. (1974) Lactate dehydrogenase from Rhizobium. Purification and role in indole metabolism. Physiologia Plantarum 32: 394–399

Tuominen, H., Östin, A., Sandberg, G. and Sundberg, B. (1994) A novel metabolic pathway for indole-3-acetic acid in apical shoots of *Populus tremula* (L.) X *Populus tremuloides* (Michx.). Plant Physiology 106: 1511–1520

Turner, J.G., Ellis, C. and Devoto, A. (2002) The jasmonate signal pathway. Plant Cell 14 Suppl: S153–164

Ueda, J. and Kato, J. (1980) Isolation and identification of a senescence-promoting substance from wormwood (*Artemisia absinthium* L.). Plant Physiol. 66: 246–249

Ulmasov, T., Murfett, J., Hagen, G. and Guilfoyle, T.J. (1997) Aux/IAA proteins repress expression of reporter genes containing natural and highly active synthetic auxin response elements. Plant Cell 9: 1963–1971

van Huizen, R., Ozga, J.A. and reinecke, D.M. (1997) Seed and hormonal regulation of gibberellin 20-oxidase expression in pea pericarp. Plant Physiology 115: 123–128

Vickery, L.E. and Purves, W.K. (1972) Isolation of indole-3-ethanol oxidase from cucumber seedlings. Plant Physiology 49: 716–721

Vieten, A., Vanneste, S., Wisniewska, J., Benkova, E., Benjamins, R., Beeckman, T., Luschnig, C. and Friml, J. (2005) Functional redundancy of PIN proteins is accompanied by auxin-dependent cross-regulation of PIN expression. Development 132: 4521–4531

Vinogradov, V., Vyazmensky, M., Engel, S., Belenky, I., Kaplun, A., Kryukov, O., Barak, Z. and Chipman D.M. (2006) Acetohydroxyacid synthase isozyme I from *Escherichia coli* has unique catalytic and regulatory properties. Biochimica et Biophysica Acta (BBA) - General Subjects 1760 (3): 356–363

Vogel, J.T., Zarka, D.G., Van Buskirk, H.A., Fowler, S.G. and Thomashow, M.F. (2005) Roles of the CBF2 and ZAT12 transcription factors in configuring the low temperature transcriptome of *Arabidopsis*. Plant J. 41: 195–211

Wang, G., Ding, X., Yuan, M., Qiu, D., Li, X., Xu, C. and Wang, S. (2006) Dual function of rice OsDR8 gene in disease resistance and thiamine accumulation. Plant Mol. Biol. 60: 437–449

Wang, Q., He, P., Lu, D., Shen, A. and Jiang, N. (2004) Purification, characterization, cloning and expression of pyruvate decarboxylase from *Torulopsis glabrata* IFO005. J. Biochem. 136(4): 447–455

Wasternack, C. (2007). Jasmonates: an update on biosynthesis, signal transduction and action in plant stress response, growth and development. Ann. Bot. 100: 681-697.

West, A.H. and Stock, A.M. (2001) Histidine kinases and response regulator proteins in two-component signaling systems. Trends Biochem. Sci. 26: 369–376

Whaley, C.M., Wilson, H.P. and Westwood, J.H. (2007) A new mutation in plant ALS confers resistance to five classes of ALS-inhibiting herbicides. Weed Science 55: 83–90

Woodward, A.W. and Bartel, B. (2005) Auxin: regulation, action, and interaction. Annals of Botany 95: 707–735

Wright, A.D. and Neuffer, M.G. (1989) Organge pericarp in maize: filial expression in a maternal tissue. Journal of Heredity 80(3): 229–233

Wright, A.D., Sampson, M.B., Neuffer, M.G., Michalczuk, L., Slovin, J.P. and Cohen, J.D. (1991) Indole-3-acetic acid biosynthesis in the mutant maize orange pericarp, a tryptophan auxotroph. Science 254: 998–1000

Xie, D.X., Feys, B.F., James, S., Nieto-Rostro, M. and Turner, J.G. (1998) COI1: an *Arabidopsis* gene required for jasmonate-regulated defense and fertility. Science 280: 1091–1094

Xu, L., Liu, F., Lechner, E., Genschik, P., Crosby, W.L., Ma, H., Peng, W., Huang, D. and Xie, D. (2002) The SCF(COI1) ubiquitin-ligase complexes are required for jasmonate response in *Arabidopsis*. Plant Cell 14: 1919–1935

Yamada, M., Greenham, K., Prigge, M.J., Jensen, P.J. and Estelle, M. The TRANSPORT INHIBITOR RESPONSE2 (TIR2) gene is required for auxin synthesis and diverse aspects of plant development. Plant Physiology (Preview DOI:10.1104/pp.109.138859)

Yamamoto, Y., Kamiya, N., Morinaka, Y., Matsuoka, M. and Sazuka, T. (2007) Auxin biosynthesis by the YUCCA genes in rice. Plant Physiology 143(3): 1362–1371

Yang, T., Law, D.M. and Davies, P.J. (1993) Magnitude and kinetics of stem elongation induced by exogenous indole-3-acetic acid in intact light-grown pea seedlings. Plant Physiology 102: 717–724

Yu, Q., Han, H. and Powles, S.B. (2008) Mutations of the ALS gene endowing resistance to ALS-inhibiting herbicides in *Lolium rigidum* populations. Pest Manag. Sci. 64: 1229–1236

Zhao, Y., Christensen, S.K., Fankhauser, C., Cashman, J.R., Cohen, J.D., Weigel, D. and Chory, J. (2001) A role for flavin monooxygenase-like enzymes in auxin biosynthesis. Science 291: 306–309

Zheng, D., Patzoldt, W.L. and Tranel P.J. (2005) Association of the W574L ALS substitution with resistance to cloransulam and imazamox in common ragweed (*Ambrosia artemisiifolia*). Weed Science 53(4): 424–430

Zheng, W., Zhai, Q., Sun, J., Li, C.B., Zhang, L., Li, H., Zhang, X., Li, S., Xu, Y., Jiang, H., Wu, X. and Li, C. (2006). Bestatin, an inhibitor of aminopeptidases, provides a chemical genetics approach to dissect jasmonate signaling in *Arabidopsis*. Plant Physiol. 141: 1400-1413

Zhu, J.S. and Scott, G.K. (1995) Purification, characterization and developmental expression of indole-3-ethanol oxidase from seeds of *Phaseolus vulgaris*. Biochemistry and molecular biology international 35: 423–432

Zimmermann, P., Hirsch-Hoffmann, M., Hennig, L. and Gruissem W. (2004) GENEVESTIGATOR, *Arabidopsis* microarray database and analysis toolbox. Plant Physiol. 136: 2621–2632

# Appendix

## The *Arabidopsis ASA1* Gene Is Important for Jasmonate-mediated Regulation of Auxin Biosynthesis and Transport during Lateral Root Formation

## 6.1 Abstract

Plant roots show an impressive degree of plasticity in adapting their branching patterns to ever-changing growth conditions. An important mechanism underlying this tremendous ability of adaptation is the interaction between hormonal and developmental signals. Here we analyze the interaction of jasmonate with auxin to regulate lateral root (LR) formation through characterization of an *Arabidopsis* mutant, *jasmonate-induced defective lateral root1* (*jdl1/asa1-1*). We demonstrate that, whereas exogenous jasmonate promotes LR formation in wild type, it represses LR formation in *jdl1/asa1-1*. *JDL1* encodes the auxin biosynthetic gene *ANTHRANILATE SYNTHASE α1* (*ASA1*), which is required for jasmonate-induced auxin biosynthesis. Inspection of auxin distribution through monitoring expression patterns of the auxin responsive-*proIAA2:GUS* reporter reveals that jasmonate elevates local auxin accumulation in the basal meristem of wild-type roots, whereas it reduces local auxin accumulation in the basal meristem of mutant roots, suggesting that in addition to activate *ASA1*-dependent auxin biosynthesis, jasmonate also affects auxin transport. Indeed, jasmonate modifies the expression of auxin transport genes in an *ASA1*-dependent manner. We further provide evidence showing that the action mechanism of jasmonate to regulate LR formation through *ASA1* differs from that of ethylene. Our results highlight the importance of *ASA1* in jasmonate-induced auxin biosynthesis and, reveal a role for jasmonate in the attenuation of polar auxin transport in the root. Jasmonate action therefore results in fine-tuning local auxin distribution in the root basal meristem that appears to be critical for LR formation.

## 6.2 Introduction

Root systems of higher plants mainly consist of an embryonic primary root and post-embryonically developed lateral roots (LRs). Root branching or LR formation in higher plants is influenced by a wide range of environmental cues such as nutrients and water availability in the soil (Malamy, 2005). The plasticity of LR formation is of critical importance for sessile plants, allowing them to compete for resources in the soil and adapt to constantly-changing growth conditions. The mechanisms by which plants incorporate diverse regulatory signals into the developmental program of LRs are under active investigation.

Extensive studies in *Arabidopsis thaliana* have detailed the developmental processes associated with the initiation and later development of the lateral root primordium (LRP). A LRP is derived from the pericycle founder cell located in vascular tissues of the primary root (Malamy and Benfey, 1997; Casimiro et al., 2001; Dubrovsky et al., 2001). An early event at the onset of LRP initiation is that a small number of mature pericycle cells adjacent to the xylem poles divide asymmetrically to form daughter cells which are shorter than the flanking undivided pericycle cells. These daughter cells then undergo a series of precisely oriented cell divisions and expansions leading to the formation of a new organ. Eventually, an emerged LR contains a meristem which has essentially the same structure as that of the primary root meristem.

Despite structural and cytological changes occurring during LRP initiation and development, the underlying molecular mechanisms are not yet fully understood. The

phytohormone auxin seems to play an important role during each stage of LR formation (Casimiro et al., 2003; De Smet et al., 2006; Fukaki et al., 2007; Nibau et al., 2008; Fukaki and Tasaka, 2009). Physiological studies have indicated that application of auxin stimulates LR formation (Celenza et al., 1995), whereas application of polar auxin transport (PAT) inhibitors prevents LR formation (Casimiro et al., 2001; Himanen et al., 2002). Whereas *Arabidopsis* mutants with elevated endogenous auxin levels have an increased number of LRs, mutants with defective auxin transport, perception or signaling consistently show reduced LR formation (Casimiro et al., 2003; De Smet et al., 2006; Nibau et al., 2008). The essential role of auxin during LRP development has been confirmed and refined by recent in-depth investigations using the auxin-responsive reporter *DR5:GUS* (Benková et al., 2003; Dubrovsky et al., 2008). These studies elegantly demonstrated that auxin is the local instructive signal for specification of founder cells that give rise to LRPs. Furthermore, establishment of an auxin gradient with its maximum at the tip is important for proper LRP development. This gradient is dependent on PAT mediated by the PIN-FORMED (PIN) auxin efflux facilitators (Tanaka et al., 2006; De Smet et al., 2006; Michniewicz et al., 2007).

In contrast to auxin, little is known about the action of jasmonate on LR formation. As a stress hormone, jasmonate plays a well-established role in regulation of defense responses to herbivore attack and pathogen infection (Creelman and Mullet, 1997; Turner et al., 2002; Browse, 2005; Wasternack, 2007; Howe and Jander, 2008; Kazan and Manners, 2008). In addition, jasmonate also regulates many aspects of plant growth and development (Creelman and Mullet, 1997; Turner et al., 2002; Browse, 2005;

Wasternack, 2007). For example, it has long been recognized that application of jasmonate inhibits root growth (Ueda and Kato, 1980). This action has been employed as the basis for the most prominent genetic assay to identify jasmonate-related mutants in *Arabidopsis* (Staswick et al., 1992; Turner et al., 2002; Wasternack, 2007), which have significantly advanced our understanding on the molecular mechanisms of the jasmonate signaling pathway (Creelman and Mullet, 1997; Turner et al., 2002; Browse, 2005; Wasternack, 2007; Howe and Jander, 2008; Kazan and Manners, 2008).

Here we report the characterization of an *Arabidopsis* mutant designated as *jdl1/asa1-1* that essentially does not form LRs in the presence of 20 µM MeJA, the methyl ester of jasmonic acid (JA). Using the mitotic promoter-reporter construct pro*CYCB1;1:GUS* as a LRP reporter, we show that while MeJA promotes LR formation in wild type, it represses LRP initiation in *jdl1/asa1-1*. Gene cloning studies indicate that *JDL1* encodes the auxin biosynthetic gene *ANTHRANILATE SYNTHASE α1* (*ASA1*), leading to a hypothesis that jasmonate regulates LR formation through crosstalk with auxin and its biosynthesis. Our results not only highlight the importance of *ASA1* in mediating jasmonate-induced auxin biosynthesis, but also reveal a hitherto masked ability of jasmonate to down-regulate PIN1 and PIN2 protein levels. We propose that jasmonate both controls *ASA1*-dependent auxin biosynthesis and, attenuates PIN-dependent auxin transport, providing a fine-tuned regulation of local auxin accumulation in the root basal meristem that is essential for LR formation.

## 6.3 Results

### 6.3.1 *jdl1/asa1-1* is a jasmonate response mutant in LR formation

The inhibitory effect of jasmonate on primary root growth has been well recognized and widely employed as a genetic assay to identify jasmonate-related mutants in *Arabidopsis*. We found that jasmonate promotes LR formation in wild-type (WT) *Arabidopsis* plants. Under our growth conditions, MeJA at 1 µM, a concentration that did not significantly affect primary root growth, increased the number of total LRs (including LRPs and emerged LRs) by 83% (Figure 6.1B). MeJA, at concentrations of 10 µM or 20 µM, significantly inhibited primary root growth (Figure 6.1C) and increased total LRs by about 33% (Figure 6.1B). When MeJA concentration was raised to 50 µM, primary root growth was severely inhibited (Figure 6.1C), and the promotional effect on LR formation was not significant (Figure 6.1B). To explore the mechanisms of jasmonate action on LR formation, we performed a forward genetic screen for seedlings that did not show LR formation when grown on medium containing 20 µM MeJA (see METHODS). Seedlings that appeared similar to WT without MeJA but had reduced LR formation in the presence of MeJA were identified as *jdl/asa1* mutants. Here we describe the characterization of the *jdl1/asa1* mutant.

In the absence of MeJA, LR formation in *jdl1/asa1-1* was only slightly reduced compared to WT (Figures 6.1A and 6.1B). Detailed morphological comparison indicated that, when grown on MeJA-free medium, LR development in *jdl1/asa1-1* was largely normal (Supplemental Figure 6.1). To gain insight into the developmental basis for

jasmonate action on LR formation, WT and *jdl1/asa1-1* seedlings were grown on medium containing a range of concentrations of MeJA and total LRs were counted. Interestingly, while MeJA application led to increased numbers of total LRs in WT, it exerted a repressive, rather than promotional, effect on LR formation in *jdl1/asa1-1* (Figure 6.1A and 6.1B). Under our experimental conditions, 20 µM MeJA was sufficient to block the overall ability of *jdl1/asa1-1* to form LR (Figure 6.1A and 6.1B, Supplemental Figure 6.1). Therefore, *jdl1/asa1-1* represents a jasmonate response mutant for LR formation.

To determine which stage of LR formation is blocked by MeJA in *jdl1/asa1-1*, the *proCYCB1;1:GUS* reporter was introduced into the *jdl1/asa1-1* mutant background through genetic crossing. The *proCYCB1;1:GUS* reporter marks the very first divisions in pericycle cells during LR initiation and serves as a useful tool to visualize the LRP initiation and later development processes (Casimiro et al., 2001; Himanen et al., 2002; Laplaze et al., 2007). Microscopic monitoring of *proCYCB1;1:GUS* expression indicated that MeJA perturbs the initial anticlinal division of pericycle cells leading to LRP initiation in the *jdl1/asa1-1* mutant. For example, in the presence of 20 µM MeJA, GUS was expressed in the primary root tip and LRP initiation sites in WT root (Figure 6.1D and 6.1E). In *jdl1/asa1-1* root, however, GUS expression was only found in the root tip, but not in pericycle cells (Figure 6.1F and 6.1G). Therefore, *jdl1/asa1-1* is impaired in LRP initiation in response to jasmonate.

Although *jdl1/asa1-1* was defective in MeJA-induced LR formation, this mutant showed normal response to MeJA in primary root growth (Figure 6.1C), suggesting that *JDL1* represents a critical component required for MeJA-regulated LR formation, but not for MeJA-induced inhibition of primary root growth.

### 6.3.2 *JDL1* codes for ASA1, a rate-limiting enzyme for the biosynthesis of tryptophan, a metabolic intermediate for IAA production

The deficiency of *jdl1/asa1-1* in MeJA-induced LR formation provides a facile assay to determine the molecular basis of this defect using a map-based cloning approach. Using 1621 individuals showing the *jdl1/asa1-1* phenotype from a F2 mapping population, the *jdl1/asa1-1* mutation was mapped to a region between two molecular markers on the BAC clone MJJ13 of chromosome 5 (Figure 6.2A). DNA sequencing and comparison of the predicted genes in this interval revealed a single G to A nucleotide substitution in the annotated gene At5g05730 (Figure 6.2B), which was previously shown to encode the α-subunit of ANTHRANILATE SYNTHASE (ASA1) (Niyogi and Fink, 1992). Anthranilate synthase converts chorismate to anthranilate, a rate-limiting step for the biosynthesis of tryptophan, a metabolic intermediate for IAA biosynthesis (Radwanski and Last, 1995; Woodward and Bartel, 2005).

The G to A mutation in *jdl1/asa1-1*-derived *ASA1* occurs in the third exon and results in a substitution of the predicted $Trp^{175}$ to a premature translational stop codon (Figure 6.2B). Reverse transcription-PCR (RT-PCR) analysis indicated that this mutation impairs the transcriptional expression of *ASA1* (Figure 6.2C). We then analyzed two

independent mutant alleles of *ASA1*. A homozygous T-DNA line, Salk_040353, which contains a T-DNA insertion in the ninth exon of *ASA1* (Figure 6.2B), showed a similar MeJA-induced LR phenotype as *jdl1/asa1-1* (Figure 6.2D). F1 plants between Salk_040353 and WT (Col-0) showed WT response to MeJA in LR formation, suggesting that homozygous Salk_040353 harbors a recessive mutation (Figure 6.2D). F1 plants from a cross between *jdl1/asa1-1* and Salk_040353 showed defective LR formation in the presence of exogenous MeJA, indicating that *jdl1/asa1-1* is allelic to Salk_040353 (Figure 6.2D). In addition, the *wei2-2* mutant, recently shown to be a null allele of the *ASA1* gene (Stepanova et al., 2005), also exhibited similar jasmonate-induced LR formation defect (Figure 6.2E). Together, these results demonstrated that the MeJA-induced LR formation defect of *jdl1/asa1-1* is caused by loss-of-function of the *ASA1* gene. We therefore refer to *JDL1* as *ASA1*, as this corresponds with the known biochemical function of this gene. Accordingly, the original *jdl1* mutant was re-designated as *asa1-1*, Salk_040353 was re-designated as *asa1-2* and *wei2-2* was re-designated as *asa1-3* hence force.

Several independent studies have demonstrated that loss-of-function of *ASA1* results in defective tryptophan biosynthesis and, as a consequence, leads to a reduction of endogenous IAA levels (Rutherford et al., 1998; Ljung et al., 2005; Stepanova et al., 2005). In this context, we reasoned that the LR formation phenotype of *jdl1/asa1-1* might be caused by defective auxin biosynthesis. In our feeding experiments, 10 mM exogenous anthranilate, a direct product of the ASA1 protein, fully rescued the LR formation defect of *jdl1/asa1-1* in the absence or presence of MeJA (Figure 6.3). Exogenous application of

tryptophan, a precursor of auxin biosynthesis, also corrected the *jdl1/asa1-1* phenotype (Figure 6.3). Finally, IAA at 10 nM, a concentration that does not show a significant effect on root growth of WT seedlings (Rahman et al., 2001; Stepanova et al., 2005), was also able to partially restore the LR formation defect of *jdl1/asa1-1* (Figure 6.3). Together, our feeding experiments support the notion that the LR formation phenotype of *jdl1/asa1-1* is, in fact, caused by a defect in auxin biosynthesis in the presence of MeJA.

### 6.3.3 *ASA1* is important for MeJA-induced IAA biosynthesis

To study the role of the *ASA1* gene in jasmonate response in LR formation, we examined the MeJA-induced expression of *ASA1*. For this experiment, 12-d-old WT plants were treated with MeJA and *ASA1* transcript levels in whole seedlings were measured with quantitative RT-PCR (qRT-PCR). As shown in Figure 6.4A, *ASA1* transcript elevation was seen as early as 0.5 h after MeJA treatment, with a maximum level reached after 2 h. The MeJA-induced *ASA1* expression showed a tendency of reduction in a time course between 2 h to 9 h after MeJA treatment (Figure 6.4A).

To study whether the MeJA-induced expression of *ASA1* requires the function of COI1, a central regulator of jasmonate-mediated processes in *Arabidopsis* (Xie et al., 1998), we compared the MeJA-induced *ASA1* expression in WT and the *coi1-1* mutant (Xie et al., 1998). Northern blot analysis using RNAs from whole seedlings showed that the MeJA-induced expression of *ASA1* is largely reduced in *coi1-1* (Figure 6.4B). We further examined the MeJA-induced *ASA1* expression in shoot and root tissues by qRT-PCR and found that the *coi1-1* mutation abolished MeJA-induced *ASA1* expression in

both shoot and root tissues (Figure 6.4C). These data indicated that MeJA activates the expression of *ASA1* in a COI1-dependent manner.

The MeJA-induced *ASA1* expression pattern was also examined with the *ASA1* promoter fused with the GUS reporter (*proASA1:GUS*). At 5-d-old seedling stage, *proASA1:GUS* was mainly expressed in the root tip and the hypocotyl/root junction (Figure 6.4D and 6.4F). MeJA treatment not only significantly enhanced *proASA1:GUS* expression in the root tip, but also expanded its expression domains to vascular tissues along the whole primary root (Figure 6.4E and 6.4G). In addition to *ASA1*, MeJA also increased the transcription levels of several other auxin biosynthesis-related genes (Supplemental Figure 6.2). Among them, *ASB1* (Stepanova et al., 2005), *NIT3* (Kutz et al., 2002) and *YUCCA2* (Cheng et al., 2006) have been shown to be directly involved in IAA biosynthesis. Our promoter-GUS assays indicated that MeJA significantly enhanced the expression of *ASB1*, *NIT3* and *YUCCA2* in the root (Supplemental Figure 6.2). These data suggest that MeJA induces IAA biosynthesis through transcriptional activation of *ASA1* and other auxin biosynthetic genes. To investigste this possibility, we measured free IAA levels of 12-d-old WT and *jdl1/asa1-1* seedlings. Without MeJA treatment, free IAA levels in *jdl1/asa1-1* seedlings were slightly lower than those in WT (Figure 6.4H). After MeJA treatment, however, free IAA levels in WT were almost doubled, whereas free IAA levels in the mutant were only increased by 50% (Figure 6.4H), indicating that *ASA1* is required for MeJA-mediated induction of IAA biosynthesis.

Taken together, these results demonstrated that the *ASA1* function is required for jasmonate-induced auxin biosynthesis and led us to hypothesize that jasmonate regulates LR formation through activation of the *ASA1*-dependent auxin biosynthesis and subsequent response. Further support to this hypothesis came from our finding that jasmonate failed to promote LR formation in the *slr1* (Fukaki et al., 2002) and *arf7-1 arf19-2* (Okushima et al., 2005) double mutants (Supplemental Figure 5.3), in which LRP initiation is abolished as a result of disrupted auxin signaling.

### 6.3.4 MeJA-regulated *proIAA2:GUS* expression in WT and *jdl1/asa1-1* roots

To explore how jasmonate interacts with auxin to differentially regulate LR formation in WT and *jdl1/asa1-1,* we examined the spatial distribution of the auxin response in WT and *jdl1/asa1-1* roots using the auxin-responsive reporter *proIAA2:GUS,* which provides a greater spatial resolution of the auxin response in the root (Swarup et al., 2001; Marchant et al., 2002). For this purpose, we introduced the *proIAA2:GUS* reporter into the *jdl1/asa1-1* mutant background and compared the MeJA-induced GUS expression between WT and *jdl1/asa1-1* roots. In this experiment, we paid special attention to the *proIAA2:GUS* expression in a region at the transition between the meristem and the elongation zone, referred to as the root basal meristem, the site of LRP initiation (Beemster et al., 2003; De Smet et al., 2007). In untreated WT roots, *proIAA2:GUS* was expressed in the stele and columella cells (Figure 6.5A). Upon MeJA treatment, *proIAA2:GUS* expression was strongly enhanced in the stele and ectopically induced in the lateral root cap and epidermal cells (Figure 6.5B), suggesting that MeJA

up-regulates auxin response in WT roots. As expected, the MeJA-mediated up-regulation of *proIAA2:GUS* expression was significantly reduced in the jasmonate-insensitive mutant *coi1-1* (Figure 6.5C and 6.5D). Consistently, the MeJA-mediated induction of LR formation was largely abolished in *coi1-2* (Xu et al., 2002), in which LR formation is largely normal in the absence of MeJA (Figure 6.5I). In *jdl1/asa1-1* roots, the basal expression of *proIAA2:GUS* was somehow lower (Figure 6.5E) and, most surprisingly, MeJA treatment led to a significant reduction of *proIAA2:GUS* expression, particularly in the root basal meristem (Figure 6.5F). These results indicated that whereas MeJA increases auxin response in basal meristem of WT roots, it attenuates auxin response in basal meristem of *jdl1/asa1-1* roots. The contrasting action of MeJA on the root auxin response between WT and *jdl1/asa1-1* is consistent with the distinct effect of MeJA on LR formation between the two genotypes. As MeJA can actually increase free IAA levels by up to 50% in *jdl1/asa1-1* whole seedlings (Figure 6.4F), a plausible explanation for the MeJA-induced reduction of *proIAA2:GUS* expression in *jdl1/asa1-1* root is that MeJA might exert a negative effect on local auxin accumulation in the mutant root, especially in the root basal meristem.

Among the two physiologically distinct auxin transport pathways, both the phloem-based auxin transport from source leaves and the local PAT in the root contribute to auxin accumulation in the basal meristem (Swarup et al., 2001; Swarup et al., 2005; Blilou et al., 2005; Leyser, 2005). It has been proposed that the auxin influx carrier protein AUX1, which functions in both auxin transport routes, plays a role in connecting the phloem-based transport of IAA to the PAT system (Swarup et al., 2001; Marchant et

al., 2002; De Smet et al., 2007). In this context, we first checked the jasmonate-induced expression of *proIAA2:GUS* expression in *aux1-22* (Swarup et al., 2007), a null mutant disrupting the function of AUX1. The results indicated that the MeJA-triggered induction of *proIAA2:GUS* expression was largely abolished in *aux1-22* (Figure 6.5G and 6.5H), suggesting that the jasmonate-mediated activation of auxin response in the root requires the function of AUX1. Next, we checked the LR promotional effect of jasmonate in several auxin transport mutants including *aux1-22*, *axr4-2* (Dharmasiri et al., 2006) and *lax3 aux1-21* (Swarup et al., 2008). Due to defective auxin transport capacities, these mutants showed reduced LR formation in the absence of MeJA (Figure 6.5I). As expected, MeJA failed to restore LR formation of these mutants to WT levels (Figure 6.5I), indicating that MeJA-mediated induction of LR formation requires auxin transport.

The idea that MeJA affects auxin transport (both phloem-based transport and PAT) during LR formation was substantiated by comparative inspection of the auxin-responsive reporters *DR5rev:GFP* (Ottenschläger et al., 2003) and *DR5:GUS* (Ulmasov et al., 1997) in WT and *jdl1/asa1-1* roots. In WT roots, MeJA up-regulated the expression of these reporters in root tips (Supplemental Figure 6.4) and at the LRP initiation sites along the primary root length (Supplemental Figure 6.5). In *jdl1/asa1-1* roots, however, MeJA down-regulated the expression of these reporters in root tips (Supplemental Figure 4) and at the LRP initiation sites along the primary root length (Supplemental Figure 6.5).

### 6.3.5 Jasmonate modulates expression of auxin transport components

To explore how jasmonate regulates auxin transport during LR formation, we investigated the effect of MeJA treatment on the expression of several important components of the auxin transport machinery. Using transgenic lines containing the *proPIN1:GUS*, *proPIN2:GUS* and *proAUX1:GUS* reporters, respectively, which have been used previously to monitor the native gene expression (Vieten et al., 2005; Ruzicka et al., 2007), we observed a general induction effect of MeJA on the expression of these auxin efflux and infux genes at the transcriptional level. For example, when 5-d-old seedlings grown on control medium were transferred to medium containing 10 μM MeJA, obvious up-regulation of *proPIN1:GUS* (Figure 6.6A and 6.6B), *proPIN2:GUS* (Figure 6C and 6D) and *proAUX1:GUS* (Figure 6.6E and 6.6F) expression was detectable within 12 h after transfer.

To quantitatively assess the effect of MeJA on the expression of these genes, we performed qRT-PCR analyses using RNAs extracted from MeJA-treated roots. To address whether the *jdl1/asa1-1* mutation affects the action of MeJA on the regulation of these genes, we examined the expression of *PIN1*, *PIN2* and *AUX1* in roots of WT and *jdl1/asa1-1*. Similar to the *promoter:GUS* assays, MeJA treatment led to a general increase of *PIN1*, *PIN2* and *AUX1* mRNAs in WT roots (Figure 6.6G). Importantly, the MeJA-mediated induction of *PIN1* and *PIN2* expression was obviously reduced in *jdl1/asa1-1* roots (Figure 6.6G). Notably, whereas MeJA up-regulated *AUX1* expression in WT roots, this hormone significantly down-regulated *AUX1* expression in *jdl1/asa1-1* roots (Figure 6.6G). These results demonstrated that MeJA regulates the expression of the

auxin transport-related genes at the transcriptional level and highlighted the importance of *ASA1* in this regulation.

Finally, we asked whether jasmonate might regulate auxin transport-related genes at the protein level. For these experiments, 4-d-old WT and *jdl1/asa1-1* seedlings grown on control medium were transferred to medium without or with 20 μM MeJA. Forty-eight hours after transfer, PIN1 and PIN2 protein levels were assessed by immunolocalization assays. As shown in Figure 6.6H to 6.6I, MeJA treatment led to substantial reduction of PIN1 and PIN2 protein levels in WT roots. Significantly, the MeJA-mediated reduction of PIN1 and PIN2 protein levels in *jdl1/asa1-1* roots was much more severe than that observed in WT roots (Figure 6.6J and 6.6K), suggesting that the *ASA1* gene function is important for jasmonate-mediated down-regulation of PIN1 and PIN2 protein levels.

### 6.3.6 The Action of Jasmonate to Regulate LR Formation Is Independent of Ethylene

Recent reports have demonstrated that ethylene regulates LR formation through interaction with auxin (Negi et al., 2008; Ivanchenco et al., 2008). To test the possibility that jasmonate might act through the ethylene pathway to regulate LR formation, we checked the MeJA-induced LR formation in ethylene insensitive mutants *etr1-2* and *ein2-5*. *ETR1* encodes one of the ethylene receptor in *Arabidopsis* (Chang et al., 1993). *EIN2* encodes a membrane protein with unknown biochemical function and plays a positive role in ethylene signaling (Alonso et al., 1999). Consistent with recent observations (Negi et al., 2008; Ivanchenco et al., 2008), *etr1-2* and *ein2-5* showed slightly increased LR

formation in the absence of MeJA (Figure 6.7A). Given that *etr1-2* and *ein2-5* exhibited increased sensitivity to MeJA in primary root growth, we treated these plants with relatively low concentrations of MeJA and compared their LR formation with that of *jdl1/asa1-1*. As shown in Figure 6.7A, whereas 0.1 μM or 1 μM MeJA significantly reduced LR formation in *jdl1/asa1-1*, these concentrations of MeJA significantly increased LR formation in *etr1-1*, *ein2-5* as well as WT. These results indicated that, in contrast to *jdl1/asa1-1* which was defective in MeJA-induced LR formation, *etr1-1* and *eni2-5* showed near WT response to MeJA in LR formation, suggesting that the MeJA action on LR formation does not require ethylene signaling.

It has been shown that the *ASA1* gene play a role in ethylene-mediated inhibition of primary root growth (Stepanova et al., 2005; Ruzicka et al., 2007; Swarup et al., 2007). To test whether *ASA1* is also important for the ethylene action in LR formation, *jdl1/asa1-1* and WT were examined for their response to the ethylene precursor 1-amino-1-cyclopropane carboxylic acid (ACC) in LR formation. As shown in Figure 6.7B, low concentration of ACC (0.02 μM) was able to promote LR formation in WT, and this promotional effect was impaired in *jdl1/asa1-1*. High concentration of ACC (0.2 μM) inhibited LR formation in WT, and there was a significant reduction in the ability of 0.2 μM ACC to inhibit LR formation in *jdl1/asa1-1* (Figure 6.7B), consistent with a recent proposal that *ASA1* plays a role in ethylene-mediated regulation of LR formation (Negi et al., 2008). In parallel, we examined the ethylene-mediated LR formation in the jasmonate-insensitive *coi1-2* mutant, which is resistant to jasmonate but partially fertile and able to produce a small quantity of seeds (Xu et al., 2002). As shown in Figure 6.7B,

the ethylene response of *coi1-2* in LR formation was essentially similar to that of WT, suggesting that the ethylene action in regulating LR formation does not require the COI1-dependent jasmonate signaling.

Together, our results imply that the action of jasmonate to regulate LR formation is possibly independent of ethylene. This hypothesis is also supported by the fact that loss-of-function of *ASA1* led to altered response to ethylene both in primary root growth (Stepanova et al., 2005; Ruzicka et al., 2007; Swarup et al., 2007) and in lateral root formation (Negi et al., 2008; Ivanchenco et al., 2008; Figure 6.7B), but the *jdl1/asa1-1* mutant only affects jasmonate-induced LR formation, does not affect MeJA-induced primary root growth (This work).

## 6.4 Discussion

### 6.4.1 JDL1/ASA1 is an interaction node through which jasmonate integrates its action with auxin to regulate LR formation

It has been long recognized that the stress hormone jasmonate inhibits primary root growth (Wasternack, 2007). We report here that jasmonate also plays a role in regulating LR formation in *Arabidopsis*. Given the established role of auxin in LR formation (Casimiro et al., 2003; De Smet et al., 2006; Nibau et al., 2008, Fukaki and Tasaka, 2009) and the previous finding that jasmonate and auxin share common components in their signaling pathways (Tiryaki and Staswick, 2002), it is reasonable to speculate that jasmonate may interact with auxin to regulate LR formation. Our characterization of the *jdl1/asa1-1* mutant, which showed defective LR formation in the presence of exogenous MeJA (Figure 6.1), proved this speculation and provided insights on the action mechanisms of jasmonate to regulate LR formation. While MeJA promoted LR formation in WT, it repressed LR formation in *jdl1/asa1-1* (Figure 6.1). The fact that the repressive effect of MeJA on LR formation can only be observed in the *jdl1/asa1-1* mutant implies that, in WT, the repressive effect of MeJA on LR formation is masked by the *JDL1* function. Therefore, elucidation of the biochemical function of the *JDL1* gene product is critical to understand the molecular mechanisms underlying the distinct effect of MeJA on LR formation between WT and *jdl1/asa1-1*.

Not surprisingly, gene cloning studies indicated that *JDL1* encodes the well-characterized auxin biosynthetic gene *ASA1* (Figure 6.2). Early studies indicated that the

expression of *ASA1* was induced by wounding and pathogen infections (Niyogi and Fink, 1992), suggesting a potential role for this gene in plant responses to abiotic or biotic stresses. Indeed, *ASA1* was also demonstrated recently to be required for ethylene-induced auxin production and, therefore, plays a role in ethylene-mediated regulation of root growth inhibition (Stepanova et al., 2005). In this context, it is reasonable to propose that *ASA1* may represent an integration node through which jasmonate exerts its effect on auxin biosynthesis and, subsequently, regulates LR formation. Supporting evidence to this hypothesis first came from our feeding experiments showing that anthranilate, tryptophan and, finally auxin, can rescue or partially rescue the LR-deficient phenotype of the *jdl1/asa1-1* mutant (Figure 6.3). Furthermore, gene expression analyses indicated that MeJA activates the expression of *ASA1* in a COI1-dependent manner (Figure 4B and 4C). In addition to *ASA1*, MeJA also induces the expression of a list of other genes known to be related to auxin biosynthesis (Supplemental Figure 6.2). Finally, our measurement of free IAA levels proved the role of *ASA1* in mediating jasmonate-induced auxin biosynthesis (Figure 6.4G). Collectively, these results support a hypothesis that jasmonate activates the transcriptional expression of *ASA1* and leads to increased free IAA levels, which eventually contributes to MeJA-induced promotion of LR formation in WT plants. It is worth to note that, MeJA can increase free IAA levels (by up to 50%) even in the *jdl1/asa1-1* mutant seedlings although not as much as in WT seedlings (Figure 6.4G), indicating the existence of other targets of MeJA in IAA biosynthesis. Indeed, our qRT-PCR assays indicated that MeJA can induce the expression of the putative IAA conjugate hydrolase gene *ILL5* (for *ILR1-like5*) (Supplemental Figure 6.2

online). However, it remains to be determined whether the *ILL5* gene product is an active IAA amidohydrolase (Davies et al., 1999; Woodward and Bartel, 2005).

### 6.4.2 Characterization of the *jdl1/asa1-1* mutant reveals a masked role of jasmonate to regulate auxin transport during LR formation

However, the above oversimplified scenario can not explain the phenomenon that MeJA represses LR formation in the *jdl1/asa1-1* mutant. Extensive studies have together demonstrated that the phytohormone auxin serves as an instructive signal for LRP initiation and later development (Casimiro et al. 2001, Bhalerao et al. 2002; Benková et al., 2003; Laplaze et al., 2007; Swarup et al., 2008; Dubrovsky et al., 2008). Notably, a recently elegant observation proposed that LR positioning is regulated in a spatiotemporal manner by auxin accumulation in the root basal meristem (Ishikawa and Evans, 1995; Beemster et al., 2003; De Smet et al., 2007). Under this paradigm, the jasmonate-induced LR formation defect of *jdl1/asa1-1* may result from suboptimal auxin accumulation in the root basal meristem. The employment of the auxin responsive reporter *proIAA2:GUS* enabled us to inspect, at cellular resolution, local auxin accumulation in the root basal meristem. Our observations indicated that, in WT, the promotional effect of MeJA on LR formation is correlated with increased *proIAA2:GUS* expression in the basal meristem (Figure 6.5A and 6.5B). In the *jdl1/asa1-1* mutant, the repressive effect of MeJA on LR formation is correlated with reduced *proIAA2:GUS* in the root basal meristem (Figure 6.5C and 6.5D). The basal meristem has been proposed to recycle the major auxin transport flows in the root, including the phloem-based shoot-

derived auxin transport flow and the local PAT flows (Swarup et al., 2001; Marchant et al., 2002; Swarup et al., 2005; Blilou et al., 2005; Leyser, 2005), therefore, basal meristem exhibits an auxin accumulation maximum which is essential for LR initiation (De Smet et al., 2007). In this context, our observations of *proIAA2:GUS* expression in WT and mutant roots point to a possibility that, in addition to activate *ASA1*-dependent IAA biosynthesis, MeJA may also affect, directly or indirectly, the auxin transport flows which are important for local auxin accumulation in the basal meristem. The ability of the *aux1-22* mutation to reduce MeJA-induced *proIAA2:GUS* expression in the basal meristem (Figure 6.5G and 6.5H) provided supporting evidence to this hypothesis, since AUX1 was reported to be involved in the two physiologically distinct auxin transport pathways (i.e., phloem-based transport and local PAT) in the basal meristem (Swarup et al., 2001; Marchant et al., 2002; De Smet et al., 2007). Furthermore, we found that jasmonate exhibits a complex regulation on the expression of several auxin influx and efflux facilitators at both transcription and protein levels (Figure 6.6). Notably, in MeJA-treated WT roots, PIN1 and PIN2 protein levels were decreased (Figure 6.6H and 6.6I). In MeJA-treated *jdl1/asa1-1* roots, the reduction was more severe than that in WT roots (Figure 6.6J and 6.6K). These results suggested that the *ASA1* function (i.e., jasmonate-induced auxin biosynthesis) is important for JA-mediated regulation of auxin transport components.

Previous characterization of independent mutant alleles of *ASA1*, including *trp5-2*$^{wvc1}$ (Rutherford et al., 1998) and *tir7* (Ruegger et al., 1997; Ljung et al., 2005), which were isolated based on altered root waving phenotype and resistance to auxin transport

inhibitors, respectively, provided evidence that mutation of the *ASA1* function might affect auxin transport. Together with our observations in this work, these results raised the interesting question of how jasmonate regulates the expression of auxin transport components. Given jasmonate promotes *ASA1*-dependent auxin biosynthesis and auxin itself can up-regulate the expression of the *PIN* genes at the transcription level (Vieten et al., 2005), it is possible that the MeJA-induced up-regulation of the transcripts of auxin transport-related genes is achieved indirectly through the auxin pathway, i.e., MeJA induces the expression of *ASA1* that leads to increased auxin synthesis which, in turn, activates the transcriptional expression of these genes. Our data that the *jdl1/asa1-1* mutation affects the jasmonate-regulated expression levels of *AUX1*, *PIN1* and *PIN2* (Figure 6.6A to 6.6G) lend support to this possibility. Considering that MeJA positively regulates the biosynthesis of flavonoids (Dombrecht et al., 2007), which act as negative regulators of auxin transport (Brown et al., 2001; Buer and Muday, 2004; Peer et al., 2004; Besseau et al., 2007), it is also possible that the MeJA-mediated regulation of auxin transport-related genes is achieved through the up-regulation of flavonoid biosynthesis by MeJA. In line with this idea, recent elegant work using flavonoid mutants with altered auxin transport indicated that flavonoids modulate the expression of the *PIN* genes at both mRNA and protein levels in a tissue specific manner (Peer et al., 2004). Further studies are required to elucidate the regulatory mechanisms of jasmonate on the expression of auxin transport-related genes.

### 6.4.3 Jasmonate mediates a fine-tuned regulation of auxin accumulation in the root basal meristem that is critical for LR formation

Based on the results described in this study, we propose a model (Figure 6.8) to explain the distinct effect of jasmonate on LR formation between WT and *jdl1/asa1-1*. In WT plants, MeJA activates the transcriptional expression of *ASA1* which leads to increased IAA biosynthesis in shoot and root tissues. *De novo* synthesized IAA by *ASA1*-dependent pathway in the aerial part was delivered through phloem-based transport or long distance PAT to the root basal meristem region. IAA synthesized locally in the root by *ASA1* was also transported through PAT to the root basal meristem. It has been shown that defect of the *ASA1* gene harbored by the *tir7-1* mutation allele has less impact on root-specific IAA synthesis than on synthesis in the aerial portion of the seedling (Ljung et al., 2005), suggesting that MeJA-induced IAA accumulation in the root basal meristem is mainly derived from *ASA1* synthesis in shoot tissues. Considering the proposed dominant role of phloem-based transport in long-distance auxin distribution (Tanaka et al., 2006), it is likely that the majority of IAA produced in the aerial part by *ASA1* is transported to the basal meristem through phloem. In addition to activate *ASA1*-dependent auxin biosynthesis, MeJA also directly or indirectly decreases PIN1 and PIN2 protein levels, which results in a negative effect on PAT-mediated local auxin accumulation in the basal meristem. The combinational effect of MeJA on IAA biosynthesis and transport leads to increased local auxin accumulation in the root basal meristem, as a result, promotes LR formation.

In *jdl1/asa1-1* mutants, the jasmonate-induced auxin biosynthesis through *ASA1* is blocked, which leads to defective auxin sources (both shoot and root tissues) for jasmonate-induced auxin accumulation in the root basal meristem. Jasmonate still exerts

its negative effect on auxin transport capacity through reducing PIN1 and PIN2 protein levels. These effects likely cause the root basal meristem to be deprived of auxin accumulation and, as a consequence, repress LR formation. It should be noted that, the repressive effect of jasmonate on local auxin accumulation in the root basal meristem (as well as LR formation) can only be observed in *jdl1/asa1-1*, but not in WT, suggesting that the *ASA1* function (i.e., jasmonate-induced auxin biosynthesis) counteracts the repressive effect of jasmonate on auxin transport. Our results not only highlight the importance of *ASA1* in mediating jasmonate-induced auxin biosynthesis, but also reveal a masked repressive role of jasmonate on auxin transport. The two aspects of jasmonate actions may represent a fine-tuned regulation of local auxin accumulation that is critical for LR formation. Given the established role of jasmonate in plant defense, the jasmonate-mediated fine-tuned regulation of LR formation may have adaptive significance under conditions in which jasmonate levels are elevated.

## 6.5 Methods

### 6.5.1 Plant materials and growth conditions

*Arabidopsis* mutants and/or transgenic lines described are in Columbia (Col-0) background. Some of the plant materials used in this study were previously described: *wei2-2* (Stepanova et al., 2005); *coi1-1* (Xie et al., 1998); *coi1-2* (Xu et al., 2002); *proCYCB1;1:GUS* (Colón-Carmona et al., 1999); *DR5:GUS* (Ulmasov et al., 1997); *proYUC2:GUS* (Cheng et al., 2006); *proNIT3:GUS* (Kutz et al., 2002); *proIAA2:GUS* and *proIAA2:GUS/aux1-22* (Swarup et al., 2007); *DR5rev:GFP* (Benková et al., 2003); *aux1-22* (Swarup et al., 2007); *axr4-2* (Dharmasiri et al., 2006); *lax3 aux1-21* (Swarup et al., 2008); *proPIN1,2:GUS* (Vieten et al., 2005) and *proAUX1:GUS* (Marchant et al., 2002). Seeds of Salk_040353 were obtained from the *Arabidopsis* Biological Resource Center (Alonso et al., 2003).

Seeds were surface-sterilized for 15 min in 10% bleach, washed four times with sterile water, and plated on half-strength Murashige and Skoog (MS) medium (Murashige and Skoog, 1962). Plants were stratified at 4℃ for 2 d in darkness and then transferred to a phytotrone set at 22℃ with a 16-h light/8-h dark photoperiod (light intensity 120 μmol $m^{-2}$ $sec^{-1}$).

### 6.5.2 Isolation of the *jdl1/asa1-1* mutant

Ethyl methanesulfonate (EMS)-mutagenized M2 seeds of the WT accession, Col-0, were kindly provided by Dr. Jianru Zuo (Institute of Genetics and Developmental

Biology, Chinese Academy of Sciences, Beijing). M2 seeds were germinated and grown vertically on medium containing 20 µM MeJA for 10 d. Seedlings with reduced LRs were selected and directly transplanted to soil. Resulting M3 seeds from the putative mutants were confirmed on medium with 20 µM MeJA by LR phenotypes. The original *jdl1/asa1-1* (*jasmonate-induced defective lateral root1-1*) mutant was backcrossed to Col-0 for three generations and the resulted homozygous progenies were used in this study.

### 6.5.3 Map-based cloning of the *JDL1* gene

For mapping, the *jdl1/asa1-1* mutant in the Col-0 background was crossed to the polymorphic ecotype Landsberg *erecta* (L*er*), and the resulting F1 plants were self pollinated to yield F2 population segregating for the *jdl1/asa1-1* mutant phenotypes. Simple sequence length polymorphism (SSLP) markers were used for linkage analysis using a previously described procedure (Lukowitz et al., 2000). In the fine mapping process, we developed several PCR-based molecular markers. The primers for the SSLP marker CER455774 are 5'-CTAATAGAAGTGGAAAGTAAGA-3' and 5'-GGGGGAGTGATCAATGGTAT-3'. The following cleaved amplified polymorphic sequence (CAPS) markers were designed: For MJJ-1, the primers 5'-TAGAGGCCAACATGCACATATC-3' and 5'-TGTTTTACCCTGCTCTTGCTTT-3' were used, and the PCR product from L*er* can be digested by *Afl* III (198 bp and 145 bp); For CER438063, the primers 5'-TACTTGTTCTTGGCTAAATCC-3' and 5'-

GACCCACCTCTAATAAATCTACTA-3' were used, the PCR product from L*er* can be digested by *Eco*RV (241 bp and 391 bp).

The T-DNA insertion line Salk_040353 contains a T-DNA inserted in the ninth exon of *ASA1* (At5g05730). Homozygous T-DNA insertion plants were identified by diagnostic PCR with the gene specific primers 5'-TGATCGAGTGGAAAAAGGTTG-3' and 5'-ATGAAAAGCAATGTGCTGAGC-3'. The homozygous Salk_040353 mutant was crossed with *jdl1/asa1-1* for allelic test.

To generate *DR5:GU*S reporter line in the *jdl1/asa1-1* mutant background, homozygous *jdl1/asa1-1* plants were crossed to a transgenic line harboring the *DR5:GUS* construct (Ulmasov et al., 1997) to produce an F2 population. Putative *DR5:GUS/jdl1/asa1-1* plants, which were homozygous for the *jdl1/asa1-1* mutation as well as the *DR5:GUS* construct, were identified in F2 and then re-tested in F3 (i.e., in F3, 100% of seedlings showed no LR formation in the presence of 20 μM MeJA; 100% of seedlings showed uniform staining for GUS). Similarly, the *DR5rev:GFP* (Benková et al., 2003), *proCYCB1;1:GUS* (Colón-Carmona et al., 1999) and *proIAA2:GUS* (Swarup et al., 2007) reporters were also introduced into the *jdl1/asa1-1* mutant background. The *proIAA2:GUS and DR5rev:GFP* constructs were also transferred into the *coi1-1* mutant (Xie et al., 1998) using a similar approach.

### 6.5.4 Plasmid construction and plant transformation

All molecular manipulations were performed according to standard methods (Sambrook and Russell, 2001). A 2.0-kb genomic fragment upstream of the *ASA1* translation start codon was amplified by PCR and cloned into the *Sal*I/B*am*HI sites of the binary vector pCAMBIA1391-Z, resulting in the transcriptional fusion of the *ASA1* promoter with the GUS coding region. Similarly, a 2.0-kb promoter region of *ASB1* was also fused with the GUS coding region in the binary vector pCAMBIA1391-Z. Primers used for PCR amplification are as follows: 5'-CGCGTCGACCTAGAATATGTTATGCTTC-3' (*Sal*I) and 5'-CTAGGATCCTGTAACGGCTAAGAACTC-3' (*Bam*HI) for *ASA1* promoter; 5'-ATCAAGCTTTTCGGGCAGAGATCGCAGAGC-3' (*Hin*dIII) and 5'-GCCGGATCCTGTCTGAGAAGCAAAGATTCCT-3' (*Bam*HI) for *ASB1* promoter.

The above constructs were then transformed into *A. tumefaciens* strain GV3101 (pMP90), which were used for transformation of *Arabidopsis* plants by vacuum infiltration (Bechtold and Pelletier, 1998).

**6.5.5 Analysis of GUS activity**

Histochemical staining for GUS activity in transgenic plants was performed as described previously (Jefferson et al., 1987). Whole seedlings or various tissues were immersed in 1 mM 5-bromo-4-chloro-3-indolyl-β-glucuronic acid solution in 100 mM sodium phosphate, pH 7.0, 0.1 mM EDTA, 0.5 mM ferricyanide, 0.5 mM ferrocyanide, and 0.1% Triton X-100, after applying vacuum for 2 min, they were incubated at 37℃

from 20 min to overnight. Chlorophyll was cleared from plant tissues by immersing them in 70% ethanol. Individual representative seedlings were photographed.

### 6.5.6 Observation of plants

Seedlings of *DR5:GUS/*Col-0, *DR5:GUS/jdl1/asa1-1*, *proIAA2:GUS/*Col-0, *proIAA2:GUS/jdl1/asa1-1*, *proIAA2:GUS/coi1-1*, *proIAA2:GUS/aux1-22*, *proASA1:GUS/*Col-0, *proASB1:GUS/*Col-0, *proPIN1,2:GUS/*Col-0, *proAUX1:GUS/*Col-0, *proYUC2:GUS/*Col-0 and *proNIT3:GUS/*Col-0 reporter lines were photographed using the Leica Microsystems (Leica DM5000B Microscope and Leica DFC490 CCD camera). To observe the LRP and emerged LR, roots were first cleared by the HCG solution (Chloroacetaldehyde : $H_2O$ : Glycerol = 8:3:1) for 30 s (Sabatini et al., 1999). The numbers of LRPs and emerged LRs were counted with the Interference Discrepancy Contrast Microscope system (Leica DM5000B Microscope). Roots of *DR5rev:GFP/*Col-0, *DR5rev:GFP/jdl1/asa1-1* and *DR5rev:GFP/coi1-1* plants in different genetic backgrounds were mounted in 10 μM propidium iodide (PI) solution for 3-5 min for confocal scanning. The fluorescence excitation and image acquisitions were monitored by the laser scanning confocal microscope (LSM 510, Zeiss, Oberkochen, Germany).

### 6.5.7 Free IAA measurement

To measure the influence of jasmonate on auxin levels, seeds of Col-0 and *jdl1/asa1-1* were surface sterilized. Approximately 30 mL of medium containing half strength Murashige and Skoog salts (Caisson Laboratories, Inc.), 1% sucrose, and 0.5%

phytagel (Sigma), pH 5.7 was poured into each square Petri-dish (100 x 100 x 15 mm) and 19 seeds were placed in a line, 1 cm from the top edge. The Petri dishes were incubated vertically at 22°C in a phytotrone. Four milliliters of 100 μM MeJA (Bedoukian Research, Inc., CT) was added to the plates in the horizontal position onto the Petri dish to cover the seedlings for 10 minutes. Petri dishes with MeJA or control solution were resealed and placed vertically in growth chamber for another 2 d. Ethanol was used to make the 100 mM MeJA stock solution, resulting in 0.1% ethanol in the final 100 μM treatment solution, and the same amount of ethanol in water was used as the control treatment. Fresh whole seedlings (25-50 mg) were harvested, weighed and then frozen in liquid nitrogen. After adding 3 ng of [$^{13}C_6$] IAA as internal standard, each sample was extracted, purified, methylated and then analyzed by using selected ion monitoring gas chromatography-mass spectrometry (GC-SIM-MS) as described (Barkawi et al., 2008). At least 10 biological replicates were analyzed for each treatment.

### 6.5.8 Immunolocalization ssay for PIN proteins

The PIN1 and PIN2 immunolocalization assays were performed using the InsituPro robot (Friml et al., 2002). The following antibodies and dilutions were used: anti-PIN1 (1:50), anti-PIN2 (1:400) and Alexa Fluor® 488 or Alexa Fluor® 555 (1:500) secondary antibodies (Molecular Probes, Oregon, USA). Fluorescent samples were inspected by confocal laser scanning microscope Zeiss Axioplan 2 Imaging and the Zeiss LSM 510 Image Browser software.

### 6.5.9 Gene expression analysis

For RNA gel blot analysis, total RNA was prepared by a guanidine thiocyanate extraction method, and RNA gel blot analysis was performed as described previously (Zheng et al., 2006). Ten micrograms of total RNA was separated in an agarose gel containing 10% formaldehyde, blotted onto Hybond $N^+$ membrane (Amersham), and probed with $^{32}$P-labeled DNA fragment for *ASA1*. Primers used to amplify the *ASA1* probe are 5'-GGCCGCCACCGAGTTCTTAG-3' and 5'-GCAAATGTTCGCCGCTCAAA-3'.

For quantitative RT-PCR (qRT-PCR) analysis, 12-d-old *Arabidopsis* seedlings (Col-0 and *jdl1/asa1-1*) grown vertically on medium plates were treated with 50 μM MeJA for 3 h, or untreated as a control. Whole seedlings or different tissues were frozen in liquid nitrogen for RNA extraction. RNA was extracted with the RNeasy kit (Qiagen). Poly(dT) cDNA was prepared from 10 μg of total RNA with Superscript III reverse transcriptase (Invitrogen) and quantified with an cycler apparatus (Bio-Rad) with the RealMasterMix (SYBR Green) kit (Tiangen) according to the manufacturer's instructions. PCR was performed in 96-well optical reaction plates heated for 5 min at 95°C to activate hot start Taq DNA polymerase, followed by 40 cycles of denaturation for 30 s at 95°C, annealing for 30 s at 59°C and extension for 20 s at 68°C. Expression levels of target genes were normalized to *ACTIN2* or *ACTIN2* expression levels. The statistical significance was evaluated by *t*-test analysis. Primers used to quantify gene expression levels were listed in Supplemental Table 1 online.

***This article was published in The Plant Cell: Sun, J., Xu, Y., Ye, S., Jiang, H., Chen, Q., Liu, F., Zhou, W., Chen, R., Li, X., Tietz, O., Wu, X., Cohen, J.D., Palme, K. and Li, C. (2009) Arabidopsis ASA1 is important for jasmonate-mediated regulation of auxin biosynthesis and transport during lateral root formation. Plant Cell 21:1495-1511***

## 6. 6 References


Alonso, J.M., Hirayama, T., Roman, G., Nourizadeh, S. and Ecker, J.R. (1999) EIN2, a bifunctional transducer of ethylene and stress responses in *Arabidopsis*. Science 284: 2148–2152

Alonso, J.M., et al. (2003) Genome-wide insertional mutagenesis of *Arabidopsis thaliana*. Science 301: 653–657

Barkawi, L.S., Tam, Y.Y., Tillman, J.A., Pederson, B., Calio, J., Al-Amier, H., Emerick, M., Normanly, J. and Cohen, J.D. (2008) A high-throughput method for the quantitative analysis of indole-3-acetic acid and other auxins from plant tissue. Anal. Biochem. 372: 177–188

Bechtold, N. and Pelletier, G. (1998) *In planta Agrobacterium*-mediated transformation of adult *Arabidopsis thaliana* plants by vacuum infiltration. Methods in Mol. Biol. 82: 259–266

Beemster, G. T. S., Fiorani, F. and Inzé, D. (2003) Cell cycle: the key to plant growth control? Trends Plant Sci. 8: 154–158

Benková, E., Michniewicz, M., Sauer, M., Teichmann, T., Seifertova, D., Jurgens, G. and Friml, J. (2003) Local, efflux-dependent auxin gradients as a common module for plant organ formation. Cell 115: 591–602

Besseau, S., Hoffmann, L., Geoffroy, P., Lapierre, C., Pollet, B. and Legrand, M. (2007) Flavonoid accumulation in *Arabidopsis* repressed in lignin synthesis affects auxin transport and plant growth. Plant Cell 19: 148–162

Bhalerao, R.P., Eklof, J., Ljung, K., Marchant, A., Bennett, M. and Sandberg, G. (2002) Shoot-derived auxin is essential for early lateral root emergence in *Arabidopsis* seedlings. Plant J. 29: 325–332

Blilou, I., Xu, J., Wildwater, M., Willemsen, V., Paponov, I., Friml, J., Heidstra, R., Aida, M., Palme, K. and Scheres, B. (2005) The PIN auxin efflux facilitator network controls growth and patterning in *Arabidopsis* roots. Nature 433: 39–44

Brown, D.E., Rashotte, A.M., Murphy, A.S., Normanly, J., Tague, B.W., Peer, W.A., Taiz, L. and Muday, G.K. (2001) Flavonoids act as negative regulators of auxin transport *in vivo* in *Arabidopsis*. Plant Physiol. 126: 524–535

Browse, J. (2005) Jasmonate: an oxylipin signal with many roles in plants. Vitamins and Hormones 72: 431–456

Buer, C.S. and Muday, G.K. (2004) The *transparent testa4* mutation prevents flavonoid synthesis and alters auxin transport and the response of *Arabidopsis* roots to gravity and light. Plant Cell 16: 1191–1205

Casimiro, I., Beeckman, T., Graham, N., Bhalerao, R., Zhang, H., Casero, P., Sandberg, G. and Bennett, M.J. (2003) Dissecting *Arabidopsis* lateral root development. Trends Plant Sci. 8: 165–171

Casimiro, I., Marchant, A., Bhalerao, R.P., Beeckman, T., Dhooge, S., Swarup, R., Graham, N., Inze, D., Sandberg, G., Casero, P.J. and Bennett, M. (2001) Auxin transport promotes *Arabidopsis* lateral root initiation. Plant Cell 13: 843–852

Celenza, J.L., Jr., Grisafi, P.L. and Fink, G.R. (1995) A pathway for lateral root formation in *Arabidopsis thaliana*. Genes Dev. 9: 2131–2142

Chang, C., Kwok, S.F., Bleecker, A.B. and Meyerowitz, E.M. (1993) *Arabidopsis* ethylene-response gene ETR1: similarity of product to two-component regulators. Science 262: 539–544

Cheng, Y., Dai, X. and Zhao, Y. (2006) Auxin biosynthesis by the YUCCA flavin monooxygenases controls the formation of floral organs and vascular tissues in *Arabidopsis*. Genes Dev. 20: 1790–1799

Colón-Carmona, A., You, R., Haimovitch-Gal, T. and Doerner, P. (1999) Technical advance: spatio-temporal analysis of mitotic activity with a labile cyclin-GUS fusion protein. Plant J. 20: 503–508

Creelman, R.A. and Mullet, J.E. (1997) Biosynthesis and action of jasmonates in plants. Annu. Rev. Plant Physiol. Plant Mol. Biol. 48: 355–381

Davies, R.T., Goetz, D.H., Lasswell, J., Anderson, M.N. and Bartel, B. (1999) *IAR3* encodes an auxin conjugate hydrolase from Arabidopsis. Plant Cell 11: 365–376

De Smet, I., Vanneste, S., Inzé, D. and Beeckman, T. (2006) Lateral root initiation or the birth of a new meristem. Plant Mol. Biol. 60: 871–887

De Smet, I., Tetsumura, T., De Rybel, B., Frey, N.F., Laplaze. L., Casimiro, I., Swarup, R., Naudts, M., Vanneste, S., Audenaert, D., Inzé, D., Bennett, M.J. and Beeckman, T. (2007) Auxin-dependent regulation of lateral root positioning in the basal meristem of *Arabidopsis*. Development 134: 681–690

Dharmasiri, S., Swarup, R., Mockaitis, K., Dharmasiri, N., Singh, S.K., Kowalchyk, M., Marchant, A., Mills, S., Sandberg, G., Bennett, M.J. and Estelle, M. (2006) AXR4 is required for localization of the auxin influx facilitator AUX1. Science 312: 1218–1220

Dombrecht, B., Xue, G.P., Sprague, S.J., Kirkegaard, J.A., Ross, J.J., Reid, J.B., Fitt, G.P., Sewelam, N., Schenk, P.M., Manners, J.M. and Kazan, K. (2007) MYC2 differentially modulates diverse jasmonate-dependent functions in *Arabidopsis*. Plant Cell 19: 2225–2245

Dubrovsky, J.G., Rost, T.L., Colón-Carmona, A. and Doerner, P. (2001) Early primordium morphogenesis during lateral root initiation in *Arabidopsis thaliana*. Planta 214: 30–36

Dubrovsky, J.G., Sauer, M., Napsucialy-Mendivil, S., Ivanchenko, M.G., Friml, J., Shishkova, S., Celenza, J. and Benkova, E. (2008) Auxin acts as a local morphogenetic trigger to specify lateral root founder cells. Proc. Natl. Acad. Sci. USA 105: 8790–8794

Friml J., Benková E., Blilou I., Wisniewska J., Hamann T., Ljung K., Woody S., Sandberg G., Scheres B., Jürgens G. and Palme K. (2002) AtPIN4 mediates sink-driven auxin gradients and root patterning in *Arabidopsis*. Cell 108: 661–673

Fukaki, H. and Tasaka, M. (2009) Hormone interactions during lateral root formation. Plant Mol. Biol. 69: 383–396

Fukaki, H., Okushima, Y. and Tasaka, M. (2007) Auxin-mediated lateral root formation in higher plants. Int. Rev. Cytol. 256: 111–137

Fukaki, H., Tameda, S., Masuda, H. and Tasaka, M. (2002) Lateral root formation is blocked by a gain-of-function mutation in the *SOLITARY-ROOT/IAA14* gene of *Arabidopsis*. Plant J. 29: 153–168

Himanen, K., Boucheron, E., Vanneste, S., de Almeida Engler, J., Inze, D. and Beeckman, T. (2002) Auxin-mediated cell cycle activation during early lateral root initiation. Plant cell 14: 2339–2351

Howe, G.A. and Jander, G. (2008) Plant immunity to insect herbivores. Annu. Rev. Plant Biol. 59: 41–66

Ishikawa, H. and Evans, M. L. (1995) Specialized zones of development in roots. Plant Physiol. 109: 725–727

Jefferson, R.A., Kavanagh, T.A. and Bevan, M.W. (1987) GUS fusions: beta-glucuronidase as a sensitive and versatile gene fusion marker in higher plants. EMBO J. 6: 3901–3907

Kazan, K. and Manners, J.M. (2008) Jasmonate signaling: toward an integrated view. Plant Physiol. 146: 1459–1468

Kutz, A., Muller, A., Hennig, P., Kaiser, W.M., Piotrowski, M. and Weiler, E.W. (2002) A role for nitrilase 3 in the regulation of root morphology in sulphur-starving *Arabidopsis thaliana*. Plant J. 30: 95–106

Laplaze, L., Benkova, E., Casimiro, I., Maes, L., Vanneste, S., Swarup, R., Weijers, D., Calvo, V., Parizot, B., Herrera-Rodriguez, M.B., Offringa, R., Graham, N., Doumas, P., Friml, J., Bogusz, D., Beeckman, T. and Bennett, M. (2007) Cytokinins act directly on lateral root founder cells to inhibit root initiation. Plant Cell 19: 3889–3900

Leyser, O. (2005) Auxin distribution and plant pattern formation: how many angels can dance on the point of PIN? Cell 121: 819–822

Ljung, K., Hull, A.K., Celenza, J., Yamada, M., Estelle, M., Normanly, J. and Sandberg, G. (2005) Sites and regulation of auxin biosynthesis in *Arabidopsis* roots. Plant Cell 17: 1090–1104

Lukowitz, W., Gillmor, C.S. and Scheible, W.R. (2000) Positional cloning in *Arabidopsis*. Why it feels good to have a genome initiative working for you. Plant Physiol. 123: 795–805

Malamy, J.E. (2005) Intrinsic and environmental response pathways that regulate root system architecture. Plant Cell Environ. 28: 67–77

Malamy, J.E. and Benfey, P.N. (1997) Organization and cell differentiation in lateral roots of *Arabidopsis thaliana*. Development 124: 33–44

Marchant, A., Bhalerao, R., Casimiro, I., Eklof, J., Casero, P.J., Bennett, M. and Sandberg, G. (2002) AUX1 promotes lateral root formation by facilitating indole-3-acetic acid distribution between sink and source tissues in the *Arabidopsis* seedling. Plant Cell 14: 589–597

Michniewicz, M., Zago, M.K., Abas, L., Weijers, D., Schweighofer, A., Meskiene, I., Heisler, M.G., Ohno, C., Zhang, J., Huang, F., Schwab, R., Weigel, D., Meyerowitz, E.M., Luschnig, C., Offringa, R. and Friml, J. (2007) Antagonistic regulation of PIN phosphorylation by PP2A and PINOID directs auxin flux. Cell 130: 1044–1056

Murashige, T. and Skoog, F. (1962) A revised medium for rapid growth and bioassays with tobacco tissue culture. Physiol. Plant 15: 473–497

Nibau, C., Gibbs, D.J. and Coates, J.C. (2008) Branching out in new directions: the control of root architecture by lateral root formation. New Phytol. 179: 595–614

Niyogi, K.K. and Fink, G.R. (1992) Two anthranilate synthase genes in *Arabidopsis*: defense-related regulation of the tryptophan pathway. Plant Cell 4: 721–733

Okushima, Y., Overvoorde, P.J., Arima, K., Alonso, J.M., Chan, A., Chang, C., Ecker, J.R., Hughes, B., Lui, A., Nguyen, D., Onodera, C., Quach, H., Smith, A., Yu, G. and Theologis, A. (2005) Functional genomic analysis of the *AUXIN RESPONSE FACTOR* gene family members in *Arabidopsis thaliana*: unique and overlapping functions of *ARF7* and *ARF19*. Plant Cell 17: 444–463

Ottenschlager, I., Wolff, P., Wolverton, C., Bhalerao, R.P., Sandberg, G., Ishikawa, H., Evans, M. and Palme, K. (2003) Gravity-regulated differential auxin transport from columella to lateral root cap cells. Proc. Natl. Acad. Sci. USA 100: 2987–2991

Peer, W.A., Bandyopadhyay, A., Blakeslee, J.J., Makam, S.N., Chen, R.J., Masson, P.H. and Murphy, A.S. (2004) Variation in expression and protein localization of the PIN family of auxin efflux facilitator proteins in flavonoid mutants with altered auxin transport in *Arabidopsis thaliana*. Plant Cell 16: 1898–1911

Radwanski, E.R. and Last, R.L. (1995) Tryptophan biosynthesis and metabolism: biochemical and molecular genetics. Plant Cell 7: 921–934

Rahman, A., Amakawa, T., Goto, N. and Tsurumi, S. (2001) Auxin is a positive regulator for ethylene-mediated response in the growth of *Arabidopsis* roots. Plant Cell Physiol. 42: 301–307

Ruegger, M., Dewey, E., Hobbie, L., Brown, D., Bernasconi, P., Turner, J., Muday, G. and Estelle, M. (1997) Reduced naphthylphthalamic acid binding in the *tir3* mutant of *Arabidopsis* is associated with a reduction in polar auxin transport and diverse morphological defects. Plant Cell 9: 745–757

Rutherford, R., Gallois, P. and Masson, P.H. (1998) Mutations in *Arabidopsis thaliana* genes involved in the tryptophan biosynthesis pathway affect root waving on tilted agar surfaces. Plant J. 16:145–154

Ruzicka, K., Ljung, K., Vanneste, S., Podhorska, R., Beeckman, T., Friml, J. and Benkova, E. (2007) Ethylene regulates root growth through effects on auxin biosynthesis and transport-dependent auxin distribution. Plant Cell 19: 2197–2212

Sabatini, S., Beis, D., Wolkenfelt, H., Murfett, J., Guilfoyle, T., Malamy, J., Benfey, P., Leyser, O., Bechtold, N., Weisbeek, P. and Scheres, B. (1999) An auxin-dependent distal organizer of pattern and polarity in the *Arabidopsis* root. Cell 99: 463–472

Sambrook, J. and Russell, D.W. (2001) Molecular cloning, 3rd edn. Cold Spring Harbor Laboratory Press, Cold Spring Harbor, New York

Staswick, P.E., Su, W. and Howell, S.H. (1992) Methyl jasmonate inhibition of root growth and induction of a leaf protein are decreased in an *Arabidopsis thaliana* mutant. Proc. Natl. Acad. Sci. USA 89: 6837–6840

Stepanova, A.N., Hoyt, J.M., Hamilton, A.A. and Alonso, J.M. (2005) A Link between ethylene and auxin uncovered by the characterization of two root-specific ethylene-insensitive mutants in *Arabidopsis*. Plant Cell 17: 2230–2242

Swarup, K., Benkova, E., Swarup, R., Casimiro, I., Peret, B., Yang, Y., Parry, G., Nielsen, E., De Smet, I., Vanneste, S., Levesque, M.P., Carrier, D., James, N., Calvo, V., Ljung, K., Kramer, E., Roberts, R., Graham, N., Marillonnet, S., Patel, K., Jones, J.D., Taylor, C.G., Schachtman, D.P., May, S., Sandberg, G., Benfey, P., Friml, J., Kerr, I., Beeckman, T., Laplaze, L. and Bennett, M.J. (2008) The auxin influx carrier LAX3 promotes lateral root emergence. Nat. Cell Biol. 10: 946–954

Swarup, R., Friml, J., Marchant, A., Ljung, K., Sandberg, G., Palme, K. and Bennett, M. (2001) Localization of the auxin permease AUX1 suggests two functionally distinct hormone transport pathways operate in the *Arabidopsis* root apex. Genes Dev. 15: 2648–2653

Swarup, R., Kramer, E. M., Perry, P., Knox, K., Leyser, H. M. O., Haseloff, J., Beemster, G. T. S., Bhalerao, R. and Bennett, M. J. (2005) Root gravitropism requires lateral root cap and epidermal cells for transport and response to a mobile auxin signal. Nat. Cell Biol. 7: 1057–1065

Swarup, R., Perry, P., Hagenbeek, D., Van Der Straeten, D., Beemster, G.T., Sandberg, G., Bhalerao, R., Ljung, K. and Bennett, M.J. (2007) Ethylene upregulates auxin biosynthesis in *Arabidopsis* seedlings to enhance inhibition of root cell elongation. Plant Cell 19: 2186–2196

Tanaka, H., Dhonukshe, P., Brewer, P.B. and Friml, J. (2006) Spatiotemporal asymmetric auxin distribution: a means to coordinate plant development. Cell Mol. Life Sci. 63: 2738–2754

Tiryaki, I. and Staswick, P.E. (2002) An *Arabidopsis* mutant defective in jasmonate response is allelic to the auxin-signaling mutant *axr1*. Plant Physiol. 130: 887–894.

Turner, J.G., Ellis, C. and Devoto, A. (2002) The jasmonate signal pathway. Plant Cell 14 Suppl: S153–164

Ueda, J. and Kato, J. (1980) Isolation and identification of a senescence-promoting substance from wormwood (*Artemisia absinthium L*.). Plant Physiol. 66: 246–249

Ulmasov, T., Murfett, J., Hagen, G. and Guilfoyle, T.J. (1997) Aux/IAA proteins repress expression of reporter genes containing natural and highly active synthetic auxin response elements. Plant Cell 9: 1963–1971

Vieten, A., Vanneste, S., Wisniewska, J., Benkova, E., Benjamins, R., Beeckman, T., Luschnig, C. and Friml, J. (2005) Functional redundancy of PIN proteins is accompanied by auxin-dependent cross-regulation of PIN expression. Development 132: 4521–4531

Wasternack, C. (2007) Jasmonates: an update on biosynthesis, signal transduction and action in plant stress response, growth and development. Ann. Bot. 100: 681–697.

Woodward, A.W. and Bartel, B. (2005) Auxin: regulation, action, and interaction. Ann. Bot. 95: 707–735

Xie, D.X., Feys, B.F., James, S., Nieto-Rostro, M. and Turner, J.G. (1998) COI1: an *Arabidopsis* gene required for jasmonate-regulated defense and fertility. Science 280: 1091–1094

Xu, L., Liu, F., Lechner, E., Genschik, P., Crosby, W.L., Ma, H., Peng, W., Huang, D. and Xie, D. (2002) The SCF(COI1) ubiquitin-ligase complexes are required for jasmonate response in *Arabidopsis*. Plant Cell 14: 1919–1935

Zheng, W., Zhai, Q., Sun, J., Li, C.B., Zhang, L., Li, H., Zhang, X., Li, S., Xu, Y., Jiang, H., Wu, X. and Li, C. (2006) Bestatin, an inhibitor of aminopeptidases, provides a chemical genetics approach to dissect jasmonate signaling in *Arabidopsis*. Plant Physiol. 141: 1400–1413

## 6.7 Figures

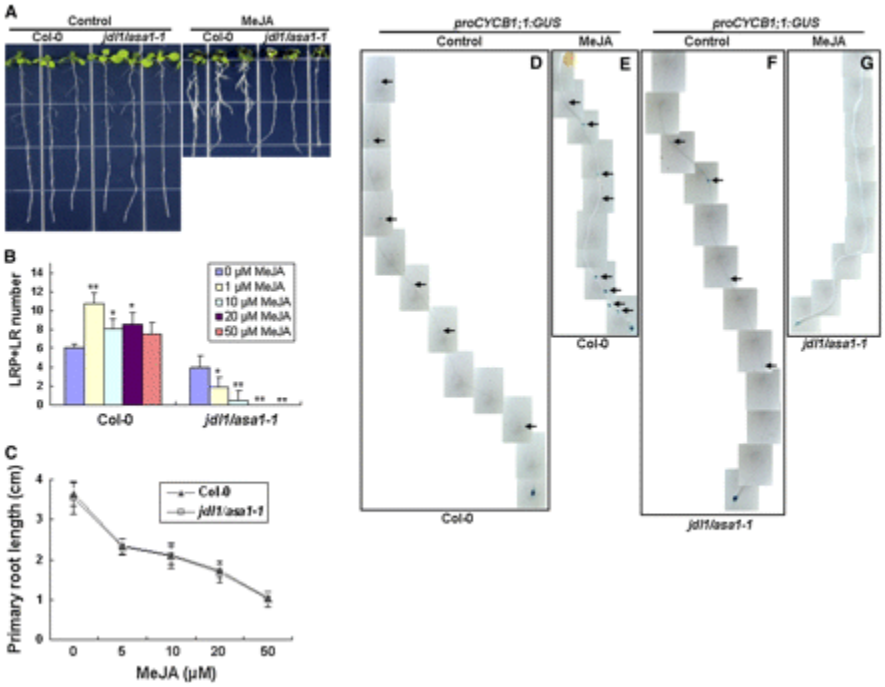


**Figure 6.1.** *jdl1/asa1-1* Shows Defective LR Formation in Response to MeJA Treatment.
**(A)** LR phenotypes of 10-d-old Col-0 and *jdl1/asa1-1* seedlings grown vertically on medium without MeJA (Control) or containing 20 µM MeJA (MeJA). Note that LR formation in the *jdl1/asa1-1* mutant was blocked by exogenous MeJA.
**(B)** Quantification of total LRs (LRPs plus emerged LRs) per primary root. Seven-day-old seedlings grown on Murashige and Skoog medium plates containing indicated concentrations of MeJA were counted for LR formation. Data show average and SD of 15 seedlings and are representative of at least three independent experiments. Asterisks denote *t* test significance compared with untreated plants: *P < 0.05; **P < 0.01.
**(C)** Measurement of primary root length of 10-d-old Col-0 and *jdl1/asa1-1* seedlings grown on medium containing indicated concentrations of MeJA. Data show average and SD of 15 seedlings and are representative of at least three independent experiments.
**(D)** to **(G)** *proCYCB1;1:GUS* staining assays showing that MeJA represses LRP initiation in *jdl1/asa1-1*. Photographs show typical roots of 6-d-old seedlings. Arrows show LRP or emerged LR, as indicated by *proCYCB1;1:GUS* staining.
**(D)** and **(E)** Expression pattern of *proCYCB1;1:GUS* at LRP initiation sites of representative Col-0 roots grown on MeJA-free medium **(D)** or on medium containing 20 µM MeJA **(E)**.
**(F)** and **(G)** Expression pattern of *proCYCB1;1:GUS* at LRP initiation sites of representative *jdl1/asa1-1* roots grown on MeJA-free medium **(F)** or on medium containing 20 µM MeJA **(G)**.

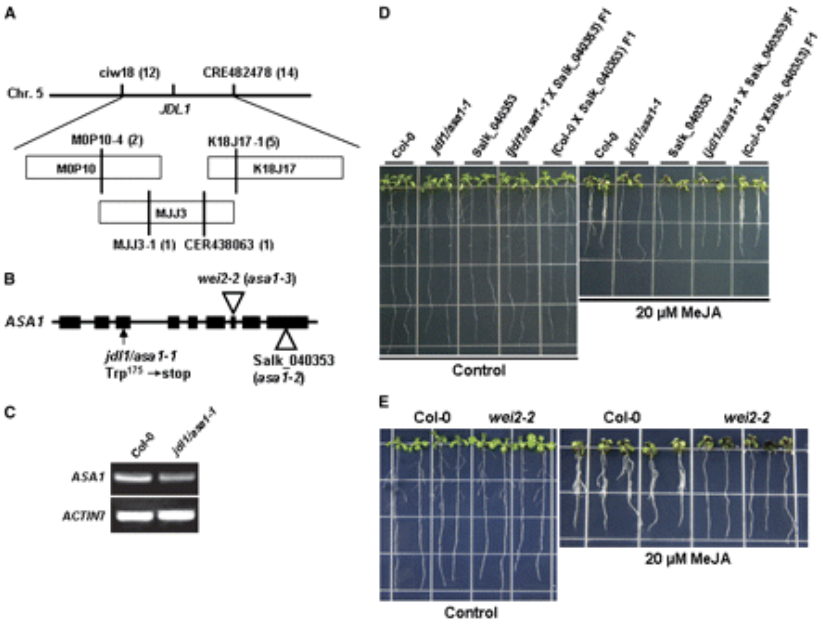


**Figure 6.2.** Map-Based Cloning of the *JDL1* Gene.
**(A)** Fine genetic and physical mapping of *JDL1*. The target gene was initially mapped to a genetic interval between markers ciw18 and CRE482478 on *Arabidopsis* chromosome 5. Analysis of a mapping population consisting of 1631 plants delimited the target gene to a region defined by markers MJJ-1 and CER438063 on the BAC clone MJJ13. Numbers in parentheses indicate the number of recombination events identified between markers and the target gene.
**(B)** Exon (box)-intron (line) structure of the *ASA1* gene (At5g05730). Sequence analysis revealed that the *ASA1* gene derived from the *jdl1/asa1-1* mutant contains a G-to-A mutation, which results in substitution of the predicted Trp-175 to a premature stop codon. Two other T-DNA insertion alleles of the *ASA1* gene, including Salk_040353 (*asa1-2*) and *wei2-2* (*asa1-3*), are indicated by open triangles.
**(C)** RT-PCR analysis of *ASA1* expression in the *jdl1/asa1-1* mutant. Twelve-day-old Col-0 and *jdl1/asa1-1* seedlings were harvested for RNA extraction and RT-PCR analysis. The primers used for PCR were *ASA1F1* and *ASA1R1* for *ASA1* and *ACTIN7F1* and *ACTIN7R1* for *ACTIN7* (see Supplemental Table 1 online).
**(D)** *jdl1/asa1-1* is allelic to the T-DNA insertion mutant Salk_040353, which contains a T-DNA insertion in the *ASA1* gene. Col-0, *jdl1/asa1-1*, Salk_040353, and F1 progenies from crosses between Salk_040353 and *jdl1/asa1-1* or Col-0 were grown vertically for 10 d on medium without MeJA (Control) or containing 20 µM MeJA (MeJA).
**(E)** LR phenotypes of the *wei2-2* mutant, which is a T-DNA insertion allele of *ASA1* (Stepanova et al., 2005). Col-0 and *wei2-2* seedlings were grown vertically for 10 d on medium without MeJA (Control) or with 20 µM MeJA (MeJA).

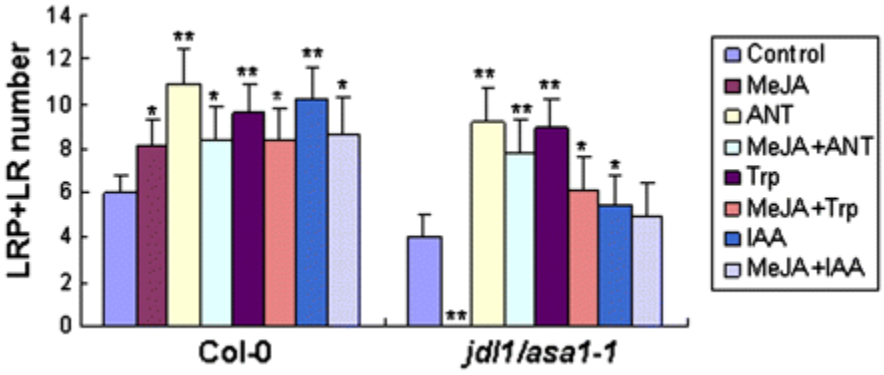


**Figure 6.3.** Rescue of the LR Formation Defect of *jdl1/asa1-1* by Anthranilate, Trp, and IAA. Col-0 and *jdl1/asa1-1* seedlings were grown vertically for 7 d on MeJA-free medium or medium containing 20 µM MeJA, with or without supplementation of 10 mM anthranilate (ANT), 10 mM Trp, or 10 nM IAA, and total LRs (LRPs plus emerged LRs) per primary root were counted. Values represent average and SD of 15 plants and are indicative of at least three independent experiments. Asterisks denote *t* test significance compared with untreated plants: *P < 0.05; **P < 0.01.

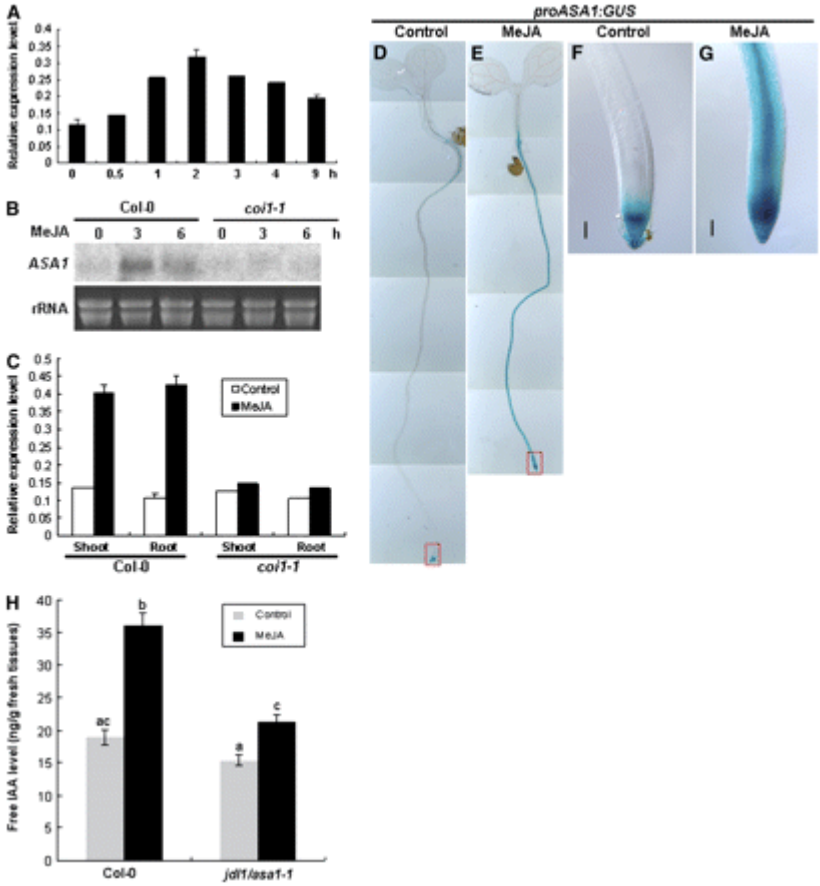


**Figure 6.4.** MeJA Treatment Induces IAA Biosynthesis through Transcriptional Activation of *ASA1* Expression.

**(A)** qRT-PCR analysis of *ASA1* expression in wild-type seedlings during the time course after MeJA treatment. Twelve-day-old Col-0 seedlings were treated with 50 µM MeJA, and whole seedlings were harvested at different time points for RNA extraction and qRT-PCR analyses. The transcript levels of *ASA1* were normalized to the *ACTIN7* expression. Error bars represent the SD of triplicate reactions.

**(B)** RNA gel blot analyses of MeJA-induced *ASA1* expression in the wild type (Col-0) and the *coi1-1* mutant. Twelve-day-old Col-0 and *coi1-1* seedlings were treated with 50 µM MeJA, and whole seedlings were harvested at the indicated times for RNA extraction. The top panel shows a RNA gel blot probed with $^{32}$P-labeled cDNA for *ASA1*, and the bottom panel shows amounts of rRNA as loading controls.

**(C)** qRT-PCR analyses of MeJA-regulated expression of *ASA1* in shoot and root tissues of Col-0 and *coi1-1*. Twelve-day-old Col-0 and *coi1-1* seedlings were treated with 50 µM MeJA for 3 h, and shoot and root tissues were harvested separately for RNA extraction and qRT-PCR analyses. The transcript levels of *ASA1* were normalized to the *ACTIN7* expression, and error bars represent the SD of triplicate reactions..

**(D)** to **(G)** MeJA-induced *proASA1:GUS* expression. Three-day-old seedlings of *proASA1:GUS* transgenic line grown on control medium were transferred either to medium without MeJA **(D)** or to medium containing 10 µM MeJA **(E)** for 2 d.

**(F)** Magnification of the framed region in **(D)**. Bar = 50 µm.

**(G)** Magnification of the framed region in **(E)**. Bar = 50 µm.
**(H)** Free IAA measurement of Col-0 and *jdl1/asa1-1* seedlings in response to MeJA treatment. Twelve-day-old Col-0 and *jdl1/asa1-1* seedlings were left untreated (Control) or treated with 100 µM MeJA (MeJA) for 2 d and then free IAA levels were measured. At least 10 biological replicates were analyzed. An analysis of variance followed by Fisher's Least Significant Difference (LSD) mean separation test (SPSS) was performed on the data. Samples with the different letters are significantly different at $P < 0.01$. Error bars represent SE.

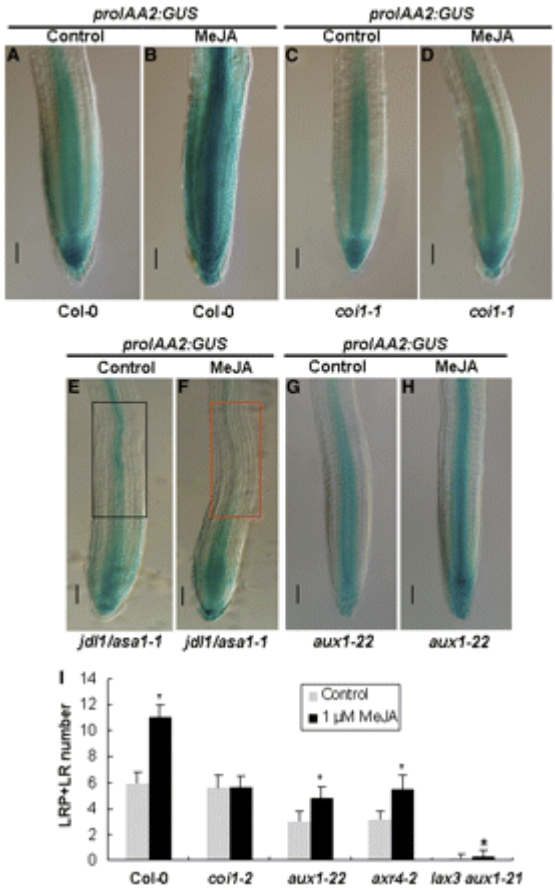


**Figure 6.5.** MeJA-Regulated *proIAA2:GUS* Expression in Roots of Col-0, *coi1-1*, *jdl1/asa1-1*, and *aux1-22*.

**(A)** and **(B)** Control **(A)** and MeJA-treated **(B)** Col-0 roots.

**(C)** and **(D)** Control **(C)** and MeJA-treated **(D)** *coi1-1* roots.

**(E)** and **(F)** Control **(E)** and MeJA-treated **(F)** *jdl1/asa1-1* roots. Framed regions indicate that MeJA reduces *proIAA2:GUS* expression in the basal meristem of *jdl1/asa1-1* roots.

**(G)** and **(H)** Control (G) and MeJA treated (H) aux1-22 roots.

For **(A)** to **(H)**, 4-d-old seedlings of the indicated genotypes grown on control medium were transferred to medium without MeJA (Control) or containing 10 µM MeJA (MeJA) for an additional 2 d, and the *proIAA2:GUS* expression was monitored. Bars = 50 µm.

**(I)** MeJA-mediated LR formation was affected in JA signaling and auxin transport mutants. Col-0, *coi1-2*, *aux1-22*, *axr4-2*, and *lax3 aux1-21* seedlings were grown vertically on medium with or without 1 µM MeJA for 7 d, and total LRs (LRPs plus emerged LRs) per primary root were counted. Values show average and SD of 15 seedlings and are representative of at least three independent experiments. Asterisks denote *t* test significance compared with untreated plants: *P < 0.01.

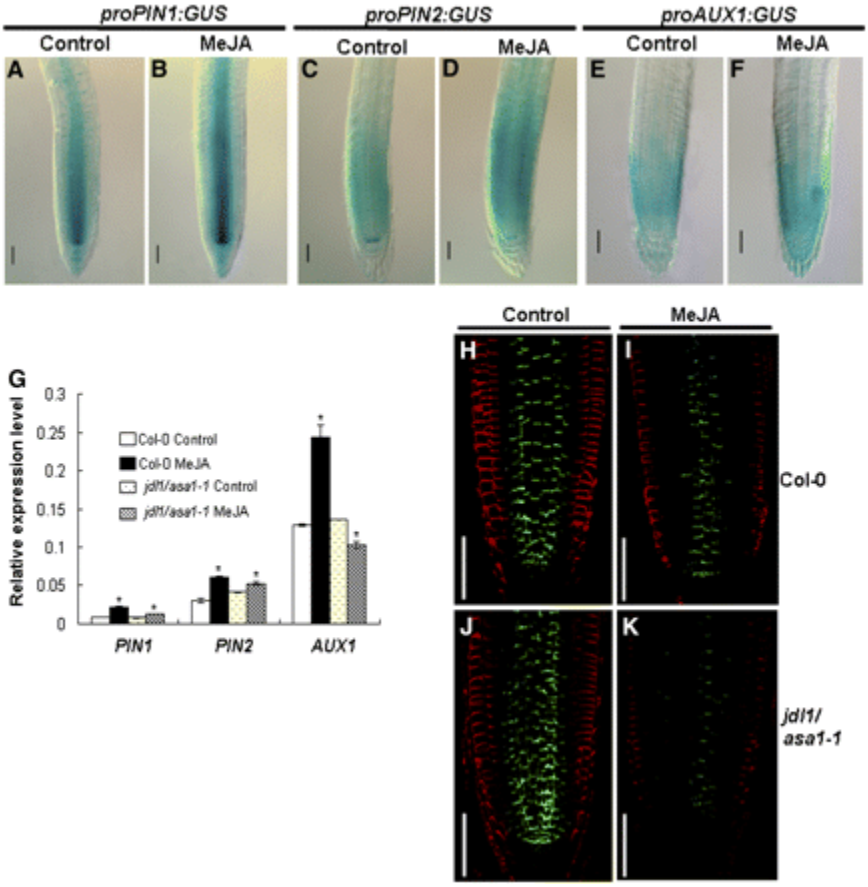


**Figure 6.6.** MeJA-Regulated Expression of Auxin Transport Components in the Roots of Wild-Type Plants.

**(A)** and **(B)** Control **(A)** and MeJA-treated **(B)** roots examined for *proPIN1:GUS* expression.

**(C)** and **(D)** Control **(C)** and MeJA-treated **(D)** roots examined for *proPIN2:GUS* expression.

**(E)** and **(F)** Control **(E)** and MeJA-treated **(F)** roots examined for *proAUX1:GUS* expression.

For **(A)** to **(F),** 5-d-old seedlings of transgenic Col-0 plants containing the indicated constructs were grown on control medium and then transferred to medium without MeJA (Control) or containing 10 µM MeJA (MeJA) for 12 h and then were collected for GUS staining. Bars = 50 µm.

**(G)** qRT-PCR analyses of MeJA-regulated expression of *PIN1*, *PIN2*, and *AUX1* in Col-0 and *jdl1/asa1-1* roots. Ten-day-old Col-0 and *jdl1/asa1-1* seedlings were treated with 50 µM MeJA for 6 h, and roots were harvested for RNA extraction and qRT-PCR analyses. The transcript levels of *PIN1*, *PIN2*, and *AUX1* were normalized to the *ACTIN2* expression. Asterisks denote *t* test significance compared with untreated plants: *P < 0.05. Results of one of three independent experiments are shown. Error bars represent the SD of triplicate reactions.

**(H)** to **(K)** MeJA treatment downregulates the PIN1 and PIN2 protein levels in wild-type and *jdl1/asa1-1* roots.

**(H)** PIN1 and PIN2 immunolocalization of untreated wild-type root.
**(I)** PIN1 and PIN2 immunolocalization of wild-type root treated with MeJA.
**(J)** PIN1 and PIN2 immunolocalization of untreated *jdl1/asa1-1* root.
**(K)** PIN1 and PIN2 immunolocalization of *jdl1/asa1-1* root treated with MeJA.
Four-day-old seedlings were transferred to medium without MeJA (Control) or with 20 µM MeJA (MeJA) for 48 h. Seedlings were fixed for PIN1 and PIN2 immunolocalization assays. Root tips were visualized and photographed with a laser scanning confocal microscope. Green, PIN1; red, PIN2. Bars = 50 µm. Images shown are representative of at least six independent experiments.

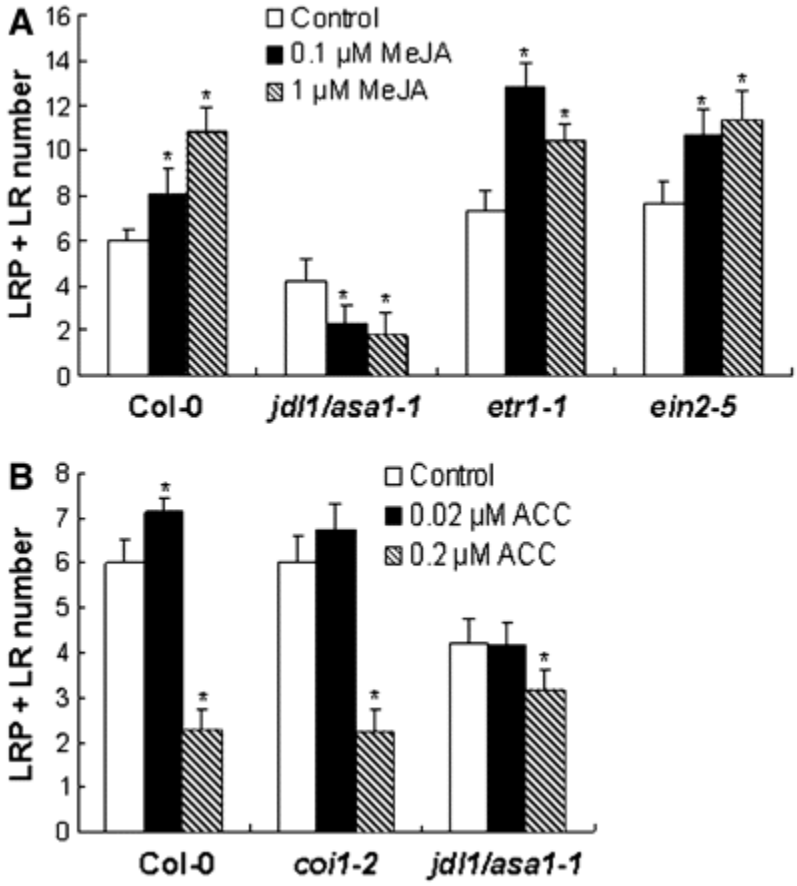


**Figure 6.7.** The Relationship between Jasmonate and Ethylene in Controlling LR Formation through the *ASA1* Gene.
**(A)** MeJA-induced LR formation of the ethylene-insensitive mutants *etr1-1* and *ein2-5*. Seven-day-old seedlings of Col-0, *jdl1/asa1-1*, *etr1-1*, and *ein2-5* grown on medium containing indicated concentrations of MeJA were counted for LR formation (LRPs plus emerged LRs). Data show average and SD of 15 seedlings and are representative of at least three independent experiments. Asterisks denote *t* test significance compared with untreated plants: *P < 0.05.
**(B)** ACC-induced LR formation in *jdl1/asa1-1* and *coi1-2*. Seven-day-old seedlings of Col-0, *jdl1/asa1-1*, and *coi1-2* grown on medium containing indicated concentrations of ethylene precursor ACC were counted for LR formation (LRPs plus emerged LRs). Data show average and SD of 15 seedlings and are representative of at least three independent experiments. Asterisks denote *t* test significance compared with untreated plants: *P < 0.05.

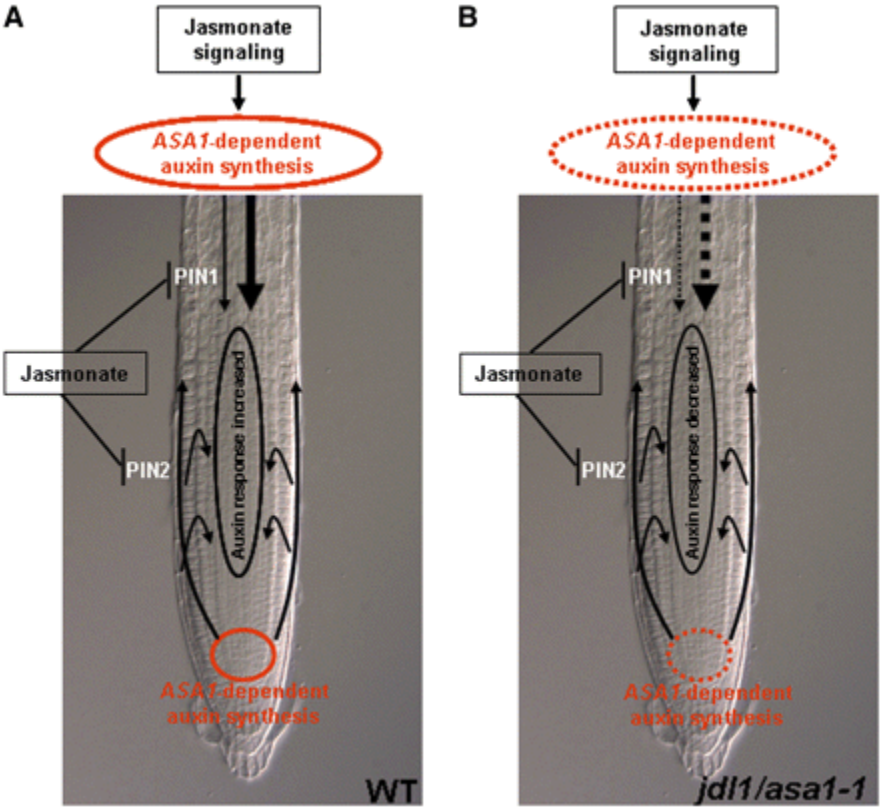


**Figure 6.8.** Model Showing Jasmonate Modulation of Auxin Accumulation in the Root Basal Meristem.

**(A)** In the wild type, JA stimulates the *ASA1*-dependent auxin synthesis in shoot and root tissues, which are transported to the root basal meristem through phloem-based and/or polar transport pathways. On the other hand, jasmonate reduces the protein levels of auxin efflux carriers (PIN1 and PIN2), which leads to decreased auxin transport capacities to the root basal meristem. The net effect of jasmonate is to increase local auxin accumulation in the root basal meristem and promote LR formation.

**(B)** In the *jdl/asa1-1* mutant, *ASA1*-dependent auxin synthesis in the shoot and root tissues is blocked. Jasmonate still represses auxin transport to the root basal meristem through reducing the levels of PIN1 and PIN2 proteins. The net effect of jasmonate in the mutant is to decrease auxin accumulation in the root basal meristem and therefore suppresses LR formation. Arrows represent auxin transport flows, ovals in red represent *ASA1*-dependent auxin synthesis in shoot and root, and dashed lines represent the *jdl1/asa1-1* mutation blocks *ASA1*-dependent auxin synthesis.

**Supplemental Figures:**

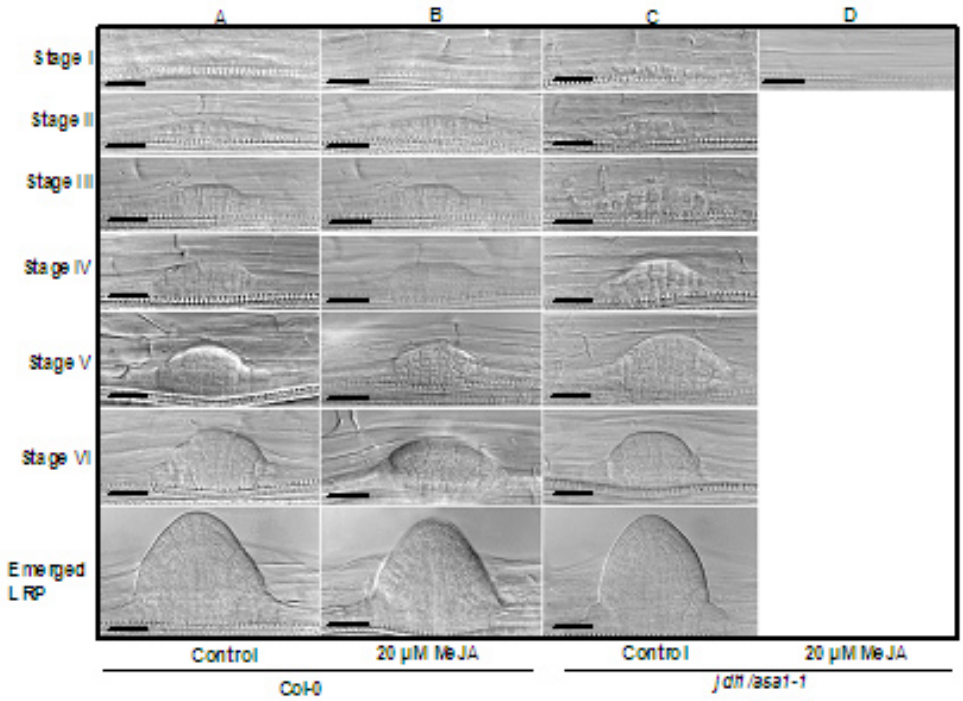


**Figure S6.1.** Morphological Comparison of LRPs in WT and *jdl1/asa1-1*.

(A) Representative image of Col-0 LRPs at different developmental stages. Seedlings were grown on MeJA-free medium (Control).

(B) Representative image of Col-0 LRPs at different developmental stages. Seedlings were grown on medium containing 20 µM MeJA (MeJA).

(C) Representative image of *jdl1/asa1-1* LRPs at different developmental stages. Seedlings were grown on MeJA-free medium (Control).

(D) MeJA represses LRP formation in *jdl1/asa1-1*. Seedlings were grown on medium containing 20 µM MeJA (MeJA).

Bars: 20 µm.

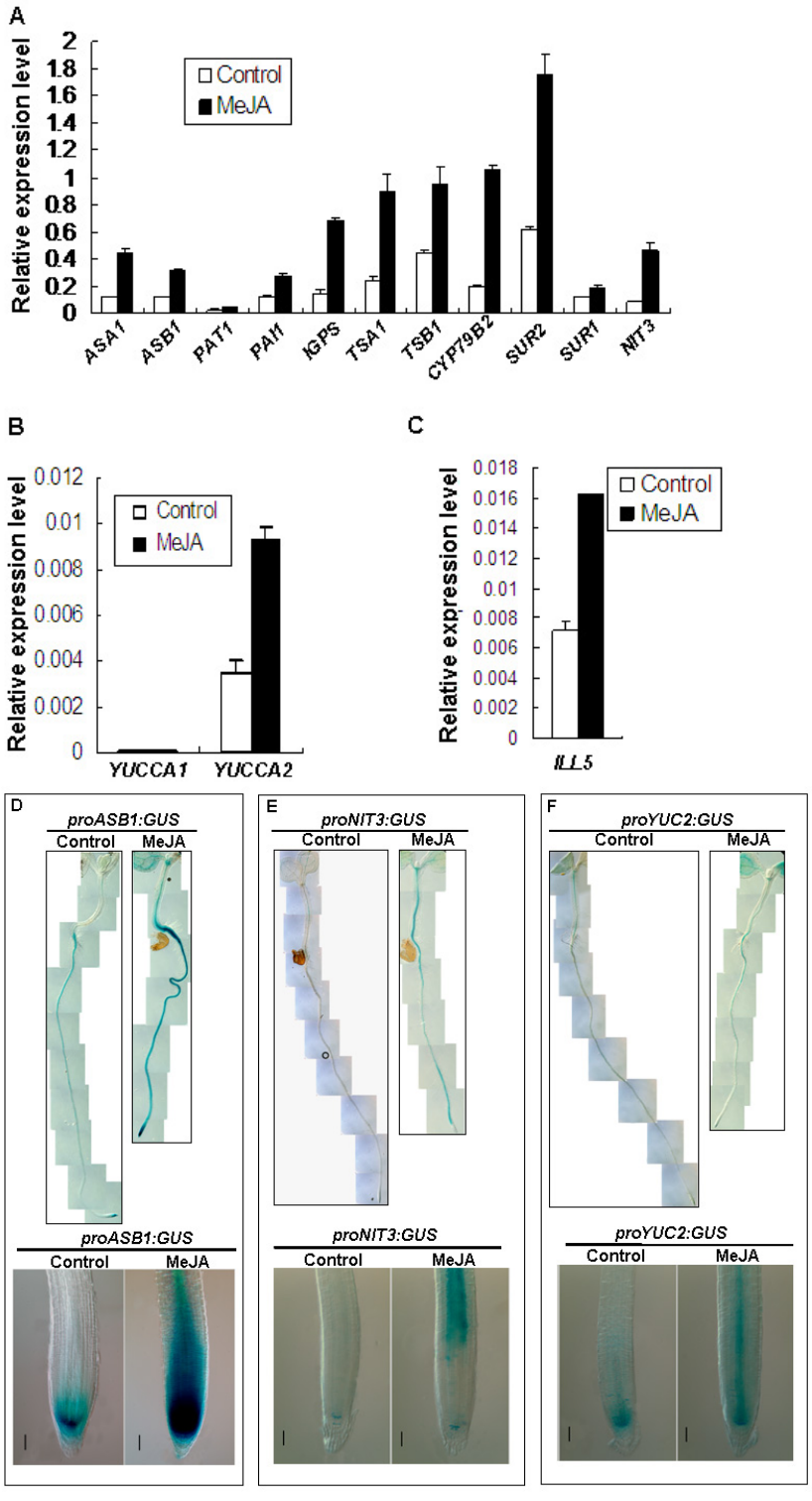
A
Relative expression level
2
1.8
1.6
1.4
1.2
1
0.8
0.6
0.4
0.2
0
Control
MeJA
ASA1
ASB1
PAT1
PAH1
IGPS
TSA1
TSB1
CYP79B2
SUR2
SUR1
NIT3
B
Relative expression level
0.012
0.01
0.008
0.006
0.004
0.002
0
Control
MeJA
YUCCA1
YUCCA2
C
Relative expression level
0.018
0.016
0.014
0.012
0.01
0.008
0.006
0.004
0.002
0
Control
MeJA
ILL5
D
proASB1:GUS
Control
MeJA
proASB1:GUS
Control
MeJA
E
proNIT3:GUS
Control
MeJA
proNIT3:GUS
Control
MeJA
F
proYUC2:GUS
Control
MeJA
proYUC2:GUS
Control
MeJA

**Figure S6.2**. MeJA-induced Expression of Auxin Biosynthesis-related Genes.
(A) - (C) MeJA-induced expression of auxin biosynthesis-related genes analyzed by qRT-PCR assays. Twelve-d-old Col-0 seedlings were treated with 50 μM MeJA for 3 h, and the whole seedlings were harvested for RNA extraction and qRT-PCR analyses. Transcript levels of target genes were normalized to the expression of *ACTIN2*. Results of one of three independent experiments are shown.
(D)-(F) MeJA-induced expression of *ASB1* (D), *NIT3* (E) and *YUCCA2* (F) analyzed by promoter-GUS assays. Four-d-old seedlings grown on control medium were transferred to medium without MeJA (Control) or containing 10 μM MeJA (MeJA) for 24 h. Bars: 50 μm. Upper panel of each figure shows promoter-GUS expression of the indicated gene in root and aerial part of whole seedling, lower panel shows promoter-GUS expression of the indicated gene in the root apical meristem and basal meristem.

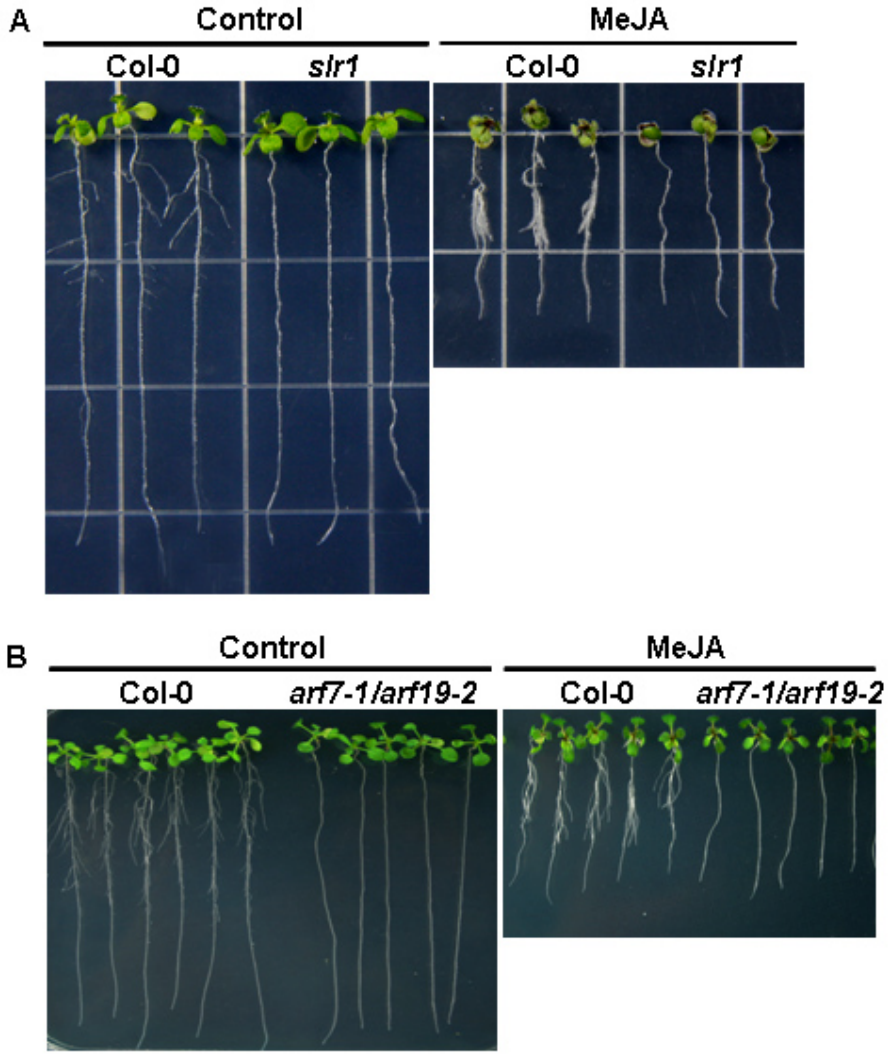


**Figure S6.3**. MeJA Fails to Promote Lateral Root Formation in *slr1* and *arf7-1 arf19-2* Double Mutants.

(A) LR phenotypes of 10-d-old Col-0 and *slr1* seedlings grown on medium without MeJA (Control) or containing 20 µM MeJA.

(B) LR phenotypes of two-week-old Col-0 and *arf7-1 arf19-2* double mutant seedlings grown on medium without MeJA (Control) or containing 20 µM MeJA (MeJA).

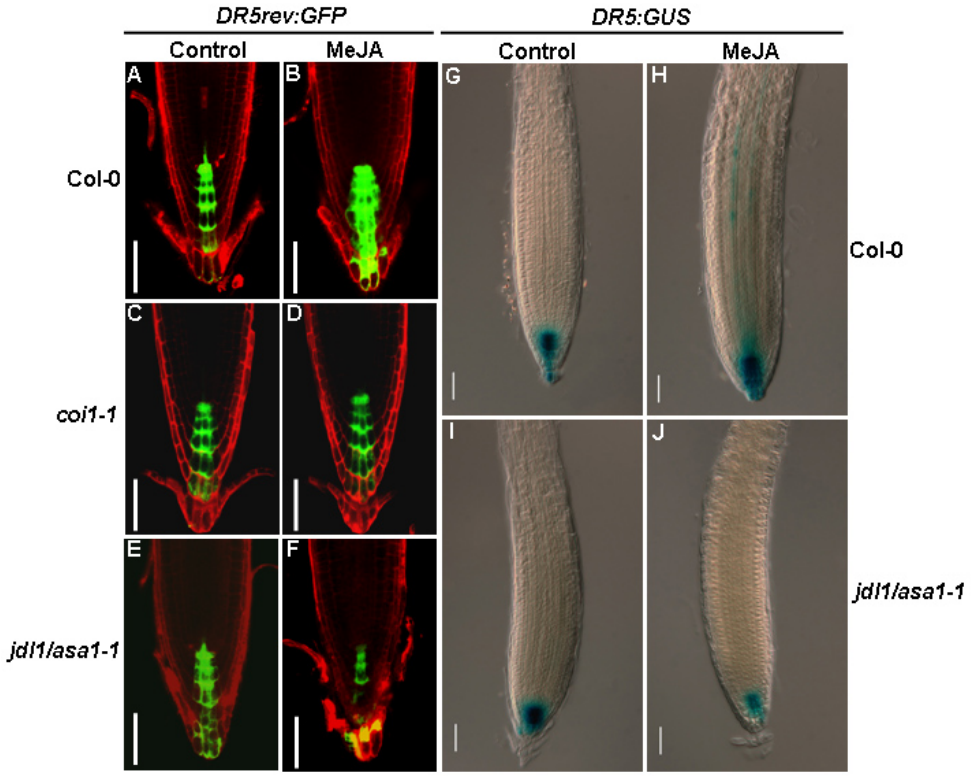


**Figure S6.4**. MeJA Differentially Regulates the Expression of *DR5*-reporters in WT, *coi1-1* and *jdl1/asa1-1* Root Tips.

Seedlings of the indicated genotypes were grown on medium without MeJA (Control) or containing 10 µM MeJA (MeJA) for 6 d, and the expression of *DR5rev:GFP* (A-F) and *DR5:GUS* (G-J) was monitored. Bars: 50 µm. Images shown are representative of at least six independent experiments.

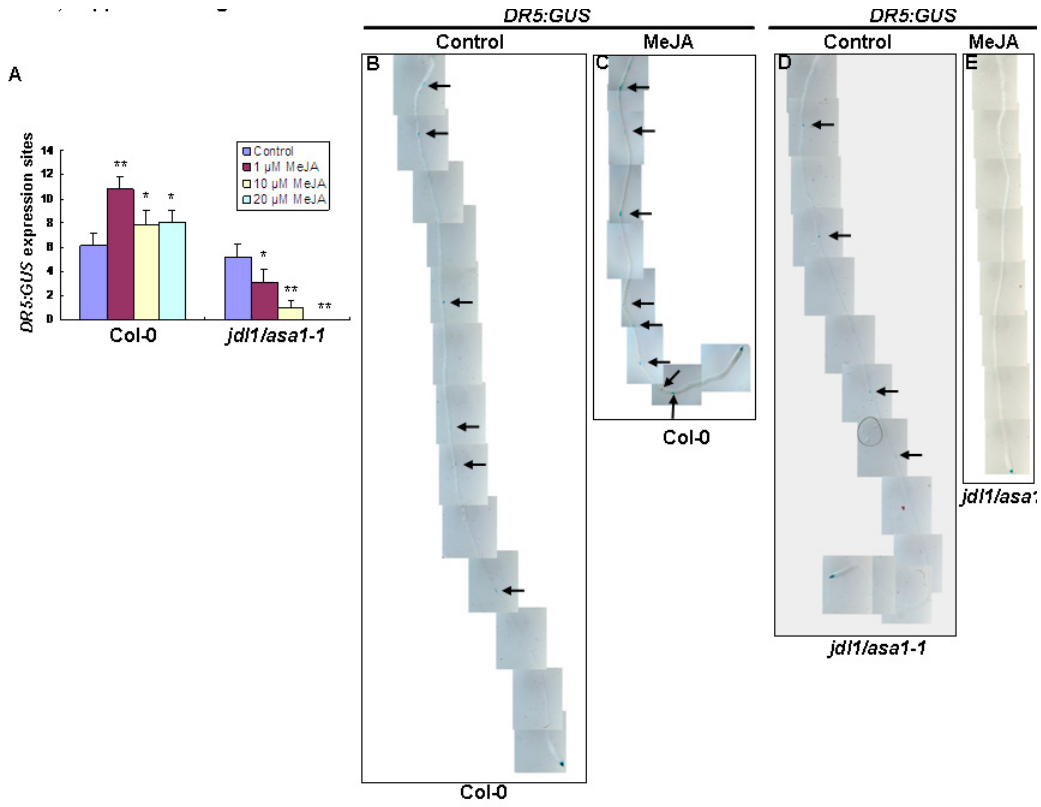


**Figure S6.5**. MeJA-Regulated *DR5:GUS* Expression along the Primary Root Length of WT and *jdl1/asa1-1*.

(A) Quantification of *DR5:GUS* staining sites along the primary root length. Seven-d-old seedlings of Col-0 and *jdl1/asa1-1* grown on medium containing indicated concentrations of MeJA were counted for *DR5:GUS* staining sites. Data show average and SD of 15 seedlings and are representative of three independent experiments. Asterisks denote *t*-test significance compared with untreated plants: *P < 0.05; **P < 0.01.

(B)-(E) *DR5:GUS* staining assays showing that MeJA represses *DR5:GUS* expression in the *jdl1/asa1-1* root.

(B) and (C) Expression pattern of *DR5:GUS* along the primary root length of representative Col-0 roots grown on MeJA-free medium (B) or on medium containing 20 μM MeJA (C).

(D) and (E) Expression pattern of *DR5:GUS* along the primary root length of representative *jdl1/asa1-1* roots grown on MeJA-free medium (D) or on medium containing 20 µM MeJA (E).
For (B) to (E), photographs show typical roots of 6-d-old seedlings. Arrows show *DR5:GUS* staining sites, which are indicative of LRP initiation sites.